The Terraces of the Conway Coast, North Canterbury: Geomorphology, Sedimentary Facies and Sequence Stratigraphy

---

A thesis submitted in partial fulfilment of the requirements for the Degree

of Doctor of Philosophy in Geological Sciences

in the University of Canterbury

by T.S. McConnico

University of Canterbury

2012

FRONTISPIECE: IN THE ~ 8 KA FOREST, CONWAY FLAT COAST, NEW ZEALAND

TABLE OF CONTENTS

ACKNOWLEDGEMENTS **5**

ABSTRACT **7**

CHAPTER 1
INTRODUCTION AND THESIS OUTLINE

1.1 GENERAL INTRODUCTION **10**

1.2 PREVIOUS WORK **11**

1.3 RESEARCH OBJECTIVES **13**

1.4 INTRODUCTION TO RESEARCH METHODS **15**
1.4.1 Geomorphic Structural Mapping 16
1.4.2 Geomorphic Terrace Mapping 17
1.4.3 Sedimentary Facies Architecture Mapping 17
1.4.4 Detailed Sedimentary Analysis 18
1.4.5 Age Control 18
1.4.6 Sequence Analysis 19

1.5 KEY TERMS **19**

1.6 THESIS OUTLINE **20**

Chapter 1 ..... *20*
Chapter 2 ..... *21*
Chapter 3 ..... *21*
Chapter 4 ..... *21*
Chapter 5 ..... *21*
Chapter 6 ..... *21*
Chapter 7 ..... *21*

Appendix A *22*
Appendix B *22*
Appendix C *22*
Appendix D *22*
Appendix E *23*
Appendix F *23*

1.7 REFERENCES **24**

CHAPTER 2
STRUCTURAL SETTING AND THE TECTONIC EVOLUTION OF THE HAWKSWOOD RANGE

2.1 INTRODUCTION **26**

2.2 BROAD TECTONIC SETTING…… 26

2.3 REGIONAL TECTONICS OF NORTH CANTERBURY…… 28
2.3.1 Previous Studies…… 28

2.4 HAWKESWOOD RANGE…… 35

2.5 NEW STRUCTURAL DATA…… 36
2.5.1 Lineament Analysis…… 36

2.6 GROUND-LEVEL DATA…… 43
2.6.1 Geomorphic Mapping…… 43
2.6.2 Local Mapping of Faults……. 45

2.7 DISCUSSION…… 53
2.7.1 Geomorphic Response to Faulting…… 53
2.7.2 Interpretation of Structural Evolution…… 56

2.8 SUMMARY……. 58

2.9 REFERENCES…….. 61

CHAPTER 3
FACIES ARCHITECTURE OF MULTIPLE GILBERT-TYPE FAN DELTA COMPLEXES

3.1 INTRODUCTION…… 68

3.2 REGIONAL SETTING…….. 69

3.3 TERRACE GEOMORPHOLOGY…… 72
3.3.1 Medina Terrace…….. 73
3.3.2 Rafa Terrace……... 73
3.3.3 Ngaroma……..……... 74
3.3.4 Inset Fluvial Terraces…….. 74
3.3.5 Modern Conway Fan Delta Surface…… 74

3.4 SEDIMENTARY LITHOFACIES…….. 75
3.4.1 Pliocene Marine Mudstones……... 75
3.4.2 Fan Delta Deposits……. 75
Angular topset beds.…….... 75
Delta Plain/Topset Beds.……... 76
Delta front beach facies.……..... 78
Delta slope foreset beds.……..... 80
Pro-delta facies.……... 81
3.4.3 Nearshore Marine Deposits……. 82
3.4.4 Estuary Deposits…… 83

3.5 SEDIMENT SOURCE ……... 88

3.6 FACIES ARCHITECTURE AND TERRACE DEVELOPMENT 87
3.6.1 Medina Terrace..... 87
Coastal transect-Medina Creek to Dawn Creek..... 87
Medina Creek transect..... 92
3.6.2 Rafa Terrace..... 93
Coastal transect- Dawn Creek to Big Bush Gully..... 94
Dawn Creek Transect..... 94
Coastal transect- Big Bush Gully to Ploughmans Creek..... 95
Big Bush Gully transect..... 96
Ploughmans Creek transect..... 97
3.6.3 Ngaroma Terrace..... 97
Coastal transect- North of Ploughmans Creek..... 97
Cross-cutting transects..... 99
3.6.4 The Modern Conway River Fan Delta..... 99

3.7 DISCUSSION OF TERRACE DEVELOPMENT..... 101
3.7.1 Terrace Development..... 101
3.7.2 Faulting and the Result of Seismic Activity..... 102

3.8 A MODEL FOR THE DEVELOPMENT OF THE TERRACES THROUGH TIME..... 104

3.9 CONCLUSIONS..... 108

3.10 REFERENCES..... 110

CHAPTER 4
GILBERT-TYPE FAN DELTA PROCESSES

4.1 GENERAL INTRODUCTION..... 120

4.2 RESEARCH OBJECTIVES..... 121

4.3 RESEARCH METHODS..... 121

4.4 GRAVELLY GILBERT-TYPE FAN DELTA ON THE CONWAY COAST, NEW ZEALAND: FORESET DEPOSITIONAL PROCESSES AND CLAST IMBRICATIONS (PUBLISHED PAPER)

CHAPTER 5
DATING TECHNIQUES AND APPLICATIONS

5.1 INTRODUCTION..... 144

5.2 DATING TECHNIQUES..... 146
5.2.1 Macro and Microfosils..... 148
5.2.2 Optically Stimulated Luminescence Dating..... 150
5.2.3 ^{14}C Dating..... 153

5.3 INTERPRETATION..... 155

5.4 DEGRADATION AND UPLIFT RATES…….. 159
5.4.1 Sediment Yield and Fan Delta Progradation…… 159
5.4.2 Uplift Rates……... 161

5.5 SUMMARY…….. 165

5.6 REFERENCES…… 168

CHAPTER 6
SEQUENCE STRATIGRAPHY

6.1 INTRODUCTION…… 172

6.2 CONWAY FLAT COAST STAGES OF DEVELOPMENT…… 175

6.3 SEQUENCE STRATIGRAPHIC FRAMEWORK…….. 177

6.4 IDENTIFICATION OF SEQUENCES……... …….. 180
Basement…….. 181
Sequence Boundary 1…….. 181
Sequence 1……... 181
Sequence Boundary 2…….. 182
Sequence 2……... 182
Sequence Boundary 3…….. 184
Sequence 3……... 184
Sequence Boundary 4…….. 184
Sequence 4…….. 185
Sequence Boundary 5……... 186
Sequence 5……... 186

6.5 KEY BOUNDING SURFACES…….. 187

6.6 FACIES ARCHITECTURE OF HIGH-FREQUENCY SEQUENCES…….. 187
6.6.1 Transgressive Tract (TST)…… 187
6.6.2 Highstand Systems Tract (HST)…… 187
6.6.3 Lowstand Systems Tract (LST)……. 188

6.7 SEQUENCE DRIVING MECHANISMS…….. 188
Tectonics as a forcing factors……..... *189*
Sediment Supply as a forcing factor…… *191*
Eustastic forcing factor of sedimentary cyclicity……... *192*

6.8 CONCLUSIONS…… 195

6.9 REFERENCES…….. 198

CHAPTER 7

CONCLUSIONS

7.1 CONCLUSIONS…….. 206

7.2 KEY FEATURES OF FAN DELTAS IN A COMPRESSIVE PLATE BOUNDARY……... 208

ACKNOWLEDGEMENTS

These last few pages give me an opportunity to reflect on and acknowledge all those people and organizations that have supported me throughout this research. I write this almost seven years after starting this project, and a huge number of people have provided scientific, financial, and general support throughout. In these short words I cannot begin to thank enough all of the people that have made this project a success.

My supervisor Professor Kari Bassett has been very patient and understanding over the years as we have encountered "unique" working and research situations. I thank her for the ideas and many reviews of work published and to be published.

Karl Spinks- has been an outstanding friend over the last seven years, and it is his confidence and encouragement that has got me through these last years; as well as standing in at the wedding..cheers mate! To think it all started at a sleeting All Blacks game.

Jarg Pettinga- offered encouragement and advice throughout the project, especially with geomorphic mapping and DEM imagery analysis.

Jim Cole – general all-around support, providing motivation, and friendly and encouraging help over the years.

Tariq Rahmin – encouragement, and helpful advice and insight when it came to the dizzying nights after staring at lines on DEM's….yes the lines did get burned into the eyelids!

Henrik Rother – for ideas and help with OSL dates

Basil Tikoff – for his active participation in the field and for acting as a sounding board during a brief visit by taking his experience in tectonic systems and applying it to the imbricated pebble problem at Conway Flat.

Becky Dorsey – for tramping along the beach and sharing ideas over the years about the deposits along Conway Flat coast

A special thank you to all of the support from the Geological Sciences Department: John Southward, Rob Speirs, Cathy Knight, Kerry Swanson, Arthur Nicholas, Julie-Anne, Alison Johnston and Janet Warburton

Maria Martin – This project got off the ground with your help and humor. Thank you for the fun trips with Spinks and for endless conversations.

Doug Lewis - for financial support, but more importantly for good company in the field, uber-interesting stories on just about any historical subject and for manuscript reviews.

Emily Cross - If anyone deserves a gold "star" it is miss es cross. Always there to provide humor, home-baked goodies and endless adventures in Dunners.

The Fulbright Family- for always providing a piece of home in Wellington, taking us on excellent adventures and for giving me the opportunity of a lifetime.

UC Doctoral scholarship- for providing funding for the research over the years.

The MacFarlaine and Handyside Families – for being terrific friends during my time out at Conway Flat, for providing somewhere to pour over maps and discuss rocks and trees, and particularly Bruce for his genuine interest in my research, and his general scientific acumen…..as well as allowing me to help blow things up!

Helen Davies – for picking a lonely American kid up at a hotel to check out a granny flat on a cold winter night 7 years ago and for the many dinners, beer tasting nights and particularly for including me in many activities over the years.

Andy Burgess, Miles Darragh, Todd & Sarah & Molly; Rob & Julie; Di; Andrea and Brian Spinks- for allowing a foreigner to feel like a Kiwi over the years…whether it was a nightly trip to Subway, a night out, watching a Bledisloe game with the boys or a bbq at the beach…thank you.

Mom and Dad – for continued and unrelenting support, and understanding that I didn't know when I would finish….and for asking other people instead of me.

My sister Laurie for appreciating the difficulty of the task at hand.

And my wife Kristin for constantly being supportive and fielding questions on the status of this project when she knew I would snap if asked☺

Abstract

A basin analysis was conducted at the Conway Flat coast (Marlborough Fault Zone, South Island, New Zealand) to investigate the interaction of regional and local structure in a transpressional plate boundary and its control on basin formation. A multi-tiered approach has been employed involving: (i) detailed analysis of sedimentary deposits; (ii) geomorphic mapping of terraces, fault traces and lineaments; (iii) dating of deposits by ^{14}C and OSL and (iv) the integration of data to form a basin-synthesis in a sequence stratigraphy framework.

A complex thrust fault zone (the Hawkswood Thrust Fault Zone), originating at the hinge of the thrust-cored Hawkswood anticline, is interpreted to be a result of west-dipping thrust faults joining at depth with the Hundalee Fault and propagating eastwards. The faults uplift and dissect alluvial fans to form terraces along the Conway Flat coast that provide the necessary relief to form the fan deltas. These terrace/fan surfaces are ~9 km long and ~3 km wide, composite features, with their upper parts representing sub-aerial alluvial fans. These grade into delta plains of Quaternary Gilbert-style fan deltas. Uplift and incision have created excellent 3D views of the underlying Gilbert-style fan delta complexes from topsets to prodelta deposits.

Erosive contacts between the Medina, Rafa, Ngaroma and modern Conway fan delta deposits, coupled with changes in terrace elevations allow an understanding of the development of multiple inset terraces along the Conway Flat coast. These terraces are divided into five stages of evolution based on variations in sedimentary facies and geomorphic mapping: Stage I involves the uplift of the Hawkswood Range and subsequent increased sedimentation rate such that alluvial fans prograded to the sea to form the Medina fan delta Terrace. Stage II began with a period of incision, from lowering sea level or changes in the uplift and sedimentation rate and continued with the deposition of the Dawn and Upham fan deltas. Stage III starts with the incision of the Rafa Terrace and deposition of aggradational terraces in the upper reaches. Stage IV initiated by a period of incision followed by deposition of estuarine facies at ~8ka and Stage V began with a period of incision and continues today with the infilling of the incised valley by the modern fan delta of the Conway River and its continued progradation.

New dates from within the Gilbert-type fan deltas along the Conway Flat coast are presented, using OSL and ^{14}C dating techniques. Faulting at the Conway Flat coast began ~ 94 ka, based on the development of the Medina Terrace fan delta with uplift rates ~1.38~1.42 m/ka. The interplay of tectonics and sea level fluctuations continued as the ~79 ka Rafa Terrace fan deltas were created, with uplift rates calculated at ~1.39 m/ka. Detailed ^{14}C ages from paleoforest (~8.4-~6.4 ka) in the Ngaroma Terrace and from the mouths of smaller streams have established uplift rates during the Holocene ~1-3 m/ka, depending on sea level.

CHAPTER 1 INTRODUCTION & THESIS OUTLINE

1.1 GENERAL INTRODUCTION

The northeast region of the South Island, New Zealand, is an active, transpressional plate boundary fault zone known as the Marlborough Fault Zone (MFZ). This zone marks the transition from oblique convergence and subduction in the North Island to the transpressional strike-slip Alpine Fault in the South Island. The mechanics of this plate boundary transition zone are poorly understood, particularly the relationship between plate kinematics, structural style and basin formation, and how this has evolved through time (Pettinga and Armstrong, 1998). The Conway Flat coastal region in North Canterbury is a large area of well-exposed marine terraces and fan-delta deposits that permitted detailed analysis of basin formation in a modern plate boundary transition zone.

Bounding the Conway Flat coastal region is the Hawkswood Range, a thrust-cored northeast plunging anticline (Pettinga and Armstrong, 1998). On the east side of the range are a series of uplifted Pleistocene-Holocene marine terraces as well as non-marine terraces (Ota et al., 1984). Uplift rates published in the literature vary between ~ 2.9 mm/yr and ~3 mm/yr for the coastal region (Ota et al; 1984, 1996). The lower terraces expose uplifted marine Gilbert-type fan delta complexes (Lewis and Ekdale, 1991), which provide an excellent opportunity to explore the connection between an evolving sedimentary basin and the overlying geomorphic expression of these marine deposits. Detailed sedimentology and terrace geomorphology has provided new data on the origin and deposition of fan deltas in an actively deforming environment.

The Conway Flat coastline straddles an area with substantial vertical topographic and bathymetric relief, as well as considerable geological complexity (Walters et al., 2006). Bathymetry along the coast increases from 0 to 800 meters between the coastline and the Conway trough in 10 kilometers offshore. Along the Kaikoura and Conway coastlines are host to major submarine canyons (i.e. Kaikoura Canyon) which incise the continental margin and are conduits for sediment transport from the Southern Alps to the Hikurangi Trough and beyond to the deep Pacific Basin (Lewis et al., 1998).

Although many studies (e.g. Falk and Dorsey, 1998; Mutti et al., 2003) have focused on Gilbert-type fan deltas in tectonically active areas, very few studies are process oriented. A process oriented analysis involving a detailed look at fan delta development is required in order to understand the detailed facies architecture. While most studies on fan deltas have focused on structure and geomorphology, this study shows that the combination of detailed sedimentology, *together with* geomorphology *and* larger scale structural analysis that provides a more robust and integrated model for the development of fan deltas.

This thesis examines the sedimentology and tectonic geomorphology of a section of North Canterbury in a complex the transitional tectonic zone, and presents a new model for the sedimentological and structural evolution of the Conway Flat and Hawkswood Range region.

1.2 PREVIOUS WORK

Warren (1995) published a 1:50 000 geologic map of the Hurunui region based on mapping largely completed in the late 1960's. Within this area he mapped the broad geology of the Conway Flat coast. The map includes basic map units correlated to the few

studies previously undertaken along this coastal section. Few structural features are identified on the east side of the Hawkswood Range.

Ota et al. (1996) conducted a study on the coastal terraces of the Kaikoura Peninsula and the Marlborough coast. This study built on the work established by Ota et al. (1984) and calculated a general uplift rate for a broad area including the Conway Flat coast and regions to the north based on the identification of uplifted beach terraces. The uplift rate was calculated based on luminescence data collected from uplifted marine terrace surfaces north of the Conway Flat coast and assumed that the Hawkswood surfaces were of the same age based on similar elevation. The data collected allowed them to establish an uplift rate of >2m/ka for the area of the Conway Flat coast south of the Conway River. They concluded that the deformation and uplift of the marine terraces was attributed to local structures. The Hundalee Fault, interpreted in the study as a southeast dipping right lateral strike-slip fault, is the causative fault south of the Conway River.

Lewis and Ekdale (1991) and Ekdale and Lewis (1991) were one study, with two publications resulting from it, largely completed at the same time on a section of the Conway Flat coast. The study focused on establishing the existence of Gilbert-type fan deltas on the east side of the Hawkswood Range and broadly looking at the depositional processes. The study not only identified the presence of marine fan deltas but also described the equivalent lateral facies. During the examination of the lateral facies Ekdale and Lewis (1991) described the unique trace fossils of the marine siltstones and concluded that the abundance, variance and species of trace fossils present in the silt beds identified the unit as nearshore marine.

Initial studies by Ota et al. (1996) identified the upper terraces of the Hawkswood Range as beach deposits. From this assumption correlations to other beach deposits north of the field area of similar heights were made. This provided the foundation for not only their uplift rates, but for the research of Hall (2004). However, these rates of deformation are still questionable at best considering the lack of age data from the individual geomorphic surfaces. Hall (2004) completed a PhD thesis that included a section on the uplift of the Hawkswood Range. Based on a detailed kinematic GPS study of the multiple terraces exposed on the east side of the Hawkswood, she calculated an uplift rate of ~ 1.7-2.3 mm/year. Hall's (2004) study was the first detailed look at the Conway Flat coast area for determining uplift rates. Research presented in this study looked in detail at the sedimentology and geomorphology of the terraces to identify that these terrace features are actually the result of uplifted beach deposits, instead they are alluvial fans offset by thrust faults. Hall concluded that the Hawkswood Range was a fault propagated, plunging anticline probably the result of a blind thrust that is located offshore.

The overall lack of relevant age control within the Conway Flat section is addressed in this study. Multiple dating techniques combined with detailed geomorphic and sedimentary facies analysis provide the basis for determining a sequence of Gilbert-type fan delta complex development. The technique of integrating geomorphology, sedimentology and structural framework allows for a complete basin synthesis to be deciphered. This technique has not been used in the Conway Flat region.

1.3 RESEARCH OBJECTIVES

The principal objective of this research was to understand the geologic evolution of the Conway Flat area of North Canterbury. Rather than focus on one particular component or

method, this study uses a combination of detailed sedimentology and tectonic geomorphology to understand the modern tectonics and sedimentology and facies architecture of Gilbert-type fan delta complexes and how these developed through time. Previous work along the Conway Flat coast was much more narrow in focus, e.g. Lewis and Ekdale (1991) and Ekdale and Lewis (1991) focused on trace fossils and the surrounding sediments; Ota et al. (1984 and 1996) and Hall (2004) collected data to determine uplift rates for the region. This is the first holistic study in the Conway Flat coast area that sets out to make connections between the structural geology, sedimentology and geomorphology that describe the evolution of this section of the Conway coast.

The completion of the following goals in this research provides new contributions to local and regional geology as well as to the literature:

1. Develop a better understanding of the structure and sedimentology of the Conway Flat coast. A basic understanding of structure in the Hawkswood Range provides the foundation for understanding the Pleistocene basin evolution along the Conway Flat coast with relation to transpressive plate boundary.
2. Provide the first mapping of geologic structures along the Hawkswood Range and Conway Flat coast.
3. Integrate the sedimentology and geomorphology data and to provide a new model of basin development, terrace development and uplift in an active plate boundary setting.
4. Undertake detailed sedimentologic study of the Gilbert-type fan delta(s) to provide new insight into depositional processes. Gilbert-type fan delta research is shrouded in controversy. The ease of access and amount of

exposure along the Conway Flat coast provide a great opportunity to highlight new features never described in the fan delta literature while at the same time clarify some of the convolute terminology that often encourages debate.

1.4 INTRODUCTION TO RESEARCH METHODS

To reconstruct the basin history the following methods will be undertaken:

1. Undertake detailed geomorphic mapping of the lower slopes of the Hawkswood Range.
2. Undertake detailed geomorphic mapping of the upper slopes of the Hawkswood Range. This mapping, coupled with general structural mapping of the upper terraces, sheds light on the modern structural evolution of the Hawkswood Range.
3. Determine the sedimentary facies architecture and geometry of the multiple Gilbert-type fan delta complexes and associated deposits along the Conway Flat coast.
4. Integrate the sedimentology and geomorphology data and to provide a new model of basin development, terrace development and uplift in an active plate boundary setting.
5. Determine the age of the deposits and surfaces on the east side of the Hawkswood Range. Carbon-14 and Optically Stimulated Luminescence (OSL) dates collected in this study combined with paleontological data from previous mapping provide a basic timeline of the formation of the

fan delta complexes and some of their surfaces. These dates allow the connection to tectonics and sea level histories to be made.

6. Identify the sediment source area for the fan deltas. The shear size of the Gilbert-type fan deltas has sparked debate on their source location. By identifying the location of the deltas a clearer picture of the Hawkswood Range development can be deciphered.

7. Provide a synthesis of the sedimentologic, geomorphic and tectonic data through sequence stratigraphy. The information garnered from this data provides a picture of the evolution of a marginal marine basin caught in a transpressional plate boundary and its evolution through time.

1.4.1 Geomorphic Structural Mapping

The Conway Flat area has many obvious geomorphic features that are directly linked to the tectonic and sedimentary evolution of the region. Detailed geomorphic structural mapping was completed by combining data collected from field mapping, aerial photo and digital elevation model (DEM) interpretations. The geomorphic mapping of the surfaces and field mapping of the structural geology exposed at the surface combined with the known fault kinematics of the region helped develop a structural model for the Hawkswood Range as well as link the underlying sedimentary deposits with geomorphic features.

An understanding of the structural history through this type of analysis will help decipher the setting for the depositional architecture of the Conway Flat coastal region. In reverse, the depositional architecture provides an age context for the fault kinematics of the Conway Flat coast.

1.4.2 Geomorphic Terrace Mapping

Detailed geomorphic mapping of uplifted terraces was done by integrating field mapping and aerial photo interpretation of the lower, coastal surfaces located on the east side of the Hawkswood Range. This mapping sets the foundation for the integration of sedimentary facies architecture and geomorphology. Mapping was completed using 1:50 000 aerial photos enlarged to A3 size. The photos were laminated and initial mapping completed with the use of mylar overlays. The interpretations from these overlays were field-proofed with additional information being added from fieldwork. The use of Digital Elevation Models (DEM) was used to highlight areas of changing elevation as were surface slope calculations completed in SURFER from Golden Software. All data was referenced against known sedimentological data collected in this study to build a complete picture of the geomorphic setting at Conway Flat.

1.4.3 Sedimentary Facies Architecture Mapping

Detailed facies analysis and sedimentary architecture of the deposits along the Conway Flat coast and inland exposures help to understand terrace development and modern tectonics. A detailed look at the architecture of the Gilbert-type fan delta complex along the Conway Flat section of the Conway coast provides keys to understanding the tectonic evolution of the region because of its direct link to terrace development and tectonic activity. Data collected from facies analysis when combined with geomorphic mapping information of the coastal terraces links the sedimentary and tectonic evolution of the basin. In turn, by understanding how the sedimentary facies connect together through their contacts, ages and location, a connection to the tectonic evolution of the Hawkswood can be made.

1.4.4 Detailed Sedimentary Analysis

Detailed sedimentary studies of the multiple Gilbert-type fan delta complexes help to interpret transport mechanisms and pin point source area for the sediments. The fan delta sedimentary characteristics provided interesting clues to the active tectonics occurring during the time of deposition. Data collected on clast imbrications provide information on foreset processes.

The Conway Flat coastal region is a perfect area to study Pleistocene to modern faulting, basin development and landscape evolution because the structural, stratigraphic and geomorphic records are well exposed and accessible. The increased geochronologic depth provided by sedimentology and facies architecture on very young deposits provides new information into active tectonics and plate kinematics.

1.4.5 Age Control

One of the keys to the success of this project is the dates of the deposits and surfaces. With geochronologic data, we can determine the age of the fan delta complexes and terraces to link deposition with the tectonic evolution of the Hawkswood Range. Various dating techniques including the use of archived paleontological data, optically stimulated luminescence (OSL) and radiocarbon-14C were used in this study.

The proximity of the coastline to this study area provides sea level as a datum for stratigraphic analysis. This absolute datum enabled calculation of general uplift rates associated with the active faults along the Conway Flat coast and in turn provided

information on depositional timing and uplift of marine Gilbert-type fan deltas. Further information about rates of uplift is provided by the age of the drowned Podocarp paleoforest located on the Conway Flat coast. The coastal paleoforest, drowned during a period of rapid sea level rise, provides both age and elevation data for calculations of uplift.

1.4.6 Sequence Analysis

Identification and mapping of unconformities and other key surfaces allows a sequence stratigraphic framework to be developed. New insights came from the integration of classic sequence stratigraphy with mapping of inset terraces and terrace elevations. The dates collected from the deposits and terrace surfaces help organize the sequence of events at Conway Flat from deposition to sea level fluctuations and tectonic deformation. The use of the dates and integration of the sedimentary data with the geomorphic data allows for a complete analysis of the region.

1.5 KEY TERMS

Included here is a set of defined key terms used throughout the thesis:

Delta – A delta is a landform that is formed at the mouth of a river, where the river flows into the ocean. Deltas are formed from the deposition of sediment carried by the river as the flow leaves the mouth of the river.

Fan delta – A fan delta is an alluvial fan that directly enters the water thus also forming a delta. Much of the sediment in a delta is derived directly from the river that feeds it.

Gilbert-type fan delta – A Gilbert-type fan delta is differentiated from other fan deltas by its distinctive morphology. The formation of a Gilbert-type delta consists of three main forms: the topset, foreset, and bottomset beds. Gilbert-type fan deltas have steep foresets representing a steep drop off or steep relief.

Marine terrace – Is a relatively flat, horizontal or gently inclined surface of marine origin. Marine terraces along the Conway Flat coast are both depositional/aggradational and erosional/degradation.

Non-marine terrace – A non-marine terrace consists of a flat or gently sloping geomorphic surface, called a tread that is typically bounded on one side by a steeper ascending slope. Non-marine terraces along the Conway Flat coast are aggradational features.

1.6 THESIS OUTLINE

This thesis is a series of integrated studies that together provide a model for depositional, geomorphic, and structural evolution of the Conway Flat coast, North Canterbury. Each chapter reflects a different aspect of this research and these chapters combine to generate an understanding of the uplift of the Hawkswood Range and its development within a transpressional plate boundary. The material from chapter 4 is already published (see appendices) with future publications from data presented in chapter 2, 3 and 6 in process.

The contents of the thesis are outlined below.

Chapter One gives a general introduction to the thesis, summarises the reasons for and objectives of the study, briefly introduces the research methods, and provides a thesis outline.

Chapter Two is a detailed look at the structure and geomorphology of the Hawkswood Range. Evidence generated by field mapping, lineament mapping and interpretation of aerial photos and Digital Elevation Models (DEM) aide in deciphering the structural history of the Hawkswood Range and its connection to regional tectonics. This chapter sets the stage for the findings of Chapters 3 and 4, which together form a complete evolutionary story of the Conway Flat coast.

Chapter Three (to be submitted to the Geological Society of America Bulletin) describes the facies architecture of nested Gilbert-type fan delta complexes. The use of terrace geomorphology when integrated with detailed analysis of the sedimentology leads to a better understanding of the fan delta complex development.

Chapter Four (published in Sedimentary Geology, McConnico and Bassett, 2007) is a detailed sedimentary analysis of steep, Gilbert-type fan delta foresets focussing on depositional processes. This data provides new insight into depositional processes occurring on foreset slopes and provides connections to the overall tectonic story for the Conway Flat coast.

Chapter Five summarizes the dates and various dating techniques used to determine ages and uplift rates along the Conway Flat coast.

Chapter Six is a synthesis of the sedimentary, geomorphic and tectonic data collected from the Conway Flat section of the Conway coast. Using sequence stratigraphy the timing of events, basin evolution and structural control on basin development in a transpressional plate boundary are discussed.

Chapter Seven summarizes the key conclusions from the thesis, highlighting the characteristics of Gilbert-type fan deltas in a transpressional plate boundary.

The Appendices contain a number of additional documents associated with this research, and the data collected during this research and reported in this thesis.

Appendix A

Lineament analysis was completed on mylar overlays over 1: 50 000 Digital Elevation Models (DEM). The reproducible lineaments were measured and record with length and trend (Chapter 2). The data is present here.

Appendix B

The initial fieldwork of this project focused on the mapping of coastal cliffs and drainages on the east side of the Hawkswood Range. This mapping was completed on a series of panoramic photos that were later transformed into line-drawings (Chapter 3). The original photos are provided here.

Appendix C

Gilbert-type fan delta deposits are frequently discussed in the literature. However, few studies focus on detailed investigations of individual foreset beds. There is new information to be found on transport processes by looking at individual beds in detail. A summary of the more than 60 beds that were the foundation for the work completed in Chapter 4 is provided here.

Appendix D

In June 2003 a test study using Ground Penetrating Radar (GPR) was undertaken to see what stratigraphy could be seen in the subsurface. The GPR line from Big Bush Gully contained here clearly shows the fan delta foresets downlapping onto a surface that is most likely the unconformity incised into Miocene muds of the Greta Formation. The GPR line is provided here.

Appendix E

The dating techniques of Radiocarbon-14C and Optically Stimulated Luminescence (OSL) and archived paleontological data were used to place age constraints on the facies along the Conway Flat coast and calculate uplift rates (Chapter 5). Presented here are the fossil data from FRED, laboratory results from Waikato Radiocarbon Laboratory, University of Waikato, Hamilton, New Zealand and Luminescence Dating Laboratory, School of Earth Sciences, Victoria University, Wellington, Wellington, New Zealand

Appendix F

In December 2005 a two-day field trip was organised for the 50th annual Geological Society of New Zealand (GSNZ) conference in Kaikoura, New Zealand. The field guide material presented data and interpretations from this thesis.

> **McConnico, TS**, and KN Bassett (2005); Field Trips 2 & 9: The Conway fan delta terraces and uplift of the Hawkswood Range; in Pettinga, JR and AM Wandres (eds.); Field Trip Guides, Geological Society of New Zealand 50 th Anniversary Conference, Kaikoura; Geological Society of New Zealand Misc. Publ 119B; p. 37-48

1.7 REFERENCES

Ekdale, A.A., and Lewis, D.W., 1991. Trace fossils and paleoenvironmental control of ichnofacies in a Late Quaternary gravel and loess fan delta complex, New Zealand. Palaeogeography, Palaeoclimatology, Palaeoecology 81, 253-279.

Falk, P., and Dorsey, R. J., 1998. Rapid development of gravelly high-density turbidity currents in marine Gilbert-type fan deltas, Loreto basin, Baja California Sur, Mexico. Sedimentology 45, 331-349.

Hall, L., 2004. Cenozoic deformation at the southern end of the Hikurangi margin, New Zealand, unpublished Ph.D. Thesis, University of Oxford, England.

Lewis, D.W. and Ekdale, A. A., 1991. Lithofacies relationships in a late Quaternary gravel and loess fan delta complex, New Zealand. Palaeogeography, Palaeoclimatology, Palaeoecology 81, 229-251.

Lewis, K.B., Garlick, R.D., Dawson, S.M., 1998. Kaikoura Canyon: depths, shelf texture, and whale dives. NIWA Chart Miscellaneous Series 78. Wellington, National Institute of Water and Atmospheric Research Limited.

Mutti, E., Tinterri, R., Benevelli, G., di Biase, D., and Cavanna, G., 2003. Deltaic, mixed and turbidite sedimentation of ancient foreland basins. Marine and Petroleum Geology 20, 733-755.

Ota, Y.Y., Torao; Iso, N., Okada, A., Yonekura, N., 1984. Marine terraces of the Conway

coast, South Island, New Zealand. New Zealand Journal of Geology and Geophysics 27, 313-325.

Ota, Y.Y., Pillans, B. Berryman, K., Beu, A., Fujimora, T., Miyauchi, T., Berger, G., Climo, F.M., 1996. Pleistocene coastal terraces of the Kaikoura Peninsula and the Marlborough coast, South Island, New Zealand. New Zealand Journal of Geology and Geophysics 39, 51-73.

Pettinga, J.R., Armstrong, M.J. 1998. North Canterbury active tectonics and earthquake hazards. Geological Society of New Zealand Miscellaneous Publication 101B: Field Trip Guides. M.G. Laird (Ed.) Field trip 3: 28 p.

Walters, R.A., Barnes, P., Goff, J.R., 2006. Locally generated tsunami along the Kaikoura coastal margin: Part 1. Fault ruptures. *New Zealand Journal of Marine and Freshwater Research 40*, 1–16

Warren, G., 1995. Geology of the Parnassus area. Institute of Geological and Nuclear Sciences Geological Map 18, 36 p.

CHAPTER 2 STRUCTURAL SETTING AND TECTONIC EVOLUTION OF THE HAWKSWOOD RANGE

2.1 INTRODUCTION

The purpose of this chapter is twofold: 1) to summarize existing work on the regional structure and tectonism of the Hawkswood range area; and 2) to present new structural data that provides a structural framework for the tectonic, geomorphic, and sedimentary evolution of the Conway Flat coast area.

2.2 BROAD TECTONIC SETTING

The modern New Zealand landmass straddles the Australian-Pacific plate boundary zone, with the relative motions of these plates controlling the position and shape of New Zealand since the Cenozoic (Pettinga et al., 2001) (Fig. 2.1). The dominant tectonic features of this active plate boundary on the South Island include the Alpine Fault and greater Marlborough Fault Zone. These features have been recognized as oblique-slip transform segments connecting opposite dipping obliquely convergent subduction zones; the younger (Pliocene ~5 Ma) west-facing Puysegur Trench in the southwest and the older (Oligocene-Miocene ~25 Ma) east-facing Kermadec-Hikurangi Trench to the northeast. Of particular importance for this thesis is the existence of the Hikurangi subduction zone from East Cape south to Kaikoura (Barnes, 1996). The interaction of the plates at the surface and at depth is reflected in both regional and local structure along the Conway Flat coast.

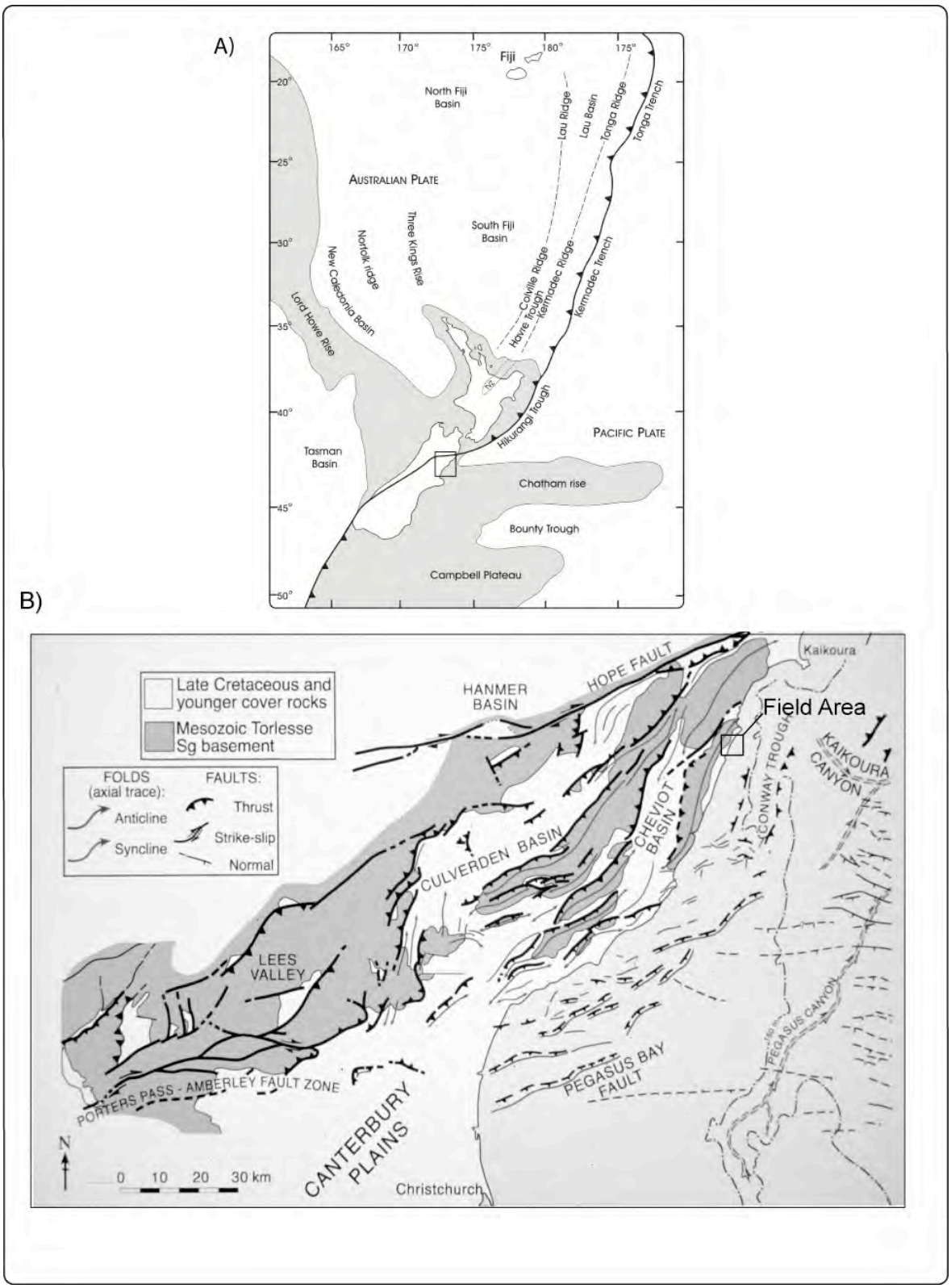

Figure 2.1. A) General location map of New Zealand. B) Modern transpressional plate tectonic setting and local structure of the Marlborough Fault Zone (MFZ) adapted from Gamble and Wright (1995) and Pettinga and Armstrong (1998). Hashed lines represent faults within the MFZ. The regional structure and Field Area box in B are further described in Figure 2.2.

Since ~ 6 Ma, the Pacific plate has moved WSW at ~42 mm/yr relative to the Australian plate creating an area of oblique convergence in the South Island (Walcott, 1998). The southeast dipping dextral-reverse Alpine Fault strikes ~18-20° anticlockwise of the plate motion vector and accommodates most of this motion (Little et al., 2002). The Alpine Fault is a linear feature that extends for 420 km along the west side of the South Island with recent data suggesting that it in fact could extend a further 200 km south towards the tip of Fiordland (Delteil at al., 1996). Bands of high-grade metamorphic rock crop out near and parallel to the Alpine Fault suggesting long periods of uplift during the Cenozoic (Wellman, 1979; Little et al., 2002). The northeast extent of the fault is not certain but geophysical data suggests that it may flatten to the east at depth extending beneath west Canterbury (Kleffman et al. 1998).

Strike-slip rates indicate that between 60-90% of the plate boundary motion is accommodated by the Alpine Fault (Barnes et al., 2005). The remainder of the oblique plate motion is dispersed across the 150-200 km wide Southern Alps and Canterbury region between various NE trending oblique-dextral fault splays of the Alpine Fault and the fold and thrust belt of North Canterbury (Pettinga and Armstrong, 1998).

2.3 Regional Tectonics of North Canterbury

2.3.1 Previous Studies on the Deformation Styles of North Canterbury

The complexity of accommodating the transition from oblique convergence to strike-slip faulting has created a widening zone of active deformation including the major strike-slip transfer faults of the Marlborough Fault Zone. Within this broad zone of strain partitioning are distinct domains of deformation. The Marlborough Fault Zone (MFZ) comprises five major and active dextral strike-slip faults dipping 60°ΔNW to vertical (Wairau, Awatere, Clarence, Kekerengu and Hope Faults). A marked change in trend of the faults from ~070°

in the south to ~055° farther north defines the boundary between the southern and northern Marlborough domains (Lamb, 1988), and the crust in these domains partly rests on the seismically active subducted slab.

In the North Canterbury region the southward transition from oblique subduction to oblique continental collision is reflected in the landforms as they respond to tectonic shortening, crustal thickening and uplift (Nicol et al., 1994; Nicol and Van Dissen, 2002; Litchfield et al., 2003). These landforms also suggest the zone of deformation has progressively widened in this region and has continued to propagate to the southeast during the Late Quaternary (Nicol, 1992). Although the zone of deformation widens the deformation rate decreases to the southeast.

The upper crust in the plate boundary transfer zone appears to consist of two distinct kinematic layers: 1) an upper-most crustal zone made up of mainly discontinuous faults, where fault slip vectors are variable but are generally not parallel to the plate motion. These faults are controlled both volumetrically and spatially by adjacent blocks of deformation and 2) a deeper zone of crustal deformation, reflected only at the surface by major structures like the Alpine and Hope faults, with slip vectors roughly parallel to plate motions (Pettinga and Wise, 1994). The trends of upper crust faults are easily seen in field fault mapping as well as in a lineament analysis completed in study on the area of North Canterbury immediately south of the Hope Fault.

The upper crust in the Hawkswood Range region is dominated by imbricate thrust fault systems that generally dip to the northwest from Conway Flat coast to the south-southeast. The topography and geomorphology of the north Canterbury region reflect the active deformation of the upper crust which accommodated ~12-15% NW-SE shortening during

the Pleistocene (Nicol et al., 1995). Examination of the Late Cretaceous–Pliocene sequence, which overlies basement, together with extrapolation of the present rates of fault displacement and uplift, suggests that the present period of deformation may have commenced during the late Pliocene or early Pleistocene (Nicol, 1991; Nicol et al., 1994). Studies within the North Canterbury Fold and Fault Belt bring to light the complexities in a plate boundary transition zone. The Hawkswood Range is situated within the North Canterbury Fault and Fold Belt (NCFFB) but is unique in its setting. In order to better understand the Hawkswood Range's place in this tectonic setting we need to briefly summarize a few studies that have been undertaken to the north, south and offshore as well as adjacent to the study area.

Structural Domains Adjacent to the Hawkswood Range

The upper crustal deformation of the oblique plate boundary convergence in North Canterbury is accommodated by the north and northeast trending folds and thrust faults presented by previous researchers as well as in this thesis (Fig 2.2). Below is a summary of the grouped styles of deformation in North Canterbury initially created to categorize the area of possible seismic hazards by Pettinga et al. (2001), but also of importance to the Conway coast region. Only domains 1, 2, 4 and 5 will be presented.

Domain 1-Marlbourough Fault Zone

Domain 1 includes the larger NE trending strike-slip faults of the NE South Island including the Awatere, Hope, Clarence and Wairau faults (Fig. 2.3) (Pettinga et al., 2001). These faults tend to splay at their SW and NE ends into several oblique reverse/thrust faults. The thrust faults adjacent to the Hope Fault mainly dip west and accommodate the

relative plate motion associated with the oblique subduction of the Pacific Plate (Pettinga et al., 2001).

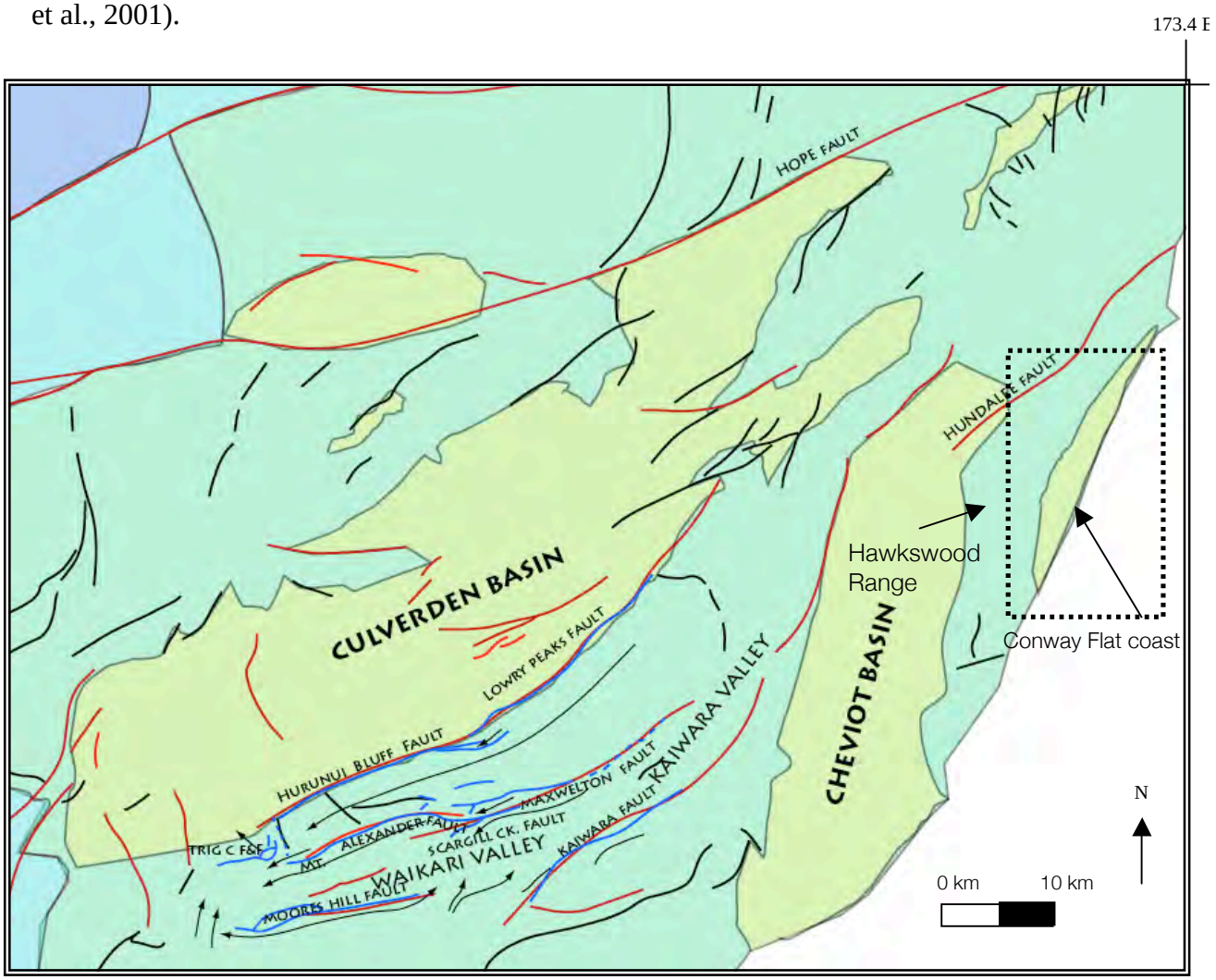

Figure 2.2. Structural map of the North Canterbury region with known faults and geologic contacts identified Note the Field area inside the hashed box.. Faults identified in Blue are from Litchfield et al. (2003). Faults identified on this map and in Red are “active” faults mapped by GNS Science. Note the absence of mapped faults east of Cheviot Basin. This study adds considerable detail to the eastern coastal region of this map.

The MFZ is the most active fault zone in the Canterbury region (Pettinga et al., 2001). Current slip rates across Domain 1 suggest a southward temporal migration of deformation along the strike-slip faults during the Quaternary. Although the Hope Fault absorbs the greatest amount of slip of any of the single faults, approximately 40 mm/yr, the summation of slip across the entire Domain is ~30-54 mm/yr (Pettinga et al, 2001). This equals a wide

zone of deformation form in response to the plate boundary transfer across the South Island.

Domain 2-West Culverden Fault Zone

The West Culverden Fault Zone comprises west dipping thrust/reverse faults and their associated fault propagated folds mapped west of Culverden Basin (Fig. 2.3). This fault system is interpreted to be a series of back-thrusts off the east dipping Alpine Fault zone and is inferred to extend to mid and lower crustal depths below the Southern Alps (Pettinga et al., 2001). The Harper and Esk faults are the major NE trending faults of this Domain and represent a period of earlier range front faulting during the Early Pleistocene during a time where the plate boundary was narrower. These faults have been active into the Holocene (GNS Science, 2009)

Domain 4 and 5- North Canterbury Fold and Thrust belt

This Domain (Fig. 2.3) includes the coastal hills southwest of Kaikoura and offshore across the continental shelf and slope. NE trending thrust faults are associated with fault-propagated folds that are forming in response to the oblique plate convergence (Pettinga et al., 2001). The faults and folds are typically asymmetric and involve basement Torlesse Supergroup and Tertiary and Quaternary cover rocks. Thrust faults from this domain extend to within 5 km of the Hope Fault with a suggestion that the Hope Fault is the southern limit of strike-slip dominated motion (Pettinga et al., 2001).

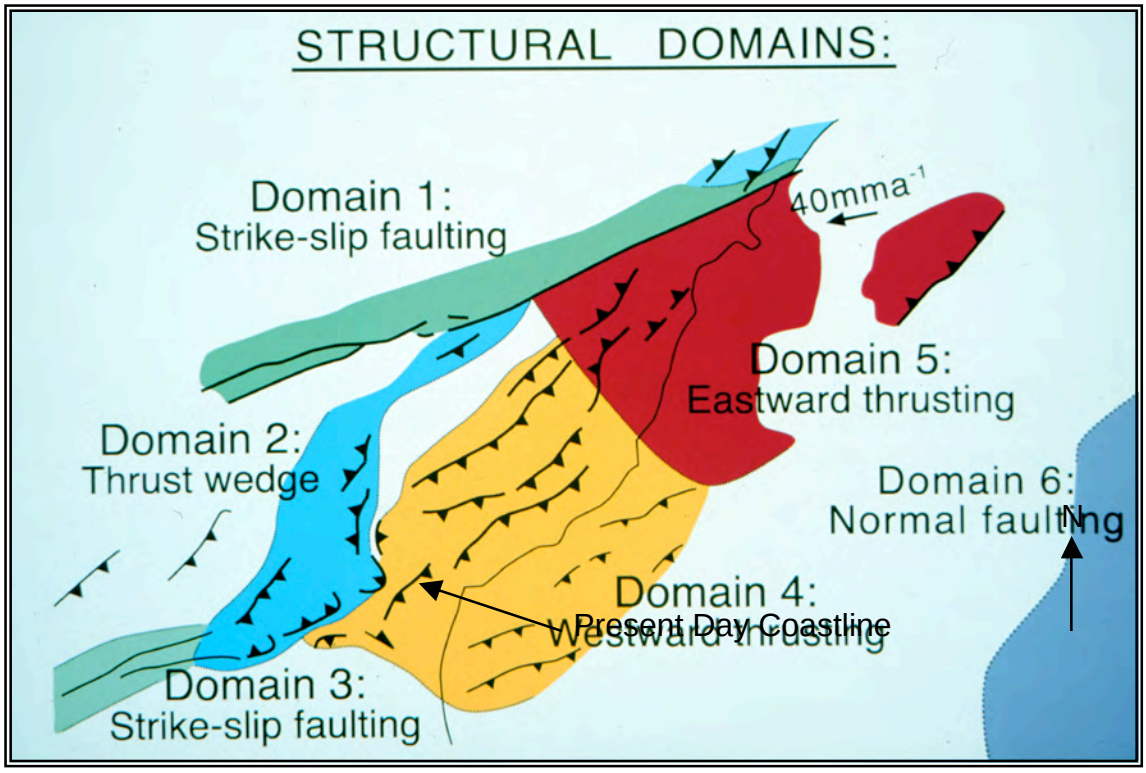

Figure 2.3. A map of structural domains for the North Canterbury region from Pettinga et al. (2001). The Hawkswood Thrust Fault Zone lies within Domain 5: Eastward thrusting. The 40 mma^{-1} indicates relative plate motion movement.

A recent study to the southeast by Litchfield et al. (2003) used geomorphic analysis and structural mapping to highlight the structural setting of a region located on the border of the North Canterbury Fold and Fault belt and the West Culverden Fault Zone, a fault zone characterized by a west dipping system of thrust faults and associated fault-propagated folds in the southwestern edge of the MFZ. Here several ENE trending reverse faults overlap with associated folding, which produced uplifted ranges cored by Torlesse Supergroup basement. Many of the faults in this system dip to the south.

The integration of conventional field mapping techniques combined with geomorphic analysis by Litchfield et al. (2003) indicated the locations and displacements of the faults. This study concluded that the Tertiary rocks remained undeformed until the late Pliocene-Pleistocene. The switch from deposition of the marine Greta Formation to the fluvial Kowai Formation marks this initiation of deformation. This change in sedimentation is also

the mark of regional uplift. The timing and nature of the structures to the south of the Hawkswood Range suggests that the deformation is entirely contractional and commenced ~1-2 Ma.

Probably one of the most influential studies of the North Canterbury Fault and Fold Belt (NCFFB) is that of Nicol et al. (1995). This study recognized that there exists a series of basins forming between two oppositely dipping thrust faults. Using a combination of outcrop and seismic data, Nicol et al. (1995) highlighted the existence of basins forming between NE-SW trending asymmetric folds. The Culverden Basin is the largest of these basins (Fig 2.2). These basins are infilled with Tertiary snd Cretaceous sediments as well as Quaternary aggradational gravels of fluvial and alluvial origin. Drill hole data used in this study shows that despite a fold amplitude of 0.7-1 km, these cover sequences remain thin.

Among the conclusions drawn by Nicol et al. (1995) are: 1) the formation of the basins are strongly driven by the underlying structures, 2) typically the basin filling sediments are not derived from the local anticline (mountains), 3) the North Canterbury folds account for 12-15% accommodation of the shortening during the Pleistocene.

Offshore Structures (Domain 4)

Offshore deformation to the south east of the Conway coastline region is included in Pettinga et al. (2001) Domain 4. The contractional deformation of North Canterbury extends up to 20 km offshore with 11 major folds between Pegasus Bay and Kaikoura with structure and topography trends similar to those on land, but with typically smaller basins. The folds are asymmetric and verge to the northwest. Barnes (1993 and 1996) integrated high resolution seismic reflection profiles of the Quaternary sequences offshore in an

attempt to identify any possible seismic hazards related to the thrust propagated folds to Christchurch and other coastal communities. The dominant structural grain is NE-SW similar to onshore structures. The trends range from 060°-070° near Pegasus Bay, to 015° at the Conway Trough (Fig. 2.1). Walters et al. (2006) identified a 22 km long, northeast-dipping reverse fault beneath the Conway Ridge, lying in 200–700 m water depth with an apparent slip rate of 1mm/year or greater.

The Pegasus Bay fault (Fig. 2.1) is the southernmost structure, and is a NE trending reverse fault. The larger asymmetric anticlines are paired with parallel asymmetric synclines similar to onshore examples like the anticlines bounding the Cheviot Basin. Seismic and sedimentologic data collected suggest the initiation of the deformation commenced at 0.65-0.80 Ma. Early Cenozoic deformation offshore near Pegasus Canyon is dominantly reactivated WNW-ESE overlapping normal faults within the Torlesse basement terrane (Barnes, 1994).

The continental strike-slip Marlborough fault zone continues offshore beneath the northeastern South Island continental shelf. A major submarine structural high referred to as the Outer Shelf fault zone and includes the Hope fault. The geometry of the faults and folds, the kinematic interactions between the faults, and sparse earthquake focal mechanisms are indicative of right-lateral motion and are seen both on land and offshore (Barnes et al., 1998).

2.4 HAWKSWOOD RANGE

The Parnassus area is part of the active convergent plate margin at the onshore extension of the Hikurangi trench. Pliocene and later movement on the subparallel Hundalee and Kaiwara Faults has resulted in the development of a small but well-delineated transform

basin where displacement has been transferred between these faults; both faults remain active. The Hundalee fault, is a high-angle fault, and is the major structural feature of the Conway Flat coast field area. Lewis and Barnes (1996) traced the Hundalee fault offshore to the head of the Kaikoura Canyon.

The Hawkswood Range is a NNE-trending thrust-bounded anticline that is ~ 120 km^2 and extends from the south at the Waiau River northwards to the Conway River. The range is up to ~8 km wide and is ~15 km long reaching an elevation of 650 m (Warren, 1995). The eastern limb of the fold is the steepest and is an area of deposition that is discussed in detail in a later chapter. The Hawkswood Range is a curvilinear anticline, located between the Conway and Waiau Rivers, which is interpreted as a fault propagation fold (Hall, 2004) that is kinematically linked to the Hawkswood Thrust Fault Zone (HTFZ) and broader Marlborough Fault Zone (MFZ). The Hawkswood Range is bounded by the Hundalee fault in the north, dominantly right lateral strike-slip fault, and the HTFZ (Fig. 2.6). The HTFZ is a complex thrust fault system. The dominant thrust faults of the Hawkswood Range trend NE and dip northwest.

2.5 New Structural Data

2.5.1 Lineament Analysis

The first order in understanding the deformation style along the Conway Flat coast is to understand the broad deformation patterns of the region. Presented are the results of the analysis that, when combined with previous research, gives a clear picture as to the structural framework of North Canterbury. Since the Hawkswood Range is located south of the Hope Fault the analysis focuses on the area south of that structural boundary.

Analysis of lineaments

Method

Regional lineaments were identified from Digital Elevation Models (DEM) produced by Landcare Research New Zealand Ltd (only lineaments along the Conway Flat coast field area have been ground-truthed, data from outside the field area is interpretation from DEM's and aerial photos). The DEM was produced from the Land Information New Zealand 1:50,000-scale topographic database, with a grid separation of 25 m, and a vertical precision of 1 m (Fig 2.4). The interpretation process was divided into two parts. A first trial lineament analysis was completed using mylar overlays. The interpretations were completed with the lighting directions of the DEM varied in SURFER© at four different azimuths (45°, 135°, 225°, 315°). The source was always kept at 45° to the horizontal. The hardcopies of traced lineaments were then scanned and imported into ARCmap©. Lineaments were rectified and geo-referenced using control points from 1: 50 000 topographic maps. Once rectified and geo-referenced the lineaments were digitized on screen in GIS. Lineaments from the DEM images were re-mapped again three months later in trial 2 after the completion of the first set, following the same procedure to test for reproducibility.

Results

The mapped lineaments once completed were compared to regional studies of the broader regional structural trends. The lineaments in the Conway Flat coast region fall within Domain 4 and 5 of Pettinga et al. (2001). Field mapping and aerial photos were used to confirm the "reality" of the lineaments mapped on DEM's.

Multiple Trial Reproducibility

In order to establish consistency in the lineament data collected, two lineament trials were conducted. The two data sets were rectified and geo-referenced and then overlain on one

another in MapINFO©. The lineaments from the first trial were highlighted in one colour and only reproducible lineaments from the second trial were retained. All irreproducible lineaments from the trials were eliminated from the data set. In selecting reproducible lineaments the procedures followed that of Wise and McCrory (1982), Wheeler and Wise (1983) and Rahimin and Pettinga (2006). All lineaments within a 10° azimuth range and between 1-2 mm at map scale from each were deemed reproducible. The data collected from reproducible lineaments is presented in Appendix A.

Lineament data extraction and data plots

The GeoMapVector program (http://www.earthsciences.uq.edu.au/~rodh/software/index.html) was used to determine azimuth parameters for all lineaments. The program generated a file that contained the trend of each lineament measured clockwise from the north and its length. The azimuth values were read to the nearest integer and the lengths of lineaments were read to the nearest metre. This technique did not allow for recording curvilinear features and as such, curvilinear lineaments with significant azimuthal deviations were digitised as segments with the minimum number of components possible, in order to preserve the original orientation of the lineament.

All data are presented as linear histograms of azimuth frequency, which were generated after double smoothing by applying a 11-degree moving-average window on every azimuth (Fig. 2.5). The two graphs presented represent the data collected from two simulated lighting directions. The counting window width was chosen to be an odd number to avoid skewing the data. The value on the Y-scale is the data concentration factor (DCF)

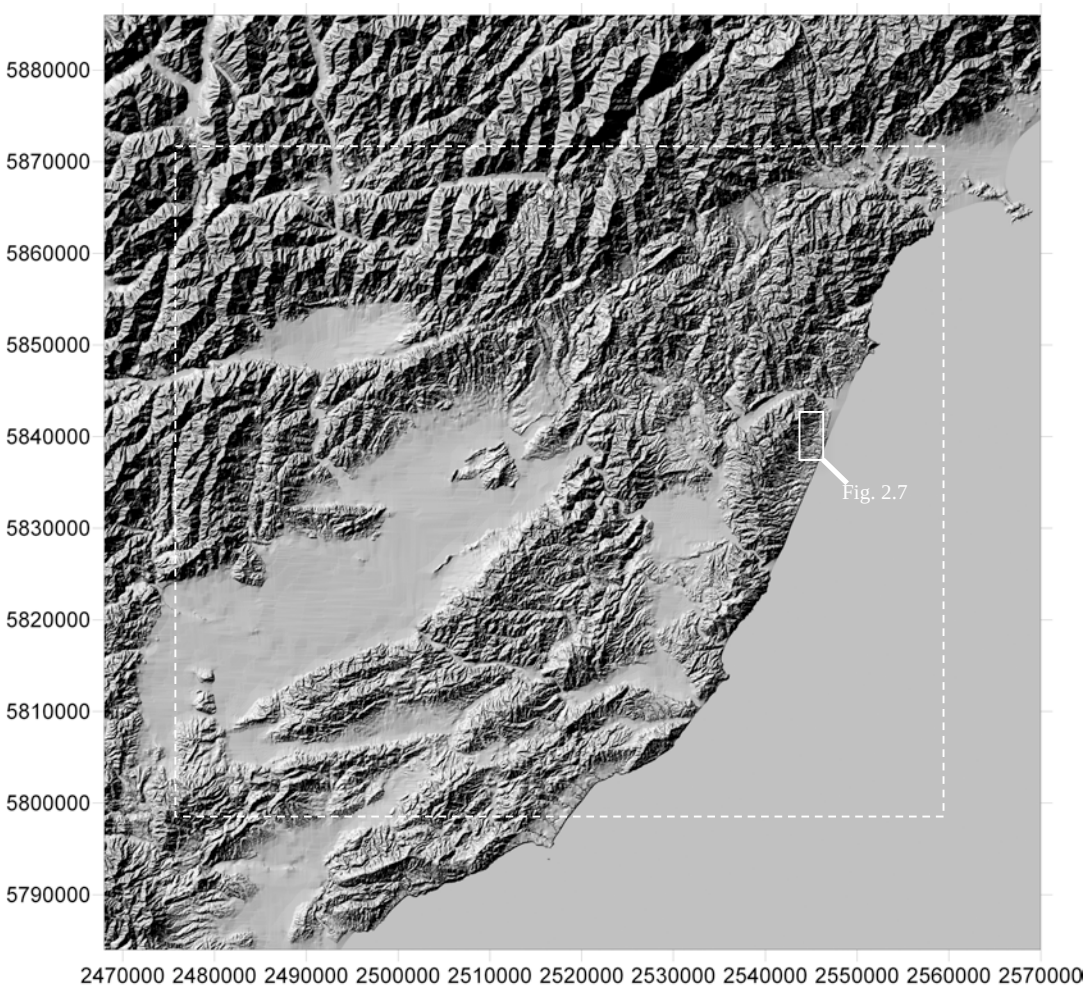

Figure 2.4. A) 1: 50 000 DEM used to map lineaments. Lineaments recorded from maps are recorded by length and azimuth in Appendix A. The mapped area is outlined in the dashed box. B) Reproducible traced lineaments from the Northeast illumination. C) Reproducible lineaments from the Northwest illumination.

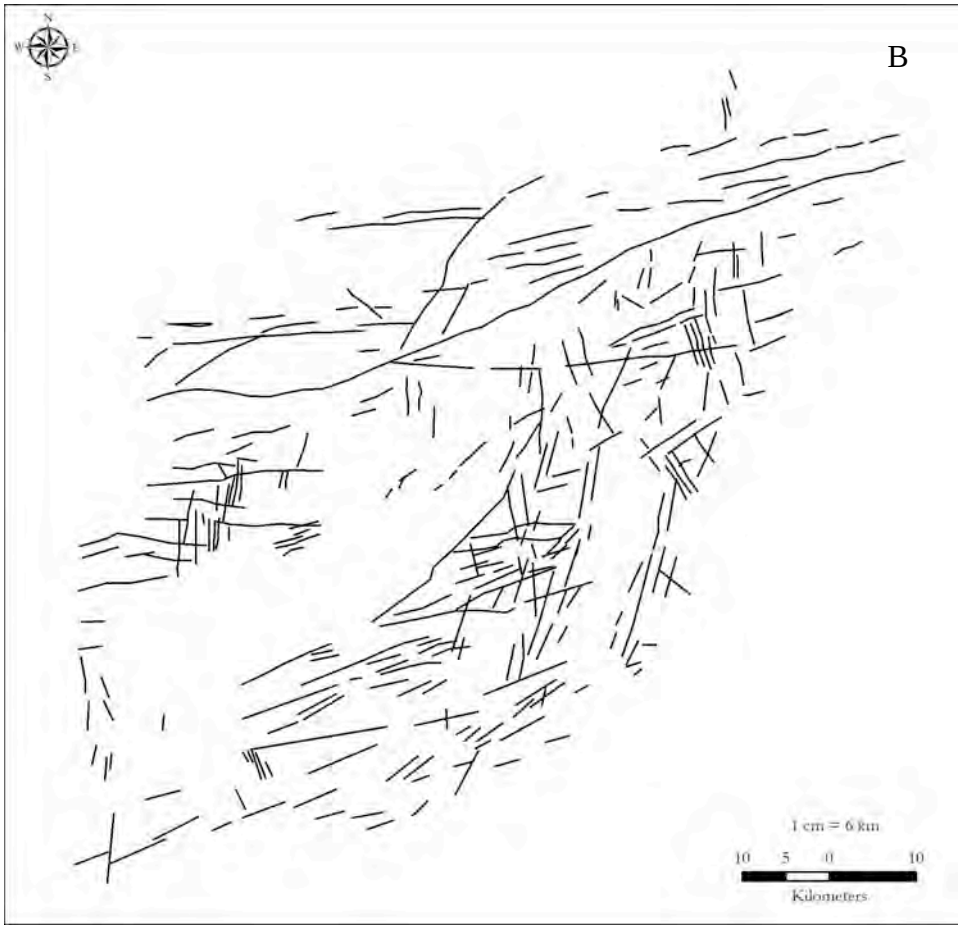
B
1 cm = 6 km
10 5 0 10
Kilometers

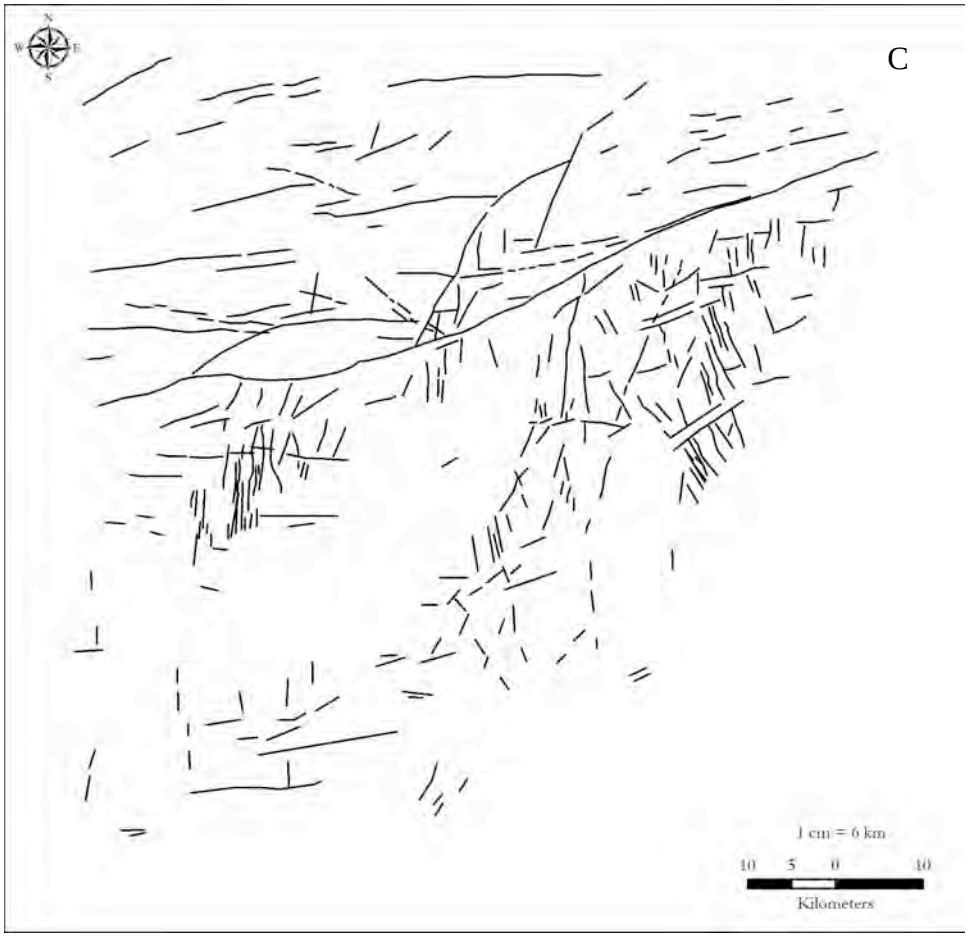
C
1 cm = 6 km
10 5 0 10
Kilometers

from Wise and McCrory (1982), which simply represents the number of times the data are concentrated beyond what is expected from an absolutely uniform data distribution. The graphs are drawn such that one unit of the concentration factor along the vertical scale is always equal in length to 10 degrees of azimuth on the horizontal scale. The above procedures eliminate the vertical scale problem and binning problem in statistical plots, highlighted in “Rule 13” and “Rule 14” of Wise and McCrory (1982).

Summary

The pattern of deformation in North Canterbury that emerges from the mapping of lineaments in this study is clear. The dominant structural features of the northeast South Island are the oblique right-lateral strike slip faults, i.e. the Alpine and Hope Faults (Pettinga et al., 2001). The northeast trend of these structures is the dominant structural grain of the region. This upper crustal mesh of faults functions as a broad zone of deformation in which faults that lie in the optimum stress orientation accommodate deformation under the present-day stress regime of the modern plate boundary.

The NE trend is associated with the pervasive pattern of high-angle, dextral faulting which imparts an excellent control on the geomorphic expression of ridges and basins in the MFZ (Litchfield et al., 2003). This NE trend is parallel with the Hope Fault and the large number of NNW trending faults does not seem to be recorded in the literature. The NE trending lineaments are typically > 10 km long where as NW trending lineaments are typically ~ 5 km long. The lineament analysis indicates a denser cluster of lineaments in the southeast section of the mapping area near the Culverden Basin. Deformation patterns are denser with proximity to known, larger, fault traces.

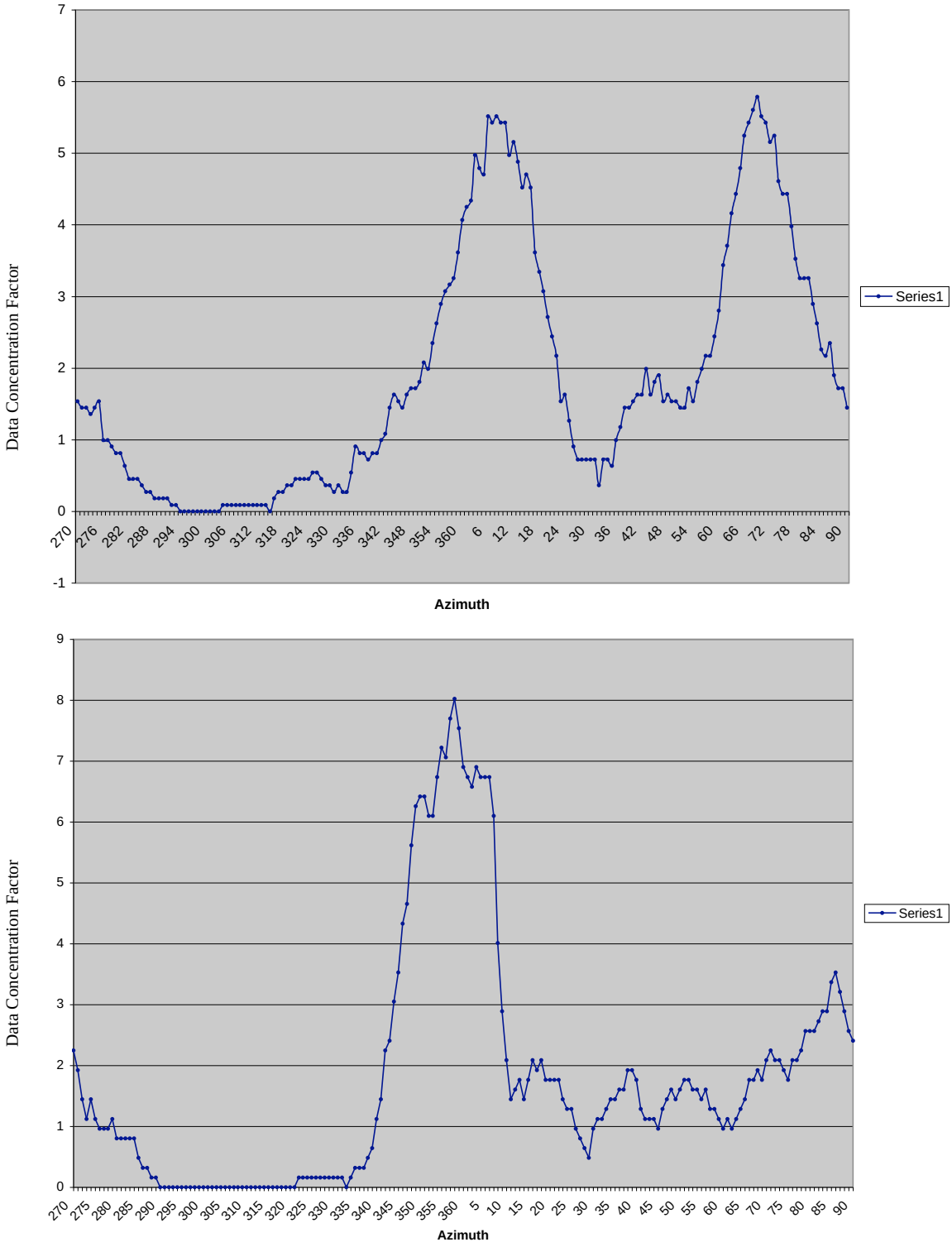

Figure 2.5. Linear histograms of azimuth frequency with 11°degree moving-average window on every azimuth. These histograms show the preferred orientation of faults in the region. The data represented here was collected from a lineament project completed on shaded relief maps for this study.

The results of the lineament analysis were consistent with the literature. The NNE trending lineaments parallel structures onshore and offshore.

2.6 GROUND-LEVEL DATA

In order to complete the foundation for a structural framework of the area ground-level data was collected through geomorphic and structural mapping. The information presented here was ground-truthed in this study, all data collected from outside the designated field area is interpretation from DEM's and aerial photos. The results of the two projects are provided below:

2.6.1 Geomorphic Mapping

The east side of the Hawkswood Range comprises several geomorphic features including a number of curvilinear scarps cut into alluvial/fluvial terraces. Here within these features is the key to deciphering the tectonic history of the Hawkswood Range (Fig. 2.7).

The Conway Flat coast is characterized by the presence of low-gradient, generally east sloping depositional alluvial-fluvial surfaces that tilt towards the coast. The proximal area of the alluvial fans is undulatory while the distal regions of the fan are quite flat. Paleo-channels can be seen on top of these surfaces suggesting that they were once active. The present drainage network flows west to east in valleys that are deeply incised into these once aggradational surfaces. The current discharge of these streams suggests that the

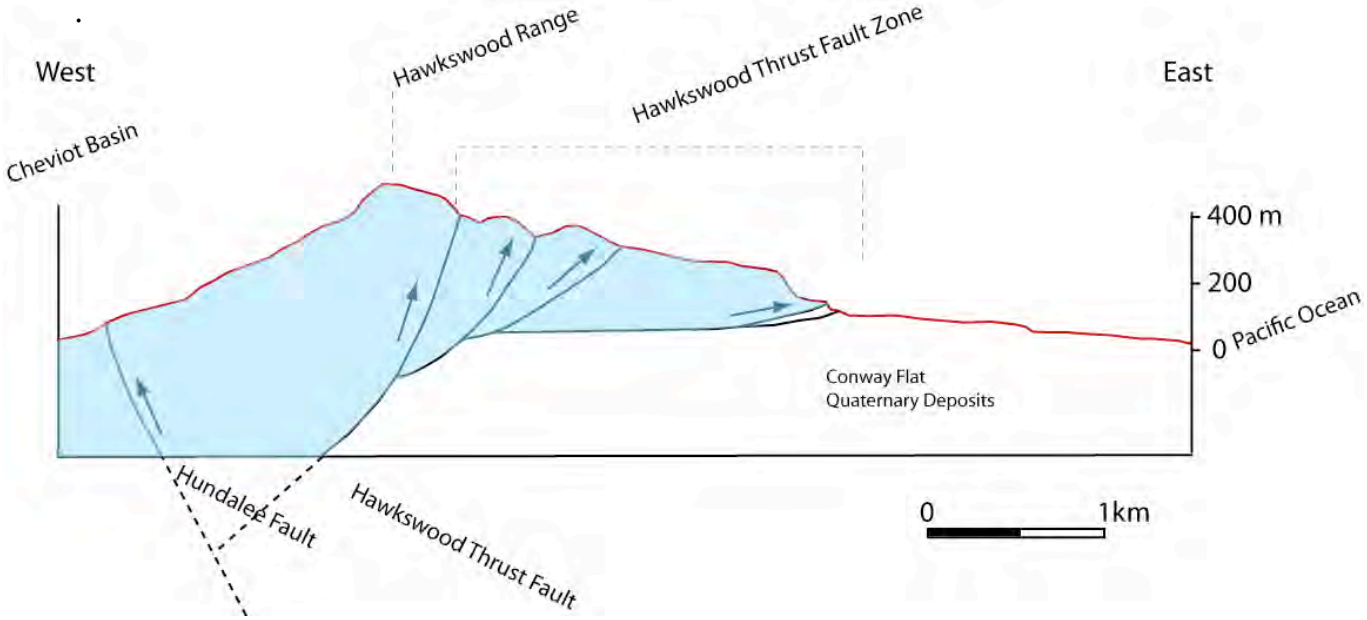

Figure 2.6. Interpretive cross section A-A' is through the Hawkswood Thrust Fault Zone (HTFZ). Note the origination of the thrust faults at depth and their eastward propagation. This fundamental structural development of the Hawkswood Range is consistent with studies by Pettinga et al. 2001. in the North Canterbury region.

current discharge rate is less now than in the past. The relic alluvial fans are dissected by major drainages at their terminus where they overlap. At the head of these major drainages exist a series of waterfalls.

The oldest surfaces of the Conway Flat coast region are located near the hinge of the anticline and give way to lower alluvial/fluvial surfaces that at one time prograded to the sea forming Gilbert-type fan deltas (Chapter 3 and 4). These marine deposits form the lower terraces of the Hawkswood Range, but contain many, smaller, inset terraces of fluvial origin. The lowest expansive surface is the Ngaroma terrace.

The geomorphic surfaces need a two-fold approach when looking at them. Although all of the surfaces are directly tied to the active tectonics of the region, they were formed by two different mechanisms. The lower flat surfaces are controlled by the underlying stratigraphy (tripartite geometry of a Gilbert-type delta, Chapter 3 and 4) and were deposited in an asymmetric basin, while the smaller inset terraces are composed of material released during episodic events (Chapter 3). The depositional environments were controlled by the interplay of active tectonics and sea-level change. In contrasting, the upper "terrace" surfaces are features created by the displacement of alluvial fans by the propagating thrust faults of the HTFZ.

The evolution of the fault zone was determined by this study's geomorphic mapping of the Hawkswood Range and comparison of field relationships between underlying structures and sedimentology. Geomorphic mapping was completed on 1: 50 000 aerial photos with mapping transferred to digital format in Adobe Illustrator. Detailed geomorphic mapping of the Conway Flat coast surfaces combined with detailed sedimentological analysis of the underlying material provides the evidence of these contrasting means of creation.

2.6.2 Local Mapping of Faults

The identification of the Conway thrust faults, and eventually the broader Hawkswood Thrust Fault Zone (HTFZ), was initially determined by an outcrop with offset alluvial fan gravels (Figs. 2.7 and 2.8). The offset gravels are located at a change in topography that was mapped along the range front (Fig. 2.7 and 2.9). Associated with this topographic break were other indicators of tectonic activity including: 1) changes in bedrock characteristics, 2) streams that originate from nowhere(?), and 3) waterfalls that form a linear pattern along the range front. In addition, the ramping up of the surface above the

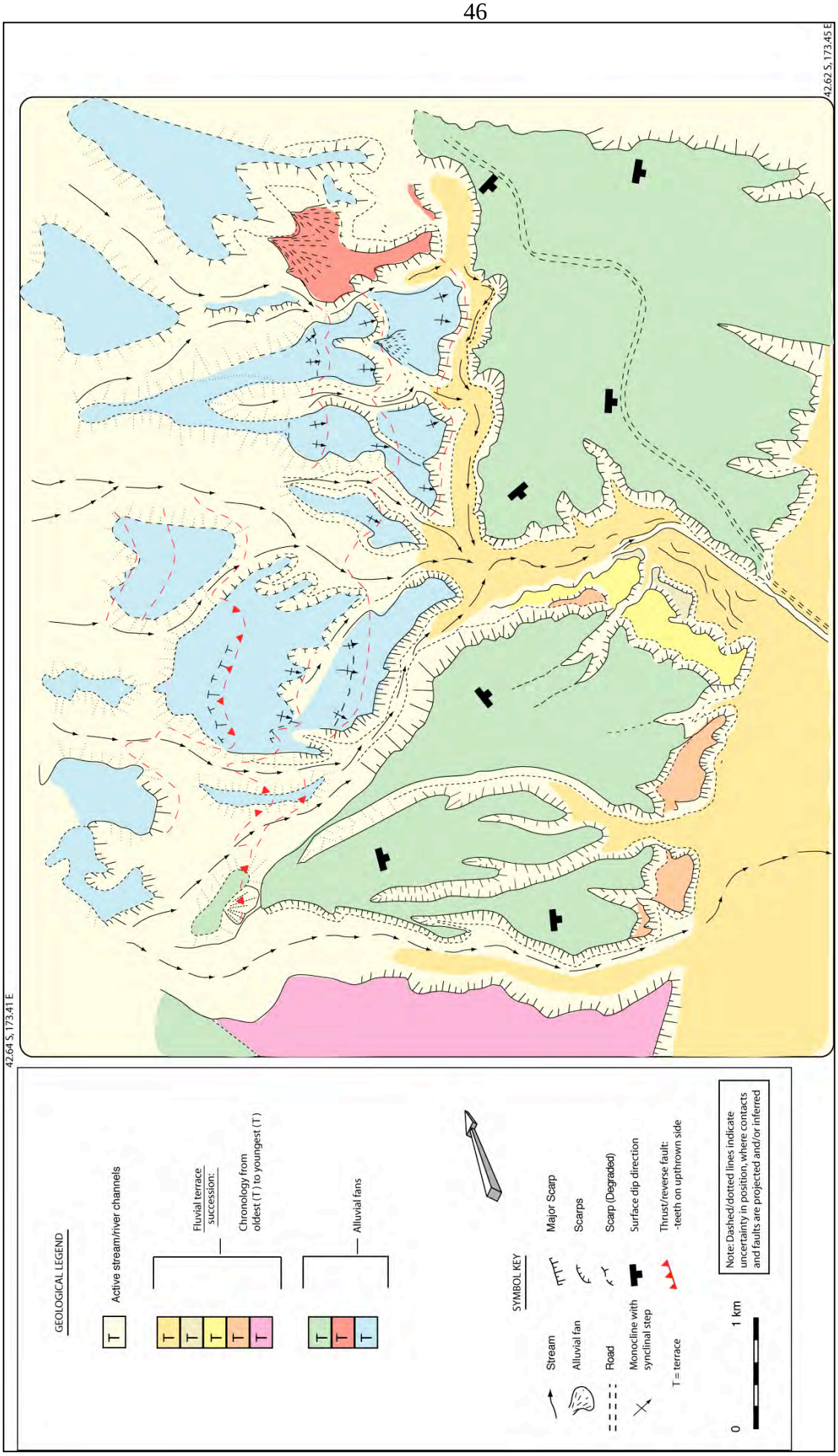

Figure 2.7. Geomorphic map of the Hawkswood Range.

identified fault plane is traceable to the South and North (Fig. 2.7). This ramping up is characteristic of the surface expression of the fault traces along the range. Similar topographic levels exist at several elevations on the east side of the Hawkswood Range. Rocks located below the inferred fault planes are fresh, well indurated and blocky in appearance (Fig. 2.10). Outcrops located above, or within the fault zones, are extremely weathered, highly fractured and friable (Fig. 2.11). These contrasting rock outcrops support fault deformation indicated in Figures 2.7 and 2.12.

Within the fault zone geomorphic expressions of thrust faults provides evidence the faults overlapped in locations. At these multiple locations faults appear to absorb the displacement within the fault zone. Within the Hawkswood Range fault segments join to form longer faults, and in other locations, overlap each other, perhaps connected by a transfer fault (Fig. 2.12). Although limited field exposures prohibit detailed mapping of the fault intersections, rock outcrops and geomorphic expressions of the faults support these interpretations.

The transfer of strain in this actively growing anticline from the eastward propagating N/NE thrust faults to the dominantly NW trending thrust fault is reflected in the structure south of the Medina farm (Fig. 2.12). Mapping in this region via aerial photography, Digital Elevation Models (DEM) and the ground proofing of these maps confirm that a second set of thrust faults override the existing thrust faults north of Medina Creek that continue to the Conway River (Fig. 2.7). This transfer of strain appears to occur at a linear feature located in a gully south of Medina Creek.

East West

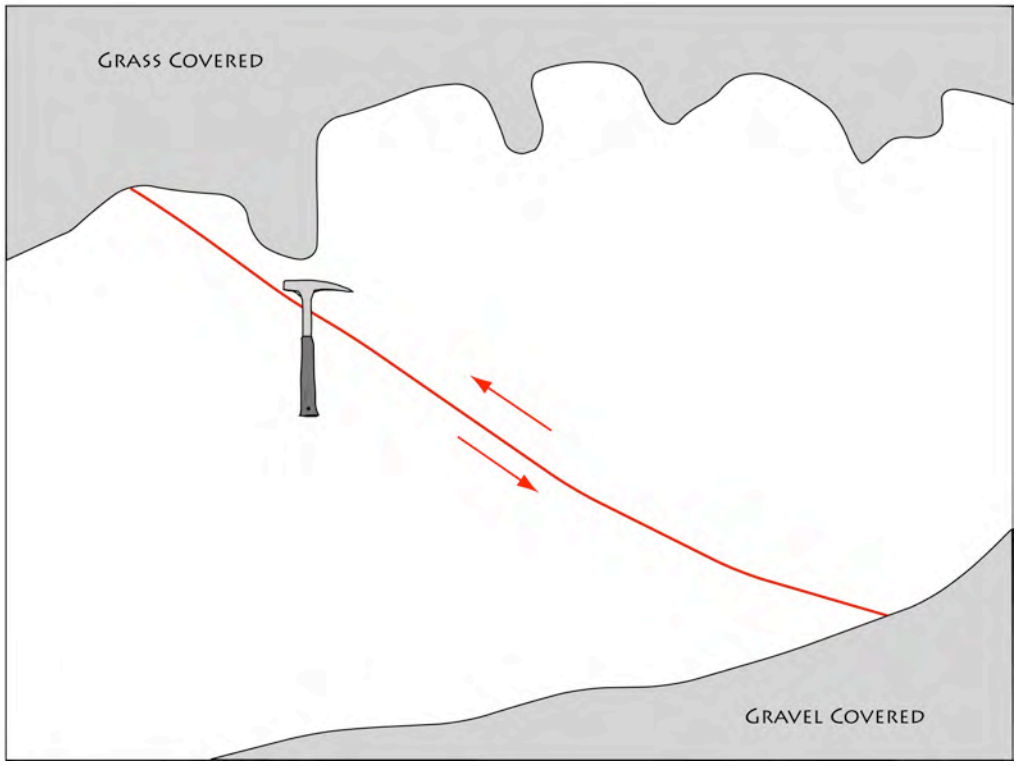

Figure 2.8. Photograph of offset alluvial gravels on the east side of the Hawkswood Range. This thrust fault coincides with geomorphic changes and can be traced through the field area. Geological hammer for scale.

Figure 2.9. Photograph of the Hawkswood Range front looking Northwest. Note the geomorphic changes in the slopes of the range indicated by arrows. The step-ups in geomorphology are caused by multiple events of thrust faulting in the Hawkswood Thrust Fault Zone.

Figure 2.10. Photo of a typical outcrop below a fault zone along Conway Flat coast. Note the fresh, well-indurated appearance of the rock. Note compass for scale (10 cm).

Figure 2.11. Photo of a typical outcrop located above and/or within the fault zone along Conway Flat coast. Note the high degree of fracturing in the rock. Although highly fractured, the rock is still indurated enough to hold together. Note compass for scale (10 cm).

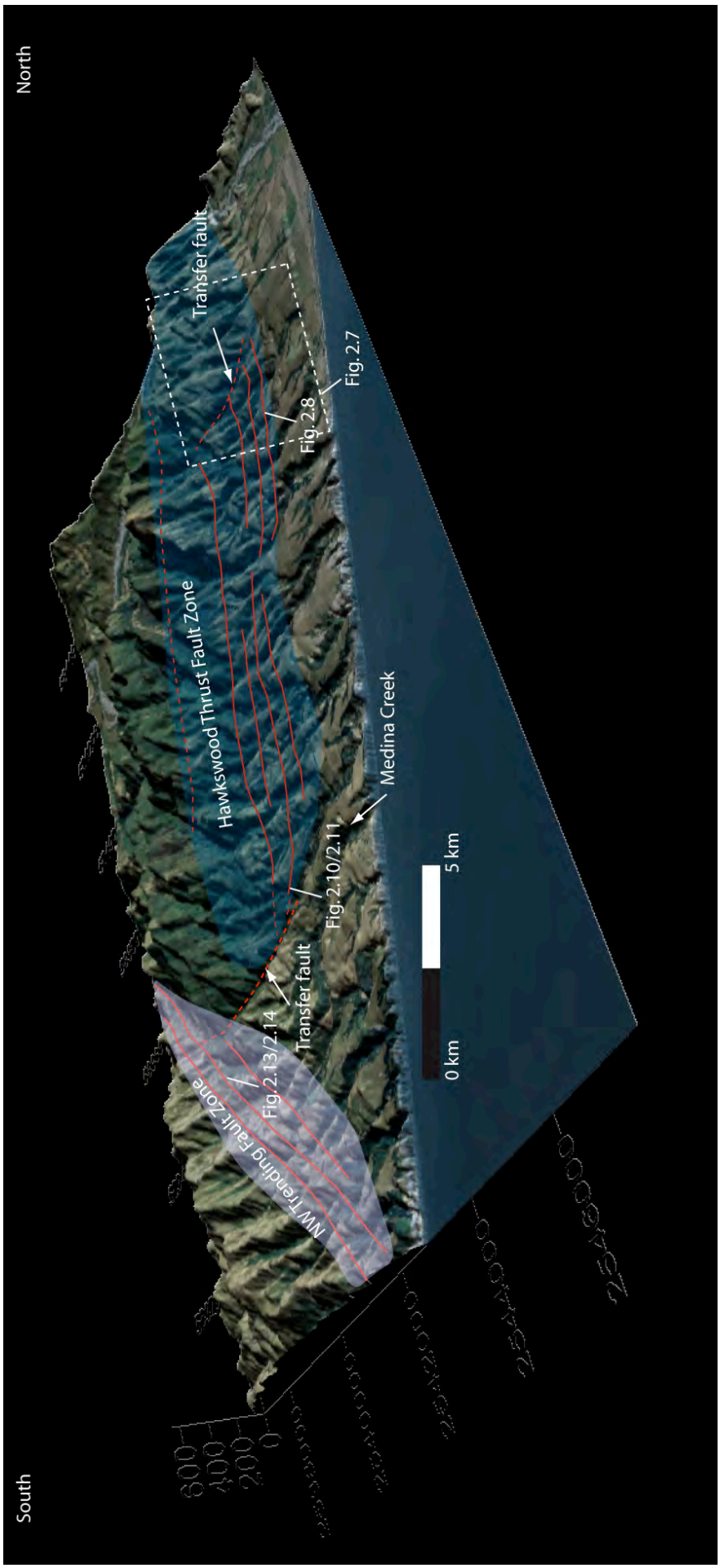

Figure 2.12. Digital elevation model (DEM) of the Hawkswood Range showing the developing HTFZ to the north and south. Note the change in trends of the geomorphic features from north to south. DEM showing the complex interaction of the multiple thrust faults (red) within the HTFZ. Note the change in the structural fabric and possible linkage of the faults.

Figure 2.13. Typical outcrop photo from south of Medina Creek. Note the change in the appearance of the rock outcrop with respect to the rock outcrop north of Medina Creek Fig. 2.10. Compass for scale (10 cm)

Figure 2.14. Typical outcrop photo from within the fault zone south of Medina Creek. This highly fractured rock in these outcrops crumbles upon touch. This rock type is typical in the fault zones south of Medina Creek. Note the change in the trends of ridges with respect to the geomorphic features north of Medina Creek (Fig. 2.13). Compass for scale (10 cm).

Deformation in the rocks (Fig. 2.13 and 2.14) and trends of ridges also support that compressional strain is accommodated on different structures in the south of the field area (Fig. 2.12).

2.7 DISCUSSION

2.7.1 Geomorphic Response to Faulting

There are numerous geological, geomorphic, and landscape features that are sensitive to movement on the faults of the HTFZ. These include: topography, thickness and shape of strata, erosional/depositional characteristics of the drainage network, and the geometry of the erosional and depositional surfaces. Burratto et al. (2003) used the Po Plain in Northern Italy to link geomorphic response to active tectonics. In a similar way, this can be done with the deposits of the Hawkswood Range by using field studies to show how the interaction between surfaces and drainage network are controlled by the geometry and kinematics of the tectonic source.

The diversion of rivers is the single best indicator that a stream is approaching a growing anticline (Holbrook and Schumm, 1999). Figure 2.15 shows the existing Conway River; the geomorphology in the photograph clearly shows the remnant border of the Conway River prior to its deflection. Sedimentological evidence provided in the following chapters also supports the claim that this cliff is representative of an erosive contact created by the deflected river.

The geomorphic response of the alluvial fans to active tectonics is another key in understanding the evolution of the fault system. As the alluvial fan deltas prograded from the Hawkswood Range into the sea, these surfaces were probably the main active fans. The

continued uplifting of the upper alluvial fans added sediment to the system over time. Periods of inactivity in fan delta formation are evident by the formation of small ponds on the surface of the alluvial fans (Fig. 2.16). The propagation of thrust faults lead to multiple displacements of the alluvial fan surfaces creating multiple “terrace” features (Fig. 2.7). This change in the geomorphic surfaces by the fault created small asymmetric folds.

Pettinga and Armstrong (1998) described similar geomorphic relief caused by smaller thrust faults in the Leonard Mound area, east Culverden Basin. At Conway Flat coast these geomorphic features created barriers that forced sediment supplied to the system to begin to stack up behind the hanging wall of the thrust faults. Sediment would continue to build up until the alluvial system would be forced to another outlet, releasing onto the lower alluvial fan surfaces. Alluvial debris flow deposits that cut into the lower alluvial fan surfaces support this interpretation.

Figure 2.15. DEM of the Ngaroma terrace and the geomorphic relief created as the Conway River dissected the terrace as it was deflected around the growing Hawkswood thrust-bounded anticline.

Figure 2.16. Photo of a small pond formed on the surface of an alluvial fan (inside dashed line). The pond was later covered by alluvial material in the upper Hawkswood Range. Note rock hammer for scale.

2.7.2 Interpretation of Structural Evolution

The existence of offset gravels, highly fractured rocks within the interpreted fault zone, and curvilinear geomorphic elevation changes support the presence of multiple fault splays on the east side of the Hawkswood Range. The fault system, based on field observations presented, developed as the original fault propagated to the east as a series of imbricate thrust faults. The loading of material on to an existing fault plane probably controlled/s the eastward propagation of these faults in the HTFZ (Fig. 2.6). This eastward propagation of thrust faults sets the scene for development of interesting non-marine and marine depositional systems that are discussed in detail in the following chapters. These sediments are stored in the basin caught between two oppositely dipping thrust faults (Hundalee fault and Conway Ridge fault).

The initial thrust fault responsible for the formation of the thrust-cored anticline is near the middle of the range on the east side of the divide (Fig. 2.6). This thrust fault splays to the east into several thrust faults that are clearly reflected in the geomorphology of the range.

It is proposed herein that the fault zone joins at depth with the Hundalee Fault and propagates to the east (Barnes, 1994; Nicol et al., 1995, Lewis and Barnes, 1999). Based on structural data published in previous studies (Nicol et al., 1995; Litchfield et al., 2003) it is plausible that the deformation along the Conway Flat coast is occurring along these thrust faults in the upper portion of the deforming Pacific Plate as the northeast of the South Island accommodates the transpressional deformation of the active plate boundary. Likewise field work done by the author supports this interpretation.

Through time, multiple fault strands may link with little departure from the expected displacement; even though multiple faults have connected. As longer continuous faults become active, the nearby adjacent faults enveloped in a “shadow zone” become inactive and eventually die out (Burbank and Anderson, 2001).

It is likely that the change in direction of faulting is a reflection of the compression, preferentially, being accommodated on older pre-existing normal faults that originated in the Cenozoic (Barnes, 1994). The northwest trend of the older normal fault fabric was reactivated as the thrust faults present in the field similar to WNW-ESE trending normal faults offshore in the Pegasus Canyon (Barnes, 1994; Pettinga, *personal communication*). The geometry of the developing fault zone created an asymmetric depositional basin. Similarly, Norris and Cooper (1997) point out that in detail at the surface in the central Southern Alps, oblique slip is partitioned onto ENE trending thrust fault structures that are connected in a zigzag pattern by WNW striking nearly pure strike-slip features and that these faults merge at depth where the slip is oblique.

A similar setting is described for the development of overlapping faults splays in the Miocene Gulf of Suez by Gupta et al., (1998). In this study Gupta et al. (1998) make the connection between fault ray evolution and its control on the stratigraphy of a rift basin. As with most studies, the geometry of the faulting described in the study occurs in an extensional regime unlike the Hawkswood Range.

The initiation of the structure in the Hawkswood Range is probably similar for the timing of events suggested by Nicol et al. (1995). Nicol et al. (1995) found deformation in the North Canterbury region commenced in late Pliocene to early Pleistocene time. The initial Hawkswood thrust fault was probably similar to the thrust faults described by Nicol et al.

(1995) in that it was restricted to the upper deforming Australian Plate as the Pacific Plate obliquely subducted. A series of terrace-like features step down from the Hawkswood Range divide (Fig. 2.17). Within these terrace features are offset gravels, abandoned streams and a linear system of waterfalls.

2.8 SUMMARY

The Hawkswood Thrust Fault Zone (HTFZ) is a complicated fault zone that provides new evidence of the plate boundary evolution and structural development in North Canterbury. It is clear that the HTFZ is located south of the dominant right-lateral oblique faults, such as the Hope Fault of the Marlborough Fault Zone (MFZ), and north of the thrust fault dominated study of Litchfield et al. (2003) in the Waikari Valley. The kinematics of the westward-verging Hundalee Fault has long been questioned and although there is little specific data on the Hundalee Fault provided in this thesis, there are some inferences that can be made.

The plunging nature of the Hawkswood anticline and propagating nature of the HTFZ faults provide information that when combined with the stratigraphy of the Conway Flat coast and regional structural information of the area allow for a general fault model to be proposed. A broad overview of the Conway Flat coast region shows the converging of a complex thrust fault zone, the HTFZ, to the northeast with the oblique strike-slip Hundalee Fault. The interaction of these structures within the modern transpressional plate boundary created the plunging Hawkswood anticline. Data collected from the Hawkswood Range, including rock deformation patterns, terrace mapping and existence of multiple fan deltas, suggest that the thrust faults of the HTFZ probably originate from the Hundalee Fault at depth as part of the upper deforming Pacific Plate (Pettinga and Wise, 1994) (Figs. 2.6 and 2.17). The fault patterns and geometric relationships between the faults along the Conway

Flat coast and the Hundalee fault support this deformation pattern. The separation of the continental and oceanic rocks of the Pacific Plate allow for the transfer of oblique compressional stress through the oblique strike-slip faults of the Marlborough Fault Zone in the northeast South Island southwards to the Conway Flat coast region (Nicol and Wise, 1992).

Based on the orientation of the northwest dipping thrust faults within the field area it is concluded that the Hundalee Fault is probably a steeply NW verging right-lateral oblique fault with a large component of reverse slip. This seems plausible when you look at the regional structural patterns of Nicol et al. (1995) and Pettinga et al. (2001). The continued accommodation of oblique compression by the northeast trending strike-slip faults eventually gives way to a dominantly thrust fault system of the HTFZ. The connection of the HTFZ to the Hundalee Fault is interesting in the fact that if this is true, the Conway Flat coast area is in fact a structural boundary between right-lateral oblique faulting and thrust faulting, a conclusion that helps provide a better constraint on the structural framework of North Canterbury.

These data set the framework for the Conway Flat coast structural setting and when combined with the following chapters on terrace development, facies architecture and sedimentary process helps to decipher the overall development of the Conway Flat coast region.

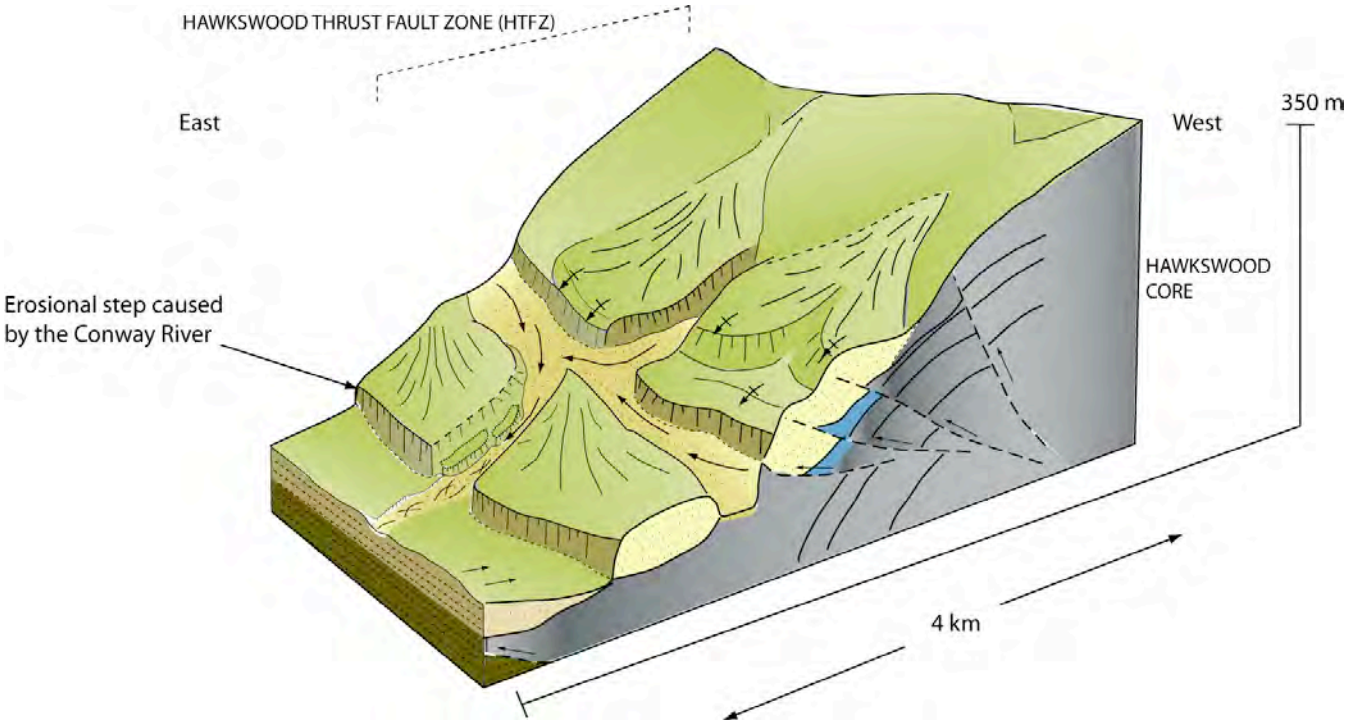

Figure 2.17. A. Block diagram showing the interpretation of the basic structural framework for the Hawkswood Range. Note the geomorphic expression of the thrust faults in the Hawkswood Thrust Fault Zone. B. Photograph of the typical geomorphic expression of the thrust faults. This is similar to the thrust fault splays described by Pettinga and Armstrong (1998) in the Leonard Mound area, east Culverden Basin.

2. 9 REFERENCES

Barnes, P.M., 1993. Structural style and sedimentation at the southern termination of the Hikuarnagi subduction zone, offshore North Canterbury, New Zealand. Unpublished Ph.D. thesis, University of Canterbury Library, Christchurch, New Zealand.

Barnes, P.M., 1994. Inherited structural control from repeated Cretaceous to Recent extension in the North Mernoo Fault Zone, western Chatham Rise, New Zealand. Tectonophysics 237, 27-46.

Barnes, P.M., 1996. Active folding of Pleistocene unconformities on the edge of the Australian–Pacific plate boundary zone, offshore North Canterbury, New Zealand. Tectonics 15, 623–640.

Barnes, P.M., Mercier de Lapinay, B., Collott, J.E., Delteil, J., Audru, J-C., 1998. Strain partitioning in the transition area between subduction and continental collision, Hikurangi margin, New Zealand. Tectonics 17, 534-557.

Barnes, P. M., Sutherland, R. Deteil, J., 2005. Strike-slip structure and sedimentary basins of the southern Alpine Fault, Fiordland, New Zealand, Geological Society of America Bulletin 117, 411-435.

Burbank, D.W., Anderson, R.S., 2001. Tectonic geomorphology. Blackwell Science, United Kingdom, 278 p.

Burrato, P., Ciucci, F., Valensise, G., 2003. An inventory of river anomalies in the Po Plain, Northern Italy: evidence for active blind thrust faulting. Annals of Geophysics, vol. 46 no, 5, 865-882.

Delteil, J., Collot, J-Y., Woody, R., Calmant, S. Christoffel, D., Coffin, M., Ferriere, J., Lamarche, G., Lebrun, J-F., Mauffret, A., Pontoise, B., Popoff, M., Ruellan, E., Sosson, M., Sutherland, R., 1996. From strike-slip faulting to oblique subduction: a survey of the Alpine-Puysegur Trench transition, New Zealand, Results of Cruise Geodynz-Sud Leg 2. Marine Geophysical Researches 18, 383-399.

Gamble, J. A., and Wright, I. C., 1995. The Southern Havre Trough: geological structure and magma petrogenesis of an active backarc rift complex. *Backarc Basins: Tectonics and magmatism*. ed B. Taylor. Plenum Press. New York, 29-62.

GNS Science, 2009. Active faults database of New Zealand. Retrieved from http://data.gns.cri.nz/af/

Gupta, S., Cowie, P. A., Dawers, N.H., Underhill, J.R., 1998. A mechanism to explain rift-basin subsidence and stratigraphic patterns through fault-array evolution. Geology 26, 595–598.

Hall, L., 2004. Cenozoic deformation at the southern end of the Hikurangi margin, New Zealand, unpublished Ph.D. Thesis, University of Oxford, England.

Holbrook, J. M., Schumm, S. A., 1999., Geomorphic and sedimentary response of rivers to tectonic deformation: a brief review and critique of a tool for recognizing subtle epeirogenic deformation in modern and ancient settings. Tectonophysics 305, 287–306.

Kleffman, S., Davey, F., Melhuish, A., Okaya, D., Stern, T., 1998. Crustal structure in the central South Island, New Zealand, from the Lake Pukaki seismic experiment. New Zealand Journal of Geology and Geophysics 41, 39-49.

Lamb, S., 1988. Tectonic rotations about vertical axes during the last 4 Ma in part of the New Zealand plate-boundary zone, Journal of Structural Geology, 10, 875 – 893.

Lewis, K.B., Barnes, K.B., 1999. Kaikoura Canyon, New Zealand: active conduit from near-shore sediment zones to trench-axis channel. Marine Geology, 162, 39-69.

Litchfield, N. J., Campbell, J.K., Nicol, A., 2003. Recognition of active reverse faults and folds in North Canterbury, New Zealand, using structural mapping and geomorphic analysis. New Zealand Journal of Geology and Geophysics 46, 563–579.

Little, T. A., Holcombe, R. J., Ilg, B. R., 2002. Kinematics of oblique collision and ramping inferred from microstructures and strain in middle crustal rocks, central Southern Alps, New Zealand, Journal of Structural Geology 24, 219-293.

Nicol, A., 1991. Structural styles and kinematics of deformation on the edge of the New Zealand plate boundary zone, mid-Waipara region, North Canterbury. Unpublished Ph.D. thesis, University of Canterbury Library.

Nicol, A., 1992. Tectonic structures developed in Oligocene limestones; implications for New Zealand plate boundary deformation in North Canterbury, New Zealand Journal of Geology and Geophysics 35, 353-362.

Nicol, A., Wise, D.U., 1992. Paleostress Adjacent to the Alpine Fault of New Zealand: Fault, Vein, and Styolite Data From the Doctors Dome Area. Journal of Geophysical Research 97/B12, 685-17.

Nicol, A., Alloway, B., Tonkin, P., 1994. Rates of deformation, uplift, and landscape development associated with active folding in the Waipara area of North Canterbury, New Zealand. Tectonics 13, 1327-1344.

Nicol, A., Van Dissen, R.J., 2002. Up-dip partitioning of displacement components on the oblique-slip Clarence Fault, New Zealand. Journal of Structural Geology 24, 1521-1535.

Nicol, A., Cowan, H., Campbell, J., Pettinga, J., 1995. Folding and the development of small sedimentary basins along the New Zealand plate boundary. Tectonophysics 241, 47-54.

Norris, R.J.; Cooper, A.F., 1997. Erosional control on the structural evolution of the range front faulting on the Alpine Fault. Geological Society of New Zealand Miscellaneous Publication 95A, 136.

Pettinga, J.R., 2004. *Personal Communication.*

Pettinga, J.R., Armstrong, M.J., 1998. North Canterbury active tectonics and earthquake hazards. Geological Society of New Zealand Miscellaneous Publication 101B: Field Trip Guides. M.G. Laird (Ed.) Field trip 3, 28 p.

Pettinga, J.R., Wise, D.U., 1994. Paleostress orientation adjacent to the Alpine Fault of New Zealand: broader implications from fault analysis near Nelson, South Island, New Zealand. Journal of Geophysical Research 99/B2, 2727-2736.

Pettinga, J.R., Yetton, M.D., Van Dissen, R.J., Downes, G., 2001. Earthquake source identification and characterization for the Canterbury region, South Island, New Zealand, Bulletin of the New Zealand Society for Earthquake Engineering 34, 282-317.

Rahiman, T. I. H., Pettinga. J.R., 2006. Fracture lineaments and seismotectonically active structures in southeastern Viti Levu, Fiji. University of Canterbury, Christchurch, New Zealand: New Zealand Workshop on Geotechnical Earthquake Engineering, In: Proceedings of New Zealand Workshop on Geotechnical Earthquake Engineering, 32-46.

Walcott, R.I., 1998. Modes of oblique compression: Late Cenozoic tectonics of the South Island of New Zealand. Reviews of Geophysics 36, 1-26.

Walters, R.A., Barnes, P., Goff, J.R., 2006. Locally generated tsunami along the Kaikoura coastal margin: Part 1. Fault ruptures. New Zealand Journal of Marine and Freshwater Research 40, 1-16.

Warren, G., 1995. Geology of the Parnassus area. Lower Hutt, Institute of Geological and Nuclear Sciences, Institute of Geological and Nuclear Sciences geologic map 18, 36 p.

Wellman, H.W., 1979. An uplift map for the South Island of New Zealand and a model for uplift of the Southern Alps, in *The origin of the Southern Alps,* eds Walcott, R.I. & Cresswell, M.M.,Wellington: Royal Society of New Zealand, 13–20.

Wise, D.U., McCrory, T. A., 1982. A new method of fracture analysis; azimuth versus traverse distance plots, Geological Society of America Bulletin *93*, 889-897.

Wheeler, R.L., Wise D.U., 1983. Linesmanship and the practice of linear geo-art; discussion and reply Geological Society of America Bulletin 94, 1377-1379.

CHAPTER 3 FACIES ARCHITECTURE

Views from a terrace:

the facies architecture of a fan delta complex

T.S. McConnico and K.N. Bassett

To be submitted to Geological Society of America Bulletin

Department of Geological Sciences, University of Canterbury, P.B. 4800, Christchurch, New Zealand

Abstract

Multiple terraces on the east side of the Hawkswood Range formed as the result of rapid uplift and erosion of a thrust-cored anticline. The terraces/fan surfaces are ~9 km long and ~3 km wide. Terrace surfaces are composite features, with their upper parts representing sub-aerial alluvial fans, which grade into delta plains of Quaternary Gilbert-style fan deltas. Uplift and incision have created excellent 3-dimensional views of the underlying Gilbert-style fan delta complexes from topsets to prodelta deposits. The flat-lying geomorphic expression of the terraces has its origin in the tripartite geometry of Gilbert-style fan deltas and is formed from the delta plain topset surfaces. These preserved geomorphic features combined with sedimentary facies analysis help uncover the complex incision of terraces and their association with the active tectonics of the region.

The Conway inset terraces are divided into four stages of evolution based on variations in sedimentary facies and geomorphic mapping. Stage I involves the uplift of the Hawkswood Range and subsequent increased sedimentation rate such that alluvial fans prograded to the sea forming the Medina fan delta terrace surface. Evidence of large slumping events is seen as the oldest fan delta onlaps onto Pliocene marine siltstones and mudstones of the Greta Formation. Stage II began with a period of incision, possibly from lowering sea level or from changes in the uplift and sedimentation rate. During Stage II, multiple fans, including the Dawn Creek and Big Bush Gully fans, prograde basinward and infill the incised paleovalleys. These form the largest of the fan delta terraces preserved along the Conway Flat coast. The beginning of Stage III is again initiated by a period of incision. Incision is followed by deposition of estuarine facies with in situ Podocarp paleoforest dated at ~ 8000 BP, possibly lateral to a fan delta similar to the modern Conway fan delta/estuary. Stage IV is marked by the appearance of small inset fluvial terraces dated at ~3,000 BP that represent smaller incision/infill events. Stage V began with a period of incision and continues today with the infill of the incised valley by the modern fan delta of the Conway River and its continued progradation.

KEYWORDS

Gilbert-type fan deltas, slumps, terrace geomorphology, tsunami, incision, New Zealand

3.1 INTRODUCTION

Gilbert-type fan deltas have been the subject of many studies (Postma 1984; Postma and

Roep, 1985; Postma et al., 1988; Colella et al., 1987; Colella, 1988; Nemec and Steel, 1988; Nemec, 1990; Massari and Parea, 1990; Allen, 1997; Falk and Dorsey, 1998; Mutti et al., 2003; Boggs, 2011). In general, Gilbert-style fan deltas form at basin margins and can act as indicators of tectonic activity as well as of changing sea-level during deposition (Hwang et al., 1995). The association of fan deltas and tectonics is addressed in many papers (Leeder and Gawthorpe, 1987; Leeder et al., 1988; Gawthorpe and Colella, 1990; Hwang et al., 1995). However recent studies combining geomorphology and sedimentology have produced insights into fan deltas and their importance to understanding tectonics (Dorsey and Roering, 2006). Gilbert-type fan deltas with steep dipping foresets and tripartite geometry can be explained by tectonic activity. The research presented here is based both on geomorphic and sedimentologic analysis of multiple terrace-forming fan deltas associated with an actively growing mountain range in a transpressional tectonic setting in New Zealand.

The aim of this research was to map in detail the terraces of the Hawkswood Range and to combine the geomorphic mapping with the information gained from detailed analysis of the sedimentary facies architecture of the fan deltas underneath. This process involved mapping the terraces' geomorphic surfaces and integrating the information with subsurface sedimentology. The combination of techniques provides a more complete picture of the development of the fan delta terraces and the controlling factors including tectonic development of the uplifting Hawkswood Range combined with possible changes in sea-level and/or sediment supply along the Conway Flat coast.

3.2 Regional Setting

Quaternary Gilbert-style fan deltas of the Conway Flat coast, New Zealand, are both formed and exposed as the result of rapid uplift on imbricate thrust faults within the

Hawkswood Range (Fig. 3.1A). The northeast region of the South Island is an active, transpressional plate boundary fault zone known as the Marlborough Fault Zone (Pettinga and Armstrong, 1998). Within this fault zone are the complex styles of structural deformation of the North Canterbury fold and thrust belt in which the Hawkswood Range is a NE plunging growing anticline over an associated east directed imbricate thrust fault (Fig. 3.1B) (Pettinga and Armstrong, 1998; Hall, 2004).

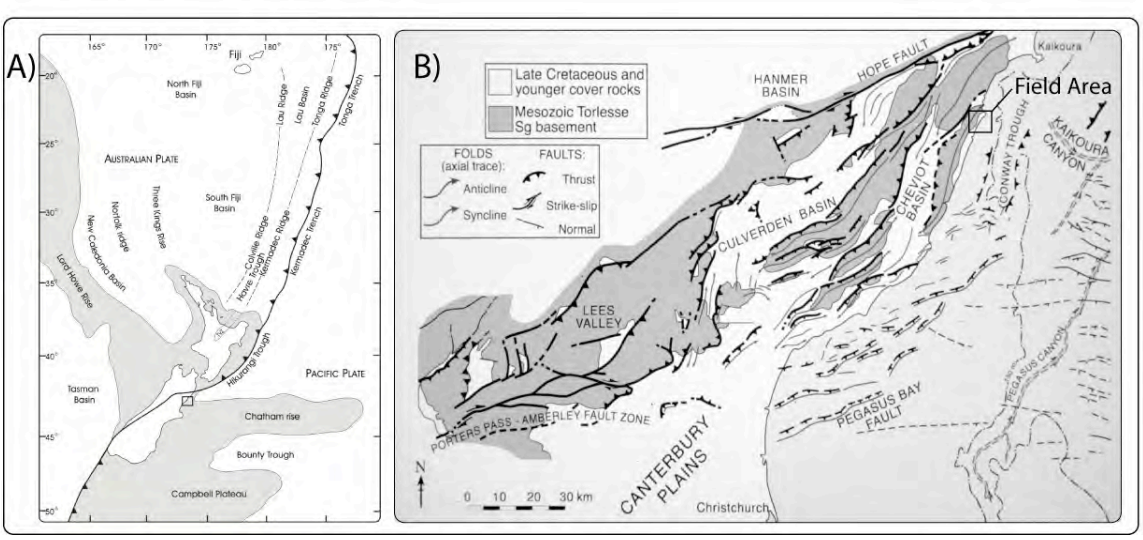

Figure 3.1. A and B) Modern transpressional plate tectonic setting and regional structure of the Marlborough fold and thrust belt adapted from Gamble and Wright (1995) and Pettinga and Armstrong (1998).

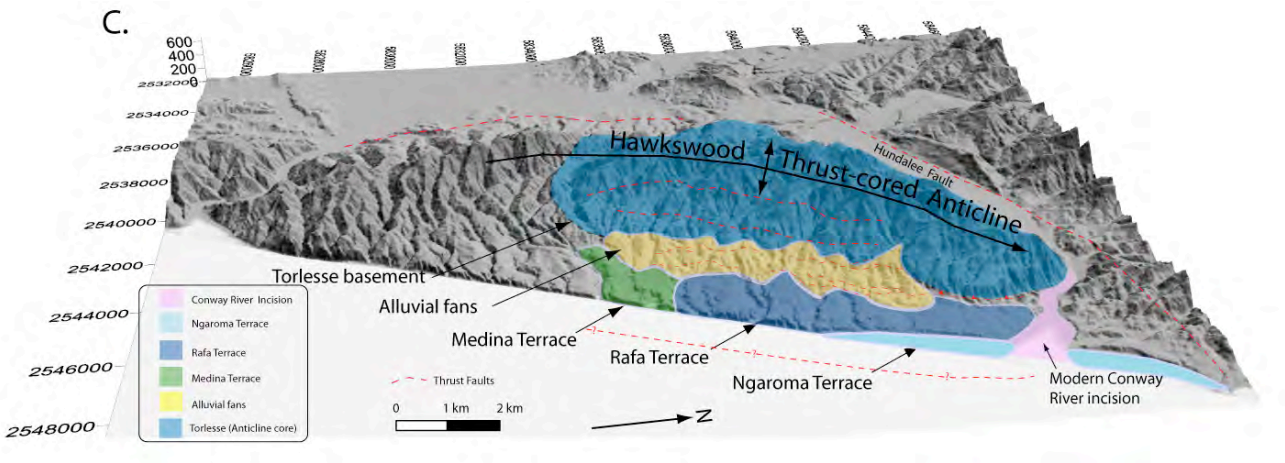

Figure 3.2. Digital elevation model (DEM) of the Hawkswood Range showing the expansive Medina, Rafa, Ngaroma terraces and older alluvial fans and the modern erosion of the beach at the Conway River mouth. These sediments are actively being uplifted as part of the growing, thrust cored, and north plunging Hawkswood Anticline.

The Hawkswood Anticline is one of many anticlines forming in the hanging wall of thrust faults which are currently accommodating most of the ~30 mm/year horizontal shortening associated with the modern convergent plate boundary (Nicol, 1991) (Fig. 3.1). The uplift associated with the growing Hawkswood Anticline formed a series of terraces that were used to document the uplift rate (Ota et al., 1984, 1996) (Fig. 3.2 and Fig. 3.4). The determined uplift rate was first calculated at 3.1 mm/year based on correlating coastal terraces along the South Island (Ota et al., 1984), but was later revised to 2.9 mm/year for the Conway coast based on nearby data collected at Haumuri Bluff (Ota et al., 1996). Recent work in the area by Hall (2004) calculated a similar ~2.9 mm/year uplift rate for the area. However, these rates of deformation are questionable due to the lack of age data from the individual geomorphic surfaces and assumptions that the terraces are remnant beach terraces. The terraces were initially misidentified and interpreted to be equivalent to beach terraces north of the Hundalee Fault.

The rapid uplift of the terraces and subsequent incision into the deposits exposes complete sections with three-dimensional views of Gilbert-style fan deltas in cliffs that dominate the Conway Flat coast (Chapter 4). The terrace surfaces are the topsets of the fan deltas. Cliff outcrops are 50-70 meters high and provide continuous sections through Quaternary to Holocene age strata (Table 5.2; Chapter 5). Outcrops also occur in recent slumps and in river gullies oriented 90° to the strike of the coastal sections thus providing three-dimensional views of the fan deltas (McConnico and Bassett, 2007; Chapter 4).

The exposures of Gilbert-style fan deltas along the Conway Flat coast in the northern part of the South Island provide an opportunity to observe and record the sedimentary facies

architecture in terraces formed by the fan delta processes. The geometry of the coastline allows for easy correlation of beds laterally and vertically, thus providing excellent exposure to understand the connection between terrace forming Gilbert-style fan deltas and active tectonics (McConnico and Bassett, 2007; Chapter 4).

3.3 TERRACE GEOMORPHOLOGY

In order to understand the relationship between terrace formation and fan delta sedimentology, terrace geomorphology must first be deciphered. The terraces are on the east side of the Hawkswood Range and have a complex geometry (Chapter 2). The terraces as a package are a group of primary terrace sets that unconformably overly each other, with a secondary set of terraces wholly contained (i.e. nested) within the older terraces (Fig. 3.3). The geomorphology of the terraces is mapped and described in detail below.

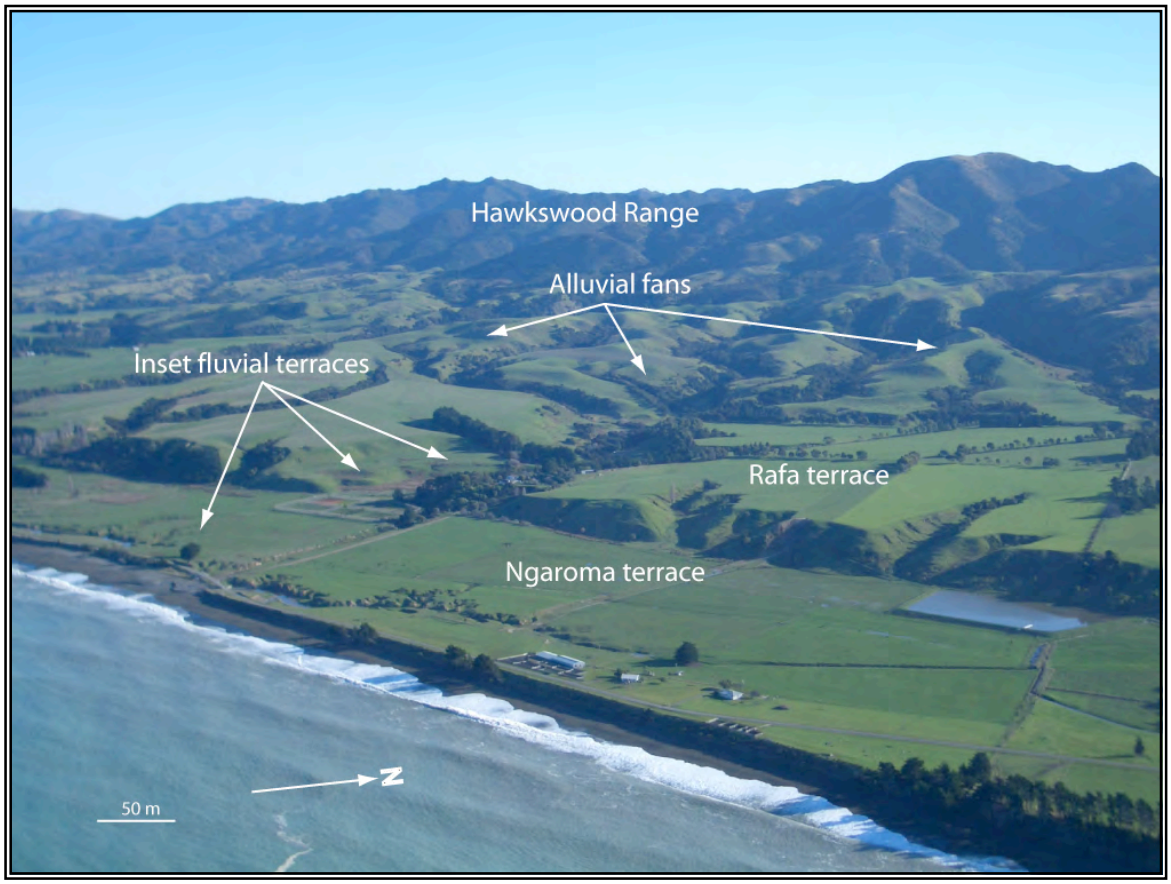

Figure 3.3. Photograph of the east side of the Hawkswood Range showing the Rafa and Ngaroma terraces and several nested fluvial terraces.

3.3.1 **Medina Terrace**

The oldest and highest terrace occurs in the southernmost portion of the area. It is 2 km long and 2 km wide at the widest point and has an elevation of ~70 m, ~10-15 m higher than the next highest terrace (Fig. 3.2). The terrace unconformably overlies, to the west and south, the basement Torlesse Supergroup of the Hawkswood Range, unconformably against alluvial fans covering the basement, and to the east in a sea cliff. The terrace has the smallest spatial distribution of all the terraces, Unconformably overlying Pliocene mudstones to the south and is in an unconformably overlain to the north by next inset terrace (Chapter 4). The terrace surface is smooth and tilts slightly to the east and has one major west-to-east running creek dissecting the surface.

3.3.2 Rafa Terrace

The Rafa Terrace is a large flat lying surface immediately north of the Medina Terrace (Fig. 3.2). The terrace is 7 km long and up to 2.5 km wide and is ~50 m in elevation, ~10-15 m lower than the Medina Terrace. The terrace terminates to the west in the basement Torlesse Supergroup rocks of the Hawkswood Range and alluvial fans developed above the basement, and to the east in a sea cliff. The terrace unconformably overlies the Medina Terrace to the south and is unconformably overlain to the north by the next terrace. The surface slopes from the west to the east at an angle of ~2° with minor undulations (Fig. 2.7). There are three major crosscutting incised valleys and several smaller creeks that dissect this terrace exposing associated underlying fan delta, marine mudstones, estuary, and fluvial deposits.

3.3.3 Ngaroma Terrace

The Ngaroma Terrace is a large flat lying terrace bound to the north by the incision of the modern Conway River, the coastal cliff to the east and unconformably overlies the Rafa Terrace to the west and south (Figs. 3.2 and 3.3). The terrace is 5 km long, up to 500 m wide and ~ 7m in elevation. The Ngaroma Terrace has a noticeably smooth surface, is horizontal to the south near Ploughmans Creek and is back tilted to the west near the Conway River mouth at the coast by three degrees. Several minor streams dissect the terrace.

3.3.4 Inset Fluvial Terraces

Within the three large terraces are several remnant inset fluvial terraces associated with incised crosscutting creeks (Chapter 4). The terraces are associated with major fluvial drainages and are located along the edges of the creeks within the incised canyons. The fluvial terraces can be up to 500 m long and 50 m wide and are often very subtle, rounded and grass covered (Fig. 3.3). The slope of the terrace surface, in a downstream orientation, is the same as the modern drainage they sit in.

3.3.5 Modern Conway Fan Delta Surface

The youngest surface along the Conway Flat coast is the currently forming fan delta of the Conway River (Fig. 3.2). The southwestern and northwestern boundaries are the erosional scarps incised into the Ngaroma and Rafa Terraces and Torlesse Supergroup basement further upstream. The eastern boundary is the modern beach ridge. The fluvial channels of

the modern Conway River dominate the surface morphology with the undulating delta plain surface, ~ 2m in elevation, gently dipping towards the sea.

3.4 SEDIMENTARY LITHOFACIES

The depositional environments that underlie each of the terraces are exposed in beach cliffs, recent slumps and in the walls of deeply incised streams. These include Pliocene-age marine deposits, Gilbert-style fan delta deposits, nearshore marine deposits, pro-delta deposits, estuary deposits, and fluvial deposits (Lewis and Ekdale, 1991;Chapter 4). All are first described below before being correlated with specific terrace surfaces.

3.4.1 Pliocene Marine Mudstones

The Pliocene marine deposits exposed along the Conway Flat coast comprise dark mudstones that are occasionally interbedded with light grey, very fine siltstones and sandstones. Mud/siltstone beds, unconformably overlain by the foreset beds of the fan deltas, contain rare laminations, occasional shell and conglomerate beds, slumping, and convoluted bedding (Chapter 4). Warren (1995) attributed the older marine mudstones and other material exposed in the large cliff faces, including the fan delta deposits described below, to the Miocene-Pliocene (Tt-Wm) Greta Formation. The deposits have been interpreted as fluvial and shallow marine conglomerate accumulated from debris flows shed from the actively rising mountain range (Rattenbury et al., 2006).

3.4.2 Fan Delta Deposits

Angular Topset beds

Angular topset beds are poorly sorted, with sub-rounded to angular clasts and comprise ~20% poorly sorted sand matrix (Fig. 3.5B) (see Chapter 4 and Appendix C for detailed stratigraphic logs). The individual beds fine upwards from cobbles to granules. Topsets

with angular clasts are commonly organized into horizontally- to subhorizontally-stacked massive beds. These beds range from a few centimeters to several decimeters thick and are truncated locally by small channels. Many of the beds are in erosional contact with each other. Topset beds with angular clasts unconformably overlie topset beds of the delta plain which contain rounded clasts. The beds are present but often inaccessible at the top of cliffs. Topset beds with angular clasts that cover the entire surfaces of both the Medina and Rafa Terraces (Fig. 3.5B) The clasts are predominantly sandstone, similar to the rock outcrops in the upper Hawkswood Range. These aggradational units are interpreted as the result of continental sedimentation in an alluvial fan. This facies represents subareial processes resulting from debris flows and stream channel in a high gradient alluvial fan (McPherson et al., 1998 and Deynoux et al., 2005; Chapter 4). This interpretation is based on the coarseness of the material, its great textural immaturity, the wide range of clast shapes, the absence of fine-grained intercalations over the whole thickness of the succession, and the presence of sedimentary structures indicative of sediment-laden stream flows. The angular sandstone and siltstone clasts on top of the rounded clasts of the Gilbert-type fan deltas represent the younger alluvial/fluvial material of the complete delta package and is derived from the Torlesse rock outcrops of the Hawkswood Range. This younger material could be sourced from a slightly different location in the Hawkswood region, but more probably represents more proximal fluvial/alluvial fan deposits prograding over the top that have not been rounded in the coastal zone.

Delta plain/Topset beds

Fan delta topset beds are present but are often inaccessible at the tops of cliffs. Topset beds contain rounded clasts that grade laterally into foreset beds (Fig. 3.5A; see Chapter 4 and Appendix C for detailed stratigraphic logs). Typical rounded topset beds are moderately to well-sorted, with subrounded to rounded clasts with random larger clasts, and < 15%

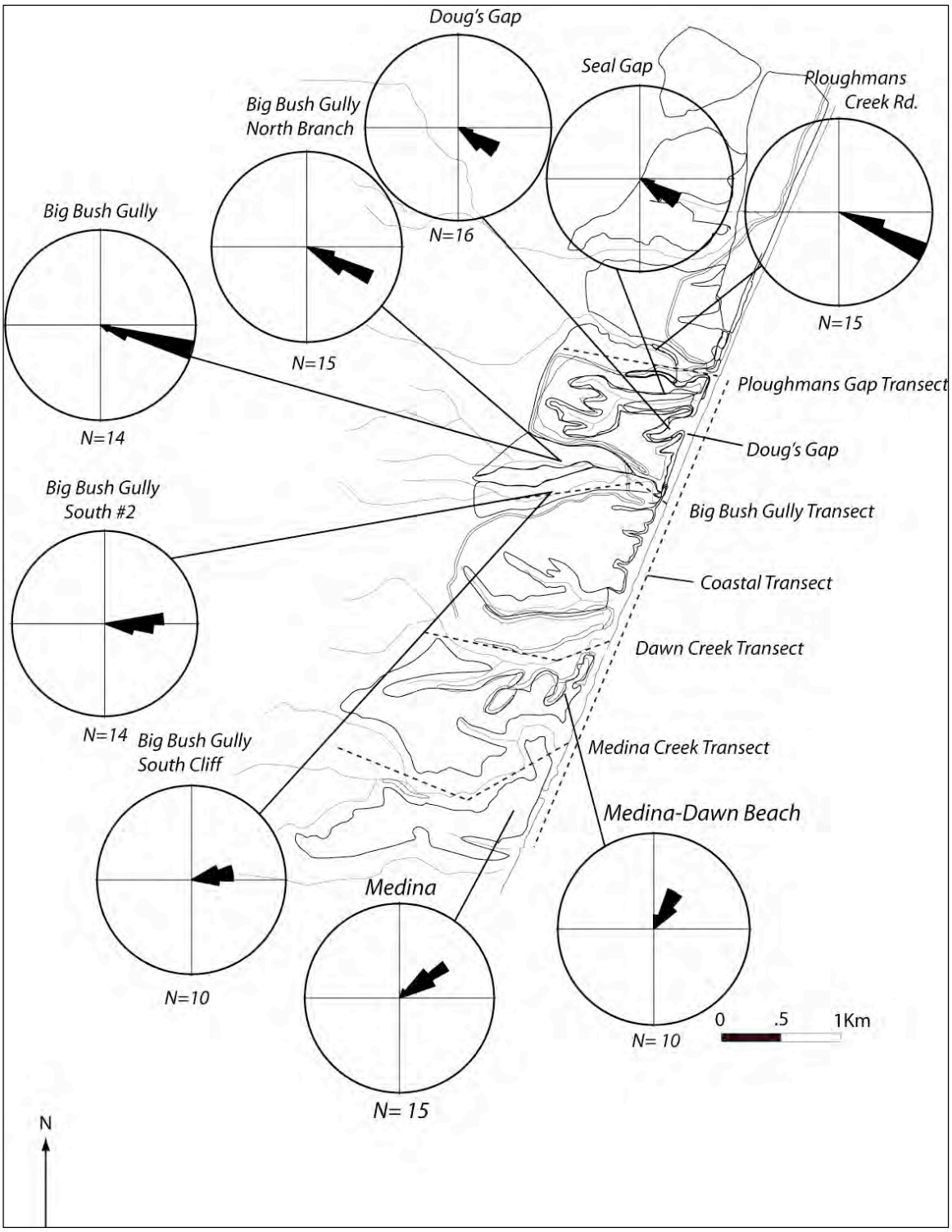

Figure 3.4. Location map of paleocurrent data collected from foreset bedding dips of the Gilbert-type fan deltas. The data suggests that the Hawkswood Range is the source for the material.

medium-coarse sand matrix, erosional basal surfaces and fine upwards. Strong-imbrication patterns of clasts exist at the topset-foreset transition (McConnico and Bassett, 2007). The base of the horizontally-bedded layers, overlying foreset beds is a widespread erosional/depositional surface, whereas the upper limit outlines the smooth present-day terrace topography (Chapter 4).

These aggradational units are interpreted as the result of continental sedimentation in a river braidplain, where repetitive pulsatory delivery and deposition of a gravelly river bedload causes vertical accretion. Individual packages of erosional basal surfaces, fining-upward trends and the high percentage of matrix are indicative of fluvial, hyperconcentrated flood and debris flow deposition on a delta plain (Miall, 1977; Nemec and Steel, 1984; Lewis and Ekdale, 1991; McConnico and Bassett, 2004). The roundness of clasts in topset beds that grade into foreset beds may be the result of reworking by coastal processes. However, the source area for the material also contains rounded clasts.

Delta front beach facies

Within the fan delta complexes are rare, well-preserved delta front beach deposits. These comprise discontinuous, well-sorted, highly stratified gravel lenses up to 20 m wide and 1 m thick (Fig. 3.5C). Gravel lenses are interbedded with fine to coarse-grained sand lenses that contain bioturbation. The clast-supported and elongated pebbles form small accretionary units, with sigmoidal- to wedge-like external geometry up to 50 cm thick. The clasts are arranged to form either planar, tangential or trough cross-bedding (Chapter 4).

The characteristics of this facies assemblage indicate beachface deposits of a reflective shoreline as is typical of wave-dominated shorelines (Massari and Parea, 1990, Postma and Nemec, 1990). The stratigraphic position of this unit, with a highly variable preservation rate in the observed sections, implies that this facies may have developed at the front of the

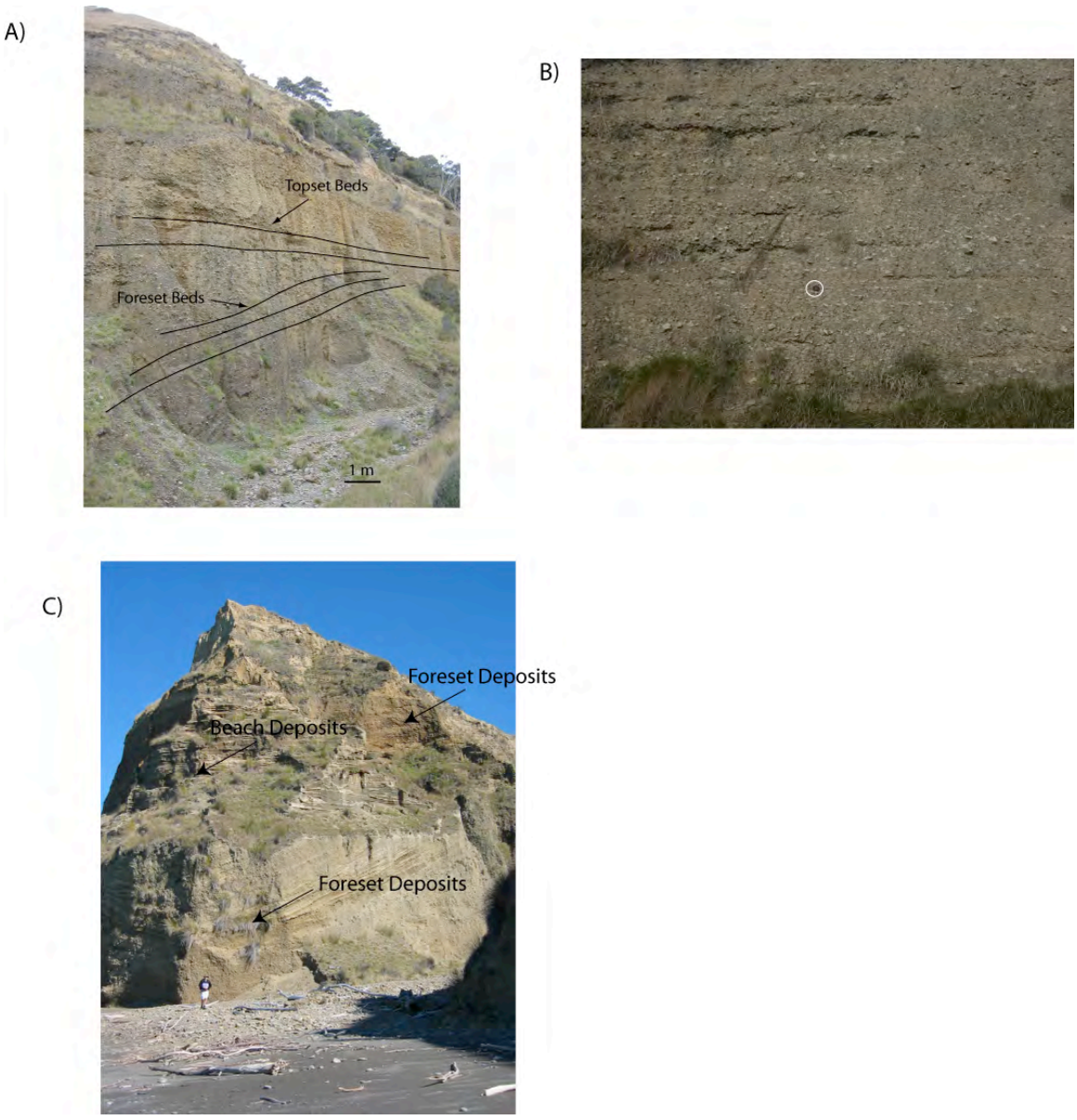

Figure 3.5. Photographs of the Gilbert-style fan delta facies. A) Topset beds grade laterally into foreset beds. B) Angular clast topset beds that blanket the terraces. C) Gilbert-style foreset beds overlain by delta front beach facies and more foreset beds from Doug's Gap. Note: camera lens for scale (Photos: K.N.

depositional system, where the sediments dropped by the river were immediately redistributed and sorted by constant wave motion. Bioturbation of *Arborichnus sparsus*, a shallow marine fauna, is indicative of a relative high-energy environment (Ekdale and Lewis, 1991).

The strongly imbricated clasts at the topset/foreset transition indicates a high density/high sediment load consistent with hyperpycnal flow (Chapter 4). The organized, laminated structure has been argued as being diagnostic of hyperpycnal flows (Petter and Steel, 2006). This flow regime would require near flood conditions with high density/high discharge; such conditions entering the sea is required to create the strong imbrication patterns visible. The existence of hyperpycnal flows in the Gilbert fan-delta settings is well documented (Dorsey et al., 1995). However, this appears to be the first description of imbricated clasts near the foreset/topset interaction in Gilbert fan delta research.

Delta slope foreset beds

The delta slope foresets are made up of a series of dipping gravel layers periodically interbedded by silt beds (Fig. 3.5C; see Chapter 4 and Appendix C for detailed stratigraphic logs). Foreset beds have high lateral persistence with a depositional dip of 23°-28°, locally up to 30° near the top to 10° near the toe. The silt lenses are up to 15 cm thick, are usually discontinuous and pinch-out in the down transport direction. Gravel beds are up to 50 cm thick and thin towards the toe of the foresets. The gravel layers are moderately sorted and clast-supported, but have high percentages (10-30%) of iron-stained, medium to coarse sand matrix. Clasts are well rounded to subangular and range from cobble to granule in size, although most average 2.5-3 cm in diameter. In the clast-supported gravel foresets, the clasts larger than 2 cm are usually imbricated while finer grains show no preferred orientation (see Chapter 4 for detailed interpretation). In coarser beds, the foresets become finer grained downslope. Matrix-supported gravels are poorly sorted with no imbrication and have medium to coarse-grained sand matrix. The foreset beds also preserve many chaotic beds and slump deposits with unusual vertical imbrication forming in the infill beds upslope of slump blocks (McConnico and Bassett, 2007; see Chapter 4 and Appendices B and C for detailed stratigraphic logs). The presence of slumps

blocks is widespread throughout fan delta foreset deposits. Slump blocks and the possible connection to coseismic events are discussed later in this chapter.

The material in the foresets is interpreted to represent sediment gravity flows originating from hyperpycnal flow from a nearby river mouth and include mass transport slumping of foreset sediments. Sediment gravity flow deposits identified include grain flow, debris flow and/or high-density turbidity current deposits (Lewis, 1976; Lewis 1980; Lewis et al., 1980; McConnico and Bassett, 2004; McConnico and Bassett, 2007). Slumps modify foreset topography promoting unusual backstacking imbrication fabrics and backset beds formed by sediment gravity flows infilling the paleo-lows produced as part of the slumping (McConnico and Bassett, 2007; see Chapter 4 and Appendix C). It is interpreted that the sediment gravity flows could be triggered by co-seismic activity or by sediment load. The process favored here is coseismic activity.

Pro-delta facies

The prodelta deposits comprised mudstone beds up to 50 cm thick with macroscopic carbonaceous material throughout. Occasionally slumping in the mud beds are deformed. Matrix-supported, chaotic shell beds, commonly with random isolated clasts, are rarely present. The shells, including *Zeacolpus symerricus,* are diagnostic fossils restricted to the pro-delta environment during the Waipipian-Nukumaruan (Placenzian-Gelasian 3.6-1.8 Ma) (Ekdale and Lewis, 1991; Chapter 4).

These descriptions are all indicative of debris flow deposition. Deformation in the mudstone layers is due to slumping of oversteepened muddy slopes possibly triggered by sediment loading and/or seismic or storm events. Fossils, including bi-valve *Chlamys*

delicatula Fossil ID-O32/f8840 (S55/f0840) (Chapter 5), are interpreted to be from a cold water, mid-outer shelf environment.

3.4.3 Nearshore Marine Deposits

The nearshore marine facies comprises mainly yellow-grey, very fine-grained silt/mud, very fine-grained sand and rare interbedded gravels (Fig. 3.6). Silt beds are laterally continuous and dip gently to the northeast (2 degrees). Bedding thicknesses range from 2-3 cm to 15 cm. Silts contain abundant trace fossils including *Anconichus horizontalis* (Ekdale and Lewis (1991) believed to be made by a burrowing animal in a low-energy environment. The beds often exhibit areas of slumping and convolute bedding (Fig. 3.6) in close proximity to foreset beds, and rare hummocky cross-stratification. Where present, convoluted bedding is contained within a package and not seen in near sequence boundaries. The interbedded sand and gravel layers are lenticular (Chapter 4).

Figure 3.6. Photograph of the fine-grained interfan marine facies. Interbedded sands and silts of the nearshore marine facies at Ploughmans Creek showing the large amounts of slumping (top left and bottom right) characteristic of the facies. Scale: Person in foreground is 1.9 m.

Abundant trace fossils, including *Diplocraterion parallelum var. lingum,* indicate shifting substrate in high-energy conditions in the nearshore marine setting (Ekdale and Lewis, 1991). A nearshore environment is further supported by the gradual shallowing of water depth recorded in the facies indicated by the interbedded fluvial and nearshore marine deposits at cliff top sections in the same horizon as the fan delta topsets. In some locations, liquefaction deposits are continuous in the same horizon for up to 500 m and are possibly indicative of co-seismic activity similar to the coeval slump deposits recorded in the fan delta.

3.4.4 Estuary Deposits

Interbedded gravels, sands and silts, and carbonaceous-rich mud crop out north of Ploughmans Creek (Fig. 3.7A). Gravels are poorly sorted, matrix supported or clast supported, subrounded to subangular with clasts ranging from 1-7 cm in diameter (Chapter 4). Within the interbedded gravels and muds exists an ~ 8000 B.P. in situ Podocarp paleoforest (Fig. 3.7B) (Ota et al, 1984). The well-preserved Podocarp paleoforest is rooted in a paleosol developed on the poorly sorted gravels. Sands and silts are laminated, with sands often displaying ripple cross-laminations. Abundant wood pieces are present ranging from <1 cm fragments to 5 cm thick pieces. Abundant rootlets up to 10 cm long and rhyzoliths are also present in the mud layers. Mud layers are dark gray, contain abundant carbonaceous material and syneresis cracks.

The depositional characteristics indicate a marginal marine setting with tidal influences similar to an estuarine environment. The gravels were deposited in channels by fluvial (clast-supported) or debris flows (matrix supported) processes. The overlying muds and rootlets are consistent with salt marsh deposits. The gravel deposits and fluvial channels

support occasional deposition of fluvial and debris flows in the estuary, creating conditions favorable for the formation of a Podocarp paleoforest. Samples of wood were taken from the drowned forest in the Ngaroma Terrace for analysis. Research with Dr. Ralph Bungard (Botany Dept.) included attempts to extract and amplify the DNA material from the trunks. The age and preservation of DNA within the samples made identification impossible. The estuary deposits were named the Rafa Formation by Warren (1995).

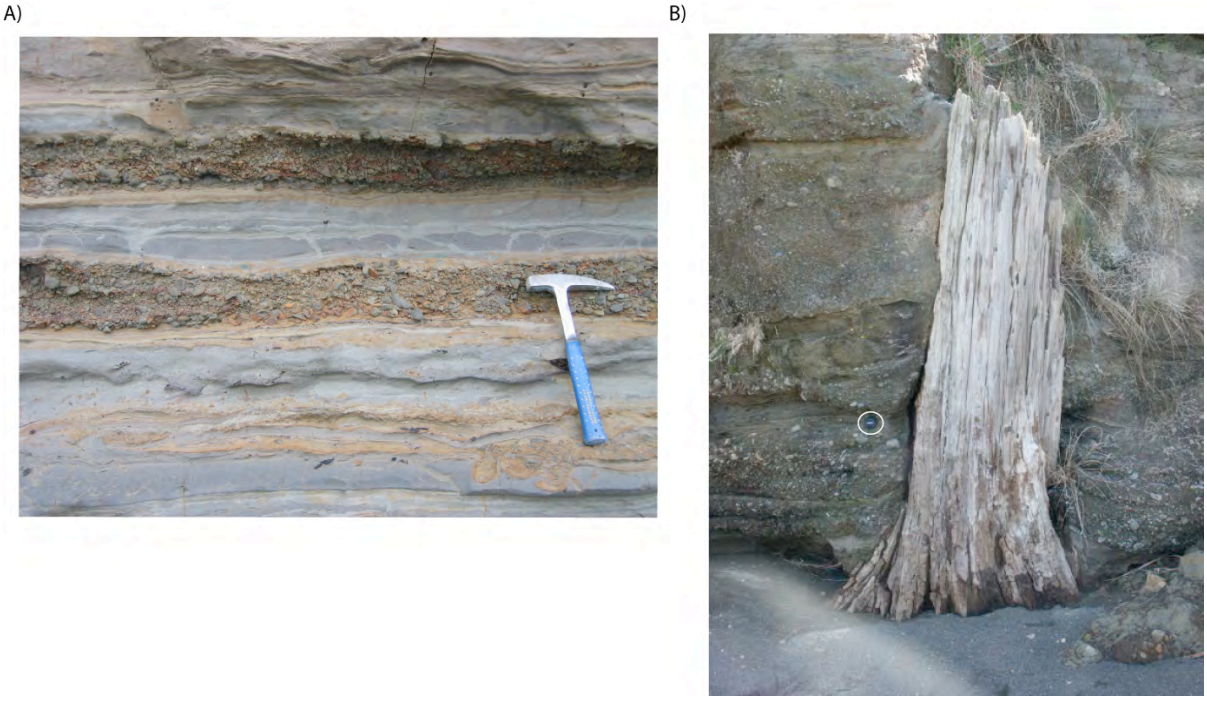

Figure 3.7. A) Photograph of estuary muds and rootlets. B) Photograph showing the Podocarp paleoforest of the Ngaroma terrace. Note the ramping of sediments against the trunk of the tree and camera lens cap for scale (4 cm) (photos: K. N. Bassett).

3.5 SEDIMENT SOURCE

The facies were mapped in detail and, where possible, paleocurrent data collected from clast imbrication and foreset bed dip direction (Fig. 3.4), clast compositions and counts were used to separate different fan deltas. Relative little paleoflow variation is observed between the successive deltaic wedges along the Conway Flat coast, which suggest an effective confinement of the deltas within the Hawkswood Range. Paleocurrent data shows the highest variation when comparing the older and younger fan deltas.

Paleocurrent measurements of imbricated clasts within the foreset beds as well as the dip of the foresets themselves were used to make correlations between coastal and inland exposures (Fig. 3.4). Correlating between the multiple fan delta deposits was confirmed by these measurements taken throughout the fan delta foresets along the coast and in the drainages and cross-cutting relationships.

The clasts of all point counts are dominantly Torlesse sandstones with varying amounts of metamorphic and volcanic clasts from the Torlesse Pahau terrane (Figs. 3.4 and 3.8). Included in the terrane are conglomerate, green sandstone, purplish-red siltstone, limestone, and volcanic clasts such as basalt and dolerite. The conglomerate lenses are present throughout the terrane but significant amounts are found in patches. The conglomerate clasts are rounded to well-rounded and include sandstone, chert and volcanic clasts (including andesite) (Rattenbury et al., 2007). Although there is ample evidence of the conglomerate patches from the Torlesse Pahau terrane found along the Conway Flat coast, the identified outcroppings from this study in the Hawkswood Range are largely indurated, highly fractured, grey thin to medium bedded sandstones and mudstones.

Clast composition analysis demonstrates that pebbles and cobbles are composed mostly of Torlesse sandstones, metamorphic and volcanic rocks (Fig. 3.8). The paleo-rivers draining the rising Hawkswood Range were the major feeder system for the deposits. Variance in the clast lithology of the fans is present from drainage to drainage. The percentage of metamorphic rocks is much greater in the Medina and Dawn fans compared to the Big Bush Gully fan. The Dawn fan also contains high percentages of fractured metamorphic rocks compared to the Big Bush Gully fan. The lithology difference across the Rafa Terrace combined with slightly different paleocurrent data suggests the Big Bush Gully

and Dawn fans are different fans (Fig. 3.2). This perhaps indicates the ancestral Big Bush Gully drainage provided the material for the Big Bush Gully fan and an ancestral Dawn Creek drainage provided the material for the Dawn fan. The appearance of limestone clasts in the Conway River count and not in other clast counts suggests different source areas. The gradual decrease in clast composition variability observed from the oldest to the youngest suggests a decrease in the size of the catchment area. The decrease in catchment area of the feeder fluvial system is probably due to the deformation and evolution of the Hawkswood Range.

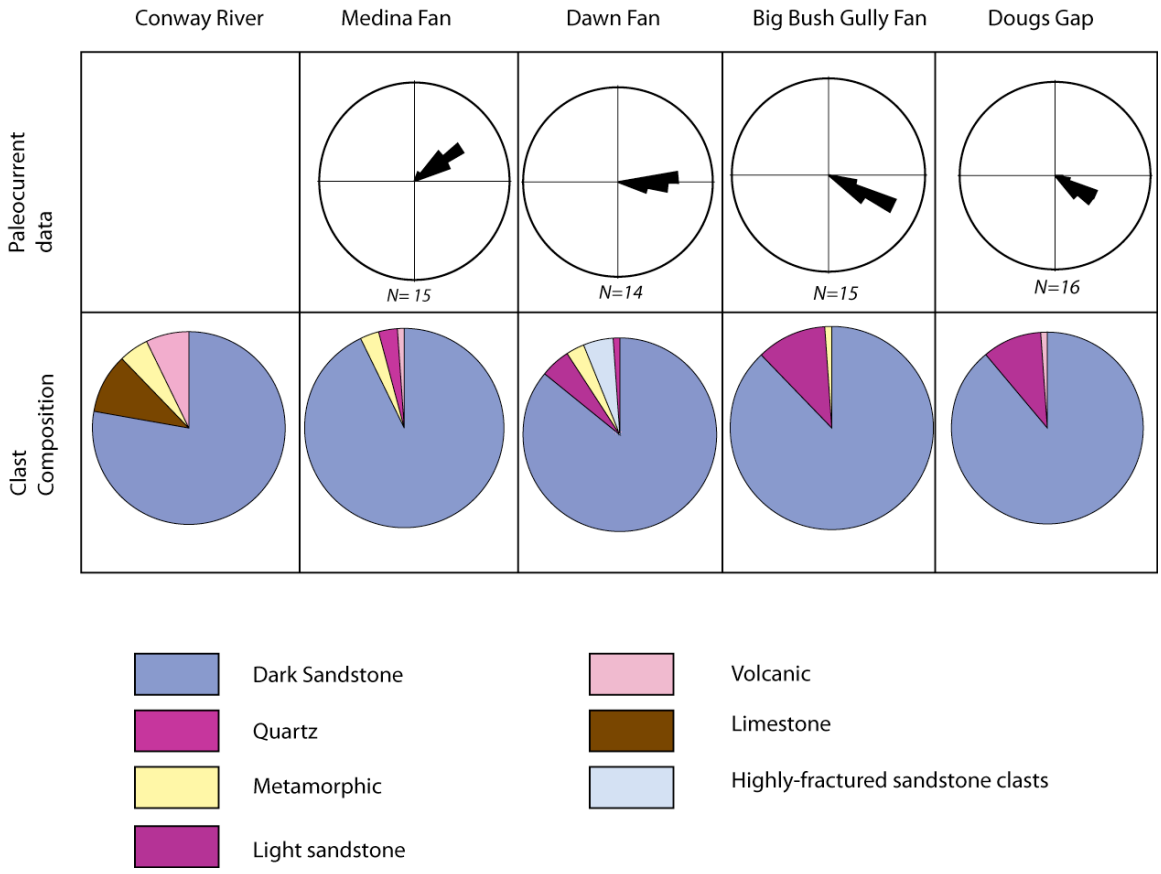

Figure 3. 8 Paleocurrent data taken from foreset dip directions (N=number of measures for each deltaic) and clast composition of the pebble-size fraction of successive delta wedges. The decrease in composition variability suggests a decrease in the catchment area of the feeder fluvial system with time.

3.6 FACIES ARCHITECTURE AND TERRACE DEVELOPMENT

An analysis of the facies architecture can be used to understand the development of the young Gilbert-style fan deltas and how they formed multiple, overlapping terraces. Five transects in total were made, four in gullies perpendicular to the coast and one transect along the coastal section in order to connect the facies architecture to the development of the individual terraces. The locations of these transects are shown on Figure 3.4 and are Medina Creek, Dawn Creek, Big Bush Gully, and Ploughmans Creek from south to north connected by the coastal transect. Photos taken along these five transects were used to create line drawings of the facies architecture (Figs. 3.9, 3.10, 3.11; Appendix B). The three-dimensional views are facilitated by meandering streams, which provide excellent views of contacts between the units.

To facilitate the correlation of each terrace's architecture and development, we present the data first from the relevant coastal segment and then the perpendicular stream segments connect the inland and coastal exposures.

3.6.1 Medina Terrace

Coastal transect - Medina Creek to Dawn Creek

This segment of the coastal transect cuts through the Medina Terrace from the southern-most section of the field area northward to the contact with the Rafa Terrace just south of Dawn Creek (Figs. 3.4 and 3.9A). The Medina fan delta deposits are the oldest in the field area. The foreset beds at any given outcrop are up to 70 m thick and crop out for 1.5 km along the coast. Unconformably overlying the foresets are topset beds of the delta plain facies. These are one-meter thick, interbedded fine-grained sand and angular clast, poorly sorted gravels.

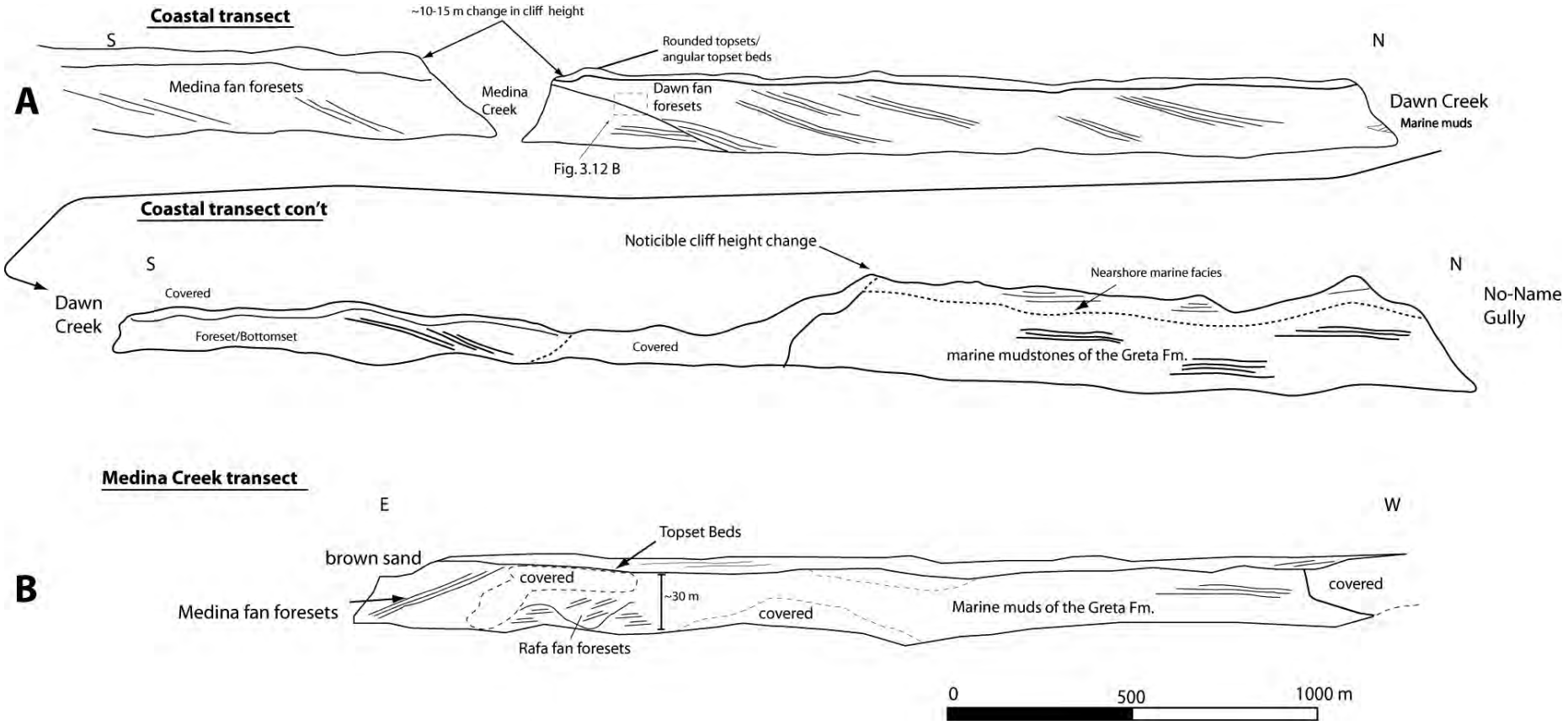

Figure 3.9. A) Line drawing of the coastal transect through the Medina terrace from Medina Creek northwards to Dawn Creek. B) Line drawing of the Medina transect providing 3-demensional control on the facies architecture of the Medina terrace (see Appendix B).

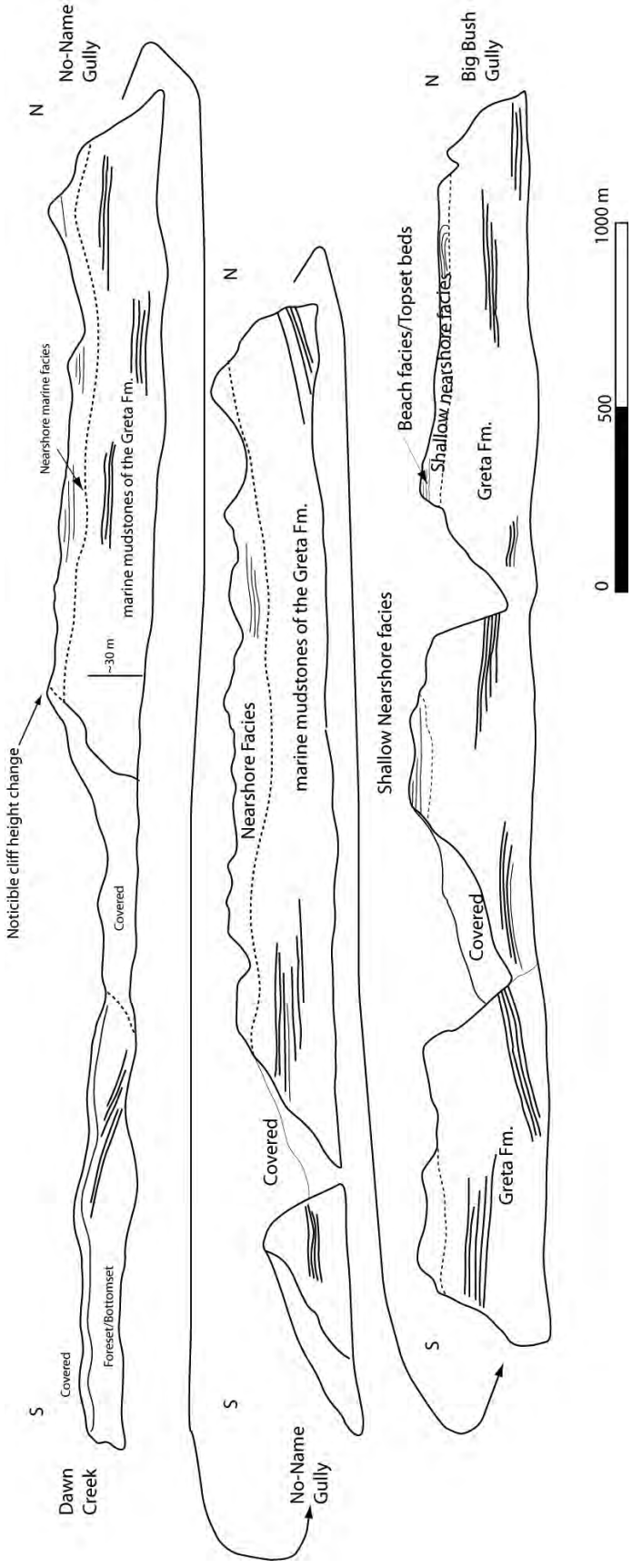

Figure 3.10. A) Line drawing of the coastal transect through the Rafa terrace from Dawn Creek northwards to Ploughmans Creek see Appendix B).

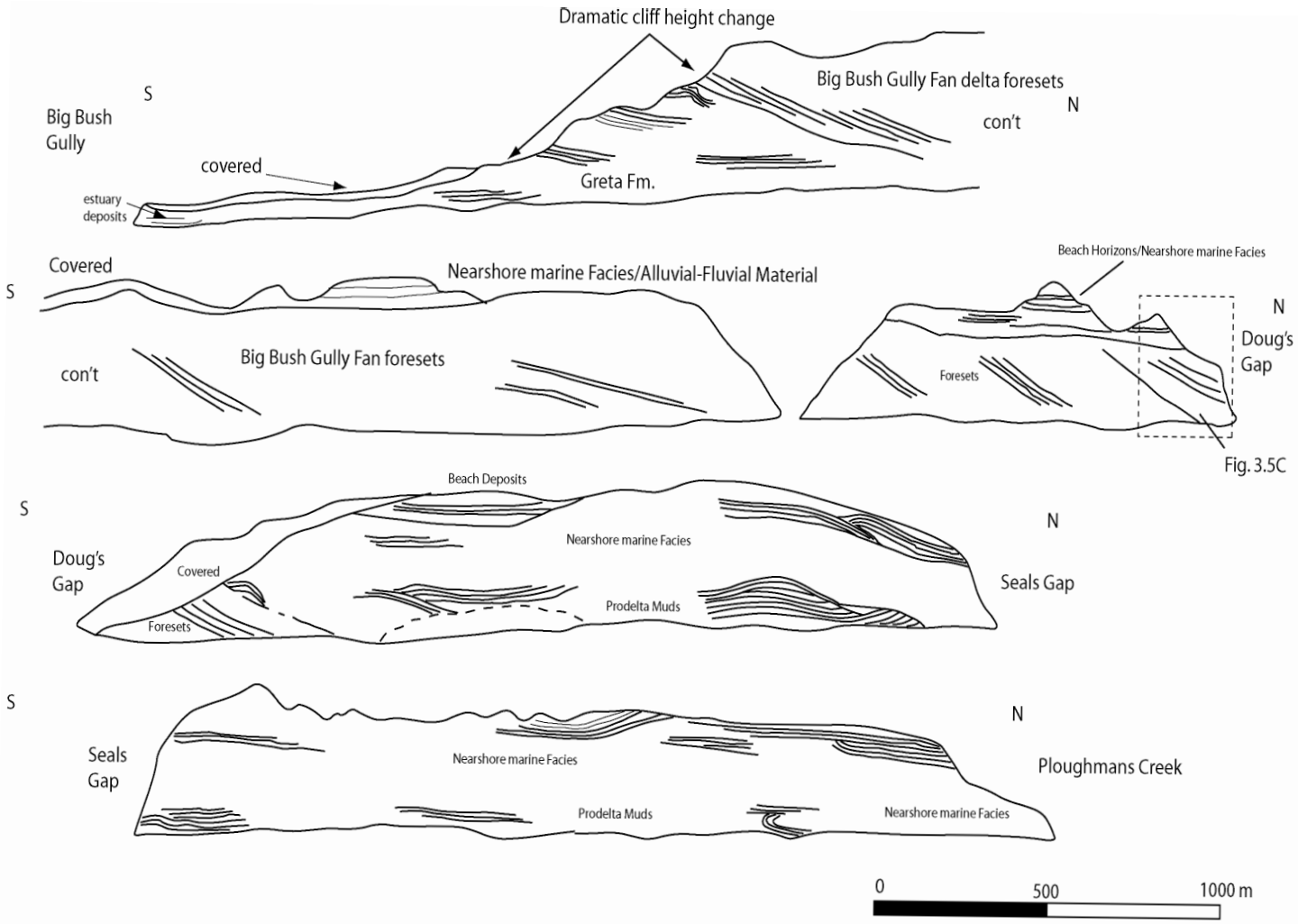

Figure 3.10 con't. A) Line drawing of the coastal transect through the Rafa terrace from Dawn Creek northwards to Ploughmans Creek (see Appendix B).

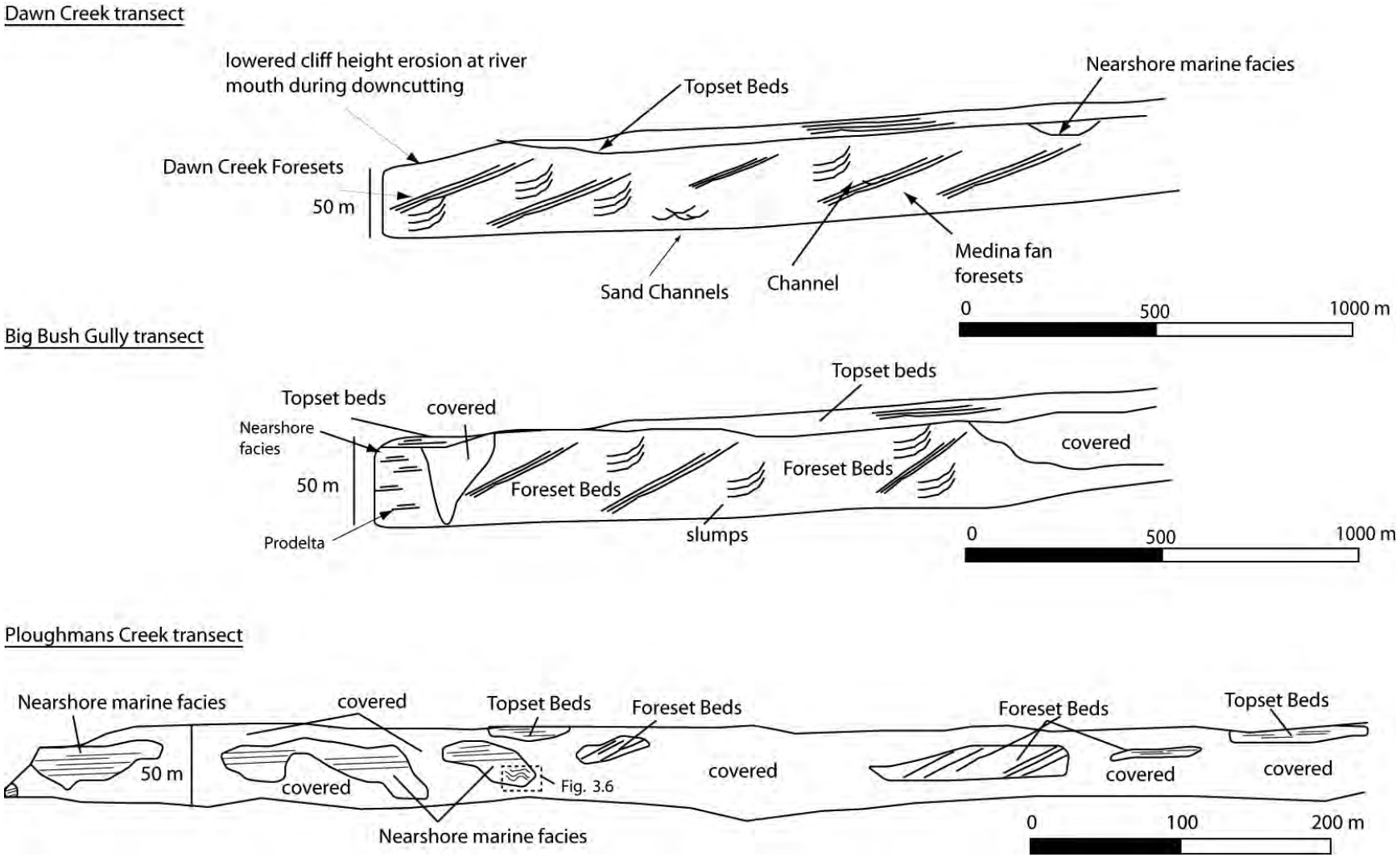

Figure 3.11. Line drawing providing 3-demensional control on the facies architecture of the Rafa terrace through Dawn creek, Big Bush Gully and Ploughmans creek (see Appendix B).

91

Laterally, the Medina fan deposits are deeply eroded and then infilled by the younger Dawn fan delta foresets deposits forming the Rafa Terrace (Figs. 3.9A, 3.12A). At this contact between the two fans the Medina fan system is truncated by the Dawn fan system. At this contact, there is a noticeable change in terrace elevation, land surface, with the Rafa Terrace ~15 m lower than the Medina Terrace.

Medina Creek Transect

The Medina Creek transect cuts through the contact between the Medina and Rafa Terraces and exposes Upper Miocene – Pliocene (Tt-Wm) marine mudstone facies that are cut by the Medina fan delta (Figs. 3.4 and 3.9B). The fan delta foresets prograde out to the coast and are ~ 30 m thick at any given outcrop in the creek exposures. These are unconformably overlain by ~1 m of fine-grained brown sand that is blanketed by ~ 3-5 m of angular clast topset material. Approximately 100 m from the coast, the meandering Medina Creek gives the first outcrop evidence of Dawn fan delta deposits from the Rafa Terrace, and, based on paleocurrent data, this matches the orientation of Dawn fan delta system crosscutting the Medina fan delta in the coastal transect between Medina and Dawn Creeks (Fig. 3.4 and 3.10B). In the Medina Creek transect, the Dawn fan delta deposits from the Rafa Terrace cross cut the Greta Formation but their relationship to the Medina fan deposits are obscured by vegetation. At the contact, the Greta Formation is truncated by the Dawn fan delta system. This contact corresponds to the ~15m elevation change between the two terraces seen along the coast (Fig. 3.9A).

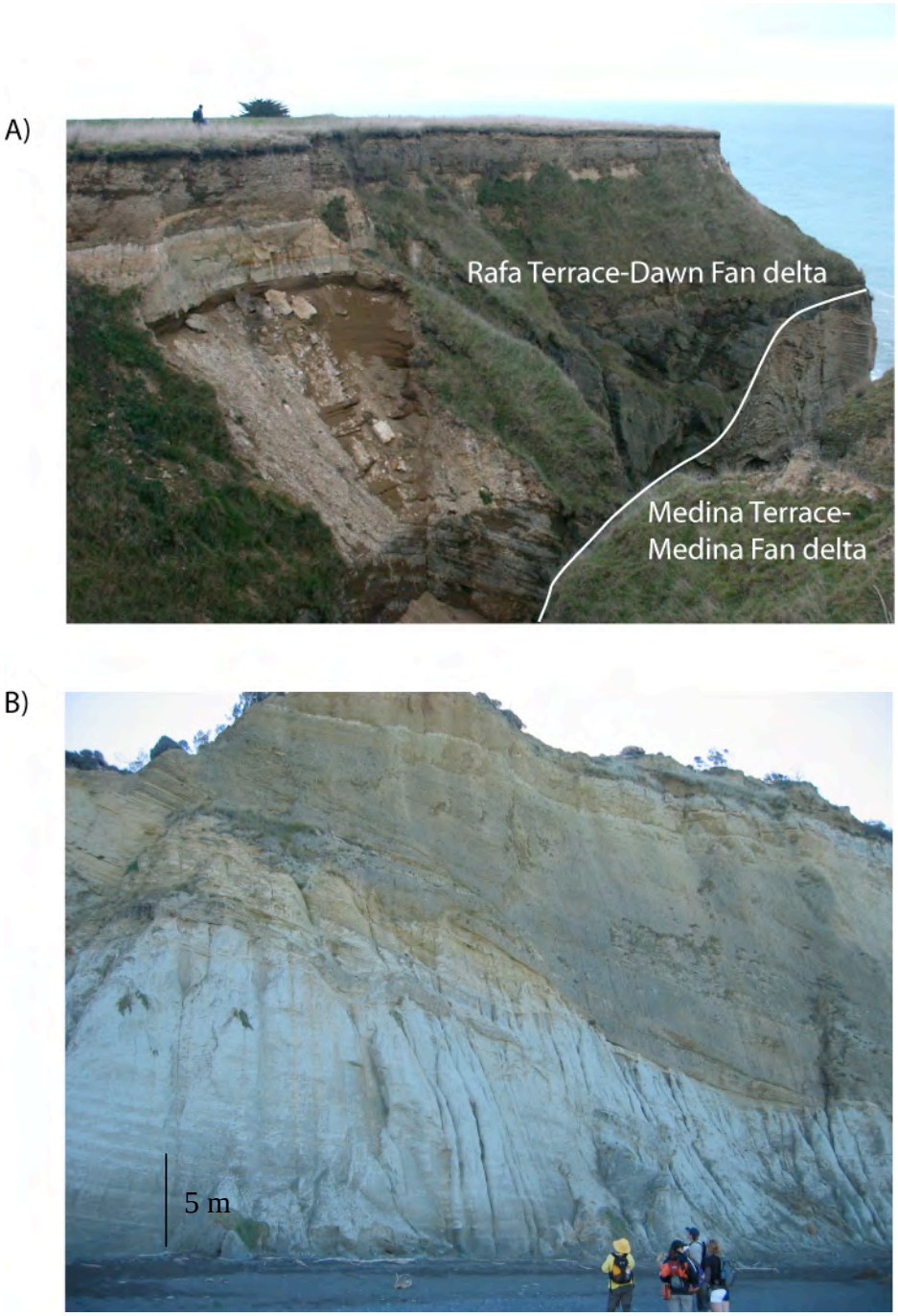

Figure 3.12. A) Photograph of the Medina fan delta just south of Medina creek. Note the Dawn fan system cutting the Medina fan system and the lack of rounded topset beds. B) Photograph of the Big Bush Gully Fan delta crosscutting the Greta Formation (Photo: K.N. Bassett).

3.6.2 Rafa Terrace

The Rafa terrace is composed of two fan delta systems, the Dawn Creek and Big Bush Gully fan deltas. The two systems are described below.

Coastal transect - Dawn Creek to Big Bush Gully

This segment of the coastal transect is entirely within the outcrops of the Rafa Terrace (Figs. 3.4, 3.10). The terrace is ~50 meters high along the coast and dips to the east at ~3 degrees. Foreset beds of the Dawn fan delta are exposed at the Dawn Creek mouth and are overlain by ~1-3 m rounded clast topset beds, ~1 m fine-grained brown sand and ~5 m of angular clast topset beds. All contacts between foresets and prodelta deposits are conformable. Prodelta sands and silts are interbedded with, and overlie, foreset deposits that outcrop on the western-side of the coastal cliffs at the mouth of Dawn Creek. This stratigraphic relationship continues for 1 km to the north, with prodelta sands thickening to 30 m and still overlying the foreset deposits of the Dawn fan delta. Prodelta marine silts are gradationally overlain by the nearshore marine facies marked by the disappearance of marine shells. The nearshore marine facies record a shallowing water depth that is marked by the appearance of both interbedded beach facies and fluvial debris flows. The nearshore marine deposits are capped by well-developed fan delta front beach facies that are capped by angular clast topset beds continuing to Big Bush Gully.

The Dawn fan delta foreset beds are conformably overlain by ~1 m of fine-grained brown sand and a ~3 m thick unit of angular topset beds. These beds continue to the mouth of Dawn Creek 250 m to the north. At the contact between the two fan deltas at the coast, the appearance of rounded clast topsets are visible above the Dawn fan delta foresets. At the coast sand and angular topset beds overlie the topset beds.

Dawn Creek Transect

The Dawn Creek cross cutting transect is wholly through the Rafa Terrace (Figs. 3.4 and 11A). The exposures are ~2.5 km long composed of prograding Dawn fan delta foresets.

The preserved foresets are up to ~50 m thick in their cliff height exposures. The foreset beds are overlain by ~1-3 m thick topset beds composed of rounded clasts, in turn overlain by ~1 m of fine-grained brown sand and finally a ~3-5 m thick package of topset beds with angular clasts. Nearshore marine deposits, interpreted as high-energy nearshore marine sediments, onlap onto the foresets at the coast. Within the prograding Dawn fan delta foresets are examples of large (>10 m thick) slump deposits with well-developed backset bedding behind the slump blocks (McConnico and Bassett, 2007). There are also examples of fine-grained sand channels developed within the fan delta foresets.

Through the Dawn Creek transect we can see the inner structure of the Rafa Terrace that consists of the prograding Dawn fan delta. This transect is the continuation of deposits exposed in the coastal transect between Medina and Dawn Creeks as supported by mapped contacts, ~35° NE paleocurrent orientations, and the ~ 15 m lower geomorphic expression of the ~30 m high Rafa Terrace (Fig. 3.4 and 3.9A).

Coastal transect - Big Bush Gully to Ploughmans Creek

This segment of the coastal transect cuts through the Rafa Terrace to its northern, unconformable, contact with the inset Ngaroma Terrace (Figs. 3.4, 3.10). At the mouth of Big Bush Gully the cliff heights are ~ 20 m lower than immediately north or south of the creek. North of Big Bush Gully (~200 m), the continuing prodelta sediments are overlain by the first appearance of a 30+ m thick package, in outcrop, of Big Bush Gully fan delta foresets (Figs. 3.10, 3.13). The Big Bush Gully fan delta is a second set of foresets that forms a second fan delta in the Rafa Terrace identified by the distance between the fan deposits and slight change from NE to SE paleocurrent orientation between the older Dawn fan foresets and the younger Big Bush Gully fan foresets (Fig. 3.4). The foresets are overlain by delta front beach deposits and continue for 0.75 km northward to Doug's

Gap. At Doug's Gap, the foresets of the Big Bush Gully fan delta are still overlain by well-developed beach deposits (Fig. 3.5C). These beach deposits are overlain by another ~10 m thick unit of foreset deposits. North of Doug's Gap the foreset beds grade laterally into interbedded sands and silts of the nearshore marine facies up to ~30 m thick in cliff exposures. The nearshore marine deposits are interbedded in the top of the cliffs with rare topset deposits containing angular clasts. The beds continue for 0.6 km to the north and overlie prodelta deposits comprised of interbedded silts and mud at Ploughmans Creek (Fig. 3.10; Lewis and Ekdale, 1991).

Big Bush Gully Transect

The Big Bush Gully crosscutting transect is 2.5 km long and cuts entirely through the Rafa Terrace (Figs. 3.4, 3.11). The sedimentary facies present are of the Big Bush Gully fan delta and coeval nearshore marine facies. The prograding Big Bush Gully fan delta foresets are ~30 m thick in their cliff height exposures and are conformably overlain by ~3 m of rounded clast topset beds, ~1 m of fine-grained brown sand, and ~2-5 m of angular clast topset beds. The foreset package decreases to ~25 m thick at the coast and, although the contact is obscured, it appears to grade laterally into ~25 m thick pro-delta deposits. The prodelta muds are gradationally overlain at the top of the cliff by the interbedded sands and silts of the nearshore marine facies.

Big Bush Gully transects the Rafa Terrace and is the primary drainage providing the material for the Big Bush Gully fan delta, a fan delta developing at the same time and from the same general direction, as the Dawn fan delta. The fan delta foresets prograded out to the coast grading into pro-delta deposits. The prodelta deposits pass upwards into nearshore marine facies as the nearshore facies aggraded in the protection of the prograding Dawn fan delta to the south; similar to an embayment of the modern coastline. The interfingering of foresets from the Big Bush Gully fan delta and nearshore marine

deposits suggests a syndepositional environment. A Ground Penetrating Radar (GPR) study during this project shows the thickness of the fan delta foresets continues to ~ 8 m below the modern day river drainage. At ~ 8 m below the surface the forests downlap onto another surface making the entire foreset package ~38 m thick.

Ploughmans Creek Transect

Ploughmans Creek represents the southernmost extent of the Rafa Terrace at the coast (Figs. 3.4, 3.11). The transect is 1.5 km long and cuts along the contact between the Rafa and Ngaroma Terraces. The south bank of Ploughmans Creek shows Rafa Terrace deposits whereas the northern bank shows the Ngaroma Terrace deposits. Here the Rafa Terrace consists of the prograding Big Bush Gully fan delta foreset deposits previously described. The foresets are conformably overlain by ~3 m of topset beds with rounded clasts, ~1 m of fine-grained brown sand, and ~3-5 m of topset beds with angular clasts. The interbedded sands and silts of the nearshore marine facies onlap the foresets fifty meters inland from the coast. The nearshore marine facies are up to ~20 m thick in the cliff and along this transect have excellent exposures of slumping and convoluted bedding (Fig. 3.6).

The Ploughman Creek transect consists mainly of the northern extent of the prograding Big Bush Gully fan delta. The overlying nearshore marine facies continued to develop in the protection of the prograding fan deltas to the south as evidenced by the lateral transition of foresets to the nearshore marine facies at Doug's Gap where the foresets interfinger with the nearshore marine deposits (McConnico and Bassett, 2007). Doug's Gap also records a change from fan delta deposits to foreshore deposits then back to a second set of fan delta material higher in the cliff.

3.6.3 Ngaroma Terrace

Coastal transect - North of Ploughmans Creek

This part of the coastal transect cuts through the Ngaroma Terrace (Figs. 3.3, 3.4, 3.13). Cliff heights at this area are 5 m and are ~10-15 m lower than in areas of the Rafa Terrace immediately to the south. An ancient Podocarp tree is located immediately north of Ploughmans Creek lateral to nearshore marine facies deposits of the Rafa Terrace's Big Bush Gully fan delta. This horizon contains ~20 *in situ* tree stumps. The paleoforest is rooted in poorly sorted, subrounded to subangular gravels overlain by dark, sulfurous muds with abundant rootcasts burying the vertical tree stumps. The gravel deposits are overlain by fine-grained sands and silts. The sands and silts contain woody material and syneresis cracks. The silts are interbedded with gravels ramping up onto and covering the Podocarp tree trunks. Individual trees and roots are dated to ~8 ka (Ota et al., 1984; this study, Ch. 5). Both the gravels and the sulfurous muds are laterally continuous for over 2 km toward the incised modern Conway River.

Laterally, the deposits at Ploughmans Creek abruptly pass from the interbedded gravel beds associated with the Podocarp paleotree horizon to nearshore marine facies muds and then back into the interbedded gravel beds of the Podocarp paleotree horizon. The changes in lithology are also marked by distinct changes in cliff height. The contacts between the paleotree deposits and the marine mudstones are associated with ancient colluvium comprised of poorly sorted, angular granule to boulder breccias. The nearshore marine muds have been dated to > 50 ka (Ota et al., 1984).

The marine muds are correlated with the nearshore marine muds preserved south of Ploughmans Creek. The change in cliff height, existence of colluvium at the contacts, age data and sedimentology suggest that a Podocarp paleoforest grew in an estuarine environment that existed on either side and possibly, in front of, a remnant high of the Rafa Terrace nearshore marine deposits.

Incised into the Ngaroma Terrace is a small channel. The channel consists of poorly sorted, angular to sub-rounded gravel deposits. The channel contains abundant woody material. The incised channel deposits with poorly sorted, matrix-rich sediment are characteristic of fluvial debris flow deposits in the inset fluvial terraces. This channel, which contains a wood fragment dated through ^{14}C at ~3 ka, help determine uplift rates during the Holocene (Chapter 5).

Cross-cutting transects

The north bank of Ploughmans Creek provides one of the few transects, perpendicular to the coast, to look at the Ngaroma Terrace. The deposits record interbedded fluvial and estuarine facies. In another locality within the Ngaroma Terrace (Fig. 3.2), a temporary trench dug by local farmers revealed more estuarine muds and paleotree stumps.

3.6.4 The Modern Conway River Fan Delta

The Ngaroma Terrace has been uplifted and incised by the Conway River and is now being infilled by the prograding Conway delta. Figure 3.2 shows the incision, based on elevations of the Ngaroma Terrace deposits infilled by the lower elevation modern delta deposits. The modern delta plain is a good analog for both the Ngaroma Terrace delta plain/estuary deposits and for the Rafa and Medina Terrace fan delta slope deposits as it is here that the modern Conway river delta plain is prograding into the open ocean and creating yet another flat geomorphic surface. At the same time all of the other smaller creeks are forming the modern infill similar to inset terraces such as at Big Bush Gully and Dawn Creek.

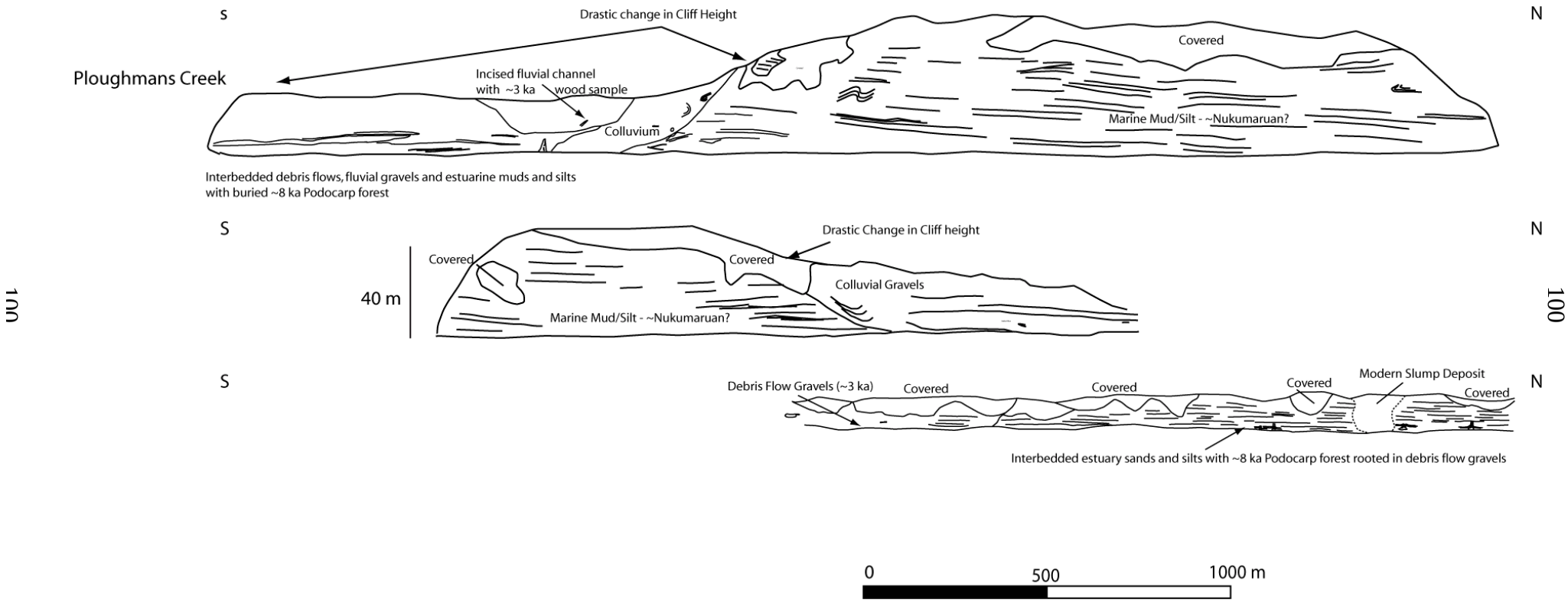

Figure 3.13. Line drawings of coastal transect along the Ngaroma terrace. Notice the contact and associated cliff height change between the estuary facies and older marine muds (see Appendix B).

3.7 DISCUSSION OF TERRACE DEVELOPMENT

3.7.1 Terrace Development

The Gilbert-type fan delta deposits of the Medina Terrace form an angular unconformity with the underlying Greta Formation mudstones. The Medina Terrace was formed by the progradation of the Medina fan delta. The deposition of the Medina fan delta was followed by planation of the fan delta's topset beds creating an erosional wave-cut platform. This is overlain by brown sands and angular clast topset beds of prograding fan delta plain/alluvial fan deposits. These angular clast topset beds form the terrace surface which is lumpy, tilts seaward, and is laterally variable.

An extended period of incision created valleys in the Medina Terrace followed by deposition of the Dawn fan delta forming the Rafa Terrace. Incision of the Medina Terrace is supported by the crosscutting sedimentary contact seen in the coastal transects and by the noticeable ~15 m change in elevation of the older, higher Medina Terrace with respect to the younger, lower Rafa Terrace.

The Rafa Terrace is the result of two fan deltas derived from sediment from Dawn and Big Bush Gully Creeks. Distinct lithologic differences between the two fans and slight variations in paleocurrent data support the existence of the two separate fans developing in the Rafa Terrace (Figs. 3.4 and 3.8).

As these two Gilbert-style fan deltas simultaneously prograded they provided protection from the dominant northward longshore currents (Barnes, 1996). This blocking of current activity allowed the nearshore marine facies to develop in an interfan delta environment as well as in a protected area north of the Big Bush Gully fan delta as seen at Ploughmans

Creek. Examples of avulsion in the development of the fan deltas is seen at Doug's Gap with overlying fan delta deposits; conversely this could mark a time of progradation following retrogradation during sea level fluctuations. The furthest progradation of the fan deltas was probably not much further than what is exposed in the modern beach cliffs today as shown by the gradation of foresets into prodelta deposits.

An extended period of incision created valleys in the Rafa Terrace. The unconformable contact between the deposits associated with the paleotree horizon and nearshore marine deposits along with the noticeable change in cliff height between the Rafa and Ngaroma Terraces at three locations are key to interpreting the estuarine facies along the coastal transect. Ground Penetrating Radar (GPR) investigation was attempted to confirm the nature of the contact, but saltwater interference made this impossible (Appendix D). The incision of the Rafa Terrace probably took place by both an ancestral Ploughmans Creek and by deflection of the paleo-Conway River around the growing Hawkswood Range leaving a remnant high between the two terraces. This deflection, and subsequently drowned river mouths, formed the estuaries around which the paleoforest grew eventually creating the Ngaroma Terrace. This is supported by cliff-height changes at the mouth of Big Bush Gully Creek and dated material from the deposits.

A minor sea level fluctuation ~ 3 ka is considered responsible for the small inset terrace in the Ngaroma Terrace and similar inset terraces located at creek mouths along the coast.

3.7.2 Faulting and the Result of Seismic Activity

Slump Deposits and Liquefaction

The slump deposits and liquefaction within the nearshore marine deposits combined with slump deposits in fan delta foresets are likely the result of seismic activity. The location of the Conway Coast within active transpressional plate boundary and the unconformable contact between the Medina Fan and underlying Greta Formation, a result of an extended period of uplift and erosion, support periods of seismic activity. The seismic activity would be a logical trigger for the liquefaction and slump deposits. The modern day analogue to this is the interaction of the Hundalee fault at the head of the Kaikoura Canyon. The Hundalee Fault is important not just as a potential earthquake source but because of its apparent role as the eastern termination (head) of Kaikoura Canyon. It is thought future earthquake ruptures of the Hundalee Fault would have a high chance of triggering submarine landslides in the canyon and generate a local tsunami (Geotech, 2009).

Fluvial Terraces and Landslides

The deposits are interpreted as interbedded fluvial and debris flow deposits sourced from loose sediments that are possibly stored in the upper catchments following large seismic events, possibly under similar flood conditions recorded in the topset deposits. There are quite possibly multiple origins for these deposits on different time scales: (short-term) seismic events, (medium-term) episodic uplift, and (long-term) sea level change.

The terraces seen in the Ngaroma Terrace and Big Bush Gully in the river gullies would have occurred simultaneous with the larger terraces and probably represent the same relative sea level changes. This is supported by dated material in the Ngaroma Terrace and at the mouth of Big Bush Gully indicating terrace development at the same time. Alternatively it is hypothesized the fluvial sediment deposits in the upper reaches of streams were most likely released and stored in the upper catchments of the Hawkswood

Range during episodic fault movements, similar co-seismic activity recorded along the Conway Flat coast in the older nearshore marine and fan delta deposits. Eventually further tectonic activity would release the material. The proposed development of these terraces is interpreted to be similar to the detailed study by Becker and Davenport (2003) of earthquake-driven rockfall deposits in Switzerland. An earthquake-triggered rockfall would have initially stored the released material in the upper catchments of the Hawkswood Range. The material subsequently was brought down in rainfall-induced landslides or normal fluvial transport. Chen et al. (2006) described the emplacement of similar debris flow deposits in Taiwan. Abundant liquefaction features and slumps in foreset and nearshore marine deposits also support earthquake triggered events occurred.

The deposits were dissected and preserved as aggradational terraces during uplift and sea level fall.

3.8 A MODEL FOR THE DEVELOPMENT OF THE TERRACES THROUGH TIME

The erosive contacts between the Medina, Rafa, Ngaroma and modern Conway fan delta systems coupled with changes in terrace elevations provide the link to understanding the development of the multiple inset terraces along the Conway Flat coast (Fig. 3.14). The inset development of the systems is supported by the crosscutting relationships of Pliocene-Holocene strata exposed along the Conway Flat coastline. The temporal evolution of the system was as follows:

Ia. Incision into the Greta Formation. The marine Greta Formation mudstones are crosscut by the Medina fan delta deposits indicating an initial erosional event marking the onset of multiple unconformities alternating with coarser deposits in the area.

Ib. Development of the Medina Terrace. The Medina Terrace is the oldest and highest in the study area. The progradation of the Medina fan delta infills the valleys created by incision into the Greta Formation marine mudstones. The fan delta foresets are as high as ~70 m indicating a high gradient sea floor at least this depth during deposition. The fan delta topsets were removed as the result of changes in uplift and/or sedimentation rate creating a wave-cut platform. This was unconformably overlain by thin alluvial fan deposits.

IIa. Incision into the Medina Terrace. Following this period of deposition was an extended period of incision.

IIb. Development of the Rafa Terrace. The Dawn and Big Bush Gully fan deltas infill the valleys cut into the Medina Terrace and prograde basinward; the Dawn fan delta is the largest (~ 50 m cliff) observed along the Conway Flat coast. The deposits of the Rafa Terrace contain fan delta foresets with rare imbrication patterns (McConnico and Bassett, 2007), large amounts of slumps and liquefaction of nearshore marine deposits.

IIIa. Incision into the Rafa Terrace. This period of deposition is again followed by an episode of incision, supported by crosscutting relationships of fan delta deposits and estuarine deposits and the associated cliff height changes. Both Ploughmans Creek and a deflected Conway River cut down into the Rafa Terrace leaving a remnant high between the two.

IIIb. Development of inset terraces. A series of inset fluvial terraces are located within Rafa Terraces in many of the drainages along the Conway Flat coast. These fluvial

deposits are varying elevations and size and are most likely the result of material being released from the upper catchment during large tectonic events. The smaller inset terraces preserved within the main drainages reflect the material released and brought down via streams as the result of large seismic events occurring during periods of incision or alternatively they could also be formed by minor incision/infill events. Although there are no age constraints on these terraces, the geomorphic and sedimentological contacts along with elevation data distinguishes these terraces from those found incised into the Ngaroma Terrace.

IVa. Incision into the inset terraces. This period of deposition is followed by an episode of incision down to modern levels.

IVb. Development of the Ngaroma Terrace. Stage 4 involves deposition of Ngaroma Terrace estuarine facies, possibly lateral to a fan delta similar to the modern Conway fan delta/estuary, with an *in situ* Podocarp paleoforest at ~8000 BP. The Podocarp paleoforest is rooted in the gravel deposits from the ancestral Conway River and probably existed until the barrier to the sea was breached creating an environment unsuitable for the paleoforest. Subsequent fluvial and debris flow deposits from the paleo-Conway River buried the tree stumps followed by drowning and deposition of the estuarine muds that comprise the ~3 m cliff deposits north of Ploughmans Creek. Small fluctuations in sea level are recorded by 3 ka channelized debris flow deposits in the Ngaroma Terrace.

Va. Incision into the Ngaroma Terrace. The deposition of the Ngaroma Terrace is again followed by a period of incision by the modern Conway River and the small creeks.

Vb. Development of the modern Conway Delta. Stage Vb represents the infilling of the incised valley by the modern fan delta of the currently prograding Conway River fan delta.

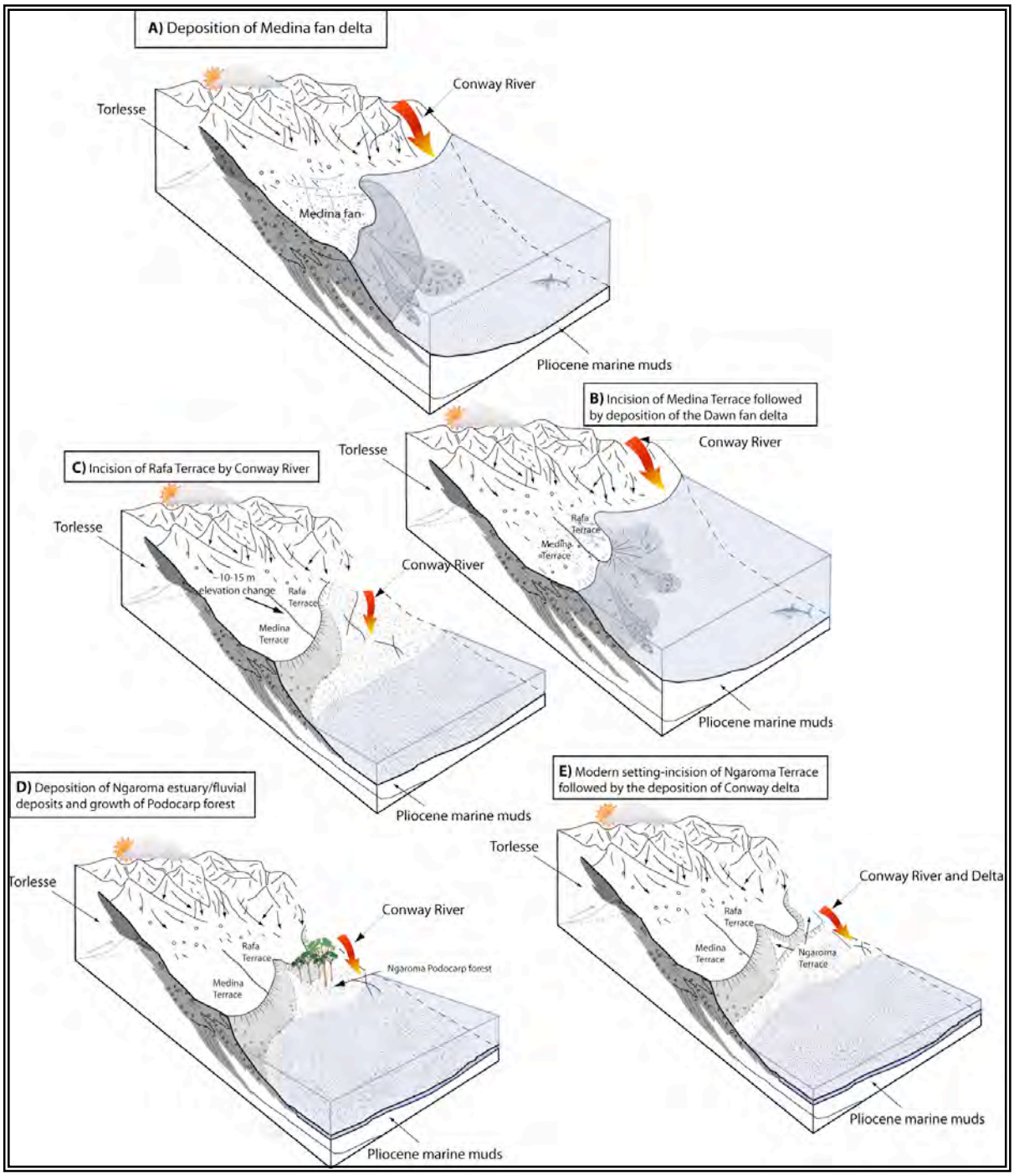

Figure 3.14. Block diagrams showing the evolution of multiple fan deltas preserved along the Conway Coast. A) Stage Ia and IIb- Incision of Pliocene Marine muds followed by the progradation of the Medina fan delta B) Stage IIa and IIb- Incision of Medina terrace followed by deposition of the Dawn fan delta. C) Stage IIIa- Incision of the Rafa terrace by the Conway River. D) Stage IIIb- Deposition of Ngaroma estuary/fluvial deposits and growth of Podocarp paleoforest. E) Stage IVa and IVb- Incision of Ngaroma terrace by the modern Conway River followed by the deposition of the Conway River delta.

3.9 CONCLUSIONS

Multiple terraces on the east side of the Hawkswood Range formed as the result of rapid uplift and erosion of a thrust-cored anticline. The terraces/fan surfaces are ~5 km long and ~2 km wide. Uplift and incision have created three-dimensional views of the underlying Gilbert-style fan delta complexes from topsets to prodelta deposits. Terrace surfaces are composite features, with their upper parts representing sub-aerial alluvial fans, which grade into delta plains of Quaternary Gilbert-style fan deltas. The geomorphic expression of the terraces, with a seaward dip and small surface channels has its origin in the tripartite geometry of Gilbert-style fan deltas and is formed from the delta plain topset surfaces. These preserved geomorphic features when combined with sedimentary facies analysis help uncover the complex nesting and overlapping of terraces and their association to the active tectonics of the region.

Depositional basins in active tectonic regions pose interesting questions with regards to controlling factors on deposition. The preserved Gilbert-type fan deltas at Conway Flat are the result of a complex interaction between factors such as regional and local uplift along fault strands, eustatic sea level, and sediment supply.

The development of the fan deltas in this compressional setting was contingent on many factors: 1) the steady uplift of the Hawkswood Anticline created an environment conducive to the formation of deltas, 2) the Hawkswood Range produced large volumes of sediment from a relatively small catchment as a result of uplift and erosion, 3) there existed a steep drop-off into the ocean and 4) thrust faults at fan apices provided the relief necessary to create Gilbert-type fan deltas.

The combination of sedimentary facies architecture and terrace geomorphology allows us to speculate about the relative significance of uplift rates vs. sea level changes in the context of regional tectonics and what roles they played in the depositional/geomorphic history of the Conway Flat coast (see Chapter 6).

3.10 REFERENCES

Alexander, J., Mulder, T., 2002. Experimental quasi-steady density current. Marine Geology 186, 195–210.

Allen, P.A., 1997. Earth Surface Processes. Blackwell Science, Oxford. Oxford, pp. 404.

Barnes, P.M., 1996. Active folding of Pliestocene unconformities on the edge of the Australian-Pacific plate boundary zone, offshore North Canterbury, New Zealand. Tectonics 15, 623-640.

Becker, A., Davenport, C.A., 2003. Rockfalls triggered by the AD 1356 Basle Earthquake. Terra Nova 15, 258–264.

Boggs, S. Jr., 2011. Principles of Sedimentology and Stratigraphy. Prentice Hall, pp. 600.

Cantalamessa, G., Di Celma, C., Ragaini, L., 2006, Tectonic controls on sequence stacking pattern and along-strike architecture in the Pleistocene Mejillones Formation, northern Chile: Implications for sequence stratigraphic models, Sedimentary Geology 183, 125–144.

Chen, H., Dadson, S., Chi, Y-G., 2006. Recent rainfall-induced landslides and debris flow in northern Taiwan. Geomorphology 77, 112–125.

Colella, A., 1988. Pliocene-Holocene fan deltas and braid deltas in the Crati Basin, southern Italy: a consequence of varying tectonic conditions. Fan Deltas-Sedimentology and Tectonic Settings. Blackie, London, pp. 50- 74.

Colella, A., de Boer, P.L., Nio, S.D., 1987. Sedimentology of a marine intermontane Pleistocene Gilbert-type fan-delta complex in the Crati Basin, Calabria, southern Italy. Sedimentology 34, 721-736.

Deynoux, M., Çiner, A., Monod, O., Karabıyıkoglu, M. ,Manatschal, Tuzcu, S., 2005. Facies architecture and depositional evolution of alluvial fan to fan-delta complexes in tectonically active Miocene Köprüçay Basin, Isparta Angle, Turkey. Sedimentary Geology 175, 315–343.

Di Celma, C., Ragaini, L., Cantalamessa, G., Landini, W., 2005. Basin-physiography and tectonic influence on sequence architecture and stacking pattern: pleistocene succession of the Canoa Basin (central Ecuador). Geol. Soc. Amer. Bull. 117, 1226 – 1241.

Dorsey, R.J., Roering, J., 2006. Quaternary Landscape Evolution in the San Jacinto Fault Zone, Peninsular Ranges of Southern California: Transient Response to Strike-Slip Fault Initiation. Geomorphology 73, 16-32.

Dorsey, R.J., Umhoefer, P.J., Renne, P. R., 1995. Rapid subsidence and stacked Gilbert-type fan deltas, Pliocene Loreto Basin, Baja California Sur, Mexico. Sedimentary Geology 98, 181-204.

Dorsey, R.J., Umhoefer, P. J., Falk, P.,1997. Earthquake clustering and stacked Gilbert-

type fan deltas in the Pliocene Loreto Basin, Baja California Sur, Mexico, Geology 25, 679–682.

Ekdale, A.A., and Lewis, D.W., 1991. Trace fossils and paleoenvironmental control of ichnofacies in a Late Quaternary gravel and loess fan delta complex, New Zealand. Palaeogeography, Palaeoclimatology, Palaeoecology 81, 253-279.

Eschard, R., Albouy, E., Deschamps, R., Euzen, T., Ayu, A., 2003. Downstream evolution of turbiditic channel complexes in the Pab Range outcrops (Maastrichtian, Pakistan). Journal of Marine and Petroleum Geology 20, 691-710.

Falk, P., and Dorsey, R. J., 1998. Rapid development of gravelly high-density turbidity currents in marine Gilbert-type fan deltas, Loreto basin, Baja California Sur, Mexico. Sedimentology 45, 331-349.

Gamble, J.A., Wright, I.C., 1995. The Southern Havre Trough geological structure and magma petrogenesis of an active backarc rift complex. In: B. Taylor (Ed.) Backarc basins: tectonics and magmatism. Plenum Press, New York, pp. 29-62.

Gawthorpe R.L., and Colella, A., 1990. Tectonic controls on coarse-grained delta depositional systems in rift basins. Special Publication International Association Sedimentology 10, 113-127.

Gilbert, G.K., 1885. The topographic features of lakeshores. Annual Report U.S. Geological Survey 5, 69-123.

Hall, L., 2004. Cenozoic deformation at the southern end of the Hikurangi margin, New Zealand, unpublished Ph.D. Thesis, University of Oxford, England.

Holt W.E., Haines, A.J., 1995. The kinematics of northern South Island, New Zealand, determined from geological strain rates. Journal of Geophysical Research 10, 17991–18010.

Hwang, I. G., Chough, S. K., Hong, S. W., Choe, M. Y., 1995. Controls and evolution of fan delta systems in the Miocene Pohang Basin, SE Korea. Sedimentary Geology 98, 147-179.

Kneller, B., 2003. The influence of flow parameters on turbidite slope channel architecture. Journal of Marine and Petroleum Geology 20, 901-910.

Leeder, M.R., and Gawthorpe, R.L., 1987. Sedimentary models for extensional tilt-block/half-graben basins. Geological Society Special Publications 28, 139-152.

Leeder, M.R., Ord, D.M., Collier, R., 1988. Development of alluvial fans and fan deltas in neotectonic extensional settings; implications for the interpretation of basin-fills. In: Fan Deltas—Sedimentology and Tectonic Settings. Nemec, W; Steel, R J (Eds.). Blackie and Son, Ltd, Glasgow, Blackie, London, UK. pp. 173-185.

Lewis, D.W., 1976. Subaqueous debris flows of early Pleistocene age at Motunau, North Canterbury, New Zealand. New Zealand Journal of Geology and Geophysics 19, 535-567.

Lewis, D.W., 1980. Storm generated graded beds and debris flow deposits with *Ophiomorpha* in a shallow offshore Oligocene sequence at Nelson, South Island, New Zealand. New Zealand Journal of Geology and Geophysics 23, 353-369.

Lewis, D.W. and Eckdale, A. A., 1991. Lithofacies relationships in a late Quaternary gravel and loess fan delta complex, New Zealand. Palaeogeography, Palaeoclimatology, Palaeoecology 81, 229-251.

Lewis, D.W., Laird, M.G., Powell, R.D., 1980. Debris flow deposits of early Miocene age, Deadman Stream, Marlborough, New Zealand. New Zealand Journal of Geology and Geophysics 27, 83-118.

Lønne, I., 1995. Sedimentary facies and depositional architecture of ice-contact glaciomarine systems. Sedimentary Geology 98, 13–43.

Massari, F., Parea, G.C., 1990. Wave-dominated Gilbert-type gravel deltas in the hinterland of the Gulf of Taranto (Pleistocene, southern Italy). Coarse-Grained Deltas, Spec. Publ. 10. Oxford, UK, pp. 311-331.

Massari, F., Rio, D., Sgavetti, M., Prosser, G., D'Alessandro, A., Asioli, A., Capraro, L., Fornaciari, E., Tateo, F., 2002. Interplay between tectonics and glacio-eustasy: Pleistocene succession of the Crotone basin, Calabria (southern Italy). Geological Society of America Bulletin. 114, 1183 – 1209.

McConnico, T.S. and Bassett, K.N., 2003. Quaternary Gilbert-style fan deltas and Podocarp forests along the modern transpressional Hope Fault, New Zealand. Abstracts

with Programs - Geological Society of America 35, no.6, pp.510.

McConnico, T.S., Bassett K.N., Pettinga, J.R., 2005. Facies architecture of the Conway fan delta complex as it formed terraces along the uplifting Hawkswood Range. Geological Society of New Zealand Miscellaneous Publication.

McConnico, T.S. and Bassett, K.N., 2007, Gravelly Gilbert-type fan delta on the Conway Coast, New Zealand: Foreset depositional processes and clast imbrications, Sedimentary Geology 198, 147-166.

McPherson, J.G., Shanmugam, G. and Moiola, R.J., 1988. Fan-deltas and braid-deltas: conceptual problems. In: Fan Deltas—Sedimentology and Tectonic Settings. Nemec and Steele (eds.). Blackie and Son, Ltd, Glasgow, Blackie, London, UK. pp. 14–22.

Miall, A.D., 1977. A review of braided river depositional environments. Earth Science Review 13, 1–62.

Mulder, T., Syvitski, J.P.M., Migeon, S., Faugeres, J-C., Savoye, B., 2003. Marine hyperpycnal flows: initiation, behavior and related deposits. A review. Marine and Petroleum Geology 20, 861–882.

Mulder T. and Alexander, 2001. The physical character of subaqueous sedimentary density flows and their deposits, Sedimentology 48, 269–299.

Mutti, E., Tinterri, R., Remacha, E., Mavilla, N., Angella, S., Fava, L., 1999. An introduction to the analysis of ancient turbidite basins from an outcrop perspective. AAPG

Course Note 39, 93

Mutti, E., Tinterri, R., Benevelli, G., di Biase, D., and Cavanna, G., 2003. Deltaic, mixed and turbidite sedimentation of ancient foreland basins. Marine and Petroleum Geology 20, 733-755.

Necker, F., Hartel, C., Kleiser, L., Meiburg, E., 2002. High-resolution simulations of particle-driven gravity currents. International Journal of Multiphase Flow 28, 279-300.

Nemec, W. and Steel, R.J., 1984. Alluvial and coastal conglomerates: their significant features and some comments on gravelly mass-flow deposits, *Memoir*, vol. 10**,**in: E.H. Koster, R.J. Steel, Editors , *Sedimentology of Gravels and Conglomerates*, pp. 1–31.

Nemec, W. and Steel, R.J. (Editors), 1988. Fan Deltas: Sedimentology and Tectonic Settings. Blackie, London, 444 pp.

Nemec, W., 1990. Aspects of sediment movement on steep delta slopes. Coarse-Grained Deltas. Special Publication, vol. 10. International Association of Sedimentologists, Oxford, UK, pp. 29-73.

Nicol, A., 1991. Structural styles and kinematics of deformation on the edge of the New Zealand plate boundary zone, Mid-Waipara Region, North Canterbury, Ph.D. Thesis, University of Canterbury, pp. 171.

Ota, Y.Y., Torao; Iso, N., Okada, A., Yonekura, N., 1984. Marine terraces of the Conway coast, South Island, New Zealand. New Zealand Journal of Geology and Geophysics 27,

313-325.

Ota, Y.Y., Pillans, B. Berryman, K., Beu, A., Fujimora, T., Miyauchi, T., Berger, G., Climo, F.M., 1996. Pleistocene coastal terraces of the Kaikoura Peninsula and the Marlborough coast, South Island, New Zealand. New Zealand Journal of Geology and Geophysics 39, 51-73.

Petter, A.L. and Steel, R.J., 2006. Hyperpycnal flow variability and slope organization on an Eocene shelf margin, Central Basin, Spitsbergen. American Association of Petroleum Geologists Bulletin 90, 1451–1472.

Pettinga, J.R. and Armstrong, M.J., 1998. Field Trip Three: North Canterbury Active Tectonics and Earthquake Hazards. In: Malcom Laird (Ed.) Geological Society of New Zealand, New Zealand Geophysical Society Joint Annual Conference Field Trip Guide. Geological Society of New Zealand Miscellaneous Publication 101 B, 1-28.

Postma, G., 1984. Slumps and their deposits in fan delta front and slope. Geology 12, 27-30.

Postma, G. and Roep, T.B., 1985. Resedimentated conglomerate in the bottomsets of Gilbert-type gravel deltas. Journal of Sedimentary Petrology 55, 874-885.

Postma, G., Nemec, W., 1990. Regressive and transgressive sequences in a raised Holocene gravelly beach, southwestern Crete. Sedimentology 37, 907-920.

Postma, G., Babic, L., Zupanic, J., Roe, S.L., 1988. Delta-front failure and associated bottomset deformation in a marine, gravelly Gilbert-style fan delta. In: Fan Deltas—Sedimentology and Tectonic Settings. Nemec and Steele (eds.). Blackie and Son, Ltd, Glasgow, Blackie, London, UK. pp. 91-102.

Rattenbury, M., 2006. Kaikoura Sheet, 1:250,000 QMAP series. Geological and Nuclear Sciences, New Zealand.

Walters, R.A., Barnes, P., Goff, J.R., 2006. Locally generated tsunami along the Kaikoura coastal margin: Part 1. Fault ruptures. New Zealand Journal of Marine and Freshwater Research 40, 1-16.

Warren, G., 1995. Geology of the Parnassus area. Lower Hutt, Institute of Geological and Nuclear Sciences, Institute of Geological and Nuclear Sciences geologic map 18, 36 p.

CHAPTER 4 GILBERT-TYPE FAN DELTA PROCESSES

4.1 GENERAL INTRODUCTION

In chapter 3, the facies architecture of multiple Gilbert-type fan delta complexes along the Conway Flat coast was deciphered, within that context, and with new detailed foreset data, a model for fan delta foreset processes and unique imbrication fabrics and bed forms are presented in chapter 4. The data presented here is published work in *Sedimentary Geology*.

Gilbert-type fan delta deposits are some of the most studied sedimentary deposits. Originally identified by GK Gilbert in Lake Bonneville (Gilbert, 1885), fan deltas have been the subject of both broad and detailed examination. Initial studies of fan deltas centered on the formation of them in coastal settings and focused on the architectural development. In recent years studies have focused on detailed interpretation of downslope sediment transport mechanisms (Sohn et al., 1999; Sohn, 2000). A few studies focused (Nemec, 1990; Dorsey et al., 1995; Sohn et al., 1999; Sohn, 2000) on development of high-density turbidity currents and their deposits in the down-transport direction. However, within these studies it becomes quite apparent that discrepancies exist in terminology when describing the same processes that occur on Gilbert-type fan delta. The main arguments arise in discussions of rapid flow transformations with the use of controversial terms, e.g. traction carpet, to describe the deposits.

The data presented in this chapter was published in a paper with Dr. Kari Bassett; approximately 90% of this paper was purely my work. The paper intended to step away from the controversy and focus on the descriptions of foreset beds by: 1) a consolidation of the terminology used when describing fan delta deposits; 2) focusing on the deposits and reasons for their presence; 3) being aware that there can be more than one interpretation for

similar looking deposits, i.e., kinematic sieving vs. traction carpets. In addition to eliminating the controversy, there was a definite need in the literature for descriptions and interpretations of the existence of odd clast imbrications and backset beds within the foreset facies. Imbrication in previous studies was rarely described in detail and in particular the steep clast fabrics of the Conway Flat fan coast deltas seemed to be unique.

4.2 RESEARCH OBJECTIVES

This chapter proposes to use detailed sedimentological analysis of individual beds of the Conway Flat coast fan delta complex to discuss process evolution and the characteristics of Gilbert-type fan delta foresets. Through detailed examination of foreset deposits this study aimed to highlight the unique sedimentary processes and structures that exist within the foresets and adjacent sedimentary facies. The following points were of particular interest when looking at the individual beds:

- Identify the multiple processes occurring on the fan delta foresets
- Identify the origin of distinct clast imbrication
- Descriptive process free of complex verbage used in prior publications

4.3 RESEARCH METHODS

Extensive fieldwork was needed to gain an understanding for the depositional processes in the multiple Gilbert-type fan deltas along the Conway Flat coast. In total, there are three individual fan deltas in the field area with excellent exposures in drainage outcrops and coastal cliffs. These exposures allowed for the construction of detailed stratigraphic columns of foreset packages. Photographs were also taken with line drawings being generated to emphasize clast imbrication patterns (Appendices C).

Gravelly Gilbert-type fan delta on the Conway Coast, New Zealand: Foreset depositional processes and clast imbrications

T.S. McConnico !, Kari N. Bassett
Department of Geological Sciences, University of Canterbury, P.B. 4800, Christchurch, New Zealand
Received 22 August 2005; received in revised form 1 May 2006; accepted 11 May 2006

Abstract
Quaternary Gilbert-style fan deltas of the Conway Coast, New Zealand, are formed and exposed by the continuing uplift and erosion of the Hawkswood Range due to transpression associated with the modern New Zealand plate boundary. The fan deltas are exposed in 50–70 m high cliffs and crop out for over 5 km along the coast and up to 2 km inland. Depositional processes on the foresets were dominated by sediment gravity flows originating from hyperpycnal river flow and gravity induced slumps. Slumps may originate at any depth on the fan delta foreset and are common in the deposits. Foreset beds are interpreted as the deposits of sediment gravity flows with preserved foreset beds that are preserving normally graded, inversely graded or massive, and change abruptly laterally and down slope.
Gravity induced slumps are the dominant mode of deposition on the foresets along the Conway Coast and presumably all Gilbert-type fan deltas. This study concludes that the sediment gravity flows developed basal traction carpets as evidenced by the regular appearance of !25° imbricated clasts in nearly all foreset beds. Behind slump deposits, there is a strong zone of ‘backstacking’ clast fabrics that prograde upslope into backset beds. These clast fabrics provide information about downslope slumps. Excellent exposures of distal foreset and nearshore marine deposits show the dynamic interface within a fan delta complex.

© 2006 Elsevier B.V. All rights reserved.

Keywords: Fan delta; Clast imbrication fabric; Debris flow; Sediment gravity flows; Turbidity currents; Submarine slumps; Foreset processes; New Zealand

0037-0738/$ - see front matter © 2006 Elsevier B.V. All rights reserved.
doi:10.1016/j.sedgeo.2006.05.026

CHAPTER 5 DATING TECHNIQUES & APPLICATIONS

5.1 INTRODUCTION

The coastal terraces along the Conway Flat coast have been interpreted a number of different ways by previous authors, particularly regarding chronology and uplift. Such differences chiefly arise from ambiguities in defining the spatial extent and lateral correlation of terraces with deposits north of the Hundalee Fault. The tectonic effects of spatially variable uplift rates and the local development of fault-related highs and lows also prevent a straight elevation correlation over wide-spread distances.

New Optically Stimulated Luminescence (OSL) and ^{14}C data was acquired in this study and reviewed alongside previous age determinations as part of the multidisciplinary approach to studying Conway Flat. Although not a principal objective of the thesis, the age dating in this study is one of the tools to understand the generation of the fan deltas and it provides some constraints and insight on erosion, uplift and deposition. Older dates used in this study were collected from the GNS Science Fossil Record electronic Database (FRED) to provide a broad identifier of the oldest rocks in the area. New samples and data targeted the Gilbert-type delta deposits and younger terrace deposits to better constrain uplift rates and erosion in the Quaternary along the Conway Flat coast. It was determined to collect multiple samples from the fan deltas to determine age and sediment yield. The locations of ^{14}C samples were selected to cross-check older dates from a previous study (Ota et al., 1984) and link to other deposits throughout the field area. In all, 12 new dates (5 OSL; 7 14C) are presented in this study. Obtaining more dates was prohibitively expensive.

The basic age range for the deposits of the Conway Flat region are 1) ~3-8 ka ^{14}C dates from the Podocarp paleoforest and associated sediments in the Ngaroma Terrace (Ota et al., 1984, 1996) and 2) Pliocene-Pleistocene macrofossil data from the mudstones underlying the Medina and Rafa Terraces (Suggate, 1965; Warren and Speden, 1978; Warren, 1995). Carbon 14 (^{14}C) is a reliable method for dating any woody material up to 50 ka, the approximate limit of the method. This method was elected for samples in the Ngaroma Terrace based on stratigraphic position and established dates (Ota et al., 1984). Based on cross-cutting relationships and facies changes, material > 50 ka were dated using Optically Stimulated Luminescence (OSL) the most viable option for dating the Rafa and Medina Terraces. Wood samples were also collected from these terraces and dated using ^{14}C to provide a cross-check by a readily available, inexpensive dating option.

Prior studies in the region (Ota et al., 1984; Hall, 2004) relied on age constraint data and interpretations mainly north of the Hundalee Fault (Chapter 2) from Kaikoura to determine uplift history for the Conway Flat coast (Ota et al., 1996). The research presented herein recognizes the tectonic complexity of the broader region and focuses on getting ages specifically from the terraces being uplifted along the Conway Flat coast to determine local tectonic development.

The ability to place age constraints on the deposits of the Conway Flat coast allowed for the detailed interpretation of facies architecture and reconstruction of the tectonic evolution. Multiple methods were used to determine the ages of sedimentary facies and therefore terraces present. Prior to this study only sparse age constraints existed for this segment of the Conway coast. Prior dates come from fossil samples collected during the mapping in the 1960's (Warren, 1995) and Carbon 14 (^{14}C) samples from wood samples

analysed in the 1980's by Ota et al. (1984; 1996). Hall (2004) analyzed samples by OSL but they did not return any usable dates.

Samples from previous studies appear to have been collected without any real understanding of their context in terms of depositional environments. In this study, by using multiple dating techniques in specific known sedimentary facies, not only are age constraints provided but the separation of depositional sequences can be determined. The use of multiple techniques in the same outcrop also provided a quality control on ages returned.

5.2 DATING TECHNIQUES

The reliable ages of the terraces coupled with the limits of age dating techniques, necessitated employing three different dating techniques including previously collected paleontological data from the Fossil Record Electronic Database (FRED) for New Zealand, ^{14}C, and Optically Stimulated Luminescence (OSL). All three types of samples for dating, including paleosamples, were collected to give a good geographic spread and to identify gaps in time across unconformities (Fig. 5.1). The detailed laboratory results from ^{14}C and OSL samples collected as a part of this thesis are provided in Appendix F. The information from these different methods provides constraints on the timing of events. The previously collected microfossils (formaminifera, nannofossils) and macrofossils (mollusca) are presented in Appendix F, combined with OSL dates, ^{14}C dates and geomorphic changes, are key in separating timing of deposition between the older muds and fan delta/nearshore marine deposits.

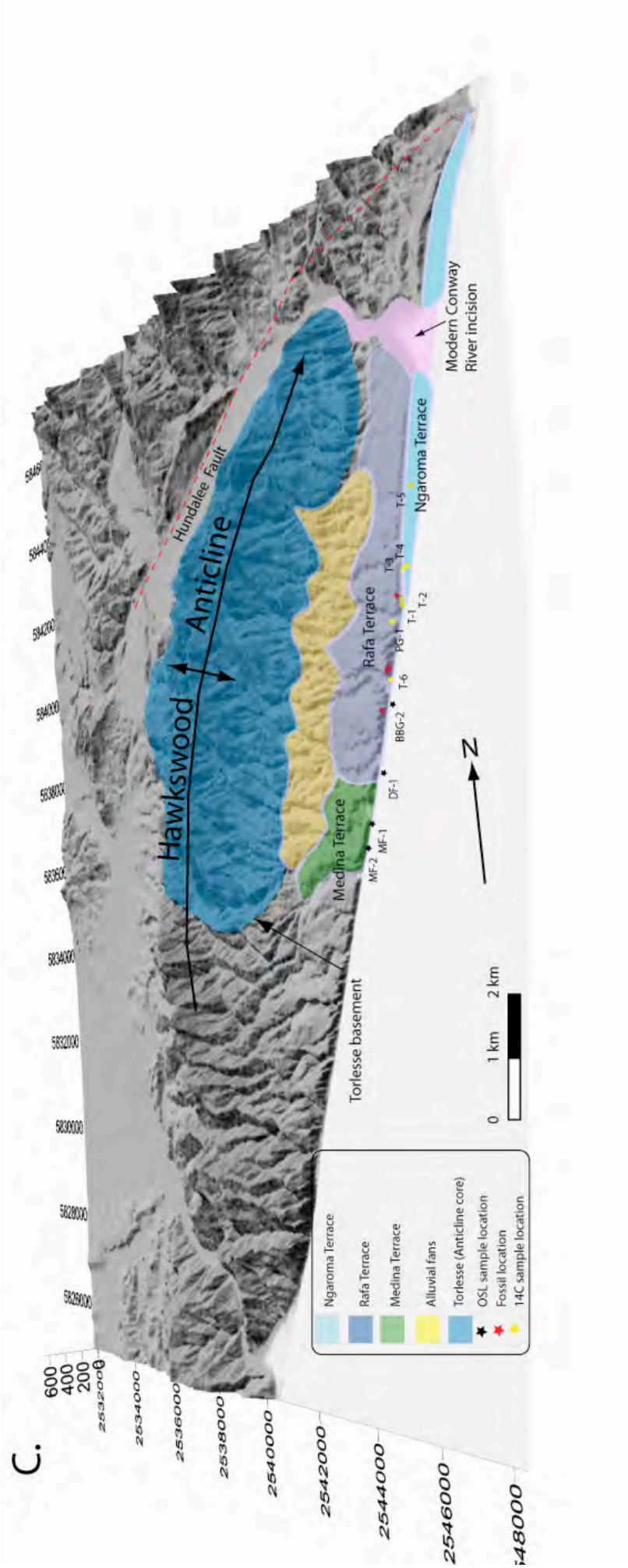

Figure 5.1. Location map of samples used for chronology collected for this study.

5.2.1 Macro and Microfossils

Paleontological data collected and stored by GNS Science (GNS) as part of the joint Geological Society of New Zealand and GNS Fossil Record File (FRED) combined with published maps (Warren, 1995) were used to place age constraints on the oldest rocks in the field area. The following samples were used to identify the oldest mudstones in the field area as being from the Pliocene – Pleistocene Greta Formation too old to date by ^{14}C (Fig. 5.2, Table 1). The fossils were all collected from the mudstones underlying the Rafa Terrace fan delta deposits and returned dates of 3-1.6 Ma (FRED-O32/f8632A and f8840). Isolated samples from the mudstones underlying the Medina Terrace fan deltas returned similar age brackets of Pliocene-Pleistocene (5.3 Ma- 1.5 Ma; Cooper, 2004). There are no catalogued fossil dates from within the Ngaroma Terrace. Samples collected from near the Ngaroma Terrace are from remnant Rafa Terrace deposits (Fig. 5.1).

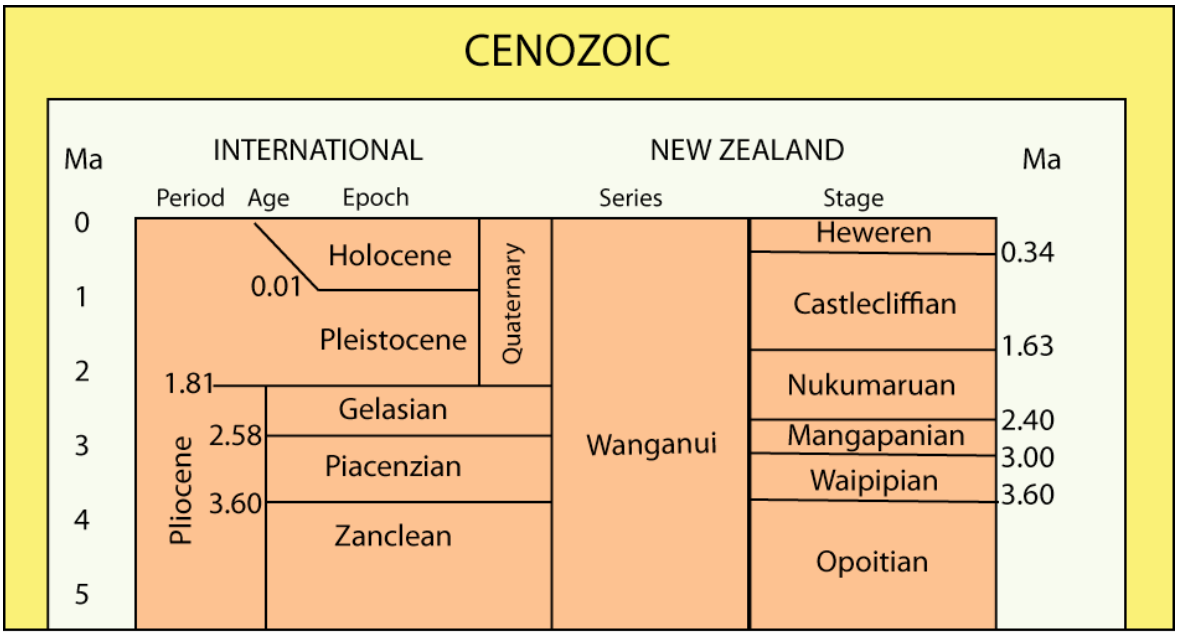

Figure 5.2 Pliocene to Quaternary geologic timescale showing New Zealand and International divisions (Cooper, 2004).

Table 5.1 Macro and microfossil dates collected from the Conway Coast. Data collected is from the IGNS FRED fossil catalogue. The complete record for each fossil Identification is provided in Appendix E.

Fossil ID-O32/f8632A (S55/f0632A)

Identified by: Beu, A.G.

Location–north of Ploughmans Creek in the Rafa Terrace

Age/Description- Mangapanian – Nukumaruan (3.0-1.63 Ma; Cooper, 2004), cold-water fauna including: *Chlamys delicatula, Paphirus largillierti, Axymene traversi, Cominella (Eucominia) nassoides otakauica, Zeacolpus (Stiracolpus) symmetricus*

Fossil ID-O32/f8628 (S55/f0628)-

Identified by: Scott, G. H.

Location – coastal cliff, north of Big Bush Creek in the Rafa Terrace

Age/Description- Waipipian (3.6-3.0 Ma; Cooper, 2004) on sparse forams, *Bulimina aculeate Nonion flemingi Notorotalia sp.* undifferentiated Tertiary on poor coccolith fauna

Fossil ID-O32/f8627 (S55/f0627)-

Identified by: Beu, A.G.

Location– north of Big Bush Gully in the Rafa Terrace

Age/Description- Waipipian to Nukumaruan (3.6-1.63 Ma; Cooper, 2004); on macrofossils, upper Waitotaran (Mangapanian) on foraminifera including: *Globorotalia inflata Notorotalia cf. finlayi Notorotalia sp.*

Fossil ID-O32/f8627A (S55/f0627A) –

Identified by: Beu, A.G.

Location - coastal cliff just north of Big Bush Creek in the Rafa Terrace

Age/Description - Waipipian – Nukumaruan (3.6-1.63 Ma; Cooper, 2004); Cold-water, outer neritic-upper bathyal molluscan fauna including: *Chlamys delicatula, Aeneator (Ellicea) orbita, Cominella (Eucominia) nassoides otakauica, Uberella aff. keyesi* n. sp., *Zeacolpus (Stiracolpus) symmetricus*

Fossil ID-O32/f8840 (S55/f0840) –

Identified by: Beu, A.G.

Location- coastal cliff south of Big Bush Creek in the Rafa Terrace

Age/Description- Mangapanian – Nukumaruan (3.0-1.63 Ma; Cooper, 2004); Mid-outer shelf fauna, cold-water including: *Anchomasa similes, Chlamys delicatula* Large. *Chlamys gemmulata, Paphirus largillierti, Pleuromeris hectori, Tawera cf. bollonsi, Axymene traversi Cominella (Eucominia) nassoides otakauica, Maurea punctulata stewartiana, Zeacolpus (Stiracolpus) symmetricus*

5.2.2 Optically Stimulated Luminescence Dating

Several samples were collected for the OSL dating technique. Due to expense, only five samples were submitted for dating. This technique was chosen for three reasons: 1) the ability to date material older than ~50 000 years, a drawback of the ^{14}C technique, 2) a cross-checking method for ^{14}C samples collected in the same deposits and 3) cross-checking the fossil ages.

The samples for OSL were all collected from sites with clean and dry and unstained outcrops well clear of the water table, as well as of leaching water. Samples were collected from multiple facies and terraces to determine timing of deposition. The chosen areas of sample collection were scraped clear to ensure that only fresh, previously unexposed, material was exposed. The samples were collected by driving a metal cylinder into the sediment with a mallet (Figs. 5.3 and 5.4).

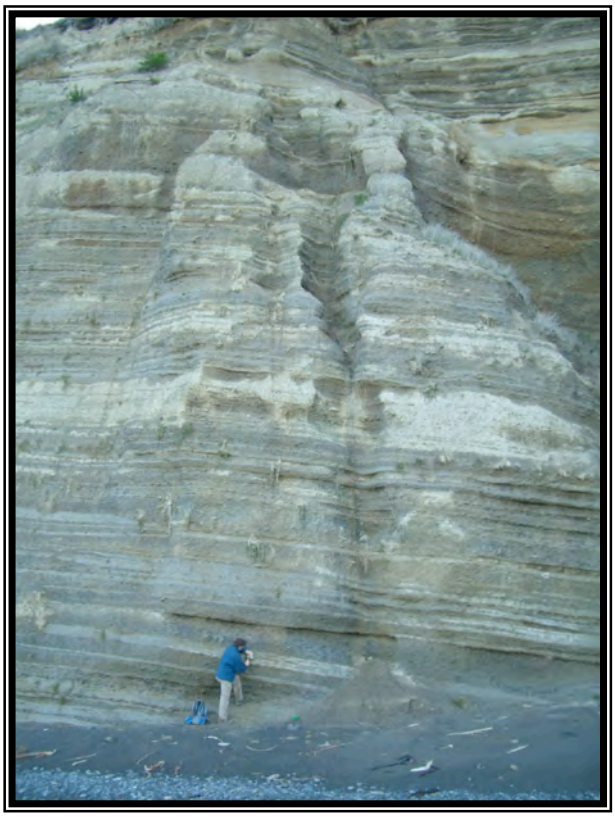

Figure 5.3 Collecting sample from Gilbert-type fan delta foresets for OSL dating. The sample is taken from a clean outcrop free from the influences of ground water or the sea. Scale: Person in foreground is 1.6 m.

Figure 5.4. OSL sample collected from Gilbert fan delta topset beds. Note the sample is covered in foil to prevent exposure to sunlight.

Once the material was collected into the metal tube the ends of the tube were wrapped in foil and taped closed (Fig. 5.4). The samples were then placed into a black bag and sealed with tape to prevent any possible exposure to light. The samples were posted as recommended by the lab to Victoria University in Wellington, New Zealand.

Five samples (laboratory code WLL549-WLL553) were submitted for OSL dating to Victoria University. The deposition ages were determined for the silt fraction of each

sample using methods proposed by Prescott and Hutton (1994). The palaeodose, i.e. the radiation dose accumulated in the sample after the last light exposure (assumed at deposition), was determined by measuring the blue luminescence output during infrared optical stimulation (which selectively stimulates the feldspar fraction). The dose rate was estimated based on a low-level gamma spectrometry measurement.

The dates for the following OSL analyzed samples place an absolute age on the Gilbert-type fan deltas where previously their age was loosely defined by widespread microfossils, macrofossils and ^{14}C samples collected from the older marine sediments below the fan deltas. Samples were collected from interbedded muds within the Gilbert-type fan deltas.

Table 5.2: Measured a-value and equivalent dose, dose rate and luminescence age for samples collected for O.S.L dating in this thesis. See figure 5.1 for sample locations.

Lab Sample #	a-value	D_e (Gy)	dD/dt (Gy/ka)	**OSL-age (ka)**	Field code	Terrace/ Facies
WLL553	0.077±0.015	448.3±9.6	4.74±0.25	**94.6±5.3**	MF2	Medina/ Fan delta
WLL552	0.094±0.024	440.4±11.8	4.70±0.42	**93.8±8.7**	MF1	Medina/ Fan delta
WLL551	0.095±0.027	387.3±10.3	4.22±0.35	**91.7±7.9**	DF1	Medina/ Fan delta
WLL550	0.067±0.005	346.6±7.0	4.39±0.17	**79.0±3.5**	BBG2	Rafa/ Fan delta
WLL549	0.119±0.006	223.6±12.8	4.27±0.27	**52.4±4.5**	PG1	Rafa/ Nearshore marine

The OSL dates from deposits in the Rafa Terrace all fall within the range ~79-52 ka. This time period represents the time of the Big Bush Gully fan delta formation. The younger ~52 ka sample collected from the Rafa Terrace represents the nearshore marine siltstones that were deposited next to, and in the protection of, the prograding Gilbert-type fan deltas.

The dates from the Medina Terrace fall within the range ~94.6-91.7 ka. This time period represents the deposition of the Medina Gilbert-type fan delta. The dates also provide information on the length of time required to produce multiple Gilbert-type fan deltas present in the field area. This duration of deposition is discussed below and gives insight into sediment supply and erosion rates along the Conway Flat coast.

5.2.3 ^{14}C dating

Based on the facies architecture and geomorphic mapping it is clear that the Ngaroma Terrace is younger than the timing of fan delta deposition. Ota et al. (1984) dated wood samples from the Ngaroma Terrace deposit and determined it was also younger than the Rafa Terrace deposits. All samples collected in this study for ^{14}C dating are wood and were collected from *in situ* tree stumps and large tree branches of the Ngaroma Terrace and inset fluvial terraces. The samples were prepared by Waikato Radiocarbon Laboratory in the following way: 1) Surfaces were scraped clean. 2) The wood was chopped up into small splinters and washed in an ultrasonic bath. 3) Samples were washed in hot 10% HCl, rinsed and treated with hot 1% NaOH. The NaOH insoluble fraction was treated with hot 10% HCl, filtered, rinsed and dried. Results were given in *Conventional Age or % Modern* as per Stuiver and Polach, (1977). These results are based on the Libby half-life of 5568 yr with correction for isotopic fractionation applied. Quoted errors are 1 standard deviation due to counting statistics multiplied by an experimentally determined Laboratory error multiplier of 1. The isotopic fractionation, $\delta 13C$, is expressed as ‰ wrt PDB. Several samples have been dated from the estuary deposits north of Ploughmans Creek in this study. The wood samples are mainly derived from the Podocarp paleoforest rooted in the estuary gravels. However, samples from inset fluvial channels were also collected to help constrain the duration of the estuarine environment and subsequent inset terrace formation.

The samples collected by this study for ^{14}C analysis and associated resulting ages, as well as those samples for ^{14}C analysis and ages provided by other authors (Ota et al., 1984; Suggate,1965) are shown in Table 5.3.

Table 5.3: ^{14}C dates collected from the Conway Flat coast

Field Sample #	Location	Material	Lab Code	Age (years ka)	Terrace/deposits
*A-1	Ploughman Gap	wood; large tree piece	N-3266	3050 +/- 85	Inset / Debris Flow
*A-2	beach cliff	wood	N-3267	7350 +/- 105	Ngaroma / Estuary
*A-3	Ploughman Gap	wood; standing tree	N-3268	7670 +/- 90	Ngaroma / Estuary
*A-4	beach cliff	wood	N-3269	7730 +/- 120	Ngaroma / Estuary
*B-1	Fan Delta	wood	GaK-7923	3550 +/- 110	Inset / Debris Flow
*B-2	beach cliff	wood	GaK-7924	8300 +/- 200	Ngaroma / Estuary
*B-3	Ploughman's Gap	wood; standing tree	GaK-7925	8400 +/- 170	Ngaroma/Estuary
+577	beach cliff	wood	NZ-533	7360 +/- 110	Ngaroma/Estuary
+578	beach cliff	wood; standing tree	NZ-546	7750 +/- 90	Ngaroma/Estuary
T-1	Ploughmans Gap	wood; standing tree	13113	7526 +/- 47	Ngaroma/Estuary
T-8	Ploughmans Gap	wood	13114	3050 +/- ??	Inset/Debris Flow
PG-	Ploughmans Gap	wood	1832	> 50, 000	Rafa Terrace/Nearshore
T-3	Ploughmans Gap	wood: standing tree	13115	7252 +/- 49	Ngaroma/Estuary
T-4	Ploughmans Gap	wood; standing tree	13349	7791 +/- 55	Ngaroma/Estuary
T-5	Ngaroma Farm	wood; large tree	13350	6437 +/- 52	Ngaroma/Estuary
T-6	Big Bush Gully	wood; large tree piece	13351	7998 +/- 55	BBGNgaroma/Estuary

* A-1-B-3 (Ota et al., 1984); + 577 and 588 (Suggate, 1965); T-1- T-8 and PG-1 (McConnico and Bassett, 2007)

The samples clearly date the estuary deposits, Podocarp paleoforest and the broader Ngaroma Terrace to the Holocene (~11.5 ka-Present). This dispersal of estuary deposits, based on the ages of existing Podocarp forests, at major drainages along the Conway Flat coastline suggests the possible existence of an extensive estuary system from the Conway River south to at least Big Bush Gully (Table 5.3). This may take the form of a system of independently forming estuaries within drowned creek mouths.

An interesting observation from this study is the difference in ages between the ~8.5 ka estuary deposits and the ~3 ka inset debris flow channel (Fig. 5.5). The age bracket from these two deposits provides a powerful tool to calculate uplift rates for the Holocene. The existence of the downcutting debris flow channels above the estuary deposits poses an interesting problem when dealing with uplift and sea- level changes. This problem is discussed later in this chapter.

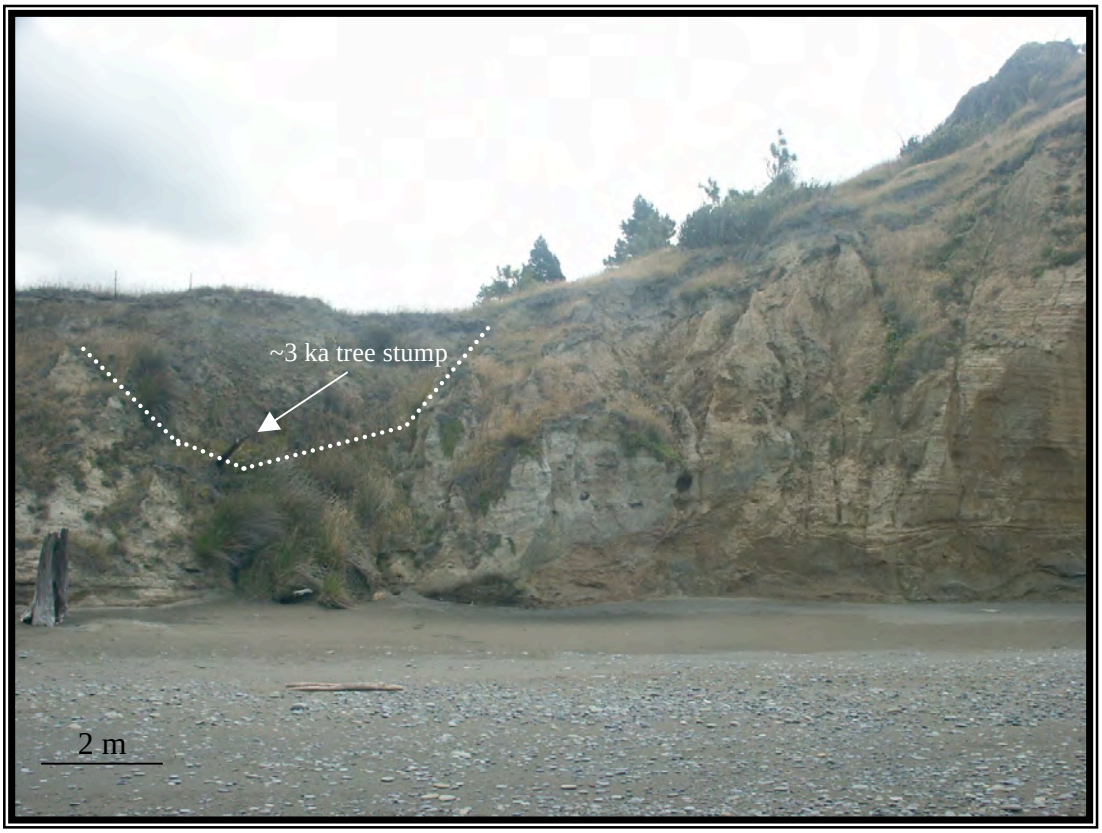

Figure 5.5 Photograph downcutting debris flow channel containing a wood stump dated ~ 3 ka (Sample T-8 incised in the Ngaroma Terrace at 2 m above sea level). This sample indicates that there was a minor sea level drop, or change in sediment supply and/or subsidence, ~ 3 ka causing incision into the Ngaroma Terrace.

5.3 INTERPRETATION

The age data presented here helps provide a framework for the development of Conway Flat coast.

1) The fossil data suggests that the pre-faulting and uplift deposits along the Conway Flat coast were mudstones from cool water, upper bathyal conditions that were deposited in relatively quiescent conditions (Warren, 1995). Since there is no coarse material, this suggests that uplift of the Hawkswood Range as a significant topographic feature didn't start until after the deposition of the Greta mudstones in the Pliocene. The fossil data does indicate there must have been an extended period of uplift and erosion of the Greta Formation (3 Mya-1.6Mya) to create accommodation space prior to the deposition of the Medina Gilbert-type fan delta at ~ 95 Ka.

2) In the Conway Flat area, the three OSL dates from the Medina Terrace and influx of coarse grained fan delta deposits indicate deposition from new source in the Hawkswood Range ~ 95 ka. The deposition of the Medina Gilbert-type fan delta following the extended period of erosion indicates that uplift during this time slowed, allowing for deposition.

3) The two OSL dates from the Rafa Terrace Gilbert-type fan delta and Nearshore marine deposits have a range of 79-52 ka. Perhaps the most interesting information to come out of the samples is from the Nearshore marine deposits and sample WLL549 dated to ~52.4 +/- 45 ka (Fig. 5.6). This sample, collected from the nearshore marine deposits south of Ploughmans Creek, is juxtaposed with older Gilbert-type fan delta deposits dated as > ~ 79 ka. It is interpreted here that these dates, along with sedimentary facies contacts, confirm that the ~79 ka fan delta deposits and ~52 ka nearshore marine deposits were coeval with the Big Bush Gully fan delta (Fig. 5.1). This interpretation is supported by the fact that the age returned for the nearshore marine deposits was younger than the fan delta. The age data supports the idea proposed in chapter 3 that the nearshore marine deposits stacked up in the shelter of prograding fan deltas. The age of the nearshore marine deposits was also

cross-checked by sample T-7, a ^{14}C sample, that indicated an age of > ~ 50 000 yrs age for the same deposits. The cross-checking of dating methods was done to validate the data.

It is important to acknowledge that gap in age dates from, ~79 - ~52 Ka could also indicate a sea-level change. This is supported by the juxtaposition of the fan delta and nearshore facies. However, the lack of erosional boundaries and interbedded gradational contact between the two facies does not support this conclusion.

4) ^{14}C dates from the Ngaroma Terrace estuary deposits and other inset fluvial terraces located at the creek mouths indicate ages between ~ 8.4- 6.4 ka. Age dates gathered from estuary deposits along the beach (T-1 to T-6; excluding T-5), from Conway River to Big Bush Gully, all returned ^{14}C dates < 8 ka. The existence of similar dates along the coast when combined with sedimentary contacts of marine deposits suggests that an extensive estuary system existed north of Ploughmans Gap and smaller estuaries at the mouths of streams south along the Conway Flat coast at this time. Although distances up to 1 km separate the deposits, this interpretation is supported by the geomorphic consistency of low-level terrace features at the minor creek mouths and ^{14}C dates.

The exposed Podocarp paleoforest within the Ngaroma Terrace probably suffered a rather unceremonious death. Dates range from ~ 6.5– 8.5 ka (Ota et al. 1984; McConnico and Bassett, 2007) collected from *in situ* paleotree stumps within the estuary deposits of the Ngaroma Terrace and geomorphic evidence including beach ridge morphology exposed within the Ngaroma Terrace provide keys to unlocking the events leading to the demise and burial of the paleoforests located in multiple drowned creek mouths. This is the environment we find trees growing in the multiple creek mouths today.

Figure 5.6 Photograph of nearshore marine facies. OSL sample collected from the base of this outcrop. The sample data from this outcrop suggests it is possible these deposits developed in the protection of prograding fan deltas; perhaps in a nearshore embayment setting.

It is interpreted here that at a time when sea-level rise out paced uplift, the beach ridge of the Ngaroma Terrace was probably breeched during the Holocene. This breeching caused the rising tide to inundate the paleoforest, slowly killing the trees. The younger Podocarp paleoforest exposed 400 m inland in the Ngaroma Terrace also supports this progressive death by gradual drowning hypothesis. These inland stumps are ~1000-2000 years younger and are representative of the paleoforest shifting further inland with the increased encroachment of the sea over a ~2 ka period.

5) Surprisingly young dates of ~3 ka came from the incised Ngaroma Terrace. These are the same as other incised/inset terraces in Dawn, Big Bush, and other minor creek mouths

based on comparison of elevations. Multiple terraces imply some sort of single controlling event (e.g. sea level change) to create multiple coeval incisions followed by deposition. The consistent elevation of the terraces located in the various creek mouths helps identify these as separate events from the significantly higher elevation, aggradational inset terraces inland (Chapter 3).

5.4 DEGRADATION AND UPLIFT RATES

5.4.1 Sediment Yield and Fan Delta Progradation

The similarity in ages between OSL samples WLL551-553 collected from the Gilbert-type fan delta of the Medina Terrace suggests us that the deposition of the Medina fan delta occurred over a short period in the range of 91-94 ka. Although the time period seems short, it is plausible based on a simple sediment yield calculation and the +/- errors in the dates. The "sediment yield", which is the flux of sediment exiting the lower end of a drainage basin normalized to the area of the catchment, is defined as mass/[(area)(time)] or volume/[(area)(time)]. This equation reduces to distance/time, and, since volume/area is vertical, this gives a vertical erosion rate averaged over the area of the catchment. Bull and Knuepfer (1987) used the term degradation rate to describe variations in sediment yield for the Charwell River near the Hope Fault in Late Quaternary time and the same approach is taken here:

(1) Volume of sediment is the area x thickness. The estimated average area of each delta is the width of the Medina surface (Fig. 5.1) measured perpendicular to the coast (~1.5 km) times the average spacing between streams measured parallel to the coast (~1 km). The thickness is the average height of the Medina fan delta as measured from outcrop

exposures (~45 m). Volume = area x height = 6.75 x 10^7 m^3. This is a minimum estimate for the average volume of sediment that came out of the catchments during a given period, since it can be figured that some sand bypassed the preserved delta deposits and that the coast has eroded back into the deposits.

(2) Duration of time is bracketed between the oldest known age for the Medina fan delta foresets (~95 ka) and the age of the youngest Medina fan delta deposits (~91 ka). This gives 4 kyrs for deposition of the deltas, with some time added as it must be taken into account that these samples are neither the oldest nor youngest material in the fan delta.

(3) Average area of the catchments is measured by tracing the divides, or locations where flow directions diverge, between the catchments. This yields an average catchment size of ~ 4 km^2.

(4) The calculation: 6.75 x 10^7 m^3 of sediment per delta was produced in ~ 4 kyrs. This equals 1.69 x 10^7 m^3 / kyr. Divide this by 4 x 10^6 m^2 (area of the catchments) and you get 4.25 m/kyr vertical degradation rate for an average catchment. This assumes that the "average" deltas were fed by the "average" catchments. This is a valid assumption because of the regular size and spacing of the catchments (*Dorsey, personal communication, 2004*). A ~ 4 m/kyr degradation rate is a good estimate.

Although 4 mm/yr is a rapid erosion rate, it is typical for the Marlborough region. Bull and Knuepfer (1987) calculated degradation rates for the Charwell River that ranged from < 4 m/kyr to 30 m/kyr and then dropped to ~1 m/kyr since 4 ka. Therefore, the degradation rate calculated for the small catchments that fed the Conway Flat coast fan deltas is similar to what you would expect for this tectonically active part of the New

Zealand coast and therefore completely possible for a < 4 kyr period. More importantly, when this data is combined with clast lithology data (Chapter 3) it is clear that the source for the fan delta deposits is the uplifted core of the Hawkswood Range. Clast lithology and imbrication data from the streams of the Hawkswood Range confirm a consistent, local, source for the Gilbert-type fan deltas (Chapter 3, Fig. 3.4).

5.4.2 Uplift Rates

The North Canterbury region of New Zealand has been the focal point of uplift studies in the past as researchers try to understand the actively deforming plate boundary transition zone (Ota et al.,1984; Nicol et al., 1995; Pettinga et al., 2001; Hall, 2004). Three studies on the uplift rates of the east coast have been conducted within the Conway Flat region, Ota et al. (1984, 1996) and Hall (2004). These studies were part of larger projects that lumped the Conway Flat coast into a larger region of terraces encompassing areas as far north as Kaikoura. The larger region crosses several major active oblique thrust and strike-slip faults and covers several structural domains (Fig. 2.3 from Chapter 2). Ota et al. (1984, 1996) established an uplift rate for the areas south of the Conway River at >2 m/ka based on ^{14}C dates collected from a series of uplifted terraces north of the Conway Flat coast. Both Ota et al. (1984, 1996) and Hall (2004) correlated the dated terraces with those of the Conway Flat coast despite crossing several mountain ranges and fault zones. Therefore both arrived at similar calculations for the uplift rates.

This study focussed on determining uplift rates specific to the Conway Flat coast and used a more detailed approach for calculating the uplift rates based on dates collected from the uplifted terraces themselves. Detailed sedimentological work, geomorphic mapping and facies architecture allow for a more reliable uplift rate model and calculations through

time. It was only through the use of all these means that the upper “terraces” were identified as not being the same marine terraces as those to the north near Kaikoura as proposed by Ota et al. (1984) and used in Hall’s (2004) thesis. Through geomorphic mapping and sedimentology, these were clearly defined as terraces created by the underlying structure and day lighting of thrust faults of the Hawkswood Thrust Fault Zone (HTFZ). The upper "terrace” features along the east flank of the Hawkswood Range are the geomorphic surfaces created by the displacement of alluvial fans by the propagating thrust faults of the HTFZ. Ota et al. (1984) previously described the geomorphic surfaces of these terraces simply as uplifted marine terraces. It is likely that the Hawkswood Fault is a splay of the Hundalee Fault, and more importantly, is the first in a series of eastward propagating thrust faults of the greater Hawkswood Thrust Fault Zone (HTFZ) introduced in Chapter 2.

This same approach and understanding of the structure, geomorphology and sedimentology also led to the recognition of the series of stacked deltas that created a series of varying coastal terraces which reflect the underlying tri-partite fan delta stratigraphy. The uplift rates presented below are for each terrace and represent the uplift rates at particular times based on dates collected from the various facies within the terraces (Fig. 5.7).

Medina Terrace

Of the terraces identified in this study, the Medina Terrace is the oldest dated between ~94 ka -91 ka. Using the formula below, an approximate uplift can be calculated based on the difference in the new location of the topset beds and the sea-level at the time of deposition:

“uplift” distance relative to sea level/sample age

During the formation of the Medina Terrace relative sea level was ~130 m lower than present (Chapter 6; Fig. 6.5) and therefore the uplift rate is calculated at ~1.42 m/Ka for

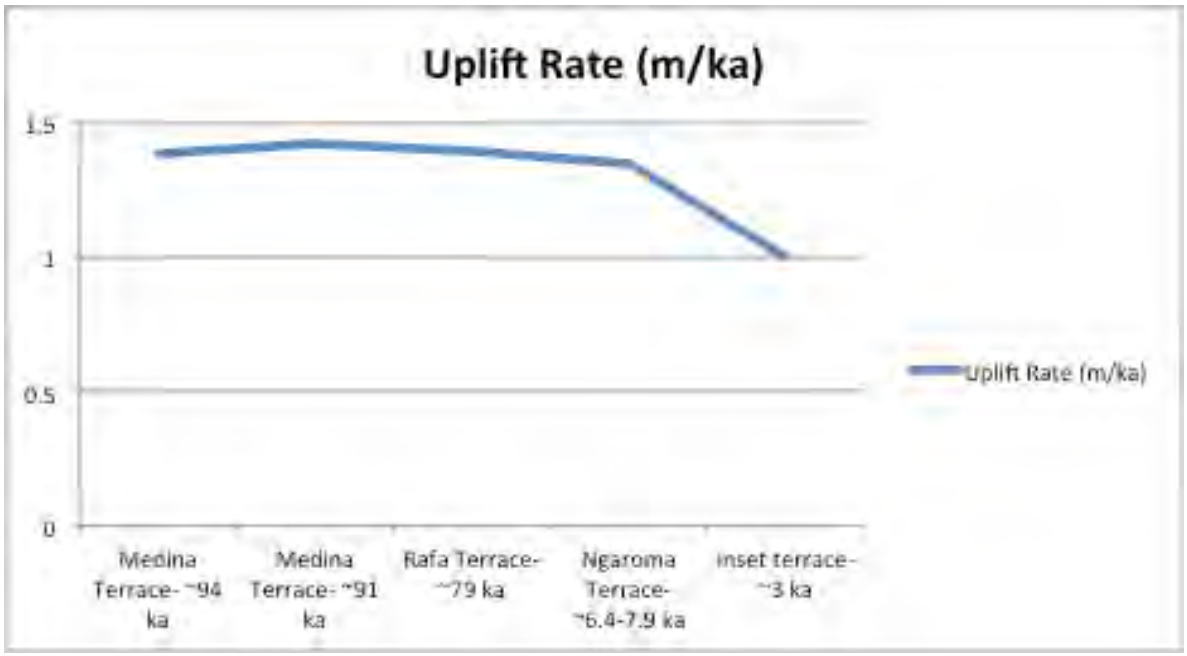

Figure 5.7 Chart showing the uplift rates of the Conway Flat coast through time. The uplift rate for the Ngaroma Terrace was determined by dividing the average location relative to sea level for the samples (10 m) divided by the average age of the sample (7.4 ka).

the oldest sample WLL-553 and ~1.38 m/Ka for the younger ~91 ka, sample WLL-551 (Fig. 5.7).

The limited data suggests there was an increase in uplift rate at the initiation of fan delta but that this rate remained fairly constant during the formation of the Medina Gilbert-type fan delta. This might suggest that the controlling factor in the depositional patterns of the fan deltas was sea level. Dorsey and Umhoefer (2000) concluded a similar interpretation for Gilbert-type fan delta deposits in the Loreto Basin and used the same method to determine uplift rates of Gilbert-type fan deltas in a tectonically active region.

Rafa Terrace

During the formation of the Rafa Terrace, relative sea level was ~110 meters lower than present day sea level. The Rafa Terrace contains two dates that provide information on the uplift rates of two facies: 1) Gilbert-type fan deltas and 2) nearshore marine deposits. Based on sample localities, sea level curves (Chapter 6; Fig. 6.5), age dates and the formula discussed above it was calculated that the Gilbert fan delta material of the Rafa Terrace records an uplift rate for sample WLL-550 of 1.39 m/ka (Fig. 5.7). The accumulation rate for the nearshore marine environment is 2.6 m/ka.

This information tells us that the initiation of the Rafa Terrace fan delta deposition was probably caused by changes in sea level, as the uplift rate is similar to that of the previous fan deltas. The accumulation rate of ~ 2.6 m/ka from the nearshore marine environment is interesting. Perhaps this is the signature for increased tectonic activity in the region.

Ngaroma Terrace

The Ngaroma Terrace contains dates that are from ~8 ka to ~6 ka. These dates, when combined with the sea level curves from the Holocene (Chapter 6; Fig. 6.4) and position relative to current sea level, results in uplift rates between ~1-3 m/ka. The exact quantification of uplift rate is difficult as the sea level during the time of the Podocarp paleoforest could have been anywhere from ~5-15m lower than present day sea-level (Chapter 6; Gibb, 1986). An approximate uplift rate is provided using the average age of the samples (7.4 ka) and relative sea level (10 m). The results of these calculations indicate the uplift rate of the Ngaroma Terrace at 1.35 m/ka (Fig. 5.7).

The uplift rate of the Ngaroma Terrace matched sea level rise during the Holocene. Ages ranging from ~8 – 6 ka for the Podocarp paleoforest rooted in estuary deposits alongside

the ocean support this. However, the gradual younging of Podocarp tree trunks inland, also tells us that from ~8 ka - ~6 ka sea-level rise began to outpace uplift and sedimentation rates. Thus the overall calculation of uplift rate is tricky because of the uncertainty around sea level rise and retrogradation of facies. We do know that uplift rates around 1.35 m/ka continue into the Holocene.

The uplift rate is further supported by the wood sample T-8 (3 ka) from the inset terrace. The samples uplifted location relative to sea level (3 meters) when divided by the samples age (~3 ka) indicates that uplift during the Holocene slowed to ~1 m/ka around 3 ka (Fig. 5.7).

5.5 SUMMARY

This study provided the first dates from within the Gilbert-type fan deltas along the Conway Flat coast by using OSL dating techniques. Locations were selected for the OSL and ^{14}C dates in this study based on prior dates and appropriate sample material. From these samples, the OSL dates suggest the development of multiple fan delta complexes along the Conway Flat coast during sea-level fluctuations and steady tectonic uplift. Earlier age dates from deposits along the Conway Flat coast were gathered by original mappers in the area and logged in the GNS Science database FRED. Sample fossil locations from along the coast yielded dates of Pliocene-Pleistocene (Waipipian -Nukumaruan, 3.6-3.0 Ma) for the older marine rocks underlying the fan deltas in the southern part of the field area.

A sequence of events determined by new data presented here confirms that the deformation along the Conway Flat coast is independent of the timing of deformation

north of the Hundalee Fault at Kaikoura (Ota et al., 1996; Hall, 2004). This is a new and significant addition to the knowledge of North Canterbury tectonic development. Based on results from data collected here and that of previous studies, the age data tell us:

1) the initiation of concentrated faulting at the Conway Flat coast was prior to ~ 94ka. The initiation of uplift and erosion was long enough to uplift and erode rocks down through deep marine rocks of the Greta Formation.
2) the ages of the oldest fan delta compared to the Greta Formation support the existence of an extended and significant period of erosion before deposition of fan delta material. The comparison of dates supports faulting in the area was initiated much earlier in the sequence than deposition of the relatively shallow Gilbert-type fan deltas.
3) uplift of the Hawkswood Range slowed down ~95ka allowing deposition of the Medina Gilbert-type fan delta to occur.
4) nearshore marine deposits in the Rafa Terrace were coeval with to slightly younger than prograding Gilbert-type fan deltas, suggesting the nearshore marine deposits formed in the lee of the prograding fan delta.
5) a large Podocarp paleoforests existed extensively inland and are discontinuous from the Conway River south to at least Big Bush Gully. These paleoforests were a victim of sea level rise as ages confirm a progressive younging of the trees inland.
6) the Hawkswood Range's catchment sizes were large enough to produce Gilbert-type fan deltas along the Conway Flat coast. This is supported by documented erosion rates for the Marlborough region.
7) that Holocene uplift rates matched sea level rise (1-3 m/ka) for most of the Holocene based on estuarine stratigraphy.

8) Although Ota et al. (1996) and Hall (2004) conclude that the reason for uplift is the result of local structures, they were quick to lump the east coast, south of Kaikoura, into one continuous structural section. In actuality what this study has shown is the complex fault zones within North Canterbury make the generality that structures north of the Hundalee fault are related to the HTFZ impossible. Although uplift rates are similar, this study provides the data to chart uplift through time that is linked with confidence by detailed sedimentology, and geomorphic and structural analysis of a complex localized fault zone (Fig. 5.7). This supports that the HTFZ and associated terraces formed independently of any terraces north of the Hundalee Fault.

5.6 REFERENCES

Bull, W.B, Kneupfer, P.L., 1987. Adjustment by the Charwell River, New Zealand to uplift and climate changes. Geomorphology 1, 15-32.

Cooper, R.A., 2004. New Zealand Geological Timescale 2004/2 wallchart. Institute of Geological and Nuclear Sciences information series 64.

Dorsey, R. J., and Umhoefer, P. J., 2000. Tectonic and eustatic controls on sequence stratigraphy of the Pliocene Loreto basin, Baja California Sur, Mexico, Geological Society of America Bulletin 112, 177–199.

Gibb, J.G., 1986. A New Zealand regional Holocene eustatic sea-level curve and its application to determination of vertical tectonic movements, Royal Society of New Zealand Bulletin 24, 377-395.

Hall, L., 2004. Cenozoic deformation at the southern end of the Hikurangi margin, New Zealand, unpublished Ph.D. Thesis, University of Oxford, England.

Holbrook J., Schumm S. A., 1999. Geomorphic and sedimentary response of rivers to tectonic deformation: a brief review and critique of a tool for recognizing subtle epeirogenic deformation in modern and ancient settings. Tectonophysics 305, 287–306.

McConnico, T.S. and Bassett, K.N., 2007. Gravelly Gilbert-type fan delta on the Conway Coast, New Zealand: Foreset depositional processes and clast imbrications, Sedimentary Geology 198, 147-166.

Nicol, A., Cowan, H., Campbell, J., Pettinga, J. 1995. Folding and the development of small sedimentary basins along the New Zealand plate boundary. Tectonophysics 241, 47-54.

Ota, Y.Y., Torao; Iso, N., Okada, A., Yonekura, N., 1984. Marine terraces of the Conway coast, South Island, New Zealand. New Zealand Journal of Geology and Geophysics 27, 313-325.

Ota, Y.Y., Pillans, B. Berryman, K., Beu, A., Fujimora, T., Miyauchi, T., Berger, G., Climo, F.M., 1996. Pleistocene coastal terraces of the Kaikoura Peninsula and the Marlborough coast, South Island, New Zealand. New Zealand Journal of Geology and Geophysics 39, 51-73.

Pettinga, J.R., Yetton, M.D., Van Dissen, R.J., Downes, G., 2001. Earthquake source identification and characterization for the Canterbury region, South Island, New Zealand, Bulletin of the New Zealand Society for Earthquake Engineering 34, 282-317.

Prescott, J.R., Hutton, J.T., 1994. Cosmic ray contributions to dose rates for luminescence and ESR dating: large depths and long-term time variations, International specialist seminar on thermoluminescence and electron spin resonance dating 7, Krems 23, 497-500.

Stuiver, M., Paloch, H.A., 1977. Discussion: reporting of 14C data. Radiocarbon 19, 353-363.

Suggate, R. P., 1965. Late Pleistocene geology of the northern part of the South Island, New Zealand, New Zealand Geological Survey bulletin 77, 91 p.

Warren, G., Speden, I., 1978. The Piripauan and Haumuriati stratotypes (Mata series, upper Cretaceous) and correlative sequences in the Haumuri Bluff district, south Marlborough, New Zealand Geological Survey bulletin 92.

Warren, G., 1995. Geology of the Parnassus area. Lower Hutt, Institute of Geological and Nuclear Sciences, Institute of Geological and Nuclear Sciences geologic map 18, 36p.

CHAPTER 6 SEQUENCE STRATIGRAPHY

6.1 INTRODUCTION

The fan delta sequence along the Conway Flat coast provides a rare opportunity to gain insights into the depositional and geomorphic characteristics of paralic marine sediments in an active tectonic setting. Significantly, this appears to be a rare study that records coseismic events uplifting and preserving marine Gilbert-type fan deltas.

The Conway Flat coast lies within an active transpressive plate-boundary zone. The main fault in this area the Hawkswood Thrust Fault Zone (HTFZ), has been absorbing relative NW-SE plate movement of the Pacific Plate during the Pleistocene (Nicol et al., 1995). The modern phase of thrust faulting has resulted in the deposition, uplift and erosion of the Medina, Dawn, Big Bush Gully fan deltas and the modern Conway fan delta/estuary systems, creating an archive ideal for studying the connections between the geomorphology and active tectonics using sequence stratigraphy (Fig. 6.1).

Along the Conway Flat coast the preserved sequences have resulted from the complex interaction of regional uplift, local fault movements, eustatic sea level changes, and fluctuations in sediment supply. In areas where all of these conditions are constrained researchers have been able to resolve the contribution of each on basin architecture (Dorsey et al. 1997; Saul et al., 1999; Massari et al., 2002; Di Celma et al., 2005; Cantalamessa et al., 2006).

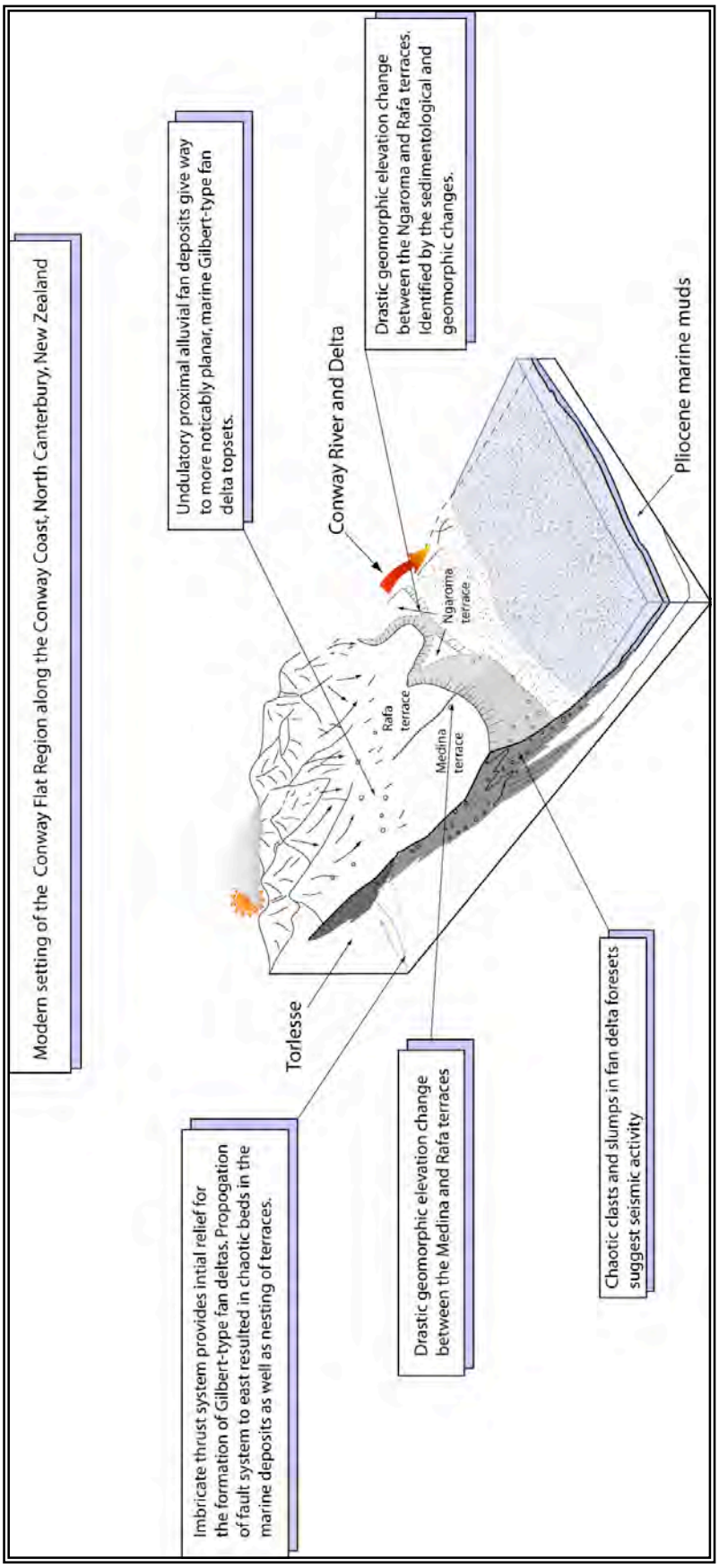

Figure 6.1. Modern setting of the Conway Flat Region. The block diagrams show a schematic setting of the depositional environment and tectonic setting.

In tectonically active marine basins, accommodation is controlled by the interplay between rate of subsidence (or uplift) and fluctuations in eustatic sea level and sediment supply. In settings similar to the Conway Flat coast study area, rapid subsidence may exceed rates of sea-level rise and fall. In such settings, preserved stratigraphic cyclicity may record continuous creation of accommodation modulated by the effects of high-frequency eustatic fluctuations (Gawthorpe et al., 1994, 1997; Dart et al., 1994; Hardy and Gawthorpe, 1998). Although the range of processes that can influence stratigraphy in tectonically active basins is generally well known, identification of those processes based on interpretation of the stratigraphic record is, at times, difficult and commonly is hindered by lack of adequate age controls on syntectonic strata.

Pioneering studies of Gilbert-type fan deltas in active tectonic settings were completed by Colella (1988), Nemec and Steel (1988) and Colella and Prior (1990) and Gawthorpe and Colella (1990). These studies relied on the assumption of rapid subsidence for basin formation and syntectonic deposition of fan delta material for basin fill. It was not until Dorsey et al. (1995) introduced detailed chrono- and bio-stratigraphy in Gilbert fan deltas in the Loreto Basin, Baja California, that rapid basin subsidence was proven. That study was not only the first to provide detailed information on the rate of basin subsidence but also provided data on the rate of fan delta development in a transform-rift system. Dorsey and Umphoefer (2000) continued research in the Loreto Basin detailing the links between stratigraphic sequences and active tectonics. The use of detailed sedimentology of non-marine and marine sediments in this transtensional plate boundary provided key answers to questions about the tectonic development of the Loreto Basin. The availability of high resolution dating in the parasequences of the Loreto Basin allowed the researchers to distinguish eustatic from tectonic controls on the sedimentary deposits.

The analysis presented in this study of the Conway Flat coast focuses on a basin in a compressional setting, and is useful for comparison with other studies in similar, tectonically active basins where high-resolution age dating may not be possible, and where geomorphic and stratigraphic markers can be used to piece together the tectonic history. Significantly, this study provides detailed analysis of Gilbert-type fan delta deposits in a compressional regime with thrusts providing the local relief at the fan apex.

6.2 CONWAY FLAT COAST STAGES OF DEVELOPMENT

Detailed study of map-scale stratal geometries, lithofacies, stratigraphic and geomorphic bounding surfaces (Chapter 4), and sequence stacking patterns has enabled the development of a sequence-stratigraphic framework for interpreting the basin history. Figure 6.2 shows the interpretation of five stages of incision followed by infill with fan delta deposits (Chapter 3). The five stages are listed below:

Ia. Incision into Pliocene marine mudstones. The Pliocene marine mudstones are crosscut by the Medina fan delta deposits indicating an initial erosional event marking the onset of multiple unconformities alternating with coarser deposits in the area.

Ib. Development of the Medina Terrace. The Medina Terrace is the oldest (~95-~91 ka) and highest in the study area. The progradation of the Medina fan delta infills the valleys created by incision into the Pliocene marine mudstones. The fan delta foresets are as high as ~70 m indicating a steep drop-off into the ocean. The fan delta topsets were removed as the result of changes in uplift and/or sedimentation rate creating a wave-cut platform. This was unconformably overlain by thin alluvial fan deposits.

IIa. Incision into the Medina Terrace. Following this was an extended period of incision, relating to lowering of sea level or from changes in the uplift and/or sedimentation rate as shown by the large incised valleys in the Medina fan delta.

IIb. Development of the Rafa Terrace. The Dawn and Big Bush Gully fan deltas infill the valleys cut into the Medina Terrace and prograde basinward. The Rafa Terrace deposits indicate ages between ~79-~52 ka. The Dawn fan delta foresets are preserved in ~50 m cliffs and the total spatial distribution of deposits makes them the largest delta deposits observed along the Conway Flat coast. The deposits of the Rafa Terrace contain fan delta foresets with rarely described imbrication patterns (McConnico and Bassett, 2007), large amounts of slumps and liquefaction of nearshore marine deposits.

IIIa. Incision into the Rafa Terrace. This deposition of the Rafa Terrace is followed by an episode of incision, supported by crosscutting relationships of fan delta deposits and estuarine deposits and the associated cliff height changes. Both Ploughmans Creek and a deflected Conway River cut down into the Rafa Terrace leaving a remnant high between the two.

IIIb. Development of the inset terraces. A series of inset fluvial terraces are located next to the Rafa Terrace in many of the drainages along the Conway Flat coast. These fluvial deposits are the result of material being released from the upper catchment during large tectonic events. The smaller inset terraces preserved within the main drainages reflect the material released and brought down via streams as the result of large seismic events occurring during periods of incision or alternatively they could also be formed by minor incision/infill events. Although there in no age constraints on these terraces, the

geomorphic and sedimentological contacts along with elevation data differentiate these terraces from those found incised into the Ngaroma Terrace.

IVa. Incision into the inset terraces. This deposition of inset terraces is followed by an episode of incision down to the Ngaroma Terrace.

IVb. Development of the Ngaroma Terrace. Stage 4 involves deposition of Ngaroma Terrace estuarine facies, possibly lateral to a fan delta similar to the modern Conway fan delta/estuary, with an *in situ* Podocarp paleoforest at ~8.5-~6.4 ka years ago. The Podocarp paleoforest is rooted in the gravel deposits from the Conway River and probably existed until the barrier to the sea was breeched creating an environment unsuitable for the paleoforest. Subsequent fluvial and debris flow deposits from the Paleo-Conway River buried the tree stumps followed by drowning and deposition of the estuarine muds that comprise the cliff deposits north of Ploughmans Creek. Small fluctuations in sea level at 3 ka are recorded by an incised channel in the Ngaroma Terrace.

Va. Incision into the Ngaroma Terrace. The deposition of the Ngaroma Terrace (~5m) is again followed by a period of incision by the modern Conway River and the small creeks.

Vb. Development of the modern Conway Delta. Stage V represents the infilling of the incised valley by the modern fan delta of the currently prograding Conway River fan delta.

6.3 SEQUENCE STRATIGRAPHIC FRAMEWORK

The effects of tectonic control on sequence stratigraphic architecture are well documented in the literature (Gawthorpe and Colella, 1990; Heller and Paola, 1992; Dorsey and

Umhoefer, 2000; Jackson et al., 2005). The Conway Flat coastal section is a very sensitive system in which the interplay of tectonics and sea level change created active and inactive periods of fan delta construction and incision respectively. The apparent recorded times of rapid sea level falls could be explained by both periods of eustatic fall in sea level or by periods of episodic uplift associated with fault movement. There is ample evidence for syndepositional earthquakes including slumps and sediment liquefaction features in the fan delta foresets and nearshore marine deposits (Chapter 3).

It is important to note that the Conway Flat coast is an asymmetric basin caught in the active tectonic fault zone (HTFZ) of a broader deforming transpressional plate boundary. The main structural feature of the Hawkswood Range is an east verging thrust fault near the range divide (Chapter 2). This thrust fault splays to the east into several faults (Fig. 2.6). These are expressed most clearly in the geomorphology of the upper alluvial fans which are dissected all along the range front by eastward propagating thrust faults. The primary result of the dissection was the formation of terrace like features. Although the timing of the initiation of these faults is not known precisely, it is inferred that they were active prior to the formation of the Gilbert-type fan delta complexes to the south which began ~95 ka (see Chapter 5). Inherent to the exposed fan delta complex along the Conway Flat coast is the implicit requirement for fault driven uplift and abrupt changes in relief at the fan apices. The uplifted estuarine deposits with their dated rooted Podocarp paleoforest indicate that by ~8 ka the imbricate thrust system had shifted east, probably offshore as there is no evidence of surface rupture, where it has uplifted the estuarine deposits and continues to uplift the modern beach sediments (Chapter 2). The back tilting of the Ngaroma Terrace supports the structural model proposed in Chapter 2 and indicates the terrace is probably located in a hanging wall of the fault zone, which is now offshore. The

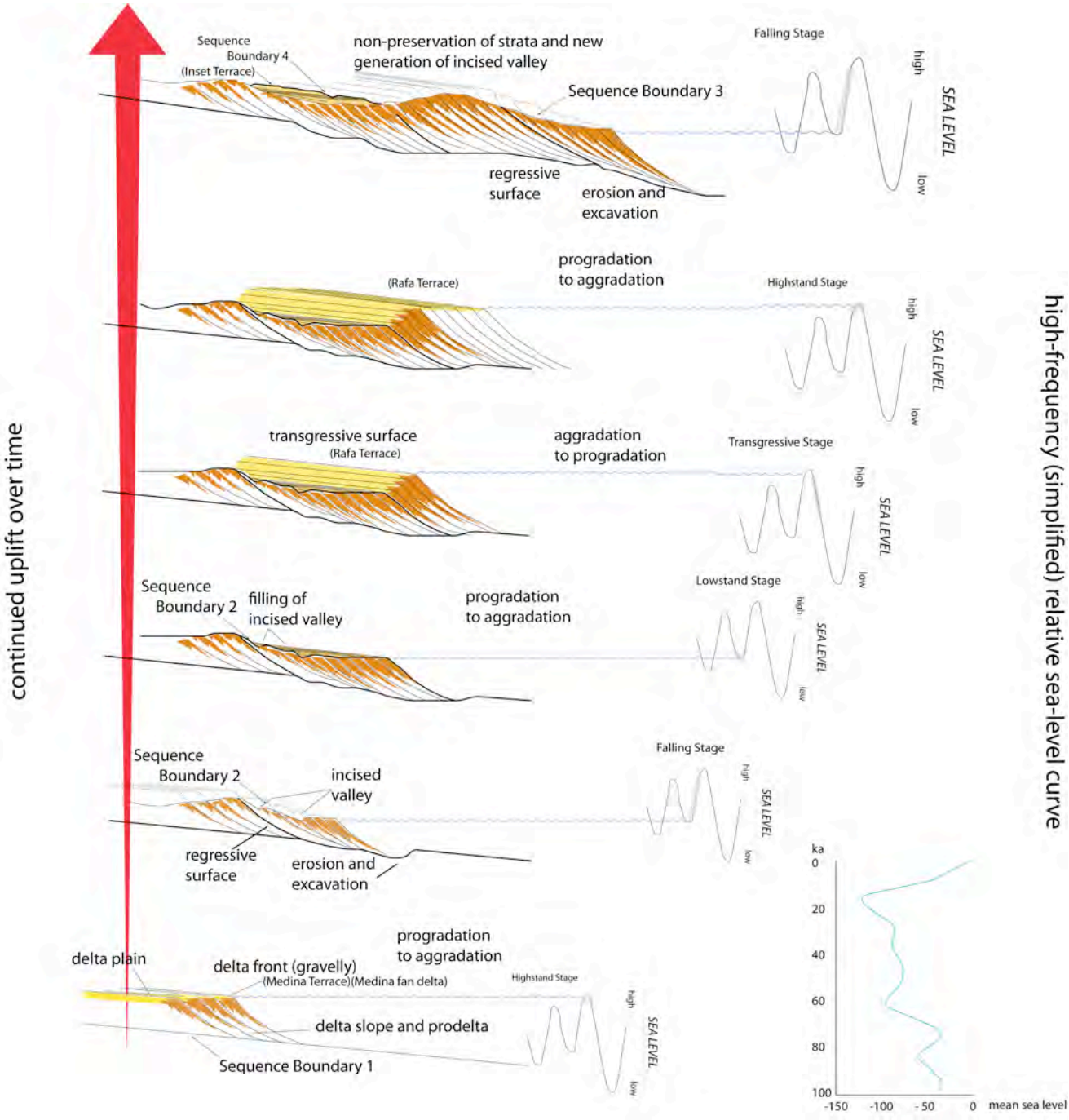

Figure 6.2. Interpretative model of a Gilbert-type fan delta sequence observed for the Conway Flat coast. Note: (i) how the sea-level oscillations produce alternating stages of delta progradation and aggradation; (ii) how gravelly avalanches along delta slopes scoured the bedrock, which was formed by non-lithified deposits, during the sea-level falls; (iii) how the delta front facies progressively shifted basinwards under the influence of continued coastal uplift; (iv) inset relative sea level curve for the Conway Flat coast modified from Figure 6. 5 (figure is modified from Longhitano, 2008).

lateral correlation of the fan delta sequences and their geomorphic boundaries provide the initial evidence of the fault zone propagation away from the Hawkswood Range divide.

The stratigraphic profile of the Conway Flat coast shows little obvious vertical cyclicity. However, a variety of characteristic features of several high-order erosional surfaces, such as morphology, geometry, and sharp non-Waltherian vertical facies transitions, regular cyclic sedimentation pattern consisting of five sequences varying from ~ 5 m to 70 m thick. The varied thickness and completeness of the systems is attributed to the complex interaction of tectonic subsidence and eustatic sea level change.

Transgressive systems tracts (TST) and highstand systems tracts (HST) are indicated by deepening-upward and shallowing-upward stacking of facies, respectively. Aggradational trends are indicated by a lack of overall shallowing or deepening. The lowstand or falling stage systems tracts have been identified through the preserved inset terraces.

The analysis of facies stacking patterns within individual sequences makes it feasible to recognize discrete deepening and aggradational upward trends depending on the relative rates of accommodation development (sea level; episodic uplift) and sediment supply. The following section describes general characteristics of the Conway Flat coast's high-frequency sequences and the criteria that define them as chronostratigraphic units.

6.4 IDENTIFICATION OF SEQUENCES

This description of sequences is based on the geomorphic mapping of terrace elevations combined with sedimentary facies architecture presented in detail in Chapter 3. The distinction between forcing factors is based on data presented in Chapter 3, 4, 5. Figure

6.2 shows the bounding surfaces for each sequence while comparing relative sea level position and depositional systems with continued uplift over time.

Basement

The oldest rocks exposed along the lower Conway Flat coast are interbedded dark mudstones and siltstones of the Greta Formation. Mud/siltstone beds contain rare laminations, are bedded, and sometimes display large scale cross bedding, slumping, and convoluted bedding. The deposits are found at the bases of the Medina and Rafa Terraces unconformably underlying the fan delta deposits. Fossil data indicate these deposits are 3-3.9 Ma (Warren, 1995).

Sequence Boundary 1

The basal erosional surface is in the Greta Formation mud/siltstones of the Medina Terrace. A transverse cross section of the Medina Terrace shows the unconformity surface is sharp and in places deeply incised into the underlying mud/siltstones. In a few localities it shows intense loadcasting.

The deeply incised Greta Formation deposits indicate a sea level fall accompanied by erosion. The eroded mud/siltstones of the Greta formation created a paleovalley that would aid in accommodating successive deposits.

Sequence 1

Sequence 1 records the deposition of coarse-grained, rounded gravels of the ~ 90-95 ka Medina fan delta forming the Medina Terrace. The foreset bedding of the fan delta is

inclined ~ 25° from horizontal as part of the typical tripartite Gilbert fan delta system. The gravels of this sequence downlap onto the erosional surface of Sequence Boundary 1. The gravels are unconformably overlain by angular, poorly sorted, coarse gravels and fine sands. Such a truncation suggests a possible parasequence (Chapter 3).

The earliest transgression along the Conway Flat coast is recorded by the deposition of the Medina Terrace Gilbert fan delta. Sequence 1 (Fig. 6.3) records the deposition of marine Gilbert-type fan delta into the asymmetric basin formed by thrust loading following the initiation of seaward propagating thrust faults along the Hawkswood Range (Chapter 2). At this time sediment accumulation in the basin outpaced accommodation causing the fan deltas to prograde basinward during a transgressive to relative highstand to forced regressive systems tract. The highstand deposits are recognized by two features: 1) the relative movement of the shoreline basinward and 2) the coarsening up deposits of the Gilbert-type fan delta.

The abrupt erosional unconformity near the top of sequence 1 indicates the erosion of the delta plain into a shore platform. It is consistent with a rapid, but short-lived, drop in sea level and corresponds with localized episodic uplift ~93 ka most likely caused by a combination of episodic uplift and relative sea level fall (Paquet et al, 2009). The eroded topset beds were reworked into the system leaving a well-defined shore platform. Then followed a brief time of sea level rise needed to cover the terrace in beach sands.

Sequence Boundary 2

An erosional unconformity at the top of Sequence 1 marks the lower boundary of Sequence 2. The boundary is marked by incision into Medina fan delta gravels. The contact is sharp and steep and is also identified by a ~15 m drop in elevation of terrace

surfaces associated with the sequences. The erosional sequence removed the delta topset beds of the Medina fan delta in sequence 1.

The sharp, deeply eroded contacts between the fan delta deposits and the dramatic changes in terrace heights at these contacts favor extended periods of incision and sediment bypass. The deeply incised Medina Terrace deposits indicate a sea level fall accompanied by erosion. The eroded Medina fan delta foresets created a paleovalley that would aid in accommodation of successive deposits.

Sequence 2

Sequence 2 records the deposition of ~79- 52ka Dawn and Big Bush Gully fan deltas and nearshore marine deposits forming the Rafa Terrace. The Dawn fan delta foresets downlap onto the erosional Sequence Boundary 2. The fan deltas are conformably overlain by horizontally stratified gravels with rounded clasts, fine-grained brown sand of the beach deposits, and gravels with angular clasts of a 2nd fan delta and its topset beds to form a parasequence. Interbedded sands and silts of the nearshore facies conformably onlap the inclined gravel beds in Sequence 2 (Chapter 3).

Sequence 2 marks renewed deposition of gravelly Gilbert-type fan deltas deposition into the basin as well as changing sediment-dispersal patterns as indicated by the gravels of the Dawn fan delta onlapping onto the erosional surface of sequence boundary 2. The construction of the two fan deltas, Dawn and Big Bush Gully, within this terrace and sequence, together represent a transgressive package. The development of nearshore marine facies in the protection of the prograding fan deltas suggests continued sea level rise throughout deposition. Several parasequences are recorded between 52-79 ka along

the Conway Flat coast with the deposition of the Dawn and Big Bush Gully Gilbert-type fan deltas and nearshore marine deposits.

Sequence Boundary 3

Sequence Boundary 3 is marked by incision into the Rafa Terrace deposits. The contact is identified by multiple ~10-15 m drop in elevation of terrace surfaces associated with the sequences. The erosional sequence removed the delta topset beds of the Dawn and Big Bush Gully fan deltas in sequence 3.

The contacts between the fan delta deposits and the dramatic changes in terrace heights at these contacts favor extended periods of incision between ~52- 20 ka.

Sequence 3

An extended period of sea level drop coupled with increased sediment input into the system indicates the initiation of Sequence 3. Sequence three is comprised of stacked beds of fluvial channel gravels with sub-rounded to angular clasts and a high percentage of matrix. The beds onlap onto Sequence 2 as exposed in several creeks in the upper reaches of the Hawkswood Range (Chapter 3). The isolated aggradational gravels were deposited as a result of a sudden influx of sediment into the system during Sequence 3.

Sequence Boundary 4

An erosional unconformity separates Sequence 2 from Sequence 4. The surface can be traced laterally along the coast for ~5 km. The termination of Sequence 2 is identified by the unconformable truncation of the interbedded sands and silts in a steep contact marked by colluvium and bank collapse. This contact is also identified by a ~10-15 m drop in elevation between the Rafa Terrace of sequence 2 and the Ngaroma Terrace of Sequence 4.

The high-angle unconformity between Sequence 2 and Sequence 4 is seen in various locations along the cliff faces along the coast and inland. This contact is highly irregular in large part due to the erosion of Sequence 2 by the Conway River as it was deflected around the growing Hawkswood Range. However, the unconformity is easily noticeable through the stratigraphy and geomorphological differences in the sequences.

The incised Rafa Terrace deposits indicate a sea level fall accompanied by erosion of the Big Bush Gully fan delta foresets and nearshore marine deposits.

Sequence 4

An eventual sea level rise is recorded by the deposition of the estuarine deposits of the Ngaroma Terrace and indicates the initiation of Sequence 4. Sequence 4 onlaps onto interbedded sands and silts of the nearshore marine facies in Sequence 2. This sequence contains fluvial delta plain gravels passing upwards into estuary deposits. These gravels are similar to the topset beds of the previous fan deltas. Multiple *in situ* ~7-8.5 ka paleotree stumps are rooted in the poorly sorted, subrounded to subangular fluvial gravels. These are overlain by dark, sulphurous muds with abundant root casts of estuary deposits (Chapter 3). There are multiple smaller estuaries preserved at the mouths of Big Bush Gully and Ploughmans Creek, also contains paleoforests that have been dated to ~7 ka (Chapter 5).

Deposition of fluvial debris flows into an estuarine environment mark the beginning of Sequence 4. Here a Podocarp paleoforest rooted in the gravels and established itself behind the protection of a beach ridge (Chapter 3). We can see the evidence of this environment with individual Podocarp tree stumps rooted in a basal conglomerate layer and interbedded

with mudstones and siltstones that are carbonization-rich. Subsequent eustatic sea level rise through the Holocene destroyed the beach ridge, essentially causing the drowning of the paleoforest. The drowned Podocarp paleoforest, gradually younging ages of the trees and remnant beach ridge deposits in eroded cliffs support the destruction of the barrier bar. The upper section of the sequence is dominated by thick packages of interbedded siltstones and mudstones with large amounts of woody debris and abundant root casts typical of a salt marsh supporting a continued estuarine environment. The fact that the estuarine environment remained for some ~5 kyrs, and the paleoforest gets progressively younger inland, indicate that at this time sea level rise and uplift rates were matched.

Sequence Boundary 5

The termination of Sequences 2 and 4 is marked by the unconformable truncation by the modern Conway River and smaller creeks along the coast.

This unconformity is also identified by a 5-10 m drop in elevation between Sequence 4 with the modern Conway delta of sequence 5.

Sequence 5

Sequence 5 is represented by poorly sorted sand, gravel and cobbles of the modern Conway River and other creeks along the range front. The unconsolidated sediments of Sequence 5 onlap the deposits of Sequences 2 and 4. The deposits represent modern fluvial deposition that form a series of river channels and bars as sediment supply keeps pace with subsidence. The material is ultimately deposited on the Conway fan in the modern Conway basin. On a smaller scale, similar deposits are recorded at the Medina, Dawn, Big Bush Gully, and Doug’s Gaps.

6.5 KEY BOUNDING SURFACES

Five bounding unconformities are recognized in the Pliocene-Holocene succession. Major, high-order unconformities are prominent surfaces marked by noticeable geomorphic change. The unconformities are indicated in Figure 6.2.

6.6 FACIES ARCHITECTURE OF HIGH-FREQUENCY SEQUENCES

6.6.1 TRANSGRESSIVE SYSTEMS TRACT (TST)

The failure of sediment supply to keep pace with the increasing rate of accommodation development during relative rise in sea-level leads to deposition of the basal sequence boundary (Di Celma and Cantalamessa, 2007).

The initiated deposition of the conglomeratic foresets along the Conway Flat coast range from 50- 70 m thick, and downlap onto an unconformity surface record the beginning of TST. The deposits forming these TST sequences are characterized by the vertically-stacked tripartite Gilbert-type fan delta deposits of the Medina and Rafa Terraces.

Transgressive sequences are also recorded with the deposition of the package of estuary deposits of the Ngaroma Terrace unconformably overlaying the Rafa Terrace deposits.

6.6.2 HIGHSTAND SYSTEMS TRACT (HST)

The HST develops as the rate of relative sea-level rise decreases towards the highstand still stand of relative sea level, accommodation is no longer created rapidly enough to satisfy the sediment supply, and the consequent progressive infill of shelf accommodation forces

the shoreline to prograde basinward. Thus, the development of the HST is strictly dependent on rates of sediment supply and relative rise in sea level.

Highstand preservation is favored by high rates of long-term subsidence, high accumulation rates and low rates of relative sea-level change (Thorne and Swift,1991). Along the Conway Flat coast these controlling factors are reflected in preserved Gilbert-type fan delta clinoforms that took advantage of such conditions and prograded basinwards.

6.6.3 LOWSTAND SYSTEMS TRACT (TST)

A LST develops as the rate of sea level fall would result in erosion causing incision with sediments bypassing inboard fan delta sequences to be deposited basinward possibly as new fan deltas or by passing into deeper water. During the lowstand systems tract, incised valleys begin to flood. It is during this time that the inset terraces that occur in the upper reaches of the Hawkswood Range are deposited. The formation of these terraces is due to increased sediment supply to the system via earthquake released fluvial/debris flows and are best described as a unique variant of a parasequence.

6.7 SEQUENCE DRIVING MECHANISMS

The stratigraphic architecture of the Conway Flat coast was analyzed using the sequence stratigraphic framework approach developed by Vail et al. (1977). Studies from Hunt and Tucker (1992) and Helland-Hansen and Gjelberg (1994) provided further information and ideas on particular depositional settings. The component five unconformity bounded units record cyclical relative changes in sea level. Sequences and system tracts were identified based on the stratal patterns, stratigraphic position, OSL and ^{14}C dates, geometry, facies characteristics and geomorphic expressions of the deposits. However, to distinguish

whether tectonics, sediment supply, eustasy, or a combination of the three controlled on development of sequences and bounding surfaces in a transpressional basin is difficult, because each to the mechanisms becomes plausible in an active plate bounndary. Information gathered from the research highlights similarities to their extensional basin counterparts, but more importantly detailed information from rarely reported compressional settings.

Tectonics forcing factors

The first forcing factor is episodic uplift within the HTFZ. Inherent to the exposed fan delta complex along the Conway Flat front is the implicit requirement for fault driven uplift. The degree to which tectonics controls or influences interpretation of the level of tectonic influence on the deposits along the Conway Flat coast is the challenge. Episodic pulses of coseismic uplift expose Gilbert-fan delta deposits and lead to the erosion of fan delta deposits. This would result in a localized sea level fall that would create the notching of existing Gilbert-type fan deltas and offset them seaward as they prograde basinward. This coseismic subsidence associated in this scenario could also mirror the drowning scenario due to readjustment of the accumulated bending. Sediments would, over time, begin to bypass the inboard system and are deposited basinward. This would in turn create an unconformable boundary. However, due to the foot-wall location of the studied succession, the development of the erosional unconformities would require significant, relative, upthrow of the hanging wall to create enough accommodation space for deposition and this not an adequate explanation for the recorded stratigraphic patterns.

The large-scale morphology of bounding unconformities is also diagnostic for distinguishing the origin of cyclicity. Indeed, the presence of incised truncation surfaces implies a significant fall in base level for their formation. Furthermore, these cycles are

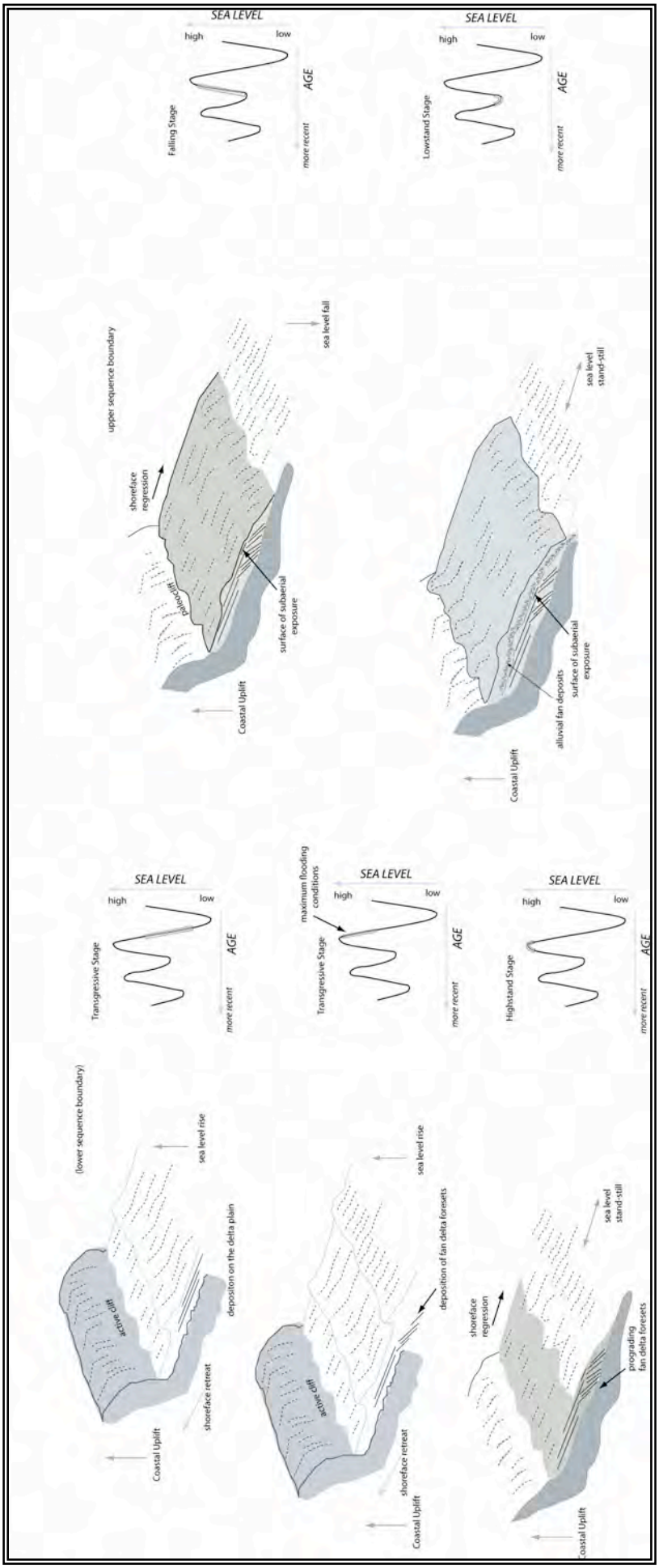

Figure 6.3. Schematic model that compares relative sea level position to depositional systems along the Conway Flat coast.

bounded by a significant change in geomorphic expression and existance of a complete package of Gilbert-type fan delta deposits implying a significant removal of material during sea level fall.

In summary, although compressional tectonics has been active during deposition of material along the Conway Flat coast its role was subordinate and probably limited to creating additional accommodation space. The tectonic activity would most likely be too erratic to create the cyclic sedimentation pattern shown by this succession. A local tectonic origin for the observed surfaces is discarded because of the large amount of episodic uplift, and subsequent erosion needed to remove all of the material of the prior TST sequences; this would require a fall in relative sea level of greater extent than the depositional basin.

Sediment Supply as a forcing factor

The second forcing factor is the variation of sediment supply to the basin. At times when excess sediment is provided to the system forcing aggradation of material. Along the Conway Flat coast it is interpreted that this could happen after periods of seismic activity released material into the upper catchment. This material is then added to the system at inconsistent times. This does not seem to be a viable option for the Conway Flat coast. Although there are potentially examples of times of increased sediment being introduced to the system (aggradational inset terraces), it is difficult to explain the observed geometries and facies architecture based solely on sediment supply. The primary piece of evidence eliminating this as a viable option is the deeply incised unconformities which cannot be generated by this mechanism. This is supported by the mere fact that entire TST sequences are eroded away prior to the deposition of the next sequence.

Eustatic forcing factor of sedimentary cyclicity

The final, and preferred, forcing factor is a viable cycle-producing mechanism which dictates changes in sea level. In this scenario, within which rates of eustatic changes in sea level were high enough to exceed those of other contemporaneous base-level control mechanisms, the predicted features of bounding unconformities and internal architecture of sequences are similar to those observed along the Conway Flat coast. Accordingly, it is suggested that eustasy is the more plausible forcing mechanism for the studied sequences.

A very important argument in favor of this kind of forcing mechanism during the Pliocene to Holocene are the correlations between the sea level change events and the unconformities bounding the five, high-frequency sequences along the Conway Flat coast. This correlation provides outcrop documentation of the link existing between sequence boundaries and the glacio-eustatic falls recorded by Paquet et al., 2009.

The depositional characteristics of Sequence 4 suggest that the Podocarp paleoforest of the Ngaroma Terrace was gradually drowned by sea level rise that outpaced uplift.

Sea level data for ~95 ka in New Zealand shows a relative highstand (Waelbroeck et al, 2002; Lisieki and Raymo, 2005; Paquet et al, 2009). This highstand follows a relative sea level fall of ~70 m from ~120-100 ka that was responsible for the notching in the Greta Formation siltstones and mudstones.

The exposed marine sections in the Wanganui Basin and Hawkes Bay were interpreted as the preserved on-land record of sea-level change (Kamp, 1981; Beu and Edwards, 1984; Turner and Kamp. 1990; Naish et al, 1998; Carter and Naish, 1999). The identification of tie-points from magnetic polarity by Turner and Kamp (1990) set the stage for widely

accepted correlations of New Zealand strata with oxygen isotope stages. Naish et al. (1998) and Carter and Naish (1998; 1999) used this to undertake a complete, integrated stratigraphic study of the Wanganui Basin. Their use of sequence stratigraphy combined with magnetic stratigraphy, tephra dates and oxygen isotope stages created a complete stratigraphic framework for the Pliocene-Pleistocene (Cooper, 2004).

Eustatic sea level change is the cause for the creation of the Medina and Rafa Terraces. Interpreted highstands from ~95-90 ka created sea level conducive for the formation of the Medina Gilbert fan deltas (Fig. 6.2 and 6.5). Oxygen isotope data record a gradual sea level fall following this period until a subsequent sea level rise and highstand from ~83 Ka to 78 ka return sea level to similar to those of ~90 ka (Paquet et al, 2009). This coincides with the deposition of the Dawn and Big Bush Gully Gilbert-type fan deltas in the Rafa Terrace.

Following the deposition of the Rafa Terrace there is a general trend of sea level fall from ~ 52- 20 ka (Paquet et al, 2009) (Fig 6.5). It is during this time that the inset terraces that occur in the upper reaches of the Hawkswood Range are deposited. The formation of these terraces is due to increased sediment supply to the system via earthquake released fluvial/debris flows and are best described as a unique variant of a parasequence. Increased sediment supply to the system is the cause for the aggradational terraces.

Gibb (1986) is the standard measurement for Holocene eustatic sea level curves based on present sea level in New Zealand (Fig 6.4). The curve created by Gibb (1986) is based on data collected from eight sites throughout New Zealand. This curve shows a range of sea level from ~9 m below today's current sea level ~7.5 ka to ~24 m lower ~9.2- 8.4 ka. The variance of paleo-sea level has an impact on determining the amount of tectonic uplift in

the region. The sea level rise and matched uplift during this period is recorded in the shallowing up sedimentary facies of the Ngaroma Terrace.

Gradual sea level rises and falls appear to be enough to create an environment conducive for the formation of the deposits in Sequence 1, 2 and 3 (Model I) (Fig. 6.2 and 6.3). The depositional characteristics of Sequence 4 suggest that the Podocarp paleoforest of the Ngaroma Terrace was gradually drowned by sea level rise that outpaced uplift.

In light of all these supporting evidence, we propose a model whereby the regular small-scale stratigraphic cyclicity exhibited along the Conway Flat coast is attributed to periodic glacio-eustatic changes in sea level. The distinctive stratigraphic architectural style of these sequences, which includes evidence of fluvial down-cutting, total removal of TSTs/ HSTs and dominance of TSTs in the section is similar to high-frequency sequences during periods of glacio-eustatic oscillations in sea level elsewhere during the Plio-Pleistocene (e.g., Cantalamessa et al., 2006; Di Celma et al. 2005).

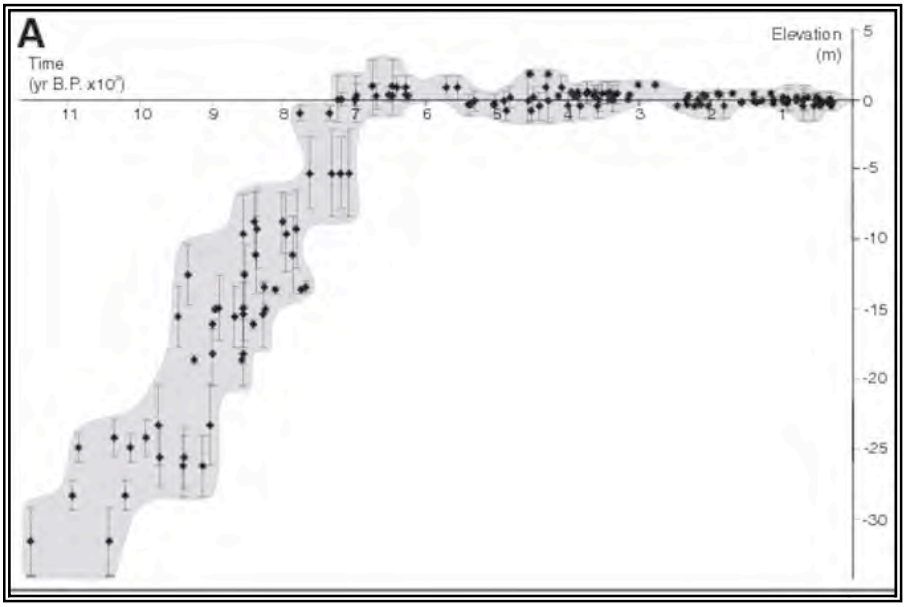

Figure 6. 4. Holocene sea level curve modified from Gibb, 1986.

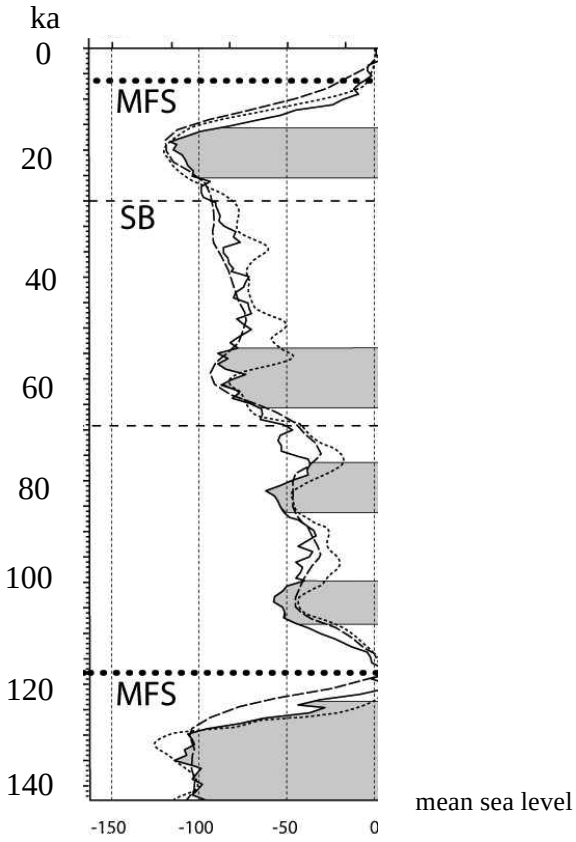

Figure 6. 5. Mean relative sea level curve based on Oxygen isotope data from Lisiecki and Raymo, 2005 (solid line); Waelbroek et al., 2002 (dashed line); Imbrie et al., 1984 (long hashed line) from Paquet et al., 2009.

6.8 CONCLUSIONS

The conclusions drawn from the sequence stratigraphic study along the Conway Flat coast provide some insight on relative tectonic and sea level change during the Pliocene-Holocene.

1) Pliocene-Holocene deposits along the Conway Flat coast include marine to shallow-marine to non-marine facies deposited in basin within a compressional-regime basin located in the Hawkswood Thurst Fault Zone (HTFZ). Four facies

combine to form five, 5 to 70 m thick unconformity-bounded depositional sequences. In general, the erosional unconformities bring Gilbert-type fan deltas sharply into contact with each other. Partitioning of each sequence into component transgressive, highstand and lowstand systems tracts has been made based on vertical facies patterns.

2) The sequence stratigraphic framework presented in this study allows speculation on the controlling factors of sequence development. After evaluating the tectonics (Chapter 2 and 5) and eustatic mechanisms (Chapter 6) for controls on the observed cyclicity, it is concluded that high frequency eustasy superimposed on steady uplift adequately explains the stratigraphic cyclicity seen along the Conway Flat coast.

3) A key outcome of the application of the sequence stratigraphic analysis to these strata is that the synsedimentary tectonics and regional climatic setting are similar to other high-frequency sequences recorded in New Zealand.

4) Steady uplift on imbricate thrust faults and fluctuations in sea level are interpreted to be controlling factors in the formation of the Conway Flat coast fan deltas. During periods of rapid relative sea level fall due to eustatic sea level fall existing fan deltas were incised and sediment by-passed the inboard system and continued out onto the shelf. The creation of sequence 1, 2, and 4 boundaries is the result of eustatic sea level change. Periods of TST to highstands resulted in the aggradation and progradation of the fan deltas into the incised valleys creating the nested fan delta sequences.

5) Sequence boundaries between multiple nested Gilbert-type fan deltas are also boundaries for geomorphic surfaces. The contacts between fan deltas coincide with

geomorphic height changes and varying terraces levels. A combination of the two techniques implies that the geomorphic flat terraces are a result of the depositional pattern of a tripartite Gilbert-type fan delta and are not reworked wave-cut platforms.

6.9 REFERENCES

Beu, A.G., Edwards, A.R., 1984. New Zealand Pleistocene and Late Pliocene glasico-eustatic cycles, Paleogeography, Paleoclimatology, Paleoecology 46, 119-142.

Burns, B.A., Heller, P.L., Marzo, M., Paolo, C., 1997. Fluvial response in a sequence stratigraphic framework: Example from the Montserrat fan delta, Spain, Journal of Sedimentary Research 67, 311-321.

Cantalamessa, G., Di Clelma, C., Ragaini, L., 2006. Tectonic controls on sequence stacking pattern and along-strike architecture in the Pleistocene Mejillones Formation, northern Chile: Implications for sequence stratigraphic models, Sedimentary Geology 183, 125–144.

Carter, R.M., Naish, T.R., 1998. A review or Wanganui Basin, New Zealand: global reference section for shallow marine, Plio-Pleistocene (2.5-0 Ma) cyclostratigraphy, Sedimentary Geology 122, 37-52.

Carter, R.M., Naish, T.R., 1999. The high resolution, chronostratigraphic and sequence stratigraphic record of the Plio-Pleistocene, Wanganui Basin, New Zealand, Institute of Geological and Nuclear Sciences Science Folio Series 2.

Di Celma, G., Cantalamessa, G., 2007. Sedimentology and high-frequency sequence stratigraphy of a forearc extensional basin: The Miocene Caleta Herradura Formation, Mejillones Peninsula, northern Chile, Sedimentary Geology 198, 29-52.

Colella, A.,1988. Pliocene–Holocene fan deltas and braid deltas in the Crati basin, southern Italy: a consequence of varying tectonic conditions. In: Nemec, W., Steel, R.J. (Eds.), Fan Deltas: Sedimentology and Tectonic Setting. Blackie and Son, pp. 50–74.

Cochran, U., Berryman, K., Zachariasen, J., Mildenhall, D., Hayward, B., Southall, K., Hollis, C, Barker, P., Wallace, L., Alloway, B., Wilson, K., 2006. Paleoecological insights into subduction zone earthquake occurrence, eastern North Island, New Zealand. Geological Society of America Bulletin 118, 1051-1074.

Colella, A., Prior, D.B. (Editors)., 1990. Coarse-grained deltas, International Association Sedimentology, Special Publication 10, 357 pp.

Cooper, R.A., 2004. The New Zealand Geological Timescale. Institute of Geological and Nuclear Sciences, Institute of Geological and Nuclear Sciences Monograph 22, 284 pp.

Dart, C.J., Collier, R.E., Gawthorpe, R.L., Keller, J.V.A., Nichols, G., 1994. Sequence stratigraphy of Pliocene-Quaternary synrift, Gilbert-type fan deltas, northern Peloponnesos, Greece, Marine and Petroleum Geology 11, 545-560.

de Lange W.P., Fraser R.J., 1999. Overview of tsunami hazard in New Zealand, Tephra 17, 3–9.

Di Celma, C., Ragaini, L., Cantalamessa, G., Landini, W., 2005. Basin-physiography and tectonic influence on sequence architecture and stacking pattern: pleistocene succession of the Canoa Basin (central Ecuador). Geological Society of America Bulletin 117, 1226 – 1241.

Dorsey, R. J., Umhoefer, P. J., 2000. Tectonic and eustatic controls on sequence stratigraphy of the Pliocene Loreto basin, Baja California Sur, Mexico, Geological Society of America Bulletin 112, no. 2, 177–199.

Dorsey, R. J., Umhoefer, P. J., and Renne, P. R., 1995. Rapid subsidence and stacked Gilbert-type fan deltas, Pliocene Loreto Basin, Baja California Sur, Mexico, Sedimentary Geology 98, 181–204.

Dorsey, R.J., Umhoefer, P. J., Falk, P., 1997. Earthquake clustering and stacked Gilbert-type fan deltas in the Pliocene Loreto Basin, Baja California Sur, Mexico, Geology 25, 679–682.

Fritz, H.M., Hager, W.H., Minor, H.-E., 2001. Lituya Bay case: rockslide impact and wave run-up, Science of Tsunami Hazards 19, 3–22.

Gawthorpe, R. L., Colella, A., 1990, Tectonic controls on coarse-grained delta depositional systems in rift basins, *in* Colella, A., and Prior, D.B. eds., Coarse-grained deltas: International Association of Sedimentologists Special Publication 10,113–127.

Gawthorpe, R.L., Fraser, A.J., Collier, R.E., 1994. Sequence stratigraphy in active extensional basins: Implications for the interpretation of ancient basin-fills, Marine and Petroleum Geology 11, 642-658.

Gawthorpe, R. L., Sharp, I., Underhill, J. R., Gupta, S., 1997. Linked sequence stratigraphic and structural evolution of propagating normal faults, Geology 25, 795–798.

Gibb, J.G., 1986. A New Zealand regional Holocene eustatic sea-level curve and its application to determination of vertical tectonic movements, Royal Society of New Zealand Bulletin 24, 377-395.

Gregg, D.R., 1963. Sheet 18, Hurunui. Geological Map of New Zealand. Department of Scientific and Industrial Research, New Zealand.

Hardy, S., Gawthorpe, R. L., 1998. Effects of variations in fault slip rate on sequence stratigraphy in fan deltas: Insights from numerical modeling, Geology 26, 911–914.

Helland-Hansen, W., Gjelberg, J.G., 1994. Conceptual basis and variability in sequence stratigraphy: a different perspective, Sedimentary Research 39, 1013-1029.

Heller, P. L., Paola, C., 1992. The large-scale dynamics of grain-size variation in alluvial basins, 2: application to syntectonic conglomerate. Basin Research 4, 91–102.

Holt W.E., Haines, A.J., 1995. The kinematics of northern South Island, New Zealand, determined from geological strain rates. Journal of Geophysical Research 10, 17991–18010.

Hunt, D., Tucker, M.E., 1992. Stranded parasequences and the forced regressive wedge systems 23 tract: deposition during base-level fall. Sedimentary Geology 81, 1-9.

Jackson, C.A.L., Gawthorpe, R.L., Carr, I.D., Sharp, I.R., 2005. Normal faulting as a control on the stratigraphic development of shallow marine syn-rift sequences: the Nukhul and Lower Rudeis Formations, Hamman Faraun Fault block, Suez Rift, Egypt. Sedimentology 52, 313 – 338.

Kamp, P.J.J., 1981. Pleistocene tephras in Hawkes Bay and their potential for dating geologic events. In: Proceedings of the Tephra Workshop, Victoria University of Wellington, 52-54.

Lewis K.B., Barnes P.M., 1999. Kaikoura Canyon, New Zealand: active sediment conduit from near-shore sediment zones to trench-axis channel. Marine Geology 162, 39–69.

Lisiecki, L.E., and Raymo, M.E., 2005. A Pliocene–Pleistocene stack of 57 globally distributed benthic δ^{18}o records: Paleoceanography 20, 1003-1029.

Massari, F., Rio, D., Sgavetti, M., Prosser, G., D'Alessandro, A., Asioli, A., Capraro, L., Fornaciari, E., Tateo, F., 2002. Interplay between tectonics and glacio-eustasy: Pleistocene

succession of the Crotone basin, Calabria (southern Italy). Geological Society of America Bulletin 114, 1183 – 1209.

McConnico, T.S., Bassett K.N., Pettinga, J.R., 2005. Facies architecture of the Conway fan delta complex as it formed terraces along the uplifting Hawkswood Range. Geological Society of New Zealand Miscellaneous Publication.

Naish, T.R., Abbott, S.T., Alloway, B.V., Beu, A.G., Carter, R.M., Edwards, A.R., Journeaux, T.D., Kamp, P.J.J., Pillans, B.J., Saul, G., Woolfe, K.J., 1998. Astronomical calibration of a southern hemisphere Plio-Pleistocene reference section, Wanganui Basin, New Zealand, Quaternary Science Reviews 17, 695-710.

Nemec, W. and Steel, R.J. (Editors), 1988. Fan Deltas: Sedimentology and Tectonic Settings. Blackie, London, 444 pp.

Newnham, R.M., Eden, D.N., Lowe, D.J., and Hendy, C.H., 2003. Rerewhakaaitu tephra, a land–sea marker for the last termination in New Zealand with implications for global climatic change: Quaternary Science Reviews 22, 289–308.

Nicol, A., Cowan, H., Campbell, J., Pettinga, J., 1995. Folding and the development of small sedimentary basins along the New Zealand plate boundary, Tectonophysics 241, 47-54.

Ota, Y., Yoshikawa, T., Iso, N., Okada, A., Yonekura, N., 1984. Marine terraces of the Conway coast, South Island, New Zealand, New Zealand Journal of Geology and Geophysics 27, 313-325.

Paquet, F., Proust, J-N., Barnes, P.M., Pettinga, J.R., 2009. inner-forearc sequence architecture in response to climatic and tectonic forcing since 150 ka: Hawke's Bay, New Zealand. Journal of Sedimentary Research 79, 97–124.

Peters, R., Jaffe, B., Gelfenbaum, G., 2007. Distribution and sedimentary characteristics of tsunami deposits along the Cascadian margin of western North America, Sedimentary Geology 200, 372-386.

Pettinga J.R., Yetton M.D., Van Dissen R.J., Downes G., 2001. Earthquake source identification and characterization for the Canterbury region, South Island, New Zealand. Bulletin of the New Zealand Society for Earthquake Engineering 34, 282–317.

Saul, G., Naish, T.R., Abbott, S.T., Carter, R.M., 1999. Sedimentary cyclicity in the marine Pliocene–Pleistocene of the Wanganui basin (New Zealand): sequence stratigraphic motifs characteristic of the past 2.5 m.y.. Geological Society of American Bulletin 111, 524 – 537.

Shulmeister, J., Goodwin, I., Renwick, J., Harle, K., Armand, L., McGlone, M.S., Cook, E., Dodson, J., Hesse, P.P., Mayewski, P., Curran, M., 2004. The southern hemisphere westerlies in the Australasian sector over the last glacial cycle: a synthesis: Quaternary International 118–119, 23–53.

Suggate, R. P., 1965. Late Pleistocene geology of the northern part of the South Island, New Zealand. New Zealand Geological Survey Bulletin 77, 91 p.

Tonkin, P., 2007. personal communication

Tsutsui, B., Campbell, J.F., Coulbourn, W.T., 1987. Storm-generated episodic sediment movements off Kahe Point, Oahu, Hawaii. Marine Geology 76, 281–299.

Turner, G.M., Kamp, P.J.J., 1990. Paleomagnetic location of the Jarmillo Subchron and the Matuyama-Brunhes transition in the Castlecliffan stratotype section, Wanganui Basin, New Zealand, Earth and Planetary Science Letters 100, 42-50.

Vail, P.R., Mitchum, R.M., Jr., Thompson, S., III., 1977. Seismic stratigraphy and global changes of sea-level. In: C.W. Payton (Editor), Seismic Stratigraphic Applications, American Association of Petroleum Geology Memoir 26, 83-97.

Van Dissen, R., Yeats, R. S., 1991. Hope Fault, Jordan thrust, and uplift of the seaward Kaikoura Range, New Zealand, Geology 19, 393 – 396.

Warren, G., 1995. Geology of the Parnassus area. Lower Hutt, Institute of Geological and Nuclear Sciences, Institute of Geological and Nuclear Sciences geologic map 18, 36p.

Waelbroeck, C., Labeyrie, L., Michel, E., Duplessy, J.C., McManus, J.F., Lambeck, K., Balbon, E., LaBracherie, M., 2002. Sea-level and deep water temperature changes derived from benthic foraminifera isotopic records: Quaternary Science Reviews 21, 295–305.

CHAPTER 7 CONCLUSIONS

7.1 CONCLUSIONS

This study focused on the structural, geomorphic, and sedimentologic development of the Conway Flat coast. Revealed through this new approach is a complicated story of marine deposition caught in the middle of a transpressional plate boundary.

The newly identified Hawkswood Thrust Fault Zone (HTFZ) is an intricate fault zone of imbricate thrust faults and connecting tear faults that link to the regional Hundalee Fault. Faults accommodate the transpressional stress being applied to the region by the modern plate boundary as the subduction continues to move southward as the boundary evolves. The reflection of this tectonic activity is seen in the thrust-bounded anticline of the Hawkswood Range and lateral sedimentary basin that is repeated regionally with basins such as the Cheviot Basin. Sequence stratigraphy helps identify and link in time and space the structural, geomorphic and sedimentological evolution of the Conway Flat coast.

As a result of the tectonic activity within the Hawkswood Range the basin exposes rare examples of depositional processes in the sedimentary deposits of Gilbert-type fan deltas. Unique clast imbrications first described here are resultant of sediment gravity flows down the slopes of the fan deltas. The mass deformations of the bedding around slump blocks, triggered by episodic earthquake events, are clues to the active tectonic setting along the Conway Flat coast. The deposits are intricately connected by sea level and tectonic change. At times, these Gilbert-type deltas were exposed in their entirety as terraces along the coast.

Chapter two presented new structural information for the Conway Flat coast in the form of lineament mapping, geomorphic mapping and the identification of new faults along the Conway Flat coast. This new data highlighted the dominant lineament trend of NNE for the region, parallel to the Hope fault and MFZ, the existence of multiple overlapping terraces and a complex, imbricate, thrust fault zone on the east side of the Hawkswood Range here called the Hawkswood Thrust Fault Zone. At a smaller scale, Chapter's three and four presented the terrace geomorphology, sedimentary lithofacies of the Conway Flat coast, the facies architecture of Gilbert-type fan deltas and detailed sedimentary investigations of the fan delta complex. This smaller scale work showed four noticeable terrace heights, deposits with high a percentage of slump deposits (both in fan deltas and nearshore marine deposits), and unique imbrication patterns of clasts within the fan delta foresets (Chapter 4). The combination of the structural and geomorphic mapping and terrace identification in chapter two with the facies architecture of chapter three shows the relationship between terrace and fault development. With detailed sedimentological studies presented in chapter four, it was shown that the facies contain many characteristics indicative of slump deposits triggered by coseismic events. Age constraints were provided by chapter five and enabled us to constrain the delta deposits to the Quaternary and initiation of deposition in the basin. The deposits at Conway Flat coast are thought to be the first Gilbert-type fan delta deposits convincingly shown to be formed in a modern compressional setting. This shows that the process of fan delta formation are controlled by local tectonics, basin

geometry and sea level fluctuations and not specific to extensional environments which dominate the fan delta literature.

Finally, the information about the terraces, earthquakes, and basin formation provided here helps understand how a basin develops through time in a transpressional plate boundary.

7.2 KEY FEATURES OF FAN DELTAS IN A COMPRESSIVE PLATE BOUNDARY

The data presented in this study supports the following conclusions:

1. Sequence boundaries between multiple nested Gilbert-type fan deltas are also boundaries for geomorphic surfaces. The contacts between fan deltas coincide with geomorphic height changes and varying terraces levels. A combination of the two techniques implies that the geomorphic flat terraces are a result of the depositional pattern of a tripartite Gilbert-type fan delta and are not reworked wave-cut platforms.

2. Coseismic activity on imbricate thrust faults and fluctuations in sea level are interpreted to be controlling factors in the formation of the Conway Flat coast fan deltas. During periods of rapid relative sea level fall due to eustatic sea level fall existing fan deltas were incised and sediment by-passed the inboard system and continued out onto the shelf. The creation of sequence boundaries are the result of eustatic sea level change superimposed on steady uplift (Chapter 5 and 6). Periods of highstands resulted in the progradation of the fan deltas into the incised valleys creating the nested fan delta sequences. Further evidence of the high stands is also recorded in the geomorphology in the form of multiple flat terraces

3. Sequences/Parasequences were created during periods of increased tectonic activity in the Hawkswood Range. The aggradational inset terraces of Sequence 3 in the upper reaches of the Hawkswood Range are a result of the increased sediment being supplied to the system.

4. The foreset deposits of the fan deltas are dominated by slumps and associated sediment gravity flows. Sediment gravity flows are the dominant means for initiating transportation along the foresets of the Conway Coasts Gilbert-style fan deltas regardless of water depth.

5. Well-preserved imbrication occurs on the delta front in less than 3 m of water indicating deposition by hyperpycnal flow.

6. Steep imbrication fabrics (~75°), referred to as ‘backstacking’, are preserved in the fan delta foreset beds. The initial imbrication fabric formed as the flow is diverted up and around the slump block is most likely caused by laminar shear in the flow.

7. Sediment gravity flows initiated by slumping on the fan delta foresets were deposited mainly under evol- ving grain flow conditions. The clast-to-clast contact and traction carpets at the base of these flows are responsible for the large amounts of foreset beds with imbrication clast dips of 30° relative to foreset slope.

APPENDIX A

Lineament analysis was completed on mylar overlays over 1: 50 000 Digital Elevation Models (DEM). The reproducible lineaments were measured and recorded with length and trend (Chapter 2). The data in excel files is presented here.

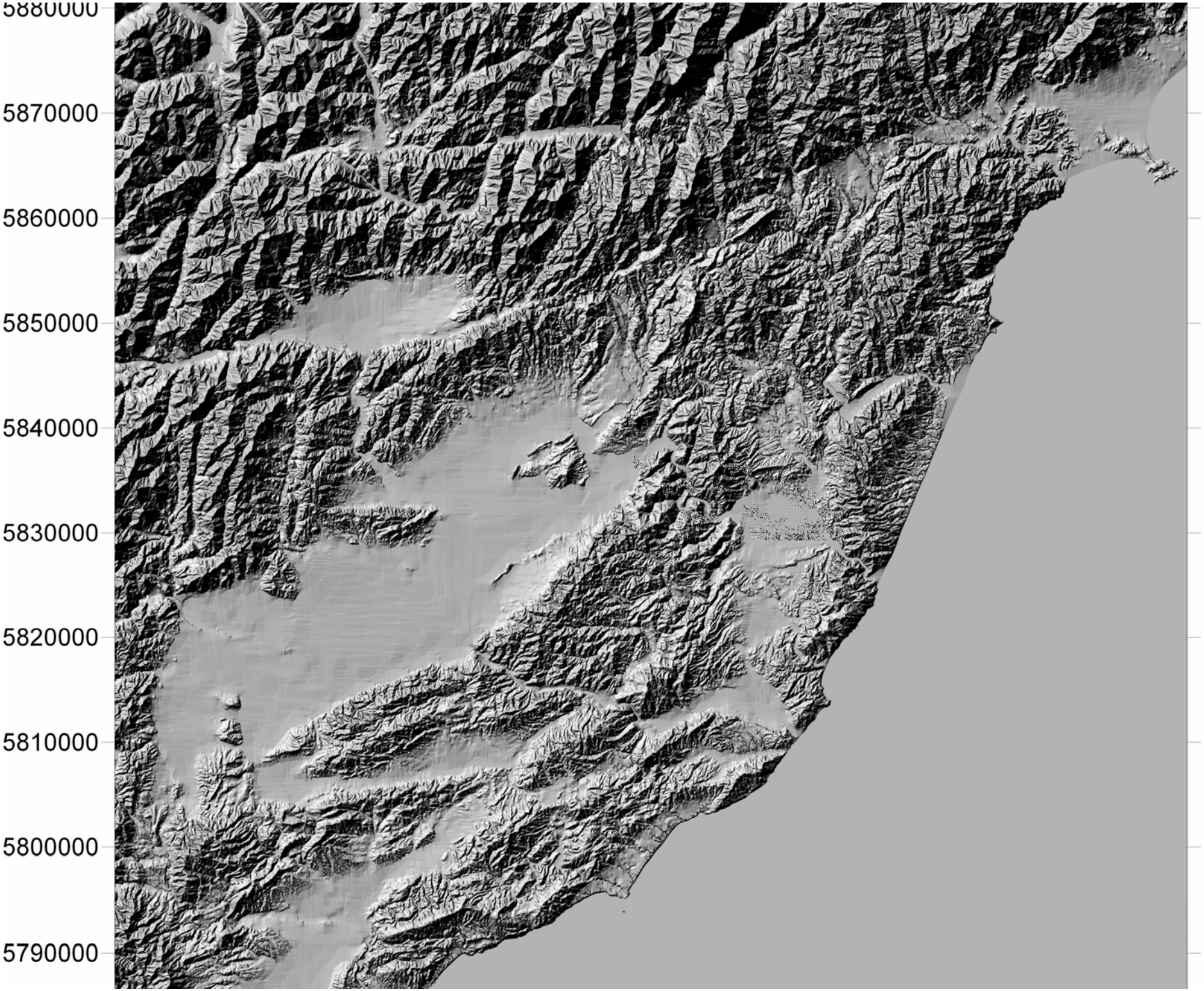
5880000
5870000
5860000
5850000
5840000
5830000
5820000
5810000
5800000
5790000

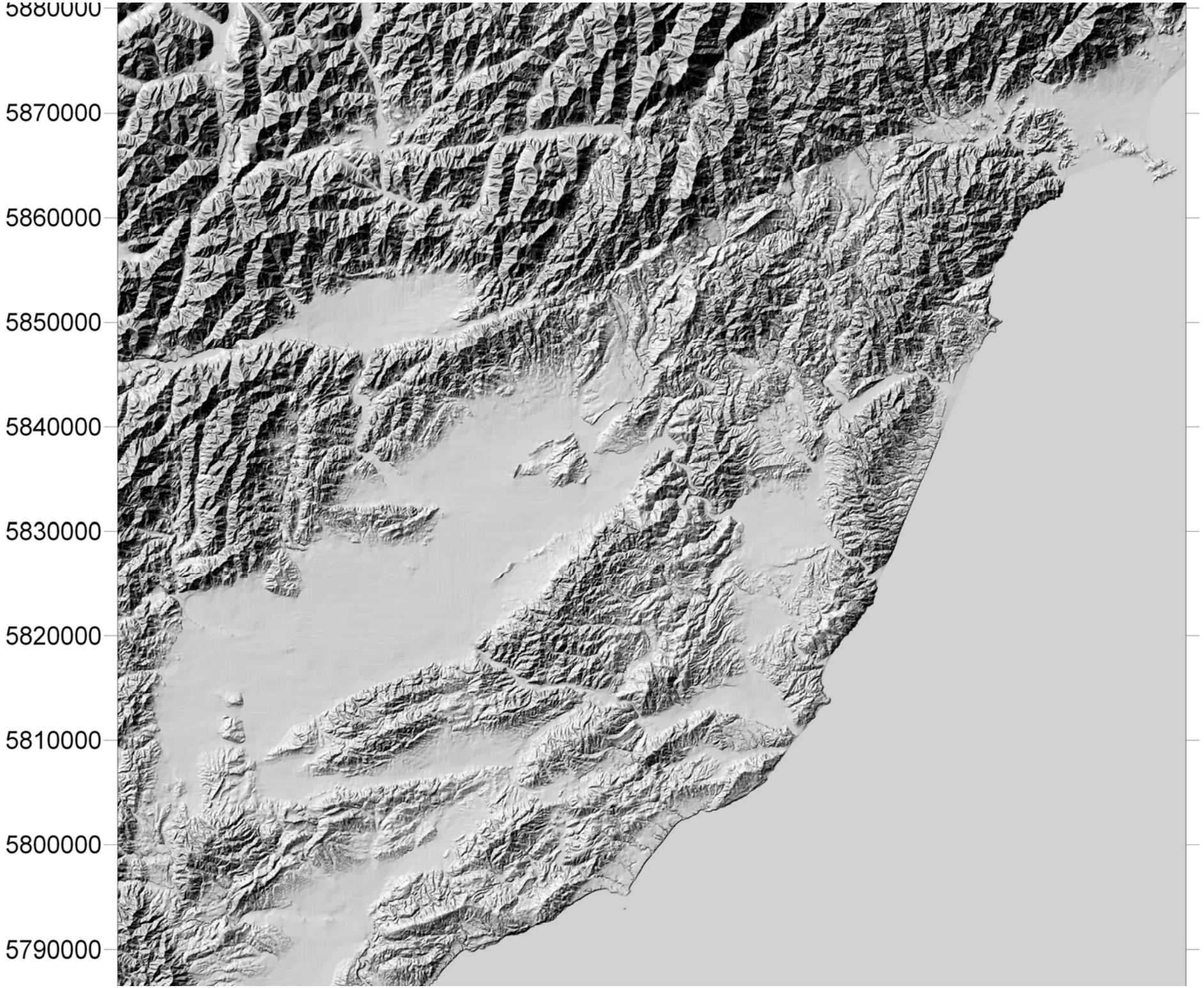
5880000
5870000
5860000
5850000
5840000
5830000
5820000
5810000
5800000
5790000

Northeast Reproducible Lineaments

Azimuth	*Frequency*	*Data Concentration Factor (dcf)*	
1	4	2.079357107	
2	4	2.260170768	
3	3	2.531391261	
4	5	2.531391261	
5	5	2.712204922	
6	2	2.983425414	
7	2	2.621798091	
8	3	2.350577599	
9	0	2.44098443	
10	2	2.260170768	
11	3	1.898543446	
12	0	1.717729784	
13	1	1.627322953	
14	4	1.356102461	
15	3	1.536916123	
16	1	1.536916123	
17	0	1.26569563	
18	1	1.26569563	
19	0	1.1752888	
20	2	0.813661477	
21	2	0.542440984	
22	0	0.452034154	
23	0	0.452034154	
24	0	0.361627323	
25	0	0.361627323	
26	0	0.180813661	
27	0	0	
28	0	0	
29	0	0	
30	0	0	
31	0	0	
32	0	0	
33	0	0.180813661	
34	0	0.180813661	
35	0	0.271220492	
36	0	0.632847815	
37	0	0.813661477	
38	2	0.904068307	
39	0	0.904068307	
40	1	0.994475138	
41	4	1.084881969	
42	2	1.084881969	
43	1	1.084881969	
44	0	0.904068307	
45	1	0.904068307	
46	1	0.994475138	
47	0	0.632847815	
48	0	0.452034154	

Northeast Reproducible Lineaments

Azimuth	*Frequency*	*Data Concentration Factor (dcf)*	
49	0	0.361627323	
50	0	0.361627323	
51	2	0.271220492	
52	0	0.271220492	
53	0	0.361627323	
54	0	0.361627323	
55	0	0.452034154	
56	0	0.542440984	
57	1	0.723254646	
58	1	0.723254646	
59	0	0.994475138	
60	1	0.994475138	
61	1	1.1752888	
62	4	1.1752888	
63	0	1.536916123	
64	3	1.717729784	
65	0	1.898543446	
66	2	2.169763938	
67	0	2.350577599	
68	5	2.260170768	
69	3	2.260170768	
70	2	2.260170768	
71	4	2.350577599	
72	3	2.531391261	
73	3	2.893018584	
74	0	2.531391261	
75	3	2.44098443	
76	1	2.621798091	
77	4	2.350577599	
78	4	2.169763938	
79	1	1.988950276	
80	2	1.988950276	
81	4	1.808136615	
82	1	1.808136615	
83	1	1.536916123	
84	1	1.1752888	
85	0	1.084881969	
86	1	1.26569563	
87	1	0.994475138	
88	1	0.994475138	
89	0	0.994475138	
90	0	0.904068307	
270	4	1.1752888	
271	1	1.26569563	
272	1	1.26569563	
273	1	1.1752888	
274	0	1.26569563	
275	3	1.356102461	

Northeast Reproducible Lineaments

Azimuth	*Frequency*	*Data Concentration Factor (dcf)*	
276	2	0.994475138	
277	1	0.994475138	
278	0	0.904068307	
279	1	0.813661477	
280	1	0.813661477	
281	0	0.632847815	
282	1	0.452034154	
283	0	0.452034154	
284	0	0.452034154	
285	0	0.361627323	
286	1	0.271220492	
287	0	0.271220492	
288	1	0.180813661	
289	0	0.180813661	
290	0	0.180813661	
291	0	0.180813661	
292	0	0.090406831	
293	0	0.090406831	
294	0	0	
295	0	0	
296	0	0	
297	0	0	
298	0	0	
299	0	0	
300	0	0	
301	0	0	
302	0	0	
303	0	0	
304	0	0.090406831	
305	0	0.090406831	
306	0	0.090406831	
307	0	0.090406831	
308	0	0.090406831	
309	1	0.090406831	
310	0	0.090406831	
311	0	0.090406831	
312	0	0.090406831	
313	0	0.090406831	
314	0	0.090406831	
315	0	0	
316	0	0.180813661	
317	0	0.271220492	
318	0	0.271220492	
319	0	0.361627323	
320	0	0.361627323	
321	2	0.452034154	
322	1	0.452034154	
323	0	0.452034154	

Northeast Reproducible Lineaments

Azimuth	*Frequency*	*Data Concentration Factor (dcf)*	
324	1	0.452034154	
325	0	0.542440984	
326	1	0.542440984	
327	0	0.452034154	
328	0	0.361627323	
329	0	0.361627323	
330	1	0.271220492	
331	0	0.361627323	
332	1	0.271220492	
333	0	0.271220492	
334	0	0.542440984	
335	0	0.723254646	
336	1	0.632847815	
337	0	0.632847815	
338	0	0.542440984	
339	3	0.632847815	
340	2	0.632847815	
341	0	0.813661477	
342	0	0.904068307	
343	0	1.26569563	
344	1	1.446509292	
345	0	1.356102461	
346	2	1.26569563	
347	2	1.446509292	
348	4	1.536916123	
349	2	1.536916123	
350	2	1.627322953	
351	1	1.898543446	
352	2	1.808136615	
353	1	1.988950276	
354	0	2.079357107	
355	2	1.988950276	
356	3	1.808136615	
357	1	1.717729784	
358	4	1.536916123	
359	5	1.446509292	
360	1	1.446509292	

Northwest Reproducible Lineaments

Azimuth	*Frequency*	*Data Concentration Factor (dcf)*	
1	3	3.529411765	
2	10	3.529411765	
3	4	3.85026738	
4	3	3.85026738	
5	1	3.85026738	
6	1	3.85026738	
7	0	3.529411765	
8	2	1.92513369	
9	0	1.443850267	
10	0	0.962566845	
11	0	0.802139037	
12	1	0.64171123	
13	0	0.802139037	
14	1	0.481283422	
15	0	0.802139037	
16	0	1.122994652	
17	0	1.28342246	
18	1	1.122994652	
19	0	1.122994652	
20	2	1.122994652	
21	2	1.122994652	
22	1	1.122994652	
23	0	1.122994652	
24	0	0.962566845	
25	1	0.962566845	
26	0	0.64171123	
27	0	0.481283422	
28	0	0.320855615	
29	0	0.481283422	
30	0	0.64171123	
31	0	0.481283422	
32	1	0.481283422	
33	0	0.64171123	
34	1	0.802139037	
35	1	0.802139037	
36	0	0.962566845	
37	0	0.962566845	
38	1	0.962566845	
39	1	0.962566845	
40	0	0.802139037	
41	1	0.64171123	
42	0	0.802139037	
43	1	0.802139037	
44	0	0.802139037	
45	0	0.64171123	
46	0	0.64171123	
47	1	0.481283422	
48	0	0.64171123	

Northwest Reproducible Lineaments

Azimuth	*Frequency*	*Data Concentration Factor (dcf)*	
49	1	0.481283422	
50	0	0.64171123	
51	0	0.802139037	
52	0	0.802139037	
53	1	0.64171123	
54	0	0.64171123	
55	1	0.481283422	
56	1	0.64171123	
57	0	0.64171123	
58	0	0.64171123	
59	0	0.481283422	
60	0	0.64171123	
61	1	0.481283422	
62	0	0.320855615	
63	0	0.481283422	
64	0	0.64171123	
65	1	0.802139037	
66	0	0.802139037	
67	0	0.802139037	
68	1	0.962566845	
69	1	1.122994652	
70	1	1.122994652	
71	0	0.962566845	
72	1	1.122994652	
73	1	1.122994652	
74	1	0.962566845	
75	0	0.802139037	
76	0	0.802139037	
77	1	0.962566845	
78	0	1.122994652	
79	0	1.122994652	
80	0	1.122994652	
81	1	1.122994652	
82	1	1.28342246	
83	2	1.122994652	
84	1	1.122994652	
85	1	1.28342246	
86	0	1.443850267	
87	1	1.443850267	
88	0	1.28342246	
89	0	0.962566845	
90	1	0.802139037	
270	1	0.64171123	
271	1	0.64171123	
272	0	0.481283422	
273	0	0.481283422	
274	0	0.481283422	
275	0	0.481283422	

Northwest Reproducible Lineaments

Azimuth	*Frequency*	*Data Concentration Factor (dcf)*	
276	0	0.320855615	
277	0	0.320855615	
278	0	0.320855615	
279	0	0.481283422	
280	1	0.481283422	
281	0	0.481283422	
282	1	0.481283422	
283	0	0.481283422	
284	1	0.481283422	
285	0	0.481283422	
286	0	0.320855615	
287	0	0.320855615	
288	0	0.160427807	
289	0	0.160427807	
290	0	0	
291	0	0	
292	0	0	
293	0	0	
294	0	0	
295	0	0	
296	0	0	
297	0	0	
298	0	0	
299	0	0	
300	0	0	
301	0	0	
302	0	0	
303	0	0	
304	0	0	
305	0	0	
306	0	0	
307	0	0	
308	0	0	
309	0	0	
310	0	0	
311	0	0	
312	0	0	
313	0	0	
314	0	0	
315	0	0	
316	0	0	
317	0	0	
318	0	0	
319	0	0	
320	0	0	
321	0	0	
322	0	0.160427807	
323	0	0.160427807	

Northwest Reproducible Lineaments

Azimuth	*Frequency*	*Data Concentration Factor (dcf)*	
324	0	0.160427807	
326	0	0.160427807	
327	1	0.160427807	
328	0	0.160427807	
329	0	0.160427807	
330	0	0.160427807	
331	0	0.160427807	
332	0	0.160427807	
333	0	0	
334	0	0.160427807	
335	0	0.320855615	
336	0	0.320855615	
337	0	0.320855615	
338	0	0.481283422	
339	1	0.64171123	
340	1	0.802139037	
341	0	1.122994652	
342	0	1.604278075	
343	1	1.764705882	
344	1	2.406417112	
345	1	2.56684492	
346	2	3.048128342	
347	3	3.368983957	
348	1	3.85026738	
349	4	4.010695187	
350	2	4.171122995	
351	4	4.171122995	
352	2	3.85026738	
353	3	3.529411765	
354	2	3.368983957	
355	2	3.048128342	
356	1	2.727272727	
357	0	2.085561497	
358	1	1.764705882	
359	0	1.28342246	
360	2	0.962566845	

Northwest Reproducible Lineaments

Azimuth	*Frequency*	*Data Concentration Factor (dcf)*	
1	1	3.214285714	
2	4	3.214285714	
3	3	3.214285714	
4	1	3.214285714	
5	2	3.214285714	
6	0	3.506493506	
7	0	3.214285714	
8	0	2.337662338	
9	0	1.461038961	
10	0	1.168831169	
11	1	0.584415584	
12	0	0.876623377	
13	1	0.876623377	
14	0	0.876623377	
15	0	0.876623377	
16	0	0.876623377	
17	1	0.584415584	
18	0	0.876623377	
19	0	0.584415584	
20	0	0.584415584	
21	0	0.584415584	
22	0	0.584415584	
23	1	0.292207792	
24	0	0.292207792	
25	0	0.292207792	
26	0	0.292207792	
27	0	0.292207792	
28	0	0.292207792	
29	0	0	
30	0	0.292207792	
31	0	0.584415584	
32	0	0.584415584	
33	0	0.584415584	
34	0	0.584415584	
35	1	0.584415584	
36	1	0.584415584	
37	0	0.584415584	
38	0	0.876623377	
39	0	0.876623377	
40	0	0.876623377	
41	0	0.584415584	
42	0	0.292207792	
43	1	0.292207792	
44	0	0.292207792	
45	0	0.292207792	
46	0	0.584415584	
47	0	0.876623377	
48	0	0.876623377	

Northwest Reproducible Lineaments

Azimuth	*Frequency*	*Data Concentration Factor (dcf)*	
49	0	0.876623377	
50	0	0.876623377	
51	1	0.876623377	
52	1	0.876623377	
53	0	0.876623377	
54	1	0.876623377	
55	0	0.876623377	
56	0	0.876623377	
57	0	0.584415584	
58	0	0.584415584	
59	0	0.584415584	
60	0	0.292207792	
61	0	0.584415584	
62	0	0.584415584	
63	1	0.584415584	
64	0	0.584415584	
65	0	0.584415584	
66	1	0.876623377	
67	0	0.876623377	
68	0	0.876623377	
69	0	0.584415584	
70	0	0.876623377	
71	1	1.168831169	
72	0	0.876623377	
73	0	0.876623377	
74	0	0.876623377	
75	1	0.876623377	
76	1	1.168831169	
77	0	1.168831169	
78	0	1.168831169	
79	0	1.461038961	
80	0	1.461038961	
81	1	1.461038961	
82	1	1.461038961	
83	0	1.753246753	
84	1	1.753246753	
85	0	2.045454545	
86	1	2.045454545	
87	1	1.753246753	
88	1	1.461038961	
89	0	1.461038961	
90	1	1.461038961	
270	0	1.461038961	
271	0	1.168831169	
272	0	0.876623377	
273	0	0.584415584	
274	1	0.876623377	
275	0	0.584415584	

Northwest Reproducible Lineaments

Azimuth	*Frequency*	*Data Concentration Factor (dcf)*	
276	0	0.584415584	
277	0	0.584415584	
278	0	0.584415584	
279	1	0.584415584	
280	0	0.292207792	
281	0	0.292207792	
282	0	0.292207792	
283	0	0.292207792	
284	0	0.292207792	
285	0	0	
286	0	0	
287	0	0	
288	0	0.292207792	
289	0	0.292207792	
290	0	0.292207792	
291	0	0.292207792	
292	0	0.292207792	
293	1	0.292207792	
294	0	0.292207792	
295	0	0.292207792	
296	0	0.292207792	
297	0	0.292207792	
298	0	0.292207792	
299	0	0	
300	0	0	
301	0	0	
302	0	0	
303	0	0	
304	0	0	
305	0	0	
306	0	0	
307	0	0	
308	0	0	
309	0	0	
310	0	0	
311	0	0	
312	0	0	
313	0	0	
314	0	0	
315	0	0	
316	0	0	
317	0	0	
318	0	0	
319	0	0	
320	0	0	
321	0	0	
322	0	0	
323	0	0	

Northwest Reproducible Lineaments

Azimuth	*Frequency*	*Data Concentration Factor (dcf)*	
324	0	0	
325	0	0	
326	0	0	
327	0	0	
328	0	0	
329	0	0	
330	0	0	
331	0	0	
332	0	0	
333	0	0	
334	0	0	
335	0	0	
336	0	0	
337	0	0	
338	0	0	
339	0	0	
340	0	0.292207792	
341	0	0.292207792	
342	0	0.584415584	
343	0	0.584415584	
344	0	0.584415584	
345	1	0.876623377	
346	0	1.168831169	
347	1	1.168831169	
348	0	1.753246753	
349	0	2.337662338	
350	1	2.337662338	
351	1	2.337662338	
352	0	2.337662338	
353	2	2.922077922	
354	2	4.090909091	
355	0	5.25974026	
356	1	4.967532468	
357	0	4.675324675	
358	3	4.675324675	
359	4	4.090909091	
360	4	3.506493506	

APPENDIX B

The initial fieldwork of this project focused on the mapping of coastal cliffs and drainages on the east side of the Hawkswood Range. This mapping was completed on a series of panoramic photos that were later transformed into line-drawings (Chapter 3). The original photos (not to scale) are provided here as a reference.

Medina Creek

N

Dawn Creek

N

Big Bush Gully

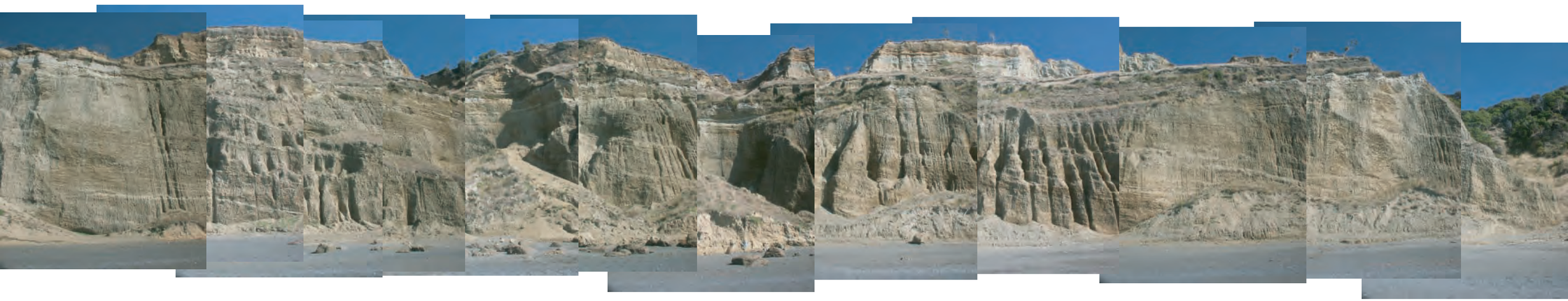

Doug's Gap

N

Doug's Gap

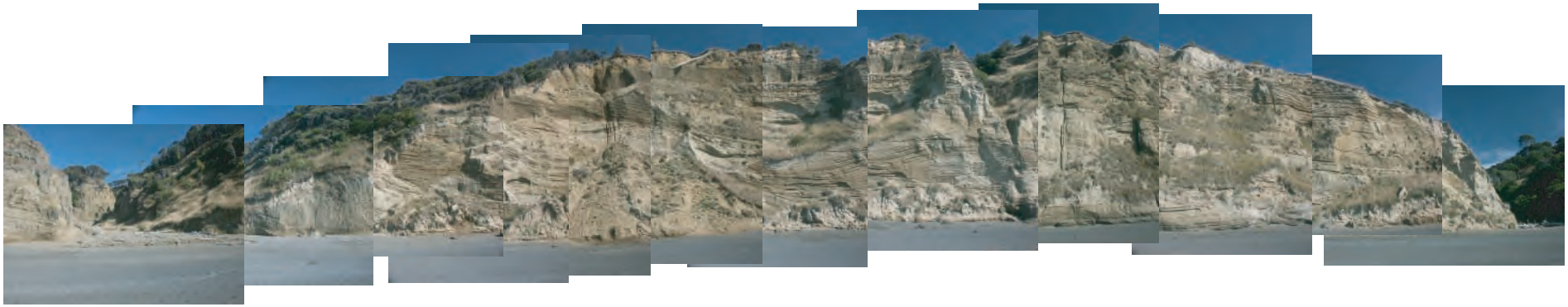

Ploughman's Creek

APPENDIX C

Gilbert-type fan delta deposits are frequently discussed in the literature. However, few studies focus on detailed investigations of individual foreset beds. There is new information to be found on transport processes by looking at individual beds in detail. A summary of the more than 60 beds that were the foundation for the work completed in Chapter 4 is provided here.

FORESET DATA

Distance below Topset	Lithology	Foreset Dip and Direction	Process	Imbrication/Reference
Doug's Gap 20+ m foreset package				
3m	Clast supported conglomerate that coarsens from 2.5cm up to 17 cm	25 ° NE	Hyperpycnal flow	Strongly imbricated 25° upslope
3m	Clast supported conglomerate that fines upwards from 2 cm to fine sand with random floating clasts; inverse grading	NE	Hyperpycnal flow	Imbricated +/- 25° upslope
3m	Clast supportes conglomerate with clast sizes up to 12 cm; inverse grading	NE	Hyperpycnal high-density flow with developed traction carpet	Weak imbrication
5m	Clast supported conglomerate fining from 8cm to 1 cm	NE	Sediment gravity flow	No imbrication
5m	Matrix supported, poorly sorted conglomerate with clasts sizes from 5cm to 2 cm	NE	Initiation of a sediment gravity flow	imbricated clasts +/- 30° upslope (Postma et al 1984)
5m	Poorly sorted conglomerate; avg. 2.5 cm with random orientations	NE	Initiation of a sediment gravity flow	
5m	Clast supported conglomerate coarsening upwards from sand to 6 cm clasts	NE	Sediment gravity flow with developed traction carpet	Weak imbrication
Seal Gap 20+ M foreset package				
8m	Inversely graded conglomerate with 2 cm to 13 cm clasts	28° NE	High density turbidity current	Strongly imbricated 25° upslope
8m	Inversely graded from coarse sand to 10 cm cobbles.	NE	Sediment gravity flow Traction carpet	Weak imbrication
8m	Inversely graded conglomerate from granule to 2 cm clasts	NE	Sediment gravity flow with developing traction carpet.	Falk and Dorsey 1998
8m	Matrix-rich conglomerate that coarsens from 1cm to 7 cm	NE	Sediment gravity flow with developing traction carpet.	
Seal Gap 30+ m foreset Package				
10 m	Clast supported onglomerate bed that coarsens from granule to 5 cm clasts	26° NE	Sediment gravity flow with developed traction carpet	Strongly imbricated 25° upslope
10 m	Matrix-rich conglomerate with clas sizes up to 8 cm	NE	Debris Flow	
10 m	Clast supported conglomerate with 2-7cm clasts at base fining to coarse sand	NE	High density current with sand over flow	Falk and Dorsey 1998, Strongly imbricated 25° upslope
10 m	Matrix supported, poorly sorted conglomerate with clasts from 2 cm to 10 cm	NE	Debris flow	
10 m	Clast supporets conglomerate that fine upwards from	NE	High-density turbidity current	Dawn Creek to

FORESET DATA

	granule to coarse sand			Ploughmans Creek
Big Bush Gully 30 + m foreset Package				
10 m	Clast supported conglomerate with Inverse grading from granules to 6cm cobbles	25° NE	High-density turbidity current with traction carpet	Lowe 1980
10 m	Clast supported conglomerate with Inverse grading from granules to 6 cm cobbles		High- density turbidity current with traction carpet	Lowe 1980, Falk and Dorsey 1996
10 m	Clast supported conglomerate with Normal grading from 4 cm cobbles to coarse grained sand		High density current with sand over flow	Lowe 1980. Postma 1984
10 m	Clast supported conglomerate with Inverse graded from sand to pebble-conglomerate up to 4 cm clasts with sand matrix.	NE	High density current with traction carpet	Lowe 1980
10 m	Matrix supported conglomerate, poorly sorted 5-8 cm clasts with medium grained sand matrix.	none	Unorganized Debris Flow	Lowe 1980
10 m	Well sorted, clast supported conglomerate with pebbles that pinch out	NE	Well-developed Turbidity Current near its run-out	Strong imbrication 25° upslope
10 m	Clast supported conglomerate with inverse graded conglomerate	NE	High density turbidity current	
Dawn Creek 30+ m foreset package				
15 m	paper			
15 m	Clast supported conglomerate with Inverse grading from granules to 6 cm clasts with 6 cm silt overflow	28° NE	Sediment gravity flow with turbulent overflow	
15 m	Clast supported conglomerate inversely graded from granules to 6 cm clasts with a 5 cm silt over flow	NE	Sediment gravity flow with a traction carpet with turbulent over flow	
15 m	Clast supported conglomerate with no internal structure	none	Debris flow that pinches out	
15 m	Clast supported conglomerate, inverse grading from 3 cm- 8 cm clasts	NE	Sediment gravity flow turbidity current with a traction carpet	
Medina Creek 30+ m foreset package				
15m	15 cm thick gravelly bed with 6cm clasts fining up to pebbles	26 ° N	Sediment gravity flow	
15 m	10 cm thick gravelly bed, well sorted with 3.5 cm clasts	N	Well developed sediment gravity flow	
15 m	15 cm thick gravelly bed fining upwards from 4 cm clasts to pebbles	N	Sediment Gravity flow	
15 m	10 cm gravelly bed that coarsens from pebbles to 7 cm clasts	N	Sediment gravity flow with developed traction carpet	
15 m	15 cm coarse silt bed with random cobbles	N	Fine-grained debris flow deposit	

FORESET DATA

20 m	Matrix supported fining upwards from cobbles to pebbles	26° N	Sediment gravity flow	Lowe 1980
20 m	Clast supported conglomerate, inverse grading from coarse sand to 2.5 cm pebbles	N	Sediment gravity flow with traction carpet	Falk and Dorsey 1998
20 m	Matrix supported pebbles	N	Debris flow	Lowe 1980
20 m	Matrix supported, fine-grained sand with random pebbles at top	N	Sediment gravity flow with outsized clasts	
20 m	Clast supported conglomerate, inversely graded from coarse sand to 4 cm pebbles	N	Sediment gravity flow with traction carpet	Falk and Dorsey 1998
Coastal Medina 50+ m foreset Package				
25 m				
Foreset 10m water depth	Clast supported conglomerate, poorly sorted with randomly oriented clasts up 8 cm	none	Slump deposits on the foresets	Colella 1988, Postma et al 1984
Marine Interfluve deposits 30+ meter cliff package				
Interfluve +/- 45m water depth	Fine-grained sand, well sorted, contorted bedding with no preserved internal features	None	Slump deposit with the Marine Interfluve deposits. The fine grained deposits are subject to slumping at the margin	
Foreset 5m water depth	Clast supported conglomerate, steeply imbricated clasts near perpendicular to foreset bedding planes	NE	'Bachstacking' clast forming behind slump blocks is responsible for steep clast imbrication	McConnico et al, submitted, Postma et al 1884
Foreset +/- 35 water depth	Fine-grained silt with clasts up to 5 cm parallel to bedding plane	None	Backset beds developed as small flows infilled depression on the foresets.	Colella 1988, Postma
Interfluve > 35 m water depth	Fine-grained sand 6 cm thick, passing up into ripple laminations.	none	Marine inerfluv deposits developing in the protection of prograding fan delta	Lewis and Ekdale 1991

APPENDIX D

GROUND PENETRATING RADAR (GPR) STUDY

Initially in this study, there were questions that arose in regards to connections between sediments on opposite sides of Ploughman creek. The apparent contrast in facies raised the question of whether or not a fault existed in front of coastal cliffs north of Ploughman creek or perpendicular to the coastline running up Ploughman creek.

Visiting Erskine Scholar Harry Jol provided many interesting discussions on the power and uses of Ground Penetrating Radar (GPR), based on these conversations it was determined that Ground Penetrating Radar (GPR) was an easily usable technique to determine whether or not faults were the reason for the apparent facies changes across Ploughman creek. In addition, we thought GPR could help identify the existence of faults within the Gilbert-type fan delta deposits by running lines across the tops of the cliffs along the Conway Coast. After deciding to use GPR we carried out the data collection at three places; 1) two lines were undertaken on the beach at Ploughman creek (Fig. 1), one parallel to the coastline and the other perpendicular to the coastline, 2) along the cliff tops on the Medina terrace and 3) in the creek beds of Big Bush Gully.

After 2 days of fieldwork and data collection during the 2003 field season it was determined, that GPR would not be able to show us the information needed. There were two problems; 1) the amount of saltwater present along the coastal beach sands prevented accurate collection of data (Fig. 2) and 2) the high amount of fine-grained silt covering the topset beds made it impossible to accurately determine what lay beneath the surface. However, from GPR data collected at Big Bush Gully a good image of the Gilbert-type fan

deltas in Big Bush Gully was produced. The image clearly shows that the ~45 m foreset packages of the Rafa fan delta extends another ~8 m into the subsurface without signs of bottomsets (Fig. 3). This information gave me a better understanding of the total thickness of the Gillbert-type fan delta foreset packages.

Figure 1. The location of the 2 GPR lines completed at Ploughman creek. See Figure 3.4 for Ploughman's Creek location.

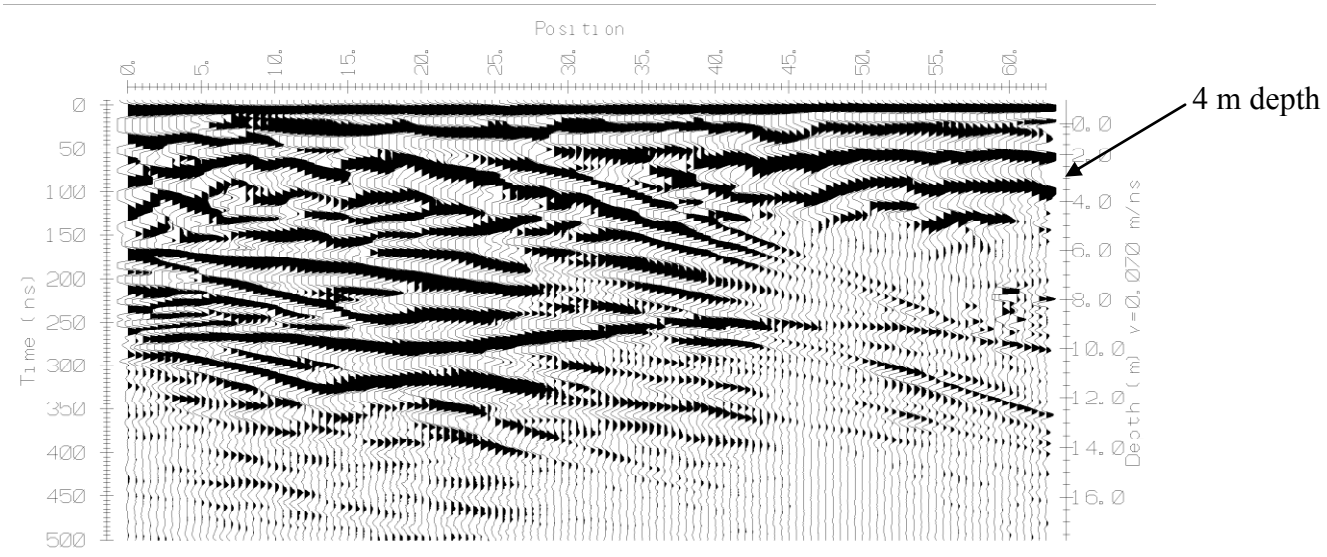

Figure 2. A) Location of GPR line along the coastline near Ploughman Creek. B) Processed data from the GPR line completed in A. Note the distortion of data near the 4 m depth mark. This is the result of saltwater interference (Photo: K. Spinks). Note, for scale person with paddle is 1.9 m.

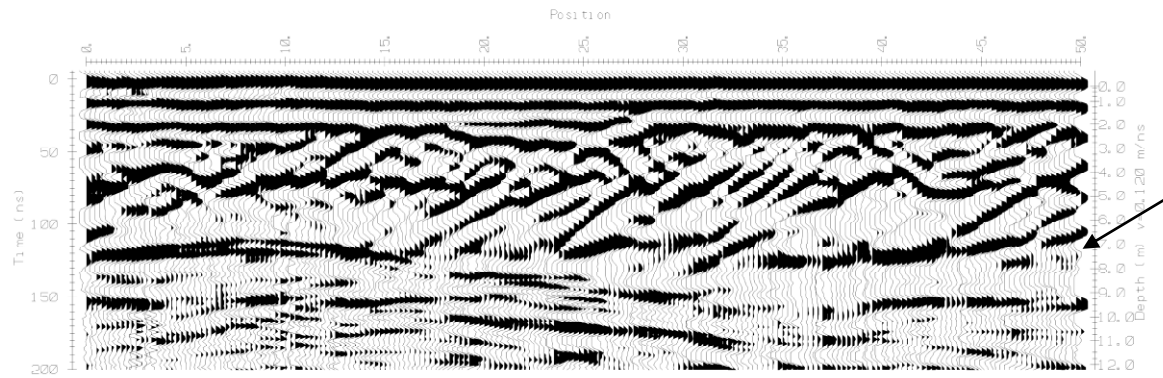

Figure 3. A) Location of GPR line conducted in Big Bush Gully. B) Processed data from the GPR line in A. Note that the foreset beds appear to downlap onto some surface at ~8m. This image provided a better constraint of the foreset package thickness.

APPENDIX E

The dating techniques of Radiocarbon-14C and Optically Stimulated Luminescence (OSL) and archived paleontological data were used to place age constraints on the facies along the Conway Flat coast and calculate uplift rates (Chapter 5). Presented here are the fossil data from FRED, laboratory results from Waikato Radiocarbon Laboratory, University of Waikato, Hamilton, New Zealand and Luminescence Dating Laboratory, School of Earth Sciences, Victoria University, Wellington, Wellington, New Zealand

Luminescence Dating of 5 samples / North Canterbury

report by: Dr. Uwe Rieser
Luminescence Dating Laboratory
School of Geography, Environment and Earth Sciences
Victoria University of Wellington
e-mail: uwe.rieser@vuw.ac.nz
tel: 0064-4-463-6125
fax: 0064-4-463-5186

Summary
5 samples (laboratory code WLL549-WLL553) were submitted for Luminescence Dating by Tim McConnico (Canterbury University). The deposition ages have been determined for all of these samples using the silt fraction. The palaeodose, i.e. the radiation dose accumulated in the sample after the last light exposure (assumed at deposition), was determined by measuring the blue luminescence output during infrared optical stimulation (which selectively stimulates the feldspar fraction). The doserate was estimated on the basis of a low level gammaspectrometry measurement.
All measurements were done in Victoria Universities Dating Laboratory.

Procedure / Luminescence measurements
Sample preparation was done under extremely subdued safe orange light in a darkroom. Outer surfaces, which may have seen light during sampling, were removed and discarded. The actual water content and the saturation content were measured using 'fresh' inside material.
The samples were treated with 10%HCl to remove carbonates until the reaction stopped, then carefully rinsed with distilled water. Thereafter, all organic matter was destroyed with 10%H_2O_2 until the reaction stopped, then carefully rinsed with distilled water. By treatment with a solution of sodium citrate, sodium bicarbonate and sodium dithionate iron oxide coatings were removed from the mineral grains and then the sample was carefully rinsed again.
The grain size 4-11μm was extracted from the samples in a water-filled (with added dispersing agent to deflocculate clay) measuring cylinder using Stokes' Law. The other fractions were discarded. The samples then are brought into suspension in pure acetone and deposited evenly in a thin layer on 70 aluminum discs (1cm diameter).
Luminescence measurements were done using a standard Riso TL-DA15 measurement system, equipped with Kopp 5-58 and Schott BG39 optical filters to select the luminescence blue band. Stimulation was done cw at about 30mW/cm^2 with infrared diodes at 880Δ80nm. β-irradiations were done on a Daybreak 801E ^{90}Sr,^{90}Y β-irradiator, calibrated against SFU, Vancouver, Canada to about 3% accuracy. α-irradiations were done on a ^{241}Am irradiator supplied and calibrated by ELSEC, Littlemore, UK.

The Paleodoses were estimated by use of the multiple aliquot additive-dose method (with late-light subtraction). After an initial test-measurement, 30 aliquots were β-irradiated in six groups up to five times of the dose result taken from the test. 9 aliquots were α-irradiated in three groups up to three times of the dose result taken from the test. These 39 disks were stored in the dark for four weeks to relax the crystal lattice after irradiation. After storage, these 39 disks and 9 unirradiated disks were preheated for 5min at 220C to remove unstable signal components, and then measured for 100sec each, resulting in 39 shinedown curves. These curves were then normalized for their luminescence response, using 0.1s shortshine measurements taken before irradiation from all aliquots.

The luminescence growth curve (β-induced luminescence intensity vs added dose) is then constructed by using the initial 10 seconds of the shine down curves and subtracting the average of the last 20 sec, the so called late light which is thought to be a mixture of background and hardly bleachable components. The shine plateau was checked to be flat after this manipulation. Extrapolation of this growth curve to the dose-axis gives the equivalent dose D_e, which is used as an estimate of the Paleodose.
A similar plot for the alpha-irradiated discs allows an estimate of the α-efficiency, the a-value (Luminescence/dose generated by the α-source divided by the luminescence/dose generated by the β-source).

Fading test
Samples containing feldspars in rare cases show an effect called anomalous fading. This effect inhibits accurate dating of the sample, as the electron traps in the crystal lattice of these feldspars are unable to store the age information over longer periods of time.
None of your samples gave an indication of this problem.

Procedure / Gamma spectrometry
The dry, ground and homogenised soil samples were encapsuled in airtight perspex containers and stored for at least 4 weeks. This procedure minimizes the loss of the short-lived noble gas ^{222}Rn and allows ^{226}Ra to reach equilibrium with its daughters ^{214}Pb and ^{214}Bi.

The samples were counted using high resolution gamma spectrometry with a broad energy Ge detector for a minimum time of 24h. The spectra were analysed using GENIE2000 software.
The doserate calculation is based on the activity concentration of the nuclides ^{40}K, ^{208}Tl, ^{212}Pb, ^{228}Ac, ^{214}Bi, ^{214}Pb, ^{226}Ra.

Results

Table1: Doserate contribution of cosmic radiation

Sample no.	depth below surface (m)	dD_c/dt (Gy/ka)[1]	Field code
WLL549	15	0.0406±0.0020	PG1
WLL550	35	0.0120±0.0006	BBG2
WLL551	20	0.0281±0.0014	DF1
WLL552	50	0.0064±0.0003	MF1
WLL553	50	0.0064±0.0003	MF2

[1] Contribution of cosmic radiation to the total doserate, calculated as proposed by Prescott & Hutton (1994), Radiation Measurements, Vol. 23.

Table2: Radionuclide and water contents

Sample no.	Water content δ[1]	U (µg/g) from ^{234}Th	U (µg/g)[2] from ^{226}Ra, ^{214}Pb, ^{214}Bi	U (µg/g) from ^{210}Pb	Th (µg/g)[2] from ^{208}Tl, ^{212}Pb, ^{228}Ac	K (%)	Field code
WLL549	1.198	2.12±0.28	2.51±0.18	2.33±0.25	10.05±0.14	2.24±0.05	PG1
WLL550	1.097	3.63±0.29	3.81±0.20	3.79±0.27	8.52±0.12	2.13±0.05	BBG2
WLL551	1.168	2.80±0.18	2.29±0.11	2.58±0.16	10.76±0.11	2.31±0.05	DF1
WLL552	1.222	3.76±0.35	3.07±0.22	3.57±0.31	12.12±0.17	2.66±0.06	MF1
WLL553	1.103	3.34±0.24	2.61±0.15	3.11±0.21	11.32±0.13	2.55±0.05	MF2

[1] Ratio wet sample to dry sample weight. Errors assumed 50% of (δ-1).
[2] U and Th-content is calculated from the error weighted mean of the isotope equivalent contents

Table3: Measured a-value and equivalent dose, doserate and luminescence age

Sample no.	a-value	D_e (Gy)	dD/dt (Gy/ka)	**OSL-age (ka)**	Field code
WLL549	0.119±0.006	223.6±12.8	4.27±0.27	**52.4±4.5**	PG1
WLL550	0.067±0.005	346.6±7.0	4.39±0.17	**79.0±3.5**	BBG2
WLL551	0.095±0.027	387.3±10.3	4.22±0.35	**91.7±7.9**	DF1
WLL552	0.094±0.024	440.4±11.8	4.70±0.42	**93.8±8.7**	MF1
WLL553	0.077±0.015	448.3±9.6	4.74±0.25	**94.6±5.3**	MF2

The University of Waikato

Radiocarbon Dating Laboratory

Private Bag 3105
Hamilton,
New Zealand.
Fax +64 7 838 4192
Ph +64 7 838 4278
email c14@waikato.ac.nz
Head: Dr Alan Hogg

Report on Radiocarbon Age Determination for Wk- 13113

Submitter	TS McConnico
Submitter's Code	sample T-1
Site & Location	Conway Coast (rafa pt-ploughmans gap section), New Zealand
Sample Material	Wood sample from tree in cliff (t-1)
Physical Pretreatment	Surfaces scraped clean. The wood was chopped up into small splinters and washed in ultrasonic bath.
Chemical Pretreatment	Sample was washed in hot 10% HCl, rinsed and treated with hot 1% NaOH. The NaOH insoluble fraction was treated with hot 10% HCl, filtered, rinsed and dried.

$\delta^{13}C$	-24.0 ±	0.2 ‰
$D^{14}C$	-608.2 ±	2.3 ‰
$F^{14}C\%$	39.2 ±	0.2 %

Result **7526 ± 47 BP**

Comments

15/12/09

- Result is *Conventional Age or Percent Modern Carbon (pMC)* following Stuiver and Polach, 1977, Radiocarbon 19, 355-363. This is based on the Libby half-life of 5568 yr with correction for isotopic fractionation applied. This age is normally quoted in publications and must include the appropriate error term and Wk number.
- Quoted errors are 1 standard deviation due to counting statistics multiplied by an experimentally determined Laboratory Error Multiplier.
- The isotopic fractionation, $\delta^{13}C$, is expressed as ‰ wrt PDB.
- $F^{14}C\%$ is also known as *Percent Modern Carbon (pMC)* .

The University of Waikato

Radiocarbon Dating Laboratory

Private Bag 3105
Hamilton,
New Zealand.
Fax +64 7 838 4192
Ph +64 7 838 4278
email c14@waikato.ac.nz
Head: Dr Alan Hogg

Report on Radiocarbon Age Determination for Wk- 13114

Submitter	TS McConnico
Submitter's Code	sample T-2
Site & Location	Conway Coast (rafa pt), New Zealand
Sample Material	wood from beach terrace
Physical Pretreatment	Surfaces scraped clean. The wood was chopped up into small splinters and washed in ultrasonic bath.
Chemical Pretreatment	Sample was washed in hot 10% HCl, rinsed and treated with hot 1% NaOH. The NaOH insoluble fraction was treated with hot 10% HCl, filtered, rinsed and dried.

$\delta^{13}C$	-25.7 ±	0.2 ‰
$D^{14}C$	-1000.4 ±	0.5 ‰
$F^{14}C\%$	0.0 ±	0.0 %

Result **>40,000 BP**

Comments

15/12/09

- Result is *Conventional Age or Percent Modern Carbon (pMC)* following Stuiver and Polach, 1977, Radiocarbon 19, 355-363. This is based on the Libby half-life of 5568 yr with correction for isotopic fractionation applied. This age is normally quoted in publications and must include the appropriate error term and Wk number.
- Quoted errors are 1 standard deviation due to counting statistics multiplied by an experimentally determined Laboratory Error Multiplier.
- The isotopic fractionation, $\delta^{13}C$, is expressed as ‰ wrt PDB.
- $F^{14}C\%$ is also known as *Percent Modern Carbon (pMC)* .

The University of Waikato

Radiocarbon Dating Laboratory

Private Bag 3105
Hamilton,
New Zealand.
Fax +64 7 838 4192
Ph +64 7 838 4278
email c14@waikato.ac.nz
Head: Dr Alan Hogg

Report on Radiocarbon Age Determination for Wk- 13115

Submitter	TS McConnico
Submitter's Code	sample T-3
Site & Location	Conway Coast (Big Bush Gully), New Zealand
Sample Material	Wood
Physical Pretreatment	Surfaces scraped clean. The wood was chopped up into small splinters and washed in ultrasonic bath.
Chemical Pretreatment	Sample was washed in hot 10% HCl, rinsed and treated with hot 0.5% NaOH. The NaOH insoluble fraction was treated with hot 10% HCl, filtered, rinsed and dried.

$\delta^{13}C$	-28.7 ±	0.2 ‰
$D^{14}C$	-594.6 ±	2.5 ‰
$F^{14}C\%$	40.5 ±	0.2 %

Result **7252 ± 49 BP**

Comments

15/12/09

- Result is *Conventional Age or Percent Modern Carbon (pMC)* following Stuiver and Polach, 1977, Radiocarbon 19, 355-363. This is based on the Libby half-life of 5568 yr with correction for isotopic fractionation applied. This age is normally quoted in publications and must include the appropriate error term and Wk number.
- Quoted errors are 1 standard deviation due to counting statistics multiplied by an experimentally determined Laboratory Error Multiplier.
- The isotopic fractionation, $\delta^{13}C$, is expressed as ‰ wrt PDB.
- $F^{14}C\%$ is also known as *Percent Modern Carbon (pMC)* .

The University of Waikato

Radiocarbon Dating Laboratory

Private Bag 3105
Hamilton,
New Zealand.
Fax +64 7 838 4192
Ph +64 7 838 4278
email c14@waikato.ac.nz
Head: Dr Alan Hogg

Report on Radiocarbon Age Determination for Wk- 13349

Submitter	TS McConnico
Submitter's Code	T-4
Site & Location	Conway Flat, New Zealand
Sample Material	Large horizontal tree stratigraphically above forest
Physical Pretreatment	Surfaces scraped clean. The wood was chopped up into small splinters and washed in ultrasonic bath.
Chemical Pretreatment	Sample was washed in hot 10% HCl, rinsed and treated with hot 1% NaOH. The NaOH insoluble fraction was treated with hot 10% HCl, filtered, rinsed and dried.

$\delta^{13}C$	-25.2 ±	0.2 ‰
$D^{14}C$	-620.9 ±	2.6 ‰
$F^{14}C\%$	37.9 ±	0.3 %

Result **7791 ± 55 BP**

Comments

15/12/09

- Result is *Conventional Age or Percent Modern Carbon (pMC)* following Stuiver and Polach, 1977, Radiocarbon 19, 355-363. This is based on the Libby half-life of 5568 yr with correction for isotopic fractionation applied. This age is normally quoted in publications and must include the appropriate error term and Wk number.
- Quoted errors are 1 standard deviation due to counting statistics multiplied by an experimentally determined Laboratory Error Multiplier.
- The isotopic fractionation, $\delta^{13}C$, is expressed as ‰ wrt PDB.
- $F^{14}C\%$ is also known as *Percent Modern Carbon (pMC)* .

The University of Waikato

Radiocarbon Dating Laboratory

Private Bag 3105
Hamilton,
New Zealand.
Fax +64 7 838 4192
Ph +64 7 838 4278
email c14@waikato.ac.nz
Head: Dr Alan Hogg

Report on Radiocarbon Age Determination for Wk- 13350

Submitter	TS McConnico
Submitter's Code	T-5
Site & Location	Conway Flat, New Zealand
Sample Material	Wood
Physical Pretreatment	Surfaces scraped clean. The wood was chopped up into small splinters and washed in ultrasonic bath.
Chemical Pretreatment	Sample was washed in hot 10% HCl, rinsed and treated with hot 1% NaOH. The NaOH insoluble fraction was treated with hot 10% HCl, filtered, rinsed and dried.

$\delta^{13}C$	-23.7 ±	0.2 ‰
$D^{14}C$	-551.3 ±	2.9 ‰
$F^{14}C\%$	44.9 ±	0.3 %

Result **6437 ± 52 BP**

Comments

15/12/09

- Result is *Conventional Age or Percent Modern Carbon (pMC)* following Stuiver and Polach, 1977, Radiocarbon 19, 355-363. This is based on the Libby half-life of 5568 yr with correction for isotopic fractionation applied. This age is normally quoted in publications and must include the appropriate error term and Wk number.
- Quoted errors are 1 standard deviation due to counting statistics multiplied by an experimentally determined Laboratory Error Multiplier.
- The isotopic fractionation, $\delta^{13}C$, is expressed as ‰ wrt PDB.
- $F^{14}C\%$ is also known as *Percent Modern Carbon (pMC)* .

The University of Waikato

Radiocarbon Dating Laboratory

Private Bag 3105
Hamilton,
New Zealand.
Fax +64 7 838 4192
Ph +64 7 838 4278
email c14@waikato.ac.nz
Head: Dr Alan Hogg

Report on Radiocarbon Age Determination for Wk- 13351

Submitter	TS McConnico
Submitter's Code	T-6
Site & Location	Conway Flat, New Zealand
Sample Material	Wood
Physical Pretreatment	Surfaces scraped clean. The wood was chopped up into small splinters and washed in ultrasonic bath.
Chemical Pretreatment	Sample was washed in hot 10% HCl, rinsed and treated with hot 1% NaOH. The NaOH insoluble fraction was treated with hot 10% HCl, filtered, rinsed and dried.

$\delta^{13}C$	-23.8 ±	0.2 ‰
$D^{14}C$	-630.5 ±	2.5 ‰
$F^{14}C\%$	36.9 ±	0.3 %

Result **7998 ± 55 BP**

Comments

15/12/09

- Result is *Conventional Age or Percent Modern Carbon (pMC)* following Stuiver and Polach, 1977, Radiocarbon 19, 355-363. This is based on the Libby half-life of 5568 yr with correction for isotopic fractionation applied. This age is normally quoted in publications and must include the appropriate error term and Wk number.
- Quoted errors are 1 standard deviation due to counting statistics multiplied by an experimentally determined Laboratory Error Multiplier.
- The isotopic fractionation, $\delta^{13}C$, is expressed as ‰ wrt PDB.
- $F^{14}C\%$ is also known as *Percent Modern Carbon (pMC)* .

The University of Waikato

Radiocarbon Dating Laboratory

Private Bag 3105
Hamilton,
New Zealand.
Fax +64 7 838 4192
Ph +64 7 838 4278
email c14@waikato.ac.nz
Head: Dr Alan Hogg

Report on Radiocarbon Age Determination for Wk- 18232

Submitter	TS McConnico
Submitter's Code	PG1
Site & Location	Conway Coast. Cliff locality 50 meters north of Ploughmans Creek, New Zealand
Sample Material	Wood
Physical Pretreatment	Surfaces scraped clean. The wood was washed in ultrasonic bath, then ground.
Chemical Pretreatment	Sample was washed in hot 10% HCl, rinsed and treated with hot 0.5% NaOH. The NaOH insoluble fraction was treated with hot 10% HCl, filtered, rinsed and dried.

$\delta^{13}C$	-25.2 ±	0.2 ‰
$D^{14}C$	-999.8 ±	0.8 ‰
$F^{14}C\%$	0.0 ±	0.1 %

Result **>50, 000 BP**

Comments

15/12/09

- Result is *Conventional Age or Percent Modern Carbon (pMC)* following Stuiver and Polach, 1977, Radiocarbon 19, 355-363. This is based on the Libby half-life of 5568 yr with correction for isotopic fractionation applied. This age is normally quoted in publications and must include the appropriate error term and Wk number.
- Quoted errors are 1 standard deviation due to counting statistics multiplied by an experimentally determined Laboratory Error Multiplier.
- The isotopic fractionation, $\delta^{13}C$, is expressed as ‰ wrt PDB.
- $F^{14}C\%$ is also known as *Percent Modern Carbon (pMC)* .

APPENDIX F

In December 2005 a two-day field trip at Conway Flat was organized for the 50th annual Geological Society of New Zealand (GSNZ) conference in Kaikoura, New Zealand. The field guide presented data and interpretations from this thesis.

> **McConnico, TS**, and KN Bassett (2005); Field Trips 2 & 9: The Conway fan delta terraces and uplift of the Hawkswood Range; in Pettinga, JR and AM Wandres (eds.); Field Trip Guides, Geological Society of New Zealand 50 th Anniversary Conference, Kaikoura; Geological Society of New Zealand Misc. Publ 119B; p. 37-48

50th Kaikoura05

The Organising Committee extends a warm welcome to all delegates and visitors to Kaikoura, where it all began 50 years ago.

Please note that all information in this publication was correct at the time of going to print. However, due to factors beyond our immediate control, such as weather, road conditions and permission for land access, some unexpected late changes in field trip routes and itineraries may be required.

Bibliographic References:

Programme & Abstracts Volume

A.N. Author (2005) What I did in my holidays. *In:* Pettinga, J.R. and Wandres, A.M. (eds.) Programme and Abstracts, Geological Society of New Zealand 50th Annual Conference, Kaikoura, New Zealand. Geological Society of New Zealand Misc. Publ. 119A, x-y p.

Field Trip Guide Volume

A.F.T. Leader (2005) A tour of my field area. *In:* Pettinga, J.R. and Wandres, A.M. (eds.) Field Trip Guides, Geological Society of New Zealand 50th Annual Conference, Kaikoura, New Zealand. Geological Society of New Zealand Misc. Publ. 119B, xx-yy p.

Geological Society of New Zealand

50th Annual Conference

28 November to 1 December 2005
Kaikoura Memorial Hall and Takahanga Marae
Kaikoura

Field Trip Guides

J. R. Pettinga and A. M. Wandres (Editors)

Organising Committee

Jarg Pettinga and Keith Lewis (Co - Conveners)
Anekant Wandres
Tim Davies
Kari Bassett
Jocelyn Campbell
Malcolm Laird
Margaret Bradshaw
Student Helpers

with administrative assistance from:

Janet Simes (Absolutely Organised Ltd)
Janet Warburton

Geological Society of New Zealand Miscellaneous Publication 119B
ISBN 0-908678-02-9

Field Trip Guides – Contents

PRE-CONFERENCE FIELD TRIPS

Trip 1: **Cretaceous-Paleogene Stratigraphy of Eastern Marlborough: Opening a South Pacific Window on a Greenhouse Earth. 1**
Leaders: Chris Hollis, Percy Strong, Malcolm Laird and James Crampton

Trip 2: **The Conway Fan Delta Terraces and the Uplift of the Hawkeswood Range 37**
Leaders: Tim McConnico and Kari Bassett

Trips 3A and 3B: **Structure, Stratigraphy and Active Tectonics of Inland North Canterbury 49**
Leaders: Jocelyn Campbell, John Bradshaw, Jarg Pettinga and Phil Tonkin

Trip 4: **Faults of Eastern Marlborough: Picton, Awatere and Kekerengu 85**
Leaders: Russ van Dissen, Tim Little, and Andy Nicol

MID-CONFERENCE FIELD TRIPS

Trip 5A: **Structure and Tectonics of the Kaikoura Peninsula 111**
Leaders: Jocelyn Campbell, Phil Tonkin and John Bradshaw

Trip 5B: **Stratigraphic and Sedimentological Teasers, Kaikoura Peninsula, Marlborough 129**
Leaders: Malcolm Laird, Greg Browne and Brad Field

Trip 6: **Mt Fyffe and Kaikoura Plains: Active Tectonics Fan Morphology and Hazards 141**
Leaders: Tim Davies, Bill Bull

Trip 7: **Structural Geomorphology and Paleoseismicity of the Hope Fault 157**
Leaders: J. Dykstra Eusden Jr, Jarg Pettinga and Rob Langridge

POST-CONFERENCE FIELD TRIPS

Trip 8: **Following in McKay's Footsteps - Iconic Cretaceous and Neogene Successions, Haumuri Bluff, Marlborough 179**
Leaders: Greg Browne, Ian Speden and Brad Field

Trip 9: **The Conway Fan Delta Terraces and the Uplift of the Hawkeswood Range 197**
Leaders: Tim McConnico and Kari Bassett

Trip 10: **Active Tectonics and Structural Geomorphology of Inland North Canterbury 199**
Leaders: Jocelyn Campbel,l Jarg Pettinga and Phil Tonkin

Field Trips 2 and 9

THE CONWAY FAN DELTA TERRACES AND THE UPLIFT OF THE HAWKESWOOD RANGE

Tim McConnico and Kari Bassett

Dept of Geological Sciences, University of Canterbury,
Private Bag 4800, Christchurch

kari.bassett*canterbury.ac.nz

Introduction

Quaternary Gilbert-style fan deltas of the Conway Coast, New Zealand, are both formed and exposed as the result of rapid uplift and erosion of the Hawkeswood Range as part of the transpressional Marlborough Fault Zone (Pettinga and Armstrong, 1998). The Hawkeswood Range is a NE plunging growing anticline over an associated thrust fault ***(Fig. 1)*** (Pettinga and Armstrong, 1998; Hall, 2003) and the northeast verging Hundalee thrust Fault on the western side of the range (Pettinga and Armstrong, 1998). It is one of many anticlines forming in the hanging wall of thrust faults which are currently accommodating most of the ~30 mm/year shortening associated with the modern convergent plate boundary (Nicol, 1991). The fantastic uplift rate of the Hawkeswood anticline was first calculated as 3.1 mm/year based on correlating coastal terraces along the South Island (Ota et al., 1984), but was later revised to 2.9 mm/year for the Conway Coast (Ota at al., 1996). Recent work in the area by Hall (2003) calculated a similar ~2.9 mm/year uplift rate for the area. These uplift rates were calculated based on the assumption that the terrace features were uplifted beach surfaces.

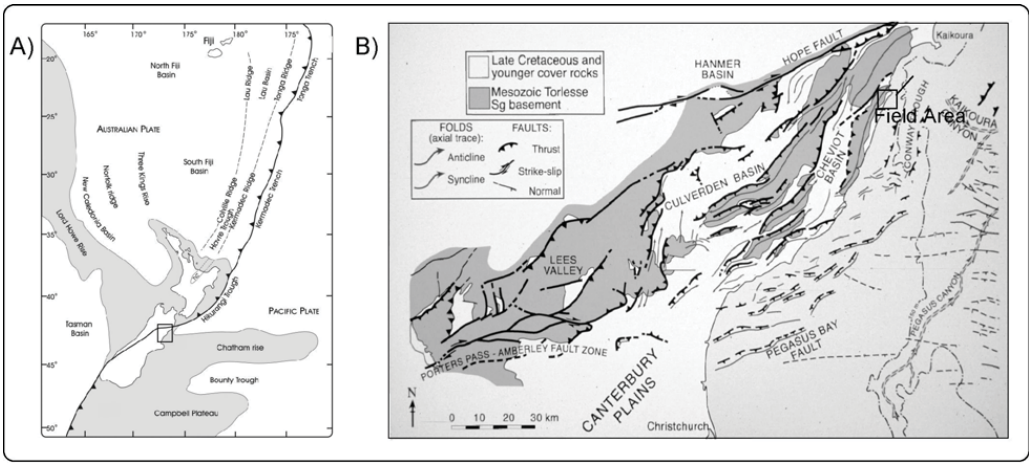

Figure 1: Map showing regional structural setting of the transpressional Marlborough Fault Zone (Pettinga and Armstrong, 1998). The Hawkeswood Range is a growing anticline formed in the hanging wall of a propagating thrust fault. The fan deltas formed on the east side of the Hawkeswood Range, marked by the rectangle.

Recent studies (McConnico and Bassett, 2003; McConnico and Bassett, 2004, McConnico et al, 2005) have found that the preserved terrace features are in fact a series of alluvial fans that have been dissected by eastward propagating thrust faults. Limited exposures make mapping difficult, but offset gravels and clast imbrication fabrics support this interpretation. The alluvial fans form Gilbert-style fan deltas where they enter the sea forming multiple terraces along the Conway Coast side of the Hawkeswood anticline. The flat-lying geomorphic expressions of the terraces have their origin in the tripartite geometry of Gilbert-style fan deltas. The rapid uplift of terraces and subsequent incision and erosion into the deposits expose complete sections with 3-dimensional exposure of Gilbert-style fan deltas in cliffs along the Coast. Cliff exposures are 50-70 meters high and expose continuous sections of Quaternary to Holocene strata. Outcrops also occur in recent slumps and in river gullies at 90° to the strike of the coastal sections thus providing 3-dimensional views of the fan deltas. The magnificent exposure of multiple Gilbert-style fan deltas provides an excellent opportunity to

observe and record the sedimentary facies architecture in terraces formed by the fan delta processes associated with rapid uplift.

Terrace Geomorphology

A series of 4 nested terraces with minor incised fluvial canyons can be identified. The Medina Terrace is the oldest and highest terrace and occurs in the southernmost portion of the field area along the coast. It is 2 km long and is 2 km wide at the widest point and has an elevation of ~10-15 m higher than the other terraces ***(Fig. 2)***. The terrace terminates to the west into the basement rocks of the Hawkeswood Range and to the east as a sea cliff containing fan delta deposits. The terrace surface is smooth and tilts slightly to the east and has one major west-to-east running creek dissecting the terrace.

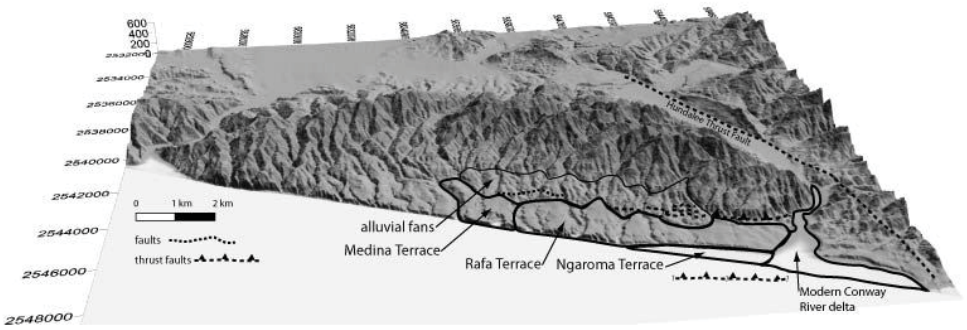

Figure 2: Map showing 4 nested terraces formed by fan deltas and the locality stops. The 4 terraces are, from north to south, the modern Conway delta, the Ngaroma Terrace, the Rafa Terrace, and the Medina Terrace. Trip 1 will focus on the Ngaroma and Rafa Terraces and Trip 2 will focus on the Medina Terrace.

The Medina Terrace is abruptly truncated to the north by incision and formation of the Rafa Terrace ***(fig. 2)***. The Rafa Terrace is 7 km long and up to 2.5 km wide and is ~10-15 m lower in elevation when compared to the Medina Terrace. The terrace terminates to the west into the basement rocks of the Hawkeswood Range and to the east as a sea cliff containing fan delta deposits. The surface slopes from the west to the east ~10-15° with minor undulations. There are 3 major drainages and several smaller creeks that dissect this terrace exposing associated fan delta plain topset deposits.

The Rafa Terrace is abruptly truncated to the north by incision and formation of the Ngaroma fluvial terrace ***(fig. 2)***. The Ngaroma Terrace is a large flat lying terrace bound to the south and west by a curvilinear contact with the Rafa Terrace and to the east by a coastal cliff containing estuary deposits. The terrace is 5 km long and up to 500 m wide. The Ngaroma Terrace has a noticeably smooth surface, is horizontal to the south near Ploughman's Creek and is back tilted near the Conway River mouth at the coast. Several minor streams dissect the terrace.

The Ngaroma Terrace is truncated to the north by incision from the modern Conway River. The youngest terrace along the Conway coast is the currently forming delta of the Conway River ***(Fig. 2)***. The southern and northern boundaries are erosional scarps into the Ngaroma Terrace deposits. The fluvial gravels of the Conway River dominate the surface morphology with the delta gently dipping towards the sea.

Within the nested terraces are several remnant fluvial terraces along the edges of incised canyons. The fluvial terraces can be up to 500 m long and 50 m wide and are often very subtle, rounded and grass covered. The slope of the terrace surfaces is the same as the modern drainages in which they sit.

Sedimentary Lithofacies

The depositional environments that formed each of the terraces are exposed in beach cliffs and in the walls of deeply incised streams. These include older (Pliocene?) marine deposits, fan delta topset fluvial and estuary deposits, fan delta foreset deposits, pro-delta deposits, and interfan shallow marine deposits ***(fig. 3)***.

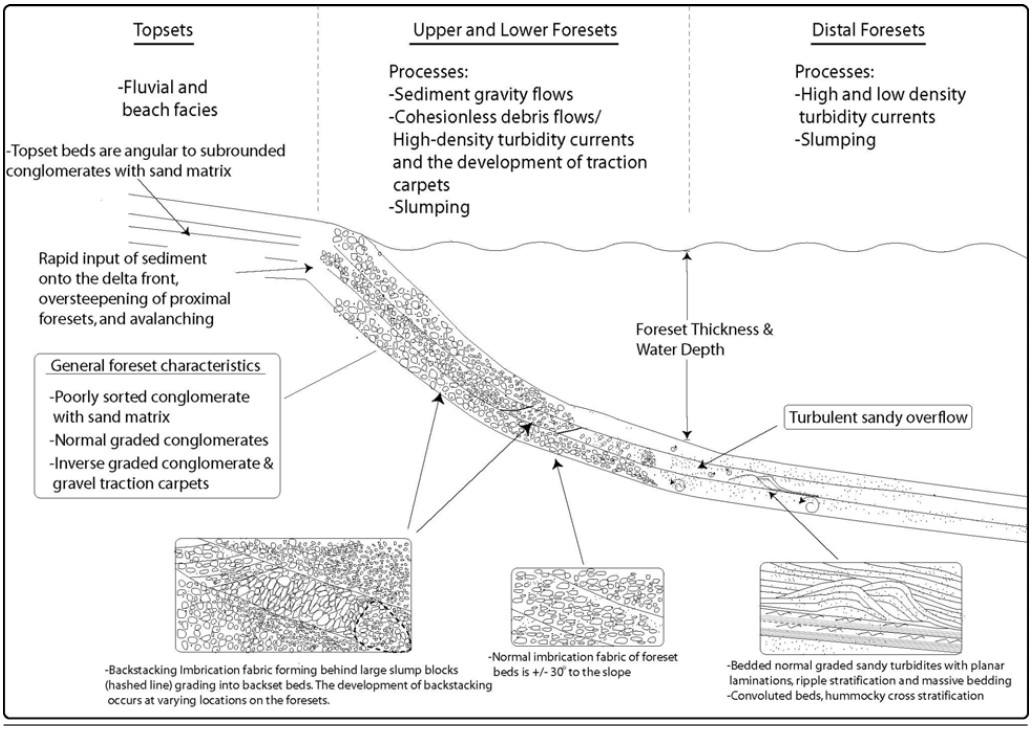

Figure 3: Schematic model of depositional processes on a Gilbert-style gravelly fan delta. Note the debris flow and fluvial bedload processes on the delta plain, the beach processes on the delta front, and slumping, debris flow, and high density turbidity currents on the delta foreset slope.

The older Marine deposits are comprised of dark muds that are occasionally interbedded with light grey, very fine silts. They contain rare laminations, are bedded, and sometimes display large scale cross bedding, slumping, and convoluted bedding. These occur beneath fan delta deposits of the Medina and Rafa Terraces and as a remnant high in the Ngaroma Terrace.

Prodelta mudstone beds typically contain diagnostic fossils, including Zeacolpus symerricus, and macroscopic carbonaceous material throughout (Ekdale and Lewis, 1991). The muds are comprised of matrix-supported, chaotic shell beds with random clasts indicative of debris flow deposition. They are similar to the older marine facies, however, a few diagnostic characteristic separate them easily: 1) the presence of shell material, 2) matrix supported, beds

containing shells and random clasts associated with debris flows, and 3) chaotic beds associated with slumps. Prodelta mudstones occur in the Medina and Rafa Terrace deposits.

The interfan nearshore marine facies comprises mainly yellow-grey, very fine-grained silt/mud, very fine-grained sand and rare interbedded gravels. Silt beds (2-25 cm thick) are continuous and dip <2º to the northeast. The beds often exhibit areas of slumping and convoluted bedding and rare hummocky cross-stratification. The interbedded sand and gravel layers are lenticular (Lewis and Ekdale, 1991). The diagnostic features of the interfan nearshore lithofacies that separate it from both the older marine and prodelta lithofacies are: 1) increased amount of silt, 2) more slumps, 3) interbedded fluvial gravels near the top of the sections, 4) lack of shell material and 5) increased carbonaceous material. The interfan marine deposits occur primarily in the Rafa Terrace along the north edge in Ploughman's Ck.

Fan delta foreset beds ***(fig. 3)*** are made of a series of stacked gravel beds (up to 50 cm thick) periodically parted by silt beds (up to 15 cm thick). Foreset beds dip to the northeast ~10° near the toe to ~30° near the top. Gravel beds fine towards the toe with silt beds thickening. The gravel layers are either moderately sorted and clast-supported with high percentages of sand matrix or poorly sorted and matrix supported. Clasts are well rounded to subangular and range from cobble to granule in size. In the clast supported gravel foresets, the clasts larger than 2 cm are usually horizontally imbricated. Slump features are relatively common in the fan delta foreset lithofacies. The foreset material is interpreted as deposited by sediment gravity flows, including grain flow, debris flow or high-density turbidity current, originating mainly from slumps or bottom hugging fluvial currents (Lewis, 1976; Lewis 1980; Lewis et al., 1980; McConnico and Bassett, 2003; McConnico and Bassett, 2004). Well developed foreset deposits occur in both the Medina and Rafa Terraces.

Within the fan delta complex are rare, well-preserved delta front deposits ***(fig. 3)***. These are comprised of discontinuous, very well sorted, very well rounded, highly stratified, and seaward imbricated gravels with interbedded sands. These are interpreted as foreshore deposits shaped by the wave activity on the beach face. These can be seen primarily in the Rafa Terrace but also rarely in the Medina Terrace.

Fan delta plain alluvial topset beds ***(fig. 3)*** are visibly present but are often inaccessible at the tops of cliffs. There are two distinct topset bed units: 1) well stratified, clast supported conglomerates with rounded clasts that laterally grade into foreset beds and 2) poorly sorted, matrix supported breccias with angular clasts. The well stratified, clast supported gravels are interpreted as fluvial bedload deposits whereas the poorly sorted, matrix supported gravels are interpreted as debris flow deposits. These cover the entire surface of the Medina and Rafa Terraces and occur in incised fluvial terraces forming the alluvial fan delta surfaces.

Fan delta plain estuarine topset deposits along the Conway coast comprise mainly carbonaceous-rich mud with interbedded sands and gravels. Mud layers are dark gray, contain abundant carbonaceous material, abundant rhyzoliths and rootlets up to 10 cm long, and syneresis cracks (Lewis and Ekdale, 1991). Sands and silts are laminated, with sands often displaying ripple laminations. Abundant wood pieces are present ranging from <1 cm fragments to 5 cm thick pieces. Gravels are poorly sorted and matrix supported or well stratified and clast supported interpreted as debris flow and fluvial stream flow deposits respectively. Rooted in the gravels is an in situ ~8000 BP Podocarp forest (Ota et al, 1984; Lewis and Ekdale, 1991). These primarily occur in the Ngaroma Terrace and the modern Conway delta.

Tectonics vs. Eustatic Sealevel

The depositional/erosional patterns of the terraces exposed along the Conway Coast probably represent a complex play between active tectonics and relative rise and falls in sea level. Relative sea level rise and fall could have created the water depths needed to produce the multiple cut and fill stages recorded within the terraces. Since the beginning of the Quaternary there have been major rise and falls in sea level (Schulmeister and Kirk, 1993; Ota et al., 1996). Most notably, rises around at 130 Ka and 12 Ka and major falls beginning around 120 Ka and 30 Ka with many other minor falls occurring also. These major rises and falls in sea level throughout the Quaternary could each account for periods of cut and fill, superimposed on the gradual uplift of the Hawkeswood Range.

Alternatively, each incision episode could represent episodic uplift along the thrust faults associated with earthquakes. Such events could have triggered large scale slumping in the shallow marine deposits to the sides of the fan deltas. If the uplift and incision of the fan deltas corresponds to tectonic motions then the timing of the fan delta deposition and incision would not correspond with eustatic sea level rises and falls.

The key to connecting the regional and local tectonics with the periods of erosion and deposition is age control. Samples have been collected for Optically Stimulated Luminescence dating from the fan deltas and marine muds in hope of determining the exact relationship of sea level rise and fall to tectonics. 14C samples from the in situ podocarp forest in the Ngaroma Terrace have already returned a date of ~8,000 BP agreeing with previous dates (Ota et al., 1984).

Field Trip 2 (Pre-conference) - fan delta sedimentary processes

From Christchurch drive north on Hwy. 1 to the Conway River (~2 hrs.)
turn right (east) to coast
at fork turn right across bridge
drive to coast

Stops 1, 3, 4, 5, 6 and 7

Field Trip 9 (Post-conf.) - tectonic setting of multiple nested fan delta terraces

From Kaikoura drive south on Hwy. 1 to the Conway River (~1 hr.)
turn left (east) to coast
at fork turn right across bridge
drive to coast and south along coast

Stops 1, 2, 3,7, 8 and 9

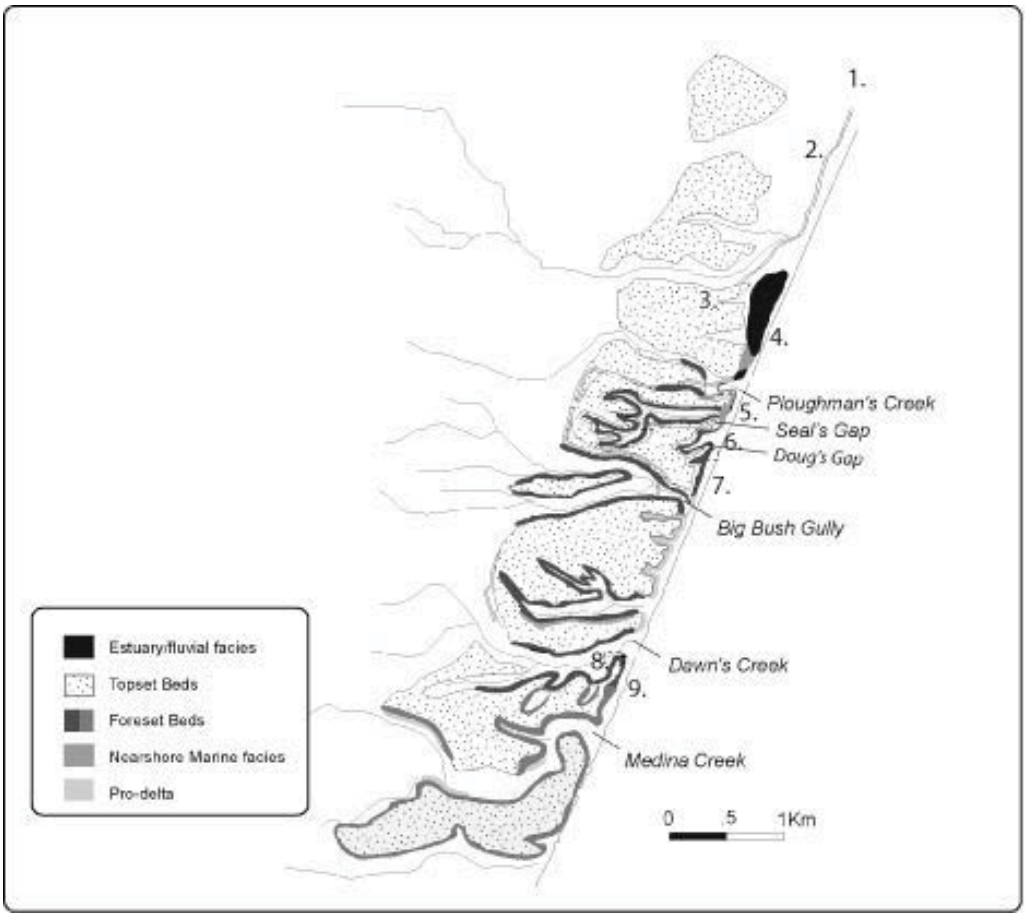

Figure 4: Map of both lithofacies and localities.

Stop 1 (On road near the mouth of the Conway River)
The youngest terrace along the Conway coast is the currently forming delta of the Conway River ***(Fig. 2)***. The modern Conway River is actively being deflected around the growing Hawkeswood anticline. The deflection of the river has created one of the numerous sets of inset terraces. The stacking of these terraces is probably a result of the play between tectonics and relative rise and falls in sea level. Note the delta surface morphology and depositional facies; delta front beach deposits for a thin strip with minor estuary deposits formed behind the beach barrier. The majority of the depositional facies is the fluvial delta plain topset beds.

Stop 2 (Ngaroma Terrace by the Ngaroma Shearing quarters)
The uplifted terraces preserved on the east side of the Hawkeswood range dip eastward with the exception of the Ngaroma Terrace ***(Fig. 2)***. The Ngaroma Terrace is also seaward dipping over most of its surface but the region near the Conway River is back tilted to the west. The back tilted section of the Ngaroma Terrace most likely overlies the active, deforming hanging wall of an eastward propagating thrust fault that roots in the Hawkeswood range.

Stop 3 (Top of the Rafa Terrace overlooking the Ngaroma Terrace)
The first example of the multiple stacking of terraces is evident by looking northwards from the contact between the Rafa and Ngaroma Terraces ***(fig. 2)***. The erosion of the Rafa Terrace, probably by the deflected ancient Conway River, was followed by deposition of the Ngaroma Terrace below. The terrace formed as an estuarine environment trapped behind a barrier beach similar to the modern system but on a larger scale. Unfortunately, due to its young age, there are only the coastal cliff exposures of the deposits (Stop 3).

Stop 4 (walking south along beach cliffs from road access to Ploughman's Gap)
The first outcrop scale connection of the nested terraces can be seen from the beach access southward along the beach cliffs to Ploughman's Creek ***(Fig. 2)***. Note the relatively low cliff height; this forms the Ngaroma Terrace. The exposed deposits are all of estuarine carbonaceous-rich mud beds with rhyzoliths and rootlets. These overlie rippled sands with abundant wood pieces (<1 cm - 5 cm) overlying gravel lenses that are either poorly sorted and matrix supported debris flow or clast supported fluvial bedload deposits. The ~8000 BP Podocarp forest (Ota et al, 1984) is rooted in the gravels of the estuary (Lewis and Ekdale, 1991). These probably formed slightly higher ground with better drainage for the trees to grow in than the surrounding estuary muds/grasslands.

Walking south along the beach to nearly at Ploughman's Creek, there is an increase in cliff height associated with an abrupt change in lithofacies to the older (Pliocene?) marine deposits. These formed a remnant high in the Ngaroma Terrace surrounded by the estuary deposits. Large scale slumps can be seen on the edges of this remnant high. On the south side of the remnant high, an incised fluvial terrace deposit can be seen with a log sticking out horizontally; this log has been dated at ~3,000 BP (Ota et al., 1984).

Just to the south of the incised fluvial deposit we return to the interbedded fluvial/estuary deposits of the Ngaroma Terrace on the north side of Ploughman's Creek. This is a fluvial gravel deposit within estuary muds with syneresis cracks. Rooted in the gravel is a podocarp tree. Ploughman's Creek itself incises the Rafa Terrace and forms the southern boundary of the Ngaroma Terrace; note the difference in both cliff height and lithofacies on the southern and northern banks of Ploughman's Creek.

Stop 5 (walking south along beach cliffs from Ploughman's Gap to Doug's Gap)
On the south side of Ploughman's Creek are the interfan marine nearshore sands and silts of the Rafa Terrace ***(Fig. 2)***. Walking up Ploughman's Creek we can see an example of slumping and convoluted bedding. Walking south along the beach we can see more slumping and rare- hummocky cross-stratification.

Walking southward along the beach cliffs, the nearshore marine sands become interbedded with more and more gravel lenses off the nearby fan delta foresets. Slumps become more evident as we approach the fan delta.

Stop 6 (Doug's Gap fan delta foresets of the Rafa Terrace)
Doug's Gap cuts through the middle of the fan delta providing a clear 3-dimensional view of the facies architecture ***(Fig. 2)***. On the north side of Doug's Gap are interesting ?levee? or hummocky cross-stratification deposits. On the south side are steeply dipping fan delta foresets overlain by well-developed beach deposits and then topset beds of a prograding fan delta. The beach deposits are extremely well rounded and well sorted gravels and contain abundant trace fossils. Doug's Gap preserves some the more interesting features from

depositional processes that occur on steep, gravelly foresets. Field evidence of traction carpets and flow transformations are well documented and support field observations of Falk and Dorsey (1998). This study also provides new information on the formation of unique clast imbrication fabrics in foreset deposits and descriptions of rarely preserved backset beds (e.g. Colella et al., 1987).

Horizontal imbrication fabrics commonly occur in the clast supported gravels of the foreset deposits in the Conway fan deltas ***(fig. 5)***. The clasts are strongly imbricated at ~30° in the upslope direction relative to the foreset slope dip. This creates a strong horizontal fabric developed from intergranular dispersive pressures in the traction carpet in a high density turbidity current. This contrasts with previous studies that show clast fabrics parallel to foreset bedding planes (e.g. Sohn et al., 1999).

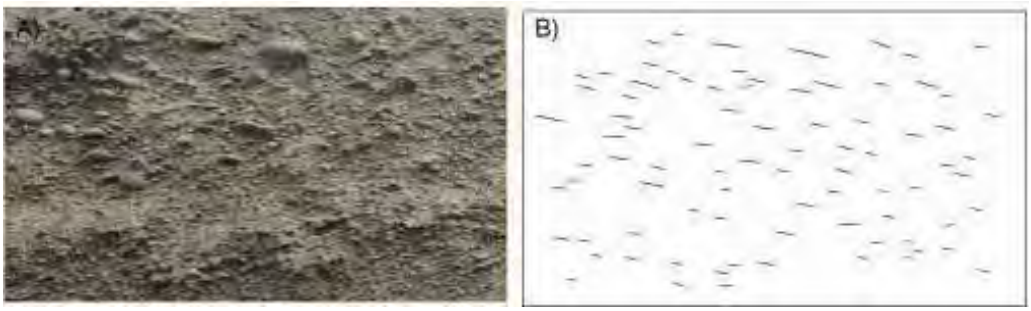

Figure 5: An example of horizontal imbrication fabric in the fan delta foresets.

Steep imbrication fabrics, referred to as 'back stacking', are also preserved in the fan delta foreset beds. The strong near vertical imbrication pattern visible near the mouth of Doug's Gap has developed behind a slump feature. The clasts range from cobble to pebble with the orientation of the clasts creating a deformed fabric around the slump block. The clasts then 'back stack' up the slope with imbrication ~75° to the foreset slope gradually becoming less steep at the top.

Beds dipping upslope, opposite to the dip of the foreset beds, overlie and are in sharp contact with the back stacking clasts. Clasts in these beds are rounded, moderately to poorly sorted and oriented parallel to backset bedding planes. The grain size of the backset beds decreases in the down slope direction and individual beds decrease in length from >6 m to < 2 m as the depression on the foreset created by the slump is gradually infilled with each backset bed. These deposits are the result of down slope sediment transport infilling the depressions left by older slumps on the delta foresets (Colella, 1988) and are similar to the backset beds of Colella et al. (1987) in the Crati Basin (Postma, 1984).

Stop 7 (along the beach cliffs from Doug's Gap to Big Bush Gully)

The fan delta foreset gravels continue in the beach cliffs as we walk south ***(Fig. 2)***. The steep dip of the foresets is not evident since we view the beds along strike thus providing an interesting view of the lateral evolution of the fan delta facies. We see the entire fan delta from just north of Doug's Gap where gravels are interbedded with shallow marine nearshore sands to just north of Big Bush Gully where gravels incise into older marine muds and prodelta deposits in a spectacular sharp contact marked by large scale soft sediment load casting. Huge flame structures in the sands separate gravel pockets forming ball and pillow structures.

The foreset gravels incise pro-delta dark muds interbedded with occasional light grey, very fine silts. Mud/silt beds below the foreset beds of the fan deltas are massive and contain beds up to 1 m thick. Lamination in the muds is rare, but areas of soft sediment deformation are visible. The mud beds typically contain fossils, including *Zeacolpus symerricus* (Ekdale and Lewis 1991), and macroscopic carbonaceous material throughout. Interbedded with the mud are occasional sand and pebble layers. The shells in these beds are randomly oriented and on occasion exist as densely packed shell beds. The densely packed shell beds are interpreted to represent storm events. The appearance of periodic *Zeacolpus symerricus* shell horizons up to 7 cm thick that dip towards the shore favor formation by storm events. Other beds with isolated floating pebbles or shells within the muds can be explained by deposition of distal fine-grained debris flows. Deformation and cross-beds in the mud layers are due to failure of over steepened muddy slopes possibly triggered by seismic or storm events.

Stop 8 (Medina House-Dawn Creek)
The largest of the Gilbert-style fan deltas along the Conway Coast is the Rafa fan delta forming the Rafa Terrace ***(Fig. 2)***. The exposures in Dawn Creek have provided an excellent opportunity to describe rarely published processes that occur on steep gravelly Gilbert-style fan deltas.

The Quaternary fan delta deposits of the Conway Coast contain a large number of slump structures. These features are located in both upper and lower foresets and in the marine interfan facies ***(fig. 3)***. The inherently steep slope of the depositional system leads to slope failures and resedimentation by gravitational processes. These include sediment slides and slumps and debris flows. Slope failures are common within fan delta complexes with high rates of sedimentation. The failures along these slopes create down slope movement of sediments that can severely alter the morphology of the slope (Postma, 1984; Postma and Roep, 1985; Colella et al*.,* 1987; Lonne, 1995). Reasons for foreset failure include over steepening combined with instigators such as earthquakes and storms. Within the foresets and nearshore marine facies of the Conway Coast the sizes of the slumps range from less than a meter to greater than 15 m.

Figure 6 is a photo of a large-scale slump in the upper foresets of the southern fan delta outcrops. In this location, decimeter bedded material dipping against the foreset bedding overlies large rip-up mud clasts and blocks of material. Clasts in the beds are rounded, moderately to well sorted, and parallel to bedding planes. Grain size gradually decreases on the down slope (but up foreset) side of these features. The gravels are interbedded with thin beds (< 10 cm) of fine-grained silt and sand. Upslope, the dip of the beds decreases relative to the foreset bed.

Bedding against the foreset slope and clasts parallel to bedding planes help distinguish these as backset beds. These deposits are the result of down slope sediment transport infilling the depressions left by older slumps on the delta foresets (Colella, 1988). Large rip-up clasts and blocks of material indicate that the material was deposited in proximity to a slump. Interbedded sands and silts are evidence of periods of sedimentation between subsequent flow deposits. These bedding features are similar to the backset beds of Postma (1984) and Colella et al. (1987) in the Crati Basin.

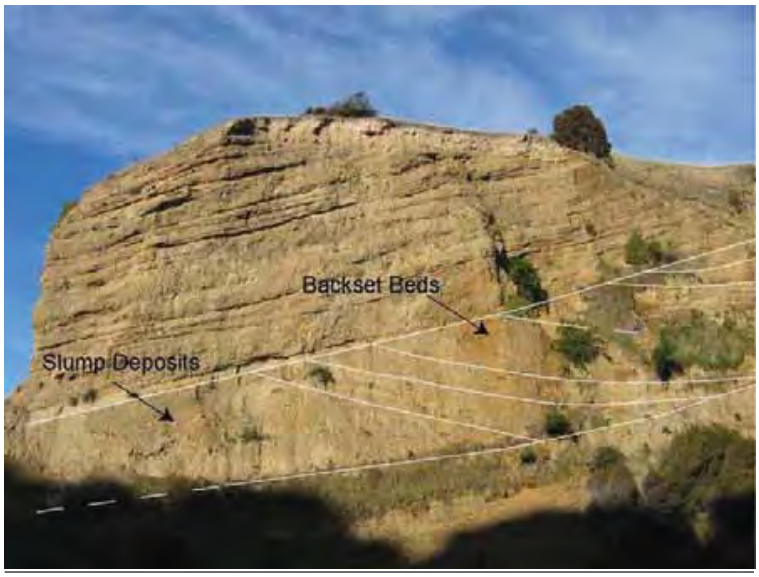

Figure 6: An example from the Rafa Terrace fan delta of backset beds forming behind a slump on the delta foresets. Slumps create depressions in the foreset slope that get progressively infilled first by gravel beds with back stacking clast imbrication followed by backset beds of alternating sands and gravels from intermittent flows.

Stop 9 (walking south along beach cliffs from Medina House)
The key to deciphering the series of nested terraces lies within the stratigraphy of the fan deltas. The Medina Terrace was formed by the progradation of the Medina fan delta ***(Fig. 2)***. The deposition of the Medina fan delta was followed by incision into the fan and removal of the fan deltas rounded topset beds (all other areas are a complete package of foresets and topsets). The Medina fan foreset beds are deeply eroded and then infilled by the younger Rafa fan delta foresets. This period of incision was followed by the deposition of the Rafa fan delta. The incised contact can be seen in the coastal transect. The formation of an inset terrace is also supported by the geomorphic expression of the Medina Terrace delta plain topset surface being ~15 m higher with respect to the Rafa Terrace. A similar contact between the two fan deltas is also seen up the Medina Creek.

References

Colella, A., 1988. Pliocene-Holocene fan deltas and braid deltas in the Crati Basin, southern Italy: a consequence of varying tectonic conditions. Fan Deltas-Sedimentology and Tectonic Settings. Blackie, London, pp. 50- 74.

Colella, A., de Boer, P.L., Nio, S.D., 1987. Sedimentology of a marine intermontane Pleistocene Gilbert-type fan-delta complex in the Crati Basin, Calabria, southern Italy. Sedimentology 34, 721-736.

Ekdale, A.A., and Lewis, D.W., 1991. Trace fossils and paleoenvironmental control of ichnofacies in a Late Quaternary gravel and loess fan delta complex, New Zealand. Palaeogeography, Palaeoclimatology, Palaeoecology 81, 253-279.

Falk, P., and Dorsey, R. J. 1998. Rapid development of gravelly high-density turbidity currents in marine Gilbert-type fan deltas, Loreto Basin, Baja California Sur, Mexico. Sedimentology 45, 331-349.

Hall, L.S., 2003. Cenozoic deformation at the southern end of the Hikurangi Margin, New Zealand. Ph.D. Thesis, University of Oxford, England.293p.

Lewis, D.W., 1976. Subaqueous debris flows of early Pleistocene age at Motunau, North Canterbury, New Zealand. New Zealand Journal of Geology and Geophysics 19, 535-567.

Lewis, D.W., 1980. Storm generated graded beds and debris flow deposits with *Ophiomorpha* in a shallow offshore Oligocene sequence at Nelson, South Island, New Zealand. New Zealand Journal of Geology and Geophysics 23, 353-369.

Lewis, D.W., Laird, M. G., Powell, R. D., 1980. Debris flow deposits of early Miocene age, Deadman Stream, Marlborough, New Zealand. Sedimentary Geology, vol.27, no.2, 83-118.

Lewis, D.W. and Eckdale, A. A., 1991. Lithofacies relationships in a late Quaternary gravel and loess fan delta complex, New Zealand. Palaeogeography, Palaeoclimatology, Palaeoecology 81, 229-251.

Lønne, I., 1995. Sedimentary facies and depositional architecture of ice-contact glaciomarine systems. Sedimentary Geology 98, 13–43.

McConnico, T.S. and Bassett, K.N., 2003. Quaternary Gilbert-style fan deltas and Podocarp forests along the modern transpressional Hope fault, New Zealand. Abstracts with Programs - Geological Society of America, vol.35, no.6, pp.510.

McConnico, T.S. and Bassett K.N., 2004. Well preserved 'antidune' and backset beds associated with slumping on the foresets of a gravelly Gilbert-style fan delta, New Zealand.Abstracts with Programs - Geological Society of America, vol.36, no.6, pp.510.

McConnico, Tim, Kari Bassett, and Jarg Pettinga, 2005, Facies architecture of the Conway fan delta complex as it formed terraces along the uplifting Hawkswood Range. New Zealand Geological Society annual conference, Kaikoura, 2005

Nicol, A., 1991, Structural styles and kinematics of deformation on the edge of the New Zealand plate boundary zone, Mid-Waipara Region, North Canterbury, Ph.D. Thesis, University of Canterbury, pp. 171.

Ota, Y.Y., Torao; Iso, N., Okada, A., Yonekura, N., 1984. Marine terraces of the Conway coast, South Island, New Zealand. New Zealand Journal of Geology and Geophysics 27, 313-325.

Ota, Y.Y., Pillans, B. Berryman, K., Beu, A., Fujimora, T., Miyauchi, T., Berger, G., Climo, F.M., 1996. Pleistocene coastal terraces of the Kaikoura Peninsula and the Marlborough coast, South Island, New Zealand. New Zealand Journal of Geology and Geophysics 39, 51-73.

Pettinga, J.R. and Armstrong, M.J., 1998. Field Trip Three: North Canterbury Active Tectonics and Earthquake Hazards. In: Malcolm Laird (Ed.) Geological Society of New Zealand, New Zealand Geophysical Society Joint Annual Conference Field Trip Guide. Geological Society of New Zealand Miscellaneous Publication 101 B, 1-28.

Postma, G., 1984. Slumps and their deposits in fan delta front and slope. Geology 12, 27-30.

Postma, G. and Roep, T.B., 1985. Resedimented conglomerate in the bottomsets of Gilbert-type gravel deltas. Journal of Sedimentary Petrology 55, 874-885.

Schulmeister, J., Kirk, R.M., 1993. Evolution of a mixed sand and gravel barrier system in North Canterbury, New Zealand, during Holocene sea-level rise and still-stand. Sedimentary Geology 87, 215-235.

Sohn, Y. K., 2000. Depositional processes of submarine debris flows in the Miocene fan deltas, Pohang Basin, SE Korea with special reference to flow transformation. Journal of Sedimentary Research 70, 491–503.